ISBN 978-82-326-1222-2 (printed version)
ISBN 978-82-326-1223-9 (electronic version)
ISSN 1503-8181

Doctoral theses at NTNU, 2015:283

Amund N. Løvik

Linkages and stock dynamics of the aluminium-gallium system

Alloying elements, impurities and by-products

NTNU
Norwegian University of
Science and Technology

NTNU
Norwegian University of
Science and Technology
Faculty of Engineering
Science and Technology
Department of Energy and Process Engineering

Doctoral theses at NTNU, 2015:283

NTNU
Norwegian University of
Science and Technology

Amund N. Løvik

Linkages and stock dynamics of the aluminium-gallium system

Alloying elements, impurities and by-products

Thesis for the degree of Philosophiae Doctor

Trondheim, October 2015
Norwegian University of Science and Technology
Faculty of Engineering Science and Technology
Department of Energy and Process Engineering

NTNU
Norwegian University of
Science and Technology

NTNU
Norwegian University of Science and Technology

Thesis for the degree of Philosophiae Doctor

Faculty of Engineering Science and Technology
Department of Energy and Process Engineering

ISBN 978-82-326-1222-2 (printed version)
ISBN 978-82-326-1223-9 (electronic version)
ISSN 1503-8181

Doctoral theses at NTNU, 2015:283

Printed by Skipnes Kommunikasjon as

Abstract

Impending global environmental- and resource related problems require a transformation of the socio-economic metabolism, the inputs, processing and outputs of materials and energy in society. The environmental impacts and resource requirements of metal cycles can be reduced significantly if they approach a steady state where in-use stocks are maintained through recycling rather than primary metal. In a steady state system, linkages between metal cycles, for example through alloys, impurities and by-products, will become increasingly important due to the high share of recycled post-consumer metal. The aluminium cycle is in this regard particularly important: It is responsible for large greenhouse gas emissions and energy use, highly sensitive to alloying elements and impurities, and has a strong linkage to gallium, which is a by-product of aluminium production. In this thesis, these linkages were studied in the context of in-use stock saturation and closed-loop material cycles, to better understand their importance, and to identify strategies that can facilitate a transition towards a steady-state socio-economic metabolism.

It was found that higher recycling rates are increasingly difficult to achieve in closed-loop steady state systems, due to the accumulation of impurities. A model of aluminium beverage can recycling showed that stable metal impurity concentrations are reached after 5-15 recycling loops with recycling rates in the range of 45-75%. It is expected that similar results would apply for systems that are more complex. The increasing availability of automotive aluminium scrap represents a future challenge for recyclers due to the large variety of alloys and limited demand for mixed scrap. A global surplus of scrap may occur in the period 2020-2030 unless measures are taken to restructure the recycling system. Allowing recycled material in safety-relevant components, together with an

improved sorting of alloys through dismantling or advanced sorting technologies, may delay the surplus with several decades.

The global system of production, manufacturing, use and recycling of gallium, and gallium-containing products was described and quantified for 2011. Gallium use is currently driven by neodymium-iron-boron magnets containing gallium as an alloying element and semiconductor applications: integrated circuits, light-emitting diodes and photovoltaic panels. Large material losses occur in the fabrication of intermediate products and devices. Currently, demand is far below the supply potential. Scenario analysis showed that a low stock saturation in the aluminium cycle might cause the supply potential of gallium to fall below future demand, given an increased market penetration of gallium-containing technologies. A number of measures was identified for improving the system-wide material efficiency, among which the most effective are related to process yield improvements or collection of production scrap.

The results showed that linkages between material cycles greatly complicate the transition to a steady-state socio-economic metabolism, and at the same time indicated priorities for measures that can be taken to facilitate this transition.

Acknowledgements

This work was carried out at the Department of Energy and Process Engineering and the Industrial Ecology Programme at Norwegian University of Science and Technology (NTNU) in Trondheim, Norway, and during a 5-month research stay at the Swiss Federal Laboratories for Materials Science and Technology (Empa) in St. Gallen, Switzerland. The work has been conducted over a period of 4 years, from 2011 to 2015.

Above all, I would like to thank my supervisor Daniel B. Müller for his clear guidance, dedication, and his unique ability to combine critical feedback and encouragement. Our discussions have been a source of inspiration and motivation throughout these years, and this work would not have been possible without his support. I express my gratitude to my co-supervisor Georg Rombach from Norsk Hydro, who played an important role in the early phase of the work and whose knowledge of the aluminium industry has been very valuable. I thank Heinz Böni, for giving me the opportunity to stay as a visitor at Empa during the last months of this work. Finally, I would like to thank my closest colleagues in the IndEcol offices: Felipe Vasquez, Franciska S. Steinhoff, Gang Liu, Helen Hamilton, Nina H. Sandberg, Stefan Pauliuk, and most of all, Eliette Restrepo and Roja Modaresi for collaborations and contributions to the papers.

Table of Contents

Abstract i

Acknowledgements iii

Table of Contents iv

List of Appended Papers and Author's Contributions vi

1. Introduction 1

1.1. End to the growth era 1

1.2. Anthropogenic metal cycles, dynamics and linkages 2

1.2.1. Metal cycles and dynamics 2

1.2.2. Linkage 1: Impurities 6

1.2.3. Linkage 2: Alloys and compounds 7

1.2.4. Linkage 3: Co-product- and by-product metals 9

1.2.5. Dynamics and linkages 9

1.3. The case of aluminium and gallium 10

1.4. Research questions and thesis structure 11

2. Methodology 15

2.1. Dynamic material flow analysis 15

2.2. Multi-element substance flow analysis and optimization 16

2.3. Monte Carlo simulation for uncertainty propagation 19

3. Summary of the papers 21

3.1. Paper I 21

3.2. Papers II and III 22

3.3. Papers IV and V 23
4. Discussion and conclusions 25
4.1. Question (i) – methodological reflections 25
4.1.1. Modelling alloying elements and impurity accumulation 25
4.1.2. Modelling by-product demand 27
4.2. Question (ii) - the significance of linkages 28
4.2.1. Alloying elements and impurities 28
4.2.2. By-product metals 29
4.2.3. In general about linkages 30
4.3. Question (iii) - solutions to linkage-related problems 31
4.4. Conclusions and outlook 32
References 35

List of Appended Papers and Author's Contributions

Paper no.	*Title*	*Contribution by A.N. Løvik*
Paper I	*A material flow model for impurity accumulation in beverage can recycling systems* Løvik, A. N.; Müller, D. B., In *TMS Light Metals*, 2014, pp. 907-911.	Research design, data collection, model development, analysis, visualization and writing.
Paper II	*Component- and alloy-specific modeling for evaluating aluminum recycling strategies for vehicles.* Modaresi, R.; Løvik, A. N.; Müller, D. B., *JOM*, 2014, 66 (11): 2262-2271.	Parts of: data collection, analysis, visualization and writing.
Paper III	*Long-term strategies for increased recycling of automotive aluminum and its alloying elements* Løvik, A. N.; Modaresi, R.; Müller, D. B., *Environ. Sci. Technol.*, 2014, 48 (8): 4258-4265.	Research design, parts of data collection, model development, analysis, visualization and writing.
Paper IV Including supporting information	*The global anthropogenic gallium system: determinants of demand, supply and efficiency improvements* Løvik, A. N.; Restrepo, E.; Müller, D. B., *Environ. Sci. Technol.*, 2015, 49(9):5704-5712.	Research design, data collection, model development, analysis, visualization and writing.
Paper V Including supporting information	*Strategies for securing rising gallium supply under boundary conditions of aluminum stock dynamics* Løvik, A. N.; Restrepo, E.; Müller, D. B., Submitted to *Environ. Sci. Technol.* (2015).	Research design, data collection, model development, analysis, visualization and writing.

1. Introduction

1.1. End to the growth era

As the world population today approaches 8 billion people (United Nations, 2015), humanity is facing unprecedented challenges related to pollution and resource availability. The most recognized example is global warming caused by anthropogenic greenhouse gas emissions (IPCC, 2014), but there are also other dramatic changes taking place, such as loss of forest cover (Hansen et al., 2013) and biodiversity (Barnosky et al., 2011). Furthermore, there are concerns about the future availability of mineral resources (Angerer et al., 2009; Graedel, 2011), especially those used in emerging technologies for climate change mitigation. While humans have always had to adapt to the limited resources and carrying capacity of their environment, it is only after industrialization, the succeeding population growth, and the emergence of international trade that these phenomena have appeared on a global level. It has been proposed that humanity should, in order to respect the limitations of a finite planet, move to a "spaceship economy" where we strive for high quality of stocks providing services to people while minimizing the throughput of energy and materials (Boulding, 1966). For material cycles, this implies a transition towards a steady state with closed loops and high recycling rates (Ayres, 1997).

These ideas stand in sharp contrast to the theory of growth as the driver of increased well-being and the element that ensures socio-economic and political stability throughout the world. Since the industrial revolution, the world has been in a state of continuous population growth, economic growth and associated growing pollution and natural resource extraction. However, population growth is expected to slow down significantly before the end of this century, possibly reaching a stable population of around 11 billion people (UN Department of Economic and Social Affairs Population Division, 2015). Efforts to solve global

environmental- and natural resource related problems and decelerating population growth both point to a coming end to the growth era, which has been a defining characteristic of the modern world since the industrial revolution.

1.2. Anthropogenic metal cycles, dynamics and linkages

1.2.1. Metal cycles and dynamics

Materials play a vital role in the socio-economic metabolism: The standard of living enjoyed in the industrialized world depends on large throughputs and stocks of materials for housing, transportation, communication, infrastructure, and energy distribution, to name a few (Gordon et al., 2006; Müller et al., 2013). Moreover, an increasing diversity of materials, to the point that almost every naturally occurring chemical element is being used, is a major ingredient in technological development (Graedel and Cao, 2010). The materials industry is a significant contributor to greenhouse gas (GHG) emissions, with more than 20% of global energy- and process related CO_2 emissions, including indirect emissions (Allwood et al., 2010). At the same time, many of the proposed technological solutions to energy/emissions problems rely on specialty metals with potential restrictions in supply, both short term and long term (Graedel, 2011).

The study of anthropogenic material cycles has emerged in an effort to understand the relationship between human activities and pollution, natural resource extraction, and energy use (Baccini and Bader, 1996). The approach is particularly useful for metals due to the importance of recycling as a measure for energy and resource conservation. There is now a large body of literature covering at least 30 different chemical elements, most of them metals, but also including plant nutrients such as phosphorus and nitrogen (Chen and Graedel, 2012). These studies, which are performed on a city, country, regional, or global level, quantify the stocks and flows of the selected material, typically a chemical element,

through the most important industrial processes and human activities. The results are used to identify options for reducing emissions of the metal to the environment (e.g. for heavy metals), conserving geological resources, and reducing associated energy needs and greenhouse gas emissions. Lately, mathematical models have been used to analyse historical and future development of the material cycles (Müller et al., 2014), and geographical aspects of material use (Liu and Müller, 2013; Pauliuk et al., 2013; Wang et al., 2007). Furthermore, dynamic models of metal cycles have been extended to include associated greenhouse gas emissions and energy requirements of processes throughout the cycle (Liu et al., 2012; Milford et al., 2013; Modaresi et al., 2014).

Above all, these studies show the importance of in-use stock dynamics for recycling of metals: the availability of end-of-life scrap for recycling is determined by the lifetime of products and the historical use of the metal. When in-use stocks are growing rapidly, e.g. due to population growth, infrastructure development, or more widespread use of the material, the end-of-life flows are small compared to the production. Consequently, recycling is limited by the availability of scrap. When stocks are stable or growing slowly, the availability of end-of-life scrap is high, and a large share of demand may be covered with recycled material (secondary production). An example of an in-use stock development pattern and associated inflow, outflow and recycled content are shown in Figure 1. In the beginning, the stock of material in use grows exponentially, reflecting exponential growth of the inflow. Scrap availability (outflow) is approximately the inflow function delayed by a certain time interval, representing the average lifetime of products in use. At the end of this time interval, the exponential function of the inflow has grown to a given multiplier times the function value at the beginning of the time interval. As long as the exponential growth rate remains the same (e.g. 3% growth per year), this multiplier will be constant, meaning that the magnitude of the outflow will always be in the same proportion to the inflow, for example 30%. Consequently, the

maximum recycled content (outflow divided by inflow) remains constant during exponential growth. In the transition phase, growth slows down; leading the outflow to "catch up" with the inflow, and recycled content grows. Finally, after stock saturation, a steady state is reached where inflow and outflow are the same. In an idealized system with perfect scrap collection and no losses in the recycling process, recycled content will approach 100%, and primary production is completely replaced by secondary production.

Global metal cycles are at different stages of development in the context of stock dynamics; however, most, if not all, have growing in-use stocks. Examples of metals with rapidly growing consumption and in-use stocks include aluminium, indium and the rare earth elements. World production of aluminium has, on average, grown about 5% per year since the year 2000, and end-of-life recycled content is stable slightly above 20 % (International Aluminium Institute, 2015). Iron, while still growing fast on a global level, has shown signs of stock saturation on a per capita level in some industrialized countries (Müller et al., 2011).

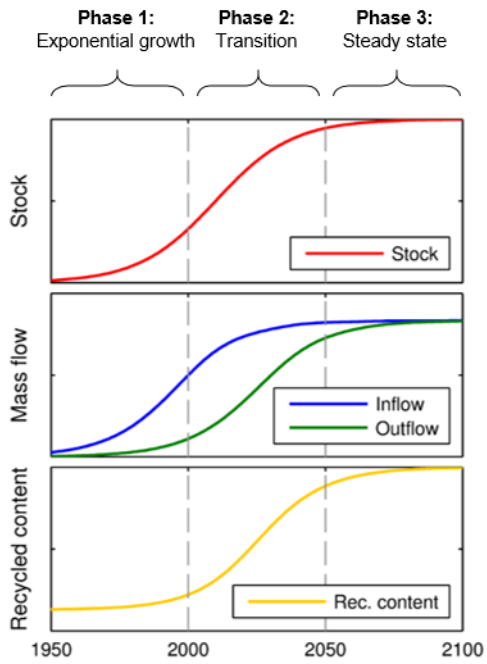

Figure 1 Example of a hypothetical in-use stock development pattern for a metal, with associated inflow, outflow and recycled content. In phase 1, the stock grows exponentially, causing exponential growth of inflow, and a constant, low recycled content. In phase 2, the stock growth slows down, more end-of-life scrap becomes available (outflow), and recycled content increases. In phase 3, the stock is stable, inflow and outflow are both high, and recycled content approaches 100% in an idealized system.

The transition of metal cycles from rapidly growing to stable stocks makes it possible, through increased recycling and replacement of primary production, to save mineral resources and energy, and reduce related emissions (Liu et al., 2012; Milford et al., 2013). Such transitions are necessary, because of the need to limit global warming, and increasingly likely to happen, because of an expected stabilisation of world population.

Most studies of anthropogenic metal cycles deal with only one chemical element. The approach of selecting one element has proven to be a powerful method, both for systems understanding and identifying options for improvement. One clear limitation however, is that linkages between the production and use of different metals are not taken into account. While all metal cycles are ultimately interwoven

in the global economy, the object of study here is linkages related to the material itself. Such linkages include at least the following: (i) common waste streams and associated mixing during recycling, (ii) alloys and compound materials, (iii) co-production of several metals from the same geological resources. Figure 2 in chapter 1.4 (page 13) illustrates these three linkages for the case of aluminium, its alloying elements, and gallium.

1.2.2. Linkage 1: Impurities

Waste streams usually consist of more than one product, and a product usually consists of different materials joined together. Hence, any waste stream contains a collection of materials, which should ideally be separated and recycled on their own to recover as much material as possible. In practice, the processes used for liberation and subsequent separation of materials are not perfect: some foreign materials will always enter the recovery process (Reuter et al., 2006). Depending on the thermodynamics and kinetics of the remelting process, these may end up in the recovered metal as an impurity (Nakajima et al., 2010). This represents a subtle linkage between material cycles. A few studies have been dedicated to the effect of impurities on recycling of metals from vehicles, showing how particle size reduction and liberation affects the contamination between different metals, and thus defines boundaries for recycling rates of metals from vehicles (Reuter et al., 2006; van Schaik et al., 2004). In addition, there has been some work on copper as an impurity in steel, and the implications for steel recycling (Ekvall et al., 2014; Hatayama et al., 2014; Nakamura et al., 2012). These studies conclude that better sorting or higher allowance of copper impurities in steel alloys can contribute to significant reductions of greenhouse gas emissions. However, they do not study the general phenomenon of impurity accumulation in itself, its dynamics and how it is affected by system characteristics such as the recycling rate.

1.2.3. Linkage 2: Alloys and compounds

Metals are usually not used in pure form, but rather in alloys or compounds with other metallic and non-metallic elements. Steel, in terms of aggregate mass the most important metal, is an alloy of iron and carbon. Alloy steels, typically used in automotive applications, industrial tools, pipelines and food handling equipment, contain additional alloying elements such as chromium, nickel, vanadium, molybdenum, niobium, manganese, silicon and tungsten (Allwood et al., 2012). Aluminium is normally used in alloys with silicon, copper, magnesium, manganese, chromium, zinc, iron and/or vanadium (Altenpohl, 1998). Many, if not most, specialty metals are mainly used in compounds where they constitute less than 50% of the mass (Graedel et al., 2015). Examples include indium, used in indium tin oxide, gallium, used in gallium arsenide, and neodymium, used in neodymium iron boron (NdFeB) magnets (Graedel et al., 2015). Furthermore, many metals are mainly used as alloying elements in materials where they constitute less than 20% of the mass (Graedel et al., 2015). Examples of such elements include the steel alloying elements nickel, chromium, manganese, vanadium and niobium (Graedel et al., 2015). The linkage of metal cycles through their use in alloys and compounds has important consequences for recycling. More complex waste streams lead to higher material losses in recycling (Reuter et al., 2013). The chemical elements constituting a single material will behave differently under a given recycling process. Hence, the more elements are present, the more difficult it becomes to optimize the recovery of all of them. In the remelting process, alloying elements will end up in the recovered metal, in the slag phase, or in the gas phase (Nakajima et al., 2010). If they are retained in the metal, alloying elements will limit the purity of recovered metal. With a large diversity of alloys in the waste stream, the recycled material will be a blend of different alloys with limited applicability compared to primary metal. If they end up in slags or in the gas phase, the alloying elements will be lost upon recycling, and will have to be replaced by primary metal.

The problem of alloying elements in metal cycles needs to be studied with a systems approach: decisions in one part of the system (alloys used in manufacturing) causes problems in a different part of the system (scrap quality issues in remelting) and solutions may lie in yet other parts of the system (better sorting of waste streams). Since the early 80's, the "alloy problem" has been studied on a society level, including material production, manufacturing, the use phase and recycling in a wider systems approach. Van Linden and Hannula (1980) developed a substance flow model of magnesium, manganese, silicon and iron in aluminium beverage can recycling, to investigate the effect of different alloy combinations (a beverage can is produced with two different aluminium alloys) on maximum recycling rate in a steady state system. Constraints to aluminium recycling caused by alloying elements has been discussed extensively since then. The publications can be divided roughly into three groups: those that (i) provide qualitative discussions of the problem and forecasts of scrap generation and demand, without explicitly modelling the flows of alloying elements (Cochran et al., 1983; D'Astolfo and Bruggink, 1994; van Linden, 1994; Modaresi and Müller, 2012; Tessieri and Ng, 1995; Zapp et al., 2003); (ii) focus on optimization of the recycling process considering different scrap types and alloy compositions, while maintaining a broader perspective (Gaustad et al., 2007; Kirchain and Cosquer, 2007; Olivetti et al., 2011; van Schaik et al., 2002); (iii) model material flows including alloying elements in a wider system, including the use phase and in-use stock dynamics (Gaustad et al., 2011; Hatayama et al., 2007a, 2009, 2012; van Schaik et al., 2002). The work on aluminium is mainly concerned with alloying elements as a potential restriction to future recycling. There has also been some work on alloying elements in the steel cycle. In contrast to the work on the aluminium cycle, the focus has been on the value of alloying elements and how to achieve a higher recycling rate of alloying elements to save energy or mineral resources, and reduce emissions. The relevant literature here includes studies on the individual alloying elements (Johnson et al., 2006; Nakajima et al., 2008; Reck et al., 2008), and studies that involve simultaneous substance flow analysis of

several alloying elements (Daigo et al., 2010; Igarashi et al., 2007; Nakajima et al., 2013; Ohno et al., 2014). Past studies have mainly focused on identification and timing of the problem, and less on the evaluation of solution options and the development of strategies.

1.2.4. Linkage 3: Co-product- and by-product metals

The third linkage considered here is that of co-product and by-product metals. Most metals are mainly produced as by-products of economically more important metals (Graedel et al., 2015). These have been referred to as carrier metal and coelement (Verhoef et al., 2004), parent and daughter metal (Graedel, 2011), or attractor- and hitch-hiker metal (Talens Peiró et al., 2013). The linkage between a byproduct element and its carrier metal is important from a resource availability perspective, because the maximum possible supply of the byproduct metal is limited by the extraction of ore for production of the base metal. Due to the small content of the byproduct metal in the ore, its aggregate value is not high enough to justify mining. Hence, future use of these metals may be severely constrained by primary resource availability. Possible supply constraints of byproduct metals to the expansion of emerging technologies have been investigated in several publications (Fizaine, 2013; Fthenakis, 2009; Houari et al., 2014; Katrak and Agarwal, 1981; Long and Smith, 1980; Nakamura et al., 2008; Stamp et al., 2014; Verhoef et al., 2004). These works have focused on the effects of a single technological shift, such as mass deployment of photovoltaics or the introduction of lead-free solder. Moreover, long-term supply potential was modelled in a simplified way without considering the stock dynamics of the carrier metal.

1.2.5. Dynamics and linkages

The importance of linkages between material cycles is closely tied to stock dynamics. In the current system phase of rapidly growing stocks, recycling of base

metals is mainly limited by availability of scrap rather than material quality issues. Likewise, linkages do not seem to restrict the supply of byproduct metals currently (Houari et al., 2014; Stamp et al., 2014), although information is scarce on this topic. For most byproduct metals, no quantification has been made of the supply potential. As shown in Figure 1, stock saturation, or even a slow-down of growth, will lead to a higher availability of scrap, which may be used to replace primary production. While this represents an opportunity to reduce energy use and emissions dramatically, it will also intensify the issue of scrap quality, and possibly reduce the potential for byproduct metal extraction. More generally: the importance of linkages, or their impacts in anthropogenic metal cycles, is closely tied to the recycled content. Because the recycled content, or rather the maximum recycled content, depends on the growth rate of the stock, there is a strong connection between linkages and stock dynamics. A transition of the metal cycle from exponential growth to saturation puts the coupled systems of individual metal cycles in a radically new relationship, where linkages may become the limiting factor of recycling or byproduct metal production.

1.3. The case of aluminium and gallium

The aluminium cycle is a particularly interesting case for studying linkages between material cycles, due to the importance of alloying elements, scrap quality, and the close connection to the gallium system.

The vast majority of aluminium is used in alloy form. There are two main types of alloys, cast and wrought, and within each type, there are eight different alloy series. An alloy belongs to a given series depending on its main alloying element(s) (or combinations thereof), which are silicon, copper, manganese, magnesium and zinc. There are more than 200 different individual alloys defined in industry standards (ASTM International, 2011; The Aluminum Association, 2009). However, the real diversity is even larger, due to internal specifications

used by the metal producers. Aluminium scrap, in particular post-consumer scrap, naturally contains a mixture of alloys, which together with external impurities prevents a direct closed-loop recycling of aluminium alloys. Furthermore, the options for refining molten aluminium are extremely limited due to its high affinity for oxygen (Gaustad et al., 2012; Nakajima et al., 2010). Most alloying elements will remain dissolved in molten aluminium during remelting and refining. In addition, foreign impurities such as iron, copper and silicon have a tendency to be picked up from mixed scrap streams, dirt, or equipment used to handle scrap and melts. Today, aluminium recycling is not severely limited by the quality of secondary material. Recycled content (end-of-life scrap), is around 20% on average (International Aluminium Institute, 2015), which leaves plenty of room for dilution with pure primary metal. With future slow-down of stock growth, the availability of scrap will increase, and alloying elements and impurities may become real limitations to aluminium recycling

Gallium, used in rapidly growing applications such as mobile phones, light-emitting diodes and photovoltaics, is almost exclusively produced as a byproduct of aluminium (United States Geological Survey, 2014). It accumulates in the sodium hydroxide solution used to dissolve bauxite and precipitate alumina in the Bayer process, and can be extracted through a series of processing steps (Hudson, 1965). Slow-down of stock growth in the aluminium cycle may lead to a replacement of primary production with recycling and reduce the potential for gallium extraction. Hence, the availability of gallium for emerging technologies depends on the development of the aluminium cycle.

1.4. Research questions and thesis structure

As has been argued above, linkages between metal cycles is potentially a limiting factor for recycling and production of by-product metals. The importance of linkages will increase dramatically with the slow-down of stock growth and

eventual saturation. These linkages should therefore be studied more in detail, to identify solutions to specific problems in the aluminium and gallium cycles, and to understand the effects of linkages in general. In this context, the following three research questions were formulated:

(i) *How can linkages between metal cycles, specifically those pertaining to alloying elements, impurities, and by-products, be modelled in a socio-economic metabolism framework? What are the strengths and limitations of different approaches?*

(ii) *How do linkages, in the context of stock dynamics and transition to a steady-state social metabolism, influence metal cycles? What are consequences for recycling of aluminium and availability of primary gallium?*

(iii) *How effective are different measures to solve problems related to linkages between material cycles, specifically in the coupled aluminium-gallium system?*

These questions were addressed in five papers. Figure 2 illustrates how the papers are related to the aluminium cycle and its linkages to other metals cycles. The papers are organized by linkage rather than by research question. Paper I deals with the impurity linkage, looking into the accumulation of a generic impurity element in an aluminium beverage can recycling system. Paper II and III address the issue of alloying elements, through a dynamic model of automotive aluminium recycling. In papers IV and V, the gallium cycle is quantified and modelled to investigate the byproduct linkage to the aluminium cycle. Question (i) is implicitly addressed in all papers through the demonstration of how material flow models can be used to examine linkages. Papers I and V have a stronger focus on new

methodological developments. Question (ii), regarding the nature and implications of linkages, is addressed in all papers. Question (iii), on solutions, is addressed in paper III for alloying elements, and in paper V for the byproduct linkage.

The rest of the thesis is structured as follows: In Chapter 2, the most important methodological elements of the work are explained. In Chapter 3, the findings of each paper are summarised. In Chapter 4, the findings are discussed in light of the research questions. The five papers are appended at the end.

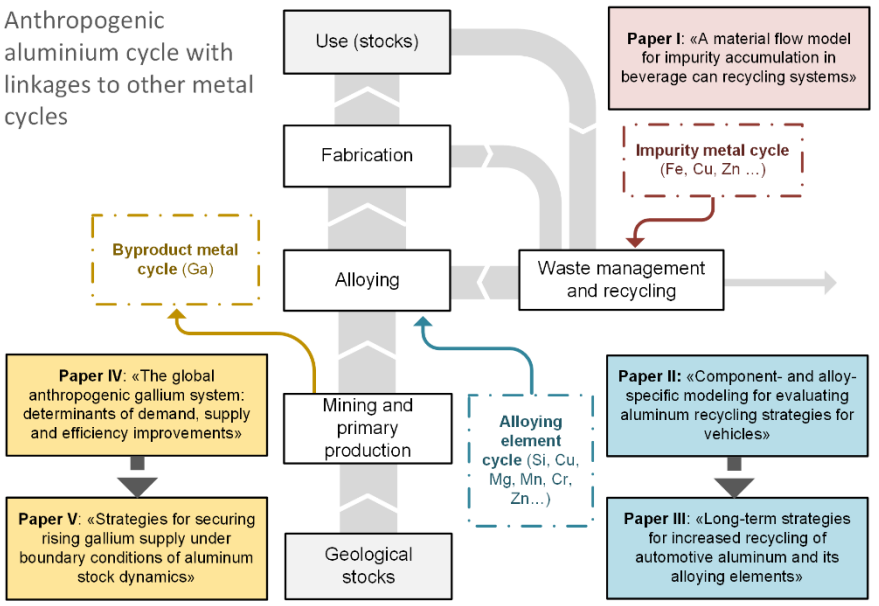

Figure 2 Overview of linkages between the anthropogenic aluminium cycle and other element cycles, and how the appended papers relate to the different linkages. Alloying element cycles are shown here as separate from the base metal cycle for visualization purposes. Strictly speaking, the cycles of the alloying element and base metal overlap in the alloying, fabrication, use and waste management and recycling processes.

2. Methodology

The methods are described in higher detail in the individual papers. In the following, some central elements are explained and commented on.

2.1. Dynamic material flow analysis

The work presented in this thesis relies on the methodology of material flow analysis (MFA) or substance flow analysis (SFA), as developed by Baccini and Brunner (1991), and Baccini and Bader (1996). In addition, the method of discrete dynamic MFA was used in papers I, II, III and V. Papers II, III and V utilize stock-driven lifetime-based approach to model future product flows from a defined development of the in-use stock (Müller, 2006). The following steps are conducted:

- In-use stock, S, in year t is given as a time series, or calculated from time series of drivers such as population, P, and service level per capita (e.g automobiles in use per capita), H:

$$S_t = P_t H_t \tag{2.1}$$

- Stock change is calculated for year t:

$$\Delta S_t = S_t - S_{t-1} \tag{2.2}$$

- Outflow from the use phase, Z, is calculated from previous inflows, X_c, and a probability function for the lifetime, $f_{t\text{-}c}$, by summing up the outflows from each individual cohort year c. The function $f_{t\text{-}c}$ gives the probability of a product to reach end-of-life at age t-c. In this work, a normal distribution was always used.

$$Z_t = \sum_{c=c_1}^{t-1} f_{t-c} X_c \tag{2.3}$$

- Required inflow is calculated as stock change plus outflow:

$$X_t = \Delta S_t + Z_t \tag{2.4}$$

These calculations are performed numerically for each model year. Due to the use of probability distribution functions and the numerical input data, an analytical solution is not possible.

The discrete dynamic model used in paper I to examine impurity accumulation assumes a fixed product lifetime of unspecified length, i.e. $Z_t = X_{t-1}$, where t indicates the number of recycling loops performed, regardless of the time it takes. Because of the simple mathematical relationship between inflows and outflows, it is possible to solve the system analytically, i.e. express impurity concentration as a function of the model input parameters.

2.2. Multi-element substance flow analysis and optimization

Papers II and III use a layered MFA approach to track alloys and/or chemical elements throughout the system as embedded in alloys, components, and passenger vehicles. Simultaneous SFA of several chemical elements is for the most part mathematically straightforward: mass flows of individual elements are obtained by multiplication of the weight fraction in alloys and the mass of each alloy. On the material layer, the total mass of aluminium alloys in different products is tracked. On the chemical element layer, the mass of each chemical element constituting the aluminium alloys is tracked. The model used in paper III also includes a component layer and an alloy level, which are situated between the

material layer and the chemical element layer. Hence, on the most detailed level, the outflow from the use phase can be described as $Z_{t,c,g,a,e}$, representing the mass of chemical element *e*, in alloy *a*, in component group *g*, from cohort *c*, at time *t*. The approach is mathematically simple, but generates an enormous number of data points, which are difficult to visualize. The layered approach makes it possible to model the compositions of scrap flows, which are determined by the degree of separation of the different component groups at end-of-life and the alloys used in each component group.

A difficulty arises when modelling the recycling process, as there are no data available on the recycling paths: which types of scrap are used in the production of which alloys, and in which amounts? Optimization by linear programming has been used to estimate likely recycling paths and maximum recycling rate (Gaustad et al., 2011; Hatayama et al., 2009; Kirchain and Cosquer, 2007), and was also used in paper III of this thesis. The linear program determines the maximum possible scrap utilization, given the amount and composition of different scrap types and the demand for a set of alloys with defined composition ranges. Let *Y(r,a)* be the mass of raw material *r* used to produce alloy *a*, *Y(r,a,e)* be the mass of element *e* in raw material *r* used to produce alloy *a*, *h(r)* be a hypothetical cost of raw material *r*, *A(a)* be the demand for alloy *a, CAU(a,e)* and *CAL(a,e)* be the upper and lower mass fraction limits of element *e* in alloy *a*, and *U(r)* be the available mass of raw material *r*. The problem can be formulated as minimization of a hypothetical total cost of raw materials, subject to five general conditions, which apply for all combinations of *a, r* and *e*:

$$\min \sum_a \sum_r Y(r,a) \cdot h(r) \quad \text{s.t.} \quad \begin{cases} \sum_r Y(r,a) = A(a) \\ \sum_r Y(r,a,e) \le CAU(a,e) \cdot A(a) \\ \sum_r Y(r,a,e) \ge CAL(a,e) \cdot A(a) \\ \sum_a Y(r,a) \le U(r) \\ \sum_a Y(r,a) \ge 0 \end{cases} \tag{2.5}$$

The first condition is a mass balance of inputs and outputs from the production process of each individual alloy. The second and third conditions are that the mass fraction of each chemical element in each alloy is within the defined range. The fourth condition is that the use of each raw material must be less than or equal to the available mass, from primary sources or scrap. It was assumed that the availability of primary aluminium and alloying elements is essentially unlimited. The fifth condition is that the use of any raw material cannot be negative. By setting the cost of scrap equal to zero, the optimal point will be equivalent to a maximization of scrap use. The problem was written on the form of a linear program:

$$\min_z f^T z \qquad \text{s.t.} \qquad \begin{cases} B \cdot z \le b \\ B_{eq} \cdot z = b_{eq} \\ lb \le z \le ub \end{cases} \tag{2.6}$$

Here, z is a vector of the variables to be changed in the optimization, i.e. the mass of each raw material used to produce each alloy; f is a vector of coefficients describing the cost of each variable in z; lb and ub are the lower and upper bounds of each variable in z; B and B_{eq} are matrices of coefficients describing the relations between the variables in z and the material compositions and production amounts; b and b_{eq} are vectors describing the compositional limits and the required production amounts. The linear program was solved with the Simplex algorithm in MATLAB (The MathWorks Inc., 2010).

2.3. Monte Carlo simulation for uncertainty propagation

Monte Carlo simulation was used for propagating parameter uncertainties to the system variables calculated by a mathematical model in paper IV. Pseudorandom values of each model input parameter are drawn from a probability distribution, and the system variables are calculated by use of the mathematical model and the drawn parameter values (Joint Committee for Guides in Metrology, 2008). This procedure is repeated many times (e.g. 10^5). The result is a distribution of values for the system variables, which can be analysed by statistics, e.g. by calculating the standard deviations or confidence intervals. An estimate of the uncertainty in model outputs is obtained.

3. Summary of the papers

3.1. Paper I

In this paper, a model is presented for analysing the accumulation of an impurity element in an aluminium beverage can recycling system. This system is a rare example of a nearly closed-loop metal recycling system, where a single product is repeatedly recycled in large quantities back into the same product. Due to the short lifetime of beverage cans, impurities picked up in scrap handling and recycling processes may quickly accumulate to detrimental levels in the material. The simplicity of the system, *i.e.* short lifetime, two alloys, one scrap type, made it possible to develop a mathematical model for the impurity weight fraction in the material and solve it analytically. The solution gives the weight fraction of the impurity as a function of number of recycling loops performed, n, recycling rate, RR, and contamination rate, h:

$$c_n = \frac{h \cdot RR}{1 - w_{lid}} \frac{1 - RR^n}{1 - RR} \tag{3.1}$$

where w_{lid} is the mass of the lid as share of the entire beverage can.

The impurity weight fraction in a steady state recycling system ($n \rightarrow \infty$) is proportional to the inverse of one minus the recycling rate; in other words, higher recycling rate leads to disproportionately higher impurity level. Furthermore, it was shown that the composition of the material reaches steady state after about 5-15 recycling loops with typical recycling rates (45-75%). Higher recycling rate leads to longer accumulation period and higher steady state impurity level.

3.2. Papers II and III

In these papers, a model was developed for tracking aluminium alloys in the global passenger vehicle fleet, and for evaluating recycling strategies to deal with constraints imposed by alloying elements. A stock-driven dynamic material flow model was built in paper II to forecast future scrap flows and their content of different aluminium alloy families. The model takes as input world population, number of vehicles per capita in use, the average lifetime of vehicles, average aluminium content in 14 different vehicle component groups, and alloy families used to produce these component groups. The results were analysed qualitatively and alternative alloy recycling pathways were discussed based on a "source-sink" diagram showing the compatibility of different alloy compositions. In paper III, the model was developed further to break down the alloy families into individual alloys and their constituent chemical elements. Future composition of scrap flows was estimated, showing that silicon and copper content will decrease due to increased use of wrought alloys. Moreover, the model was coupled to an optimisation model (linear program), to determine the maximum recycled content in the system under different conditions of component dismantling and scrap sorting. Results from earlier studies were confirmed, showing that a scrap surplus may appear in the coming decade if current practice in recycling of automotive aluminium continues. Furthermore, it showed that a combination of measures is needed to avoid such surplus. Firstly, it is necessary to allow for use of recycled material in so-called "safety-relevant" components, e.g. wheels. Secondly, it is necessary to improve scrap quality through segregation of alloys, for example by dismantling selected components, or advanced post-shredder sorting. Notably, the latter measure will have limited effect unless the first measure is also implemented.

3.3. Papers IV and V

In these papers, the linkage between the aluminium cycle and the gallium cycle was studied. Paper IV presents the first global material flow analysis of gallium. It provides an in-depth description of the whole system including primary production, refining, manufacturing of semi-finished products, fabrication of devices and recycling. The system was quantified through use of technical process parameters found in literature and provided by industry contacts. It revealed the main applications of gallium, the losses occurring throughout the system, and the relationship to the aluminium cycle. Specifically, it was found that use of gallium as a dopant in NdFeB magnets is the single largest driver for primary gallium consumption, which has not been acknowledged in earlier publications. The second and third most important applications are integrated circuits (mainly for mobile phones and wireless applications), and coloured light emitting diodes (in the red-green part of the spectrum) respectively. Only a small fraction of gallium enters use in semiconductor applications: most of the material is lost in the manufacturing processes. In paper V, this work is developed further in a dynamic model. This model was used to estimate future primary gallium demand based on various development paths for the five main applications. Furthermore, the gallium supply potential was estimated from extraction efficiencies, concentration in bauxite resources and future stock development patterns in the aluminium cycle. It was shown that both the future demand and supply potential of gallium are highly unpredictable. In a scenario where the in-use stock of aluminium grows slowly from 100 to 200 kg/cap globally and gallium-based technology penetrates in the photovoltaics and permanent magnet markets, the gallium supply from bauxite may be too low to meet demand. A sensitivity analysis on system-wide material efficiency measures showed that a shortage could be avoided even in this case by a combination of measures. The most effective measures for reducing primary demand today are related to recycling or avoiding scrap from GaAs crystal growth, substrate manufacturing, and fabrication of devices. In the future, depending on how the demand for individual applications develop, the most

important measures could be recovery of Ga from production- and end-of-life scrap of NdFeB magnets and copper indium gallium diselenide (CIGS) photovoltaics.

4. Discussion and conclusions

4.1. Question (i) – methodological reflections

4.1.1. Modelling alloying elements and impurity accumulation

In the work presented in this thesis, material flow analysis was used to study the influence of alloying elements and impurities in the aluminium cycle. The problems related to alloying elements and impurities are directly related to the stocks and flows of chemical elements. Any analysis of these problems must necessarily consider these flows and their relative magnitudes; it is by definition a study of material flows and stocks, and they both need to be clearly defined in a *system definition*. A layered approach, which for example connects a product level, a component level, an alloy level, and a chemical element level, is useful: the demand for services is defined at the product level; decisions regarding manufacturing and end-of-life treatment take place on the component- or alloy level, while the chemical element layer defines the boundary conditions of the material production. The layered approach makes it possible to model how changes on one level, e.g. dismantling of components before end-of-life vehicle shredding, affects the conditions in material production.

While for example input-output analysis has been used to investigate similar problems (Nakajima et al., 2013; Nakamura et al., 2012; Ohno et al., 2014), this is mainly an additional tool to enable quantification of flows; in the end, it is still a form of material flow analysis. Yet, it may be discussed whether the specific material flow models that have been used are adequate. The typical MFA model used is dynamic, data-intensive and calculates future scrap flows numerically, based on lifetime distribution functions (Gaustad et al., 2011; Hatayama et al., 2007b, 2009, 2012). This is also the method used in paper III in this thesis. Furthermore, a numerical approach (linear programming) was used to solve the complex problem of maximizing recycling with a large number of scrap flows and

alloys. This method is the only feasible option solve such complex problems, and enables answering specific questions that cannot be addressed properly with an analytical model. For example, the model used in paper III can be used to estimate the upper limit to recycled content in aluminium in vehicles for a certain set of alloys and components, provided that input data are accurate. Furthermore, it can be used to estimate how scrap compositions change over time. However, due to the lack of analytical mathematical solutions, it has limited capacity for generalization. The approach used in paper I, while only addressing a very simple system, allows for conclusions that potentially reach much wider. It shows how the steady state impurity concentration is related to the recycling rate and other key parameters of the system. The difficulty of reaching high recycling rates is shown on a general basis: when recycling rates approach 100%, impurities accumulate to very high concentrations. The pattern is the same, regardless of the contamination rate and other system parameters. Hence, these results illustrate more directly how radically different the system becomes with high recycled content, which in general only occurs after stock saturation or substantial slow-down of stock growth.

The models that were used in this work to analyse problems related to alloying elements and impurities do not explicitly include the thermodynamics and process metallurgy of recycling processes, such as discussed for example by Xiao and Reuter (2002) and Meskers et al. (2008). In the model used in paper III, material losses due to oxidation in remelting are implicitly included in the remelting yield parameter. Similarly, a shredder yield parameter takes into account the losses due to incomplete liberation of aluminium from the other materials in the car. However, these losses were assumed to be constant, while in reality they depend on particle shape, coatings and the physical connections between components of different materials (Xiao and Reuter, 2002; Reuter et al., 2006). Moreover, external impurities other than iron were not included due to a lack of quantitative estimates. Such simplifications, along with the optimization procedure used, mean

that the model is inherently optimistic regarding the possible recycling routes. Hence, the simulated recycling rate should be regarded as a maximum, given that additional problems with scrap quality are resolved. Nevertheless, the results can indicate the restructuring of the recycling system that is needed to utilize future aluminium scrap flows, and thereby serve as a starting point for more detailed investigations.

4.1.2. Modelling by-product demand

The importance of the linkage between a byproduct metal and its carrier metal depends on the demand for the byproduct metal relative to the supply potential. The linkage will only be felt once demand approaches the supply potential, after which the price of the byproduct metal may increase dramatically (Katrak and Agarwal, 1981). The study of the byproduct linkage must necessarily involve a study of the demand for this metal and its drivers. Base metals such as iron and aluminium are used in very large quantities for construction, transportation, infrastructure and other applications fundamental to modern society; their demand can therefore be coupled to population growth, industrialisation and urbanisation as the main drivers. Minor metals on the other hand, are typically used in a few highly specialized applications. Demand for these metals can change by an order of magnitude in few years. Such rapid changes can be explained by technological shifts, for example a breakthrough enabling widespread use of an entirely new application. Moreover, the byproduct metal normally constitutes a tiny fraction of the product in which it is used, and the amount used is highly dependent on technical parameters such as the thickness of semiconductor devices. The importance of such technical parameters was demonstrated in papers IV and V: for example, the average amount of gallium in a mobile phone is now four to five times larger than in year 2000, due to an increasing number and size of GaAs power amplifiers. The dependence on such parameters makes forecasting of demand more challenging than for base metals. Studies that do not go in depth on

individual technologies, but rather try to cover a large range of products with a simplified approach and generalizations, for example through use of input-output tables (Nansai et al., 2014), risk overlooking the most important parameters. In the case of gallium, the three most important applications (integrated circuits, light emitting diodes, and NdFeB magnets) are responsible for more than 60% of demand. However, the demand from each of them is highly sensitive to specific parameters. An in-depth understanding of the fabrication processes for these three applications seems more important than including all possible applications of gallium.

4.2. Question (ii) - the significance of linkages

4.2.1. Alloying elements and impurities

The results presented in papers I, II and III show the importance of alloying elements and impurities for recycling of aluminium: in the coming decade, aluminium scrap from passenger vehicles may exceed the amount that can be absorbed by the production of new vehicle components globally, due to the limitations to recycling imposed by alloying elements. While alloying elements already have a large influence on the recycling *paths* of aluminium, by restricting recycling to a few "recycling-friendly" alloys, e.g. for engine blocks, they do not currently limit the *amount* of aluminium recycled: there is still a high demand for the lowest quality scrap. This might change relatively soon, when scrap availability increases relative to demand. It was shown in paper III that a restructuring of the recycling system will be required to facilitate closed-loop recycling of alloys and ensure that all scrap is utilized.

The term *accumulation* is sometimes used in the discussion of alloying elements and impurities as a constraint to metal recycling (Gaustad et al., 2011; Ohno et al., 2014). This term signifies a build-up of alloying elements as impurities in alloys where they are not desirable or growing concentration of external impurities over

time due to repeated recycling. In a system of short-lived products such as the beverage can recycling system, this is actually the case. Even when all overall mass flows are constant, the concentration of an uncontrolled external impurity will increase until it reaches steady state, and end up at a level much higher than the impurity concentration after only one cycle. When it comes to alloying elements and external impurities in a large, diverse system with rapidly growing stocks, this accumulation effect is less important. The problem is in a way more direct: the concentrations of alloying elements intentionally used causes problems without the dynamic effect of accumulation. Already in the first recycling loop, the constraint due to external impurities and mixing of different alloys is severe. In the beverage can example, it was shown that accumulation occurs over a period over 5-15 recycling loops, for typical recycling rates. Considering the long lifetime and growing stocks of other aluminium-containing products, it is clear that the problem of accumulation as seen in beverage can recycling is something that would only emerge in the distant future in other sectors.

4.2.2. By-product metals

The results presented in papers IV and V show that future gallium demand and supply potential are both highly uncertain. Different technological developments may lead to completely different demand; different stock development patterns in the aluminium cycle will create completely different boundary conditions for gallium extraction. However, the demand for gallium is currently much lower than the supply potential, and there are plenty of options for improving the system-wide material efficiency of gallium. Considering that there are also alternative routes for gallium extraction, it seems that no fundamental restriction to supply will be seen any time soon, although system improvements may be needed.

The specific conclusions drawn for gallium are of course not automatically applicable to other byproduct metals, but some general observations can

nevertheless be made. Firstly, the future availability of byproduct metals is closely linked to the stock development pattern of the carrier metal. Secondly, as was discussed in paper V, the use of byproduct metals does not on its own cause depletion of geological resources, since mining is driven by extraction of the carrier metal. It could even be argued that byproduct metals should be extracted at higher rates, and possibly stockpiled: In the future, stock saturation in the carrier metal cycle may reduce the need for primary production and make byproduct extraction more expensive and/or costly in terms of energy use and emissions. Of course, this strategy involves high risk, since we cannot know with certainty that the byproduct metal will be needed in the future, or that alternative production routes will not be developed.

4.2.3. In general about linkages

Some connections exist between the three types of linkages examined here. The availability of gallium depends on the primary production of aluminium. With increased availability of aluminium scrap, the problem of alloying elements and impurities may become a limitation for aluminium recycling and associated reduction of primary production. Hence, solution of these problems may indirectly cause the supply potential for gallium to decrease. Moreover, gallium is a natural impurity in aluminium with detrimental effects on material properties (Senel et al., 2014). Due to the nature of the gallium extraction process (Hudson, 1965), more extraction of gallium can lead to lower concentration of gallium in primary aluminium, and thereby slightly improve material quality.

The work presented in this thesis illustrate the importance of dynamics and long-term developments in the context of linkages between material cycles. More specifically, these linkages emerge as problems when stock growth slows down. In an ideal system, recycling rates could approach 100% after the in-use stock saturates. In this extreme case, impurities would accumulate to very high

concentrations, alloys would have to be sorted perfectly, and the supply potential for gallium would be reduced to zero. While this is unrealistic, for example due to unavoidable losses in the collection, handling and remelting of metal scrap, it illustrates how these coupled systems depend on growth. The current functioning of the recycling system, related to the recycled content, persists only as long as there is exponential growth. When growth slows down, there will be an increasing availability of scrap until recycling is limited by insufficient collection, losses in the recycling processes, or material quality issues. This kind of growth addiction is similar to what has been described for the world economy (Jackson, 2011), and illustrates the wide-reaching challenges related to a transition to a steady-state socio-economic metabolism.

4.3. Question (iii) - solutions to linkage-related problems

In papers II and III, some strategies for increased recycling of automotive aluminium were studied. Specifically, it was found that use of recycled material in safety-relevant components should be introduced and combined with better scrap segregation, for example by dismantling of vehicle components or alloy sorting after shredding. The alloying element problem in the aluminium cycle is complex, and requires collaboration between different actors in the system: The aluminium industry, which has the highest incentive to increase recycling, may implement advanced scrap sorting technologies to enable production of a wider range of secondary alloys. However, the success of this strategy depends on an increased acceptance for secondary material among automotive manufacturers.

Paper V considered measures to avoid a gallium shortage in the case that demand outstrips supply potential in the future. A number of measures were found to have a significant impact on primary gallium demand and supply potential. Among these are increased recycling of production scrap, reduced thickness of

photovoltaic cells and improved yield in primary production. These solutions are relatively simple, in the sense that they can be implemented separately by individual actors in the system. In the case of a shortage, increased prices may facilitate recycling of production scrap that was previously lost, and encourage primary producers to improve the extraction process.

The alloy problem seems to be both more urgent and difficult to solve than a potential gallium shortage: A scrap surplus from the automotive sector is expected already between 2020 and 2030, while only the extreme combination of highest demand and lowest supply potential for gallium led to a shortage within the same period. Moreover, the lowest supply potential scenarios implicitly assume that the alloy problem is solved, in that they involve a very high end-of-life recycling rate of aluminium.

4.4. Conclusions and outlook

The work presented in this thesis has pointed out some potential problems and solutions related to linkages between the aluminium cycle, its alloying elements and the gallium cycle. It has been shown that linkages between material cycles make the transition to a steady-state social metabolism (circular economy) extremely difficult. Some specific solution strategies related to the aluminium and gallium cycles that may facilitate such a transition have been demonstrated. Naturally, many questions remain to be answered. The following three topics were identified as important areas of research in the future:

- In paper I, it was shown how impurities accumulate over time in a simple closed-loop recycling system. Furthermore, it was shown that the steady-state concentration is highly dependent on the recycling rate. It was suggested that similar conclusions would hold also for systems with a higher complexity. This should be investigated further by generalizations

of the analytical model to include a larger number of alloys, several scrap types, and growing stocks.

- The work presented here has illustrated the importance of stock dynamics for linkage-related problems. Saturation of the in-use stock, or slow-down of growth, can push the material cycle into a completely different state. The timing of these emerging phenomena is closely tied to the temporal development of the in-use stocks. Hence, the results presented here point back to in-use stocks, their growth patterns, and their drivers as an important topic for future research.
- The problems investigated here lie in the future. Modelling of these problems requires many assumptions regarding the future technological system and is inherently very uncertain. As was shown for gallium, the range of possible developments for demand is huge. Efforts should be made to understand how technologies develop over time with regard to material use, for example by looking into specific technologies and the historic development of material intensity and diversity to find common patterns.

References

Allwood, J.M., Cullen, J.M., and Milford, R.L. (2010). Options for Achieving a 50% Cut in Industrial Carbon Emissions by 2050. Environ. Sci. Technol. *44*, 1888–1894.

Allwood, J.M., Cullen, J.M., and Carruth, M.A. (2012). Sustainable materials: with both eyes open (Cambridge: UIT).

Altenpohl, D. (1998). Aluminum: technology, applications, and environment: a profile of a modern metal (Washington, D.C.: Aluminum Association).

Angerer, G., Erdmann, L., Marscheider-Weidemann, F., Scharp, M., Lüllmann, A., Handke, V., and Marwede, M. (2009). Rohstoffe für Zukunftstechnologien: Einfluss des branchenspezifischen Rohstoffbedarfs in rohstoffintensiven Zukunftstechnologien auf die zukünftige Rohstoffnachfrage (Stuttgart: Fraunhofer ISI).

ASTM International (2011). Standard specification for aluminum alloys in ingot and molten forms for castings from all casting processes (ASTM International).

Ayres, R.U. (1997). Metals recycling: economic and environmental implications. Resour. Conserv. Recycl. *21*, 145–173.

Baccini, P., and Bader, H.-P. (1996). Regionaler Stoffhaushalt: Erfassung, Bewertung und Steuerung (Heidelberg: Spektrum Akademischer Verlag).

Baccini, P., and Brunner, P.H. (1991). Metabolism of the anthroposphere (Springer-Verlag).

Barnosky, A.D., Matzke, N., Tomiya, S., Wogan, G.O.U., Swartz, B., Quental, T.B., Marshall, C., McGuire, J.L., Lindsey, E.L., Maguire, K.C., et al. (2011). Has the Earth/'s sixth mass extinction already arrived? Nature *471*, 51–57.

Boulding, K.E. (1966). The Economics of the Coming Spaceship Earth. In Environmental Quality in a Growing Economy, (Baltimore, MD: Resources for the Future; John Hopkins University Press), pp. 3–14.

Chen, W.-Q., and Graedel, T.E. (2012). Anthropogenic Cycles of the Elements: A Critical Review. Environ. Sci. Technol. *46*, 8574–8586.

Cochran, C.N., McClure, R.H.G., and Tribendis, J.J. (1983). Recycling of Automotive Aluminum - Present and Future (Warrendale, PA: SAE International).

Daigo, I., Matsuno, Y., and Adachi, Y. (2010). Substance flow analysis of chromium and nickel in the material flow of stainless steel in Japan. Resour. Conserv. Recycl. *54*, 851–863.

D'Astolfo, L.E., and Bruggink, P.R. (1994). Preserving the value-chain in automotive aluminum recycling. In Light Metals 1994, (San Francisco, CA), pp. 1121–1127.

Ekvall, T., Fråne, A., Hallgren, F., and Holmgren, K. (2014). Material pinch analysis: a pilot study on global steel flows. Metall. Res. Technol. *111*, 359–367.

Fizaine, F. (2013). Byproduct production of minor metals: Threat or opportunity for the development of clean technologies? The PV sector as an illustration. Resour. Policy *38*, 373–383.

Fthenakis, V. (2009). Sustainability of photovoltaics: The case for thin-film solar cells. Renew. Sustain. Energy Rev. *13*, 2746–2750.

Gaustad, G., Li, P., and Kirchain, R. (2007). Modeling methods for managing raw material compositional uncertainty in alloy production. Resour. Conserv. Recycl. *52*, 180–207.

Gaustad, G., Olivetti, E., and Kirchain, R. (2011). Toward Sustainable Material Usage: Evaluating the Importance of Market Motivated Agency in Modeling Material Flows. Environ. Sci. Technol. *45*, 4110–4117.

Gaustad, G., Olivetti, E., and Kirchain, R. (2012). Improving aluminum recycling: A survey of sorting and impurity removal technologies. Resour. Conserv. Recycl. *58*, 79–87.

Gordon, R.B., Bertram, M., and Graedel, T.E. (2006). Metal stocks and sustainability. Proc. Natl. Acad. Sci. *103*, 1209–1214.

Graedel, T.E. (2011). On the Future Availability of the Energy Metals. Annu. Rev. Mater. Res. *41*, 323–335.

Graedel, T.E., and Cao, J. (2010). Metal spectra as indicators of development. Proc. Natl. Acad. Sci. *107*, 20905–20910.

Graedel, T.E., Harper, E.M., Nassar, N.T., Nuss, P., and Reck, B.K. (2015). Criticality of metals and metalloids. Proc. Natl. Acad. Sci. *112*, 4257–4262.

Hansen, M.C., Potapov, P.V., Moore, R., Hancher, M., Turubanova, S.A., Tyukavina, A., Thau, D., Stehman, S.V., Goetz, S.J., Loveland, T.R., et al. (2013). High-Resolution Global Maps of 21st-Century Forest Cover Change. Science *342*, 850–853.

Hatayama, H., Yamada, H., Daigo, I., Matsuno, Y., and Adachi, Y. (2007a). Dynamic Substance Flow Analysis of Aluminum and Its Alloying Elements. Mater. Trans. *48*, 2518–2524.

Hatayama, H., Yamada, H., Daigo, I., Matsuno, Y., and Adachi, Y. (2007b). Dynamic substance flow analysis of aluminum and its alloying elements. Mater. Trans. *48*, 2518–2524.

Hatayama, H., Daigo, I., Matsuno, Y., and Adachi, Y. (2009). Assessment of the Recycling Potential of Aluminum in Japan, the United States, Europe and China. Mater. Trans. *50*, 650–656.

Hatayama, H., Daigo, I., Matsuno, Y., and Adachi, Y. (2012). Evolution of aluminum recycling initiated by the introduction of next-generation vehicles and scrap sorting technology. Resour. Conserv. Recycl. *66*, 8–14.

Hatayama, H., Daigo, I., and Tahara, K. (2014). Tracking effective measures for closed-loop recycling of automobile steel in China. Resour. Conserv. Recycl. *87*, 65–71.

Houari, Y., Speirs, J., Candelise, C., and Gross, R. (2014). A system dynamics model of tellurium availability for CdTe PV. Prog. Photovolt. Res. Appl. *22*, 129–146.

Hudson, L.K. (1965). Gallium as a by-Product of Alumina Manufacture. J. Met. *17*, 948–951.

Igarashi, Y., Daigo, I., Matsuno, Y., and Adachi, Y. (2007). Dynamic Material Flow Analysis for Stainless Steels in Japan - Reductions Potential of CO2 Emissions by Promoting Closed Loop Recycling of Stainless Steels. ISIJ Int. *47*, 758–763.

International Aluminium Institute (2015). Global Mass Flow Model 2013 (2014 draft) (London, UK: International Aluminium Institute).

IPCC (2014). Climate Change 2014: Synthesis Report. Contribution of Working Groups I, II, III to the Fifth Assessment Report of the Intergovernmental Panel on Climate Change [Core Writing Team, R.K. Pachauri and L.A. Meyer (eds.)] (Geneva, Switzerland: IPCC).

Jackson, T. (2011). Prosperity without Growth: Economics for a Finite Planet (London ; Routledge).

Johnson, J., Schewel, L., and Graedel, T.E. (2006). The Contemporary Anthropogenic Chromium Cycle. Environ. Sci. Technol. *40*, 7060–7069.

Joint Committee for Guides in Metrology (2008). Evaluation of measurement data - Supplement 1 to the "Guide to the expression of uncertainty in measurement" - Propagation of distributions using a Monte Carlo method.

Katrak, F.E., and Agarwal, J.C. (1981). Gallium: Long-Run Supply. JOM *33*, 33–36.

Kirchain, R., and Cosquer, A. (2007). Strategies for maintaining light metal reuse: Insights from modeling of firm-wide raw materials availability and demand. Resour. Conserv. Recycl. *51*, 367–396.

Linden, J.H.L. van, and Hannula, R.E. (1980). Mathematical model of the aluminum beverage can recycling system. In Light Metals: Proceedings of Technical Sessions, AIME Annual Meeting, (Chicago, IL, USA: Metallurgical Society of AIME), pp. 813–825.

Van Linden, J.H.L. (1994). Automotive aluminum recycling changes ahead. In Light Metals 1994, (San Francisco, CA), pp. 1115–1120.

Liu, G., and Müller, D.B. (2013). Mapping the Global Journey of Anthropogenic Aluminum: A Trade-Linked Multilevel Material Flow Analysis. Environ. Sci. Technol. *47*, 11873–11881.

Liu, G., Bangs, C.E., and Müller, D.B. (2012). Stock dynamics and emission pathways of the global aluminium cycle. Nat. Clim. Change *3*, 338–342.

Long, L.W., and Smith, S. (1980). Possible material supply constraints for photovoltaic solar cells. Min. Congr. J. *66*, 43–44.

Meskers, C.E.M., Reuter, M.A., Boin, U., Kvithyld, A. (2008). A fundamental metric for metal recycling applied to coated magnesium. Metallurgical and Materials Transactions B. *39B* 500-517.

Milford, R.L., Pauliuk, S., Allwood, J.M., and Müller, D.B. (2013). The Roles of Energy and Material Efficiency in Meeting Steel Industry CO2 Targets. Environ. Sci. Technol. *47*, 3455–3462.

Modaresi, R., and Müller, D.B. (2012). The role of automobiles for the future of aluminum recycling. Env. Sci Technol *46*, 8587–8594.

Modaresi, R., Pauliuk, S., Løvik, A.N., and Müller, D.B. (2014). Global Carbon Benefits of Material Substitution in Passenger Cars until 2050 and the Impact on the Steel and Aluminum Industries. Environ. Sci. Technol. *48*, 10776–10784.

Müller, D.B. (2006). Stock dynamics for forecasting material flows—Case study for housing in The Netherlands. Ecol. Econ. *59*, 142–156.

Müller, D.B., Wang, T., and Duval, B. (2011). Patterns of Iron Use in Societal Evolution. Environ. Sci. Technol. *45*, 182–188.

Müller, D.B., Liu, G., Løvik, A.N., Modaresi, R., Pauliuk, S., Steinhoff, F.S., and Brattebø, H. (2013). Carbon Emissions of Infrastructure Development. Environ. Sci. Technol. *47*, 11739–11746.

Müller, E., Hilty, L.M., Widmer, R., Schluep, M., and Faulstich, M. (2014). Modeling Metal Stocks and Flows: A Review of Dynamic Material Flow Analysis Methods. Environ. Sci. Technol. *48*, 2102–2113.

Nakajima, K., Yokoyama, K., and Nagasaka, T. (2008). Substance Flow Analysis of Manganese Associated with Iron and Steel Flow in Japan. ISIJ Int. *48*, 549–553.

Nakajima, K., Takeda, O., Miki, T., Matsubae, K., Nakamura, S., and Nagasaka, T. (2010). Thermodynamic Analysis of Contamination by Alloying Elements in Aluminum Recycling. Environ. Sci. Technol. *44*, 5594–5600.

Nakajima, K., Ohno, H., Kondo, Y., Matsubae, K., Takeda, O., Miki, T., Nakamura, S., and Nagasaka, T. (2013). Simultaneous Material Flow Analysis of Nickel, Chromium, and Molybdenum Used in Alloy Steel by Means of Input–Output Analysis. Environ. Sci. Technol. *47*, 4653–4660.

Nakamura, S., Murakami, S., Nakajima, K., and Nagasaka, T. (2008). Hybrid Input−Output Approach to Metal Production and Its Application to the Introduction of Lead-Free Solders. Environ. Sci. Technol. *42*, 3843–3848.

Nakamura, S., Kondo, Y., Matsubae, K., Nakajima, K., Tasaki, T., and Nagasaka, T. (2012). Quality- and Dilution Losses in the Recycling of Ferrous Materials from End-of-Life Passenger Cars: Input-Output Analysis under Explicit Consideration of Scrap Quality. Environ. Sci. Technol. *46*, 9266–9273.

Nansai, K., Nakajima, K., Kagawa, S., Kondo, Y., Suh, S., Shigetomi, Y., and Oshita, Y. (2014). Global Flows of Critical Metals Necessary for Low-Carbon Technologies: The Case of Neodymium, Cobalt, and Platinum. Environ. Sci. Technol. *48*, 1391–1400.

Ohno, H., Matsubae, K., Nakajima, K., Nakamura, S., and Nagasaka, T. (2014). Unintentional Flow of Alloying Elements in Steel during Recycling of End-of-Life Vehicles. J. Ind. Ecol. *18*, 242–253.

Olivetti, E.A., Gaustad, G.G., Field, F.R., and Kirchain, R.E. (2011). Increasing Secondary and Renewable Material Use: A Chance Constrained Modeling Approach To Manage Feedstock Quality Variation. Environ. Sci. Technol. *45*, 4118–4126.

Pauliuk, S., Wang, T., and Müller, D.B. (2013). Steel all over the world: Estimating in-use stocks of iron for 200 countries. Resour. Conserv. Recycl. *71*, 22–30.

Reck, B.K., Müller, D.B., Rostkowski, K., and Graedel, T.E. (2008). Anthropogenic Nickel Cycle: Insights into Use, Trade, and Recycling. Environ. Sci. Technol. *42*, 3394–3400.

Reuter, M.A., van Schaik, A., Ignatenko, O., and de Haan, G.J. (2006). Fundamental limits for the recycling of end-of-life vehicles. Miner. Eng. *19*, 433–449.

Reuter, M.A., Hudson, C., van Schaik, A., Heiskanen, K., Meskers, C., and Hagelüken, C. (2013). Metal Recycling: Opportunities, limits, infrastructure, A Report of the Working Group on the Global Metal Flows to the International Resource Panel (UNEP).

Van Schaik, A., Reuter, M.A., Boin, U.M.J., and Dalmijn, W.L. (2002). Dynamic modelling and optimisation of the resource cycle of passenger vehicles. Miner. Eng. *15*, 1001–1016.

Van Schaik, A., Reuter, M.A., and Heiskanen, K. (2004). The influence of particle size reduction and liberation on the recycling rate of end-of-life vehicles. Miner. Eng. *17*, 331–347.

Senel, E., Walmsley, J.C., Diplas, S., and Nisancioglu, K. (2014). Liquid metal embrittlement of aluminium by segregation of trace element gallium. Corros. Sci. *85*, 167–173.

Stamp, A., Wäger, P.A., and Hellweg, S. (2014). Linking energy scenarios with metal demand modeling–The case of indium in CIGS solar cells. Resour. Conserv. Recycl. *93*, 156–167.

Talens Peiró, L., Villalba Méndez, G., and Ayres, R.U. (2013). Material Flow Analysis of Scarce Metals: Sources, Functions, End-Uses and Aspects for Future Supply. Environ. Sci. Technol. *47*, 2939–2947.

Tessieri, M.B., and Ng, G.K. (1995). Forecast of aluminum usage in the automotive market and subsequent impact on the recycling infrastructure. In Proceedings of the TMS Fall Meeting, P.B. Queneau, and R.D. Peterson, eds. (Warrendale: Minerals, Metals & Materials Soc), pp. 713–727.

The Aluminum Association (2009). International alloy designations and chemical composition limits for wrought aluminum and wrought aluminum alloys (The Aluminum Association, Inc.).

The MathWorks Inc. (2010). MATLAB Version 7.11.0.584 (R2010b).

UN Department of Economic and Social Affairs Population Division (2015). World Population Prospects: The 2015 Revision, DVD Edition.

United Nations (2015). Population, consumption and the environment 2015 (New York: United Nations, Department of Economic and Social Affairs, Population Division).

United States Geological Survey (2014). Gallium. In 2012 Minerals Yearbook, B.W. Jaskula, ed. (Washington DC).

Verhoef, E.V., Dijkema, G.P.J., and Reuter, M.A. (2004). Process Knowledge, System Dynamics, and Metal Ecology. J. Ind. Ecol. *8*, 23–43.

Wang, T., Müller, D.B., and Graedel, T.E. (2007). Forging the Anthropogenic Iron Cycle. Environ. Sci. Technol. *41*, 5120–5129.

Xiao, Y., Reuter, M.A. (2002). Recycling of distributed aluminium turning scrap. Minerals Engineering *15*, 963-970.

Zapp, P., Rombach, G., and Kuchshinrichs, W. (2003). Long term supply of aluminium to the European automotive indsutry. World Metall. - Erzmetall *57*, 258–265.

Paper I

A material flow model for impurity accumulation in beverage can recycling systems

Løvik, A. N.; Müller, D. B., In *TMS Light Metals* 2014, pp. 907-911

Light Metals 2014
Edited by: John Grandfield
TMS (The Minerals, Metals & Materials Society), 2014

A Material Flow Model for Impurity Accumulation in Beverage Can Recycling Systems

Amund N. Løvik[1], Daniel B. Müller[1]

[1]Industrial Ecology Programme, Department of Energy and Process Engineering, Norwegian University of Science and Technology, Trondheim, NO-7491, Norway

Keywords: Aluminum, Recycling, UBC, Impurity, Accumulation

Abstract

Recycling of aluminum is beneficial due to reduced energy inputs, greenhouse gas emissions and raw material costs. Beverage cans are currently the second largest source of old scrap, and could become even larger with improved collection. However, impurities such as iron, titanium or lead may impede end-of-life recycling at higher levels, especially in closed-loop systems where they can accumulate over time. A generic material flow model for impurity accumulation in a simple recycling system is presented here. Sensitivity analysis was used to investigate the effect of key parameters on dynamics of accumulation and concentration at steady state. It was found that it takes longer to reach steady state at high collection rates, and that the steady state concentration is disproportionally higher. Increasing the U.S. beverage can collection rate from today's 54% to the goal of 75% may cause more than a doubling of impurity concentrations unless better scrap treatment and remelting are developed in parallel or the scrap is used in other applications.

Introduction

Primary production of aluminum is energy intensive and causes large emissions of greenhouse gases (GHG). Ingot production from secondary sources can cut the energy input by more than 90% [1], and process related GHG emissions are essentially eliminated. Considering the limited potential for energy and emission improvements in the primary production chain [2], it is clear that increased recycling is the most important measure for a more sustainable aluminum industry. Beverage cans represent one of the largest end uses, and due to the short lifetime it is the second largest source of end-of-life aluminum scrap globally [3]. However, the recycling rate is low in many countries, especially for those without a deposit scheme for collection. The collection rate is above 80% in several European countries [4], but only about 50% in the U.S. [5], the largest consumer of this product. Hence, there is a large potential for increased recycled content if better systems for scrap collection are developed.

Like any type of end-of-life scrap, used beverage cans (UBC) come with impurities such as other metals or glass from commingled collection systems, dirt, or titanium dioxide particles from the lacquer used for decoration [6, 7]. Due to the repeated recycling of the material, these impurities may accumulate over time in the system if not properly controlled in the scrap beneficiation processes. The concentration of impurities in remelted material is adjusted by diluting with primary aluminum or higher quality scrap. With a higher recycled content, the possibility for dilution is smaller, and impurities that are unproblematic today may become constraints to recycling in the future.

Previous material flow models of aluminum recycling that include quality differences have mainly focused on complex systems, such as automotive aluminum, with long lifetimes, a large number of alloys and several scrap streams [8-13]. In all of these works, optimization models were used to determine maximum scrap utilization, given the demand for various alloys, supply of scrap of different types, and the composition of these. The results are calculated numerically year by year. This is a powerful way to assess recyclability in complex systems, but because of the numerical methods the models depend on quantified parameters and have a limited capacity to explain the underlying drivers for accumulation. None of these studies include real measurements of scrap compositions, and most ignore external contaminants (e.g. free iron particles) entirely. Only one study considered the accumulation of impurities or alloying elements over time due to repeated recycling of the same material [9]. It was assumed there that the concentration of each alloying element in remelted material increases by a certain fraction, the "accumulation ratio", for each loop. This approach overestimates the accumulation effect, since it assumes that the flow of impurities into the system is proportional to the concentration of impurities already there.

An analytical model of accumulation can lead to better understanding of the mechanisms causing it and inform about possible future developments without knowing the real level of scrap contaminations. This is more easily done with a simple system such as beverage can recycling where there is only one type of scrap and the lifetime is short. We therefore developed an analytical, dynamic substance flow model for a generic impurity in a simple UBC recycling system, and performed a sensitivity analysis to investigate the effect of collection and contamination rates on steady state impurity concentration and the time it takes to reach it.

Methods

System definition

The system of interest for this work is defined as shown in Figure 1. It is a simplified representation of a closed system of aluminum beverage can production, use and recycling. No statistics exist that specify the destination of scrap, but it has been claimed that 95% of collected UBC scrap in the U.S. is used for production of new cans [14]. This is largely consistent with the Aluminum Association's estimate of recycled content in beverage cans [15], after adjusting for production scrap.

The beverage cans are manufactured from two parts, the lid and the body, which have different material compositions. The body is made from an alloy (AA3104) with around 1% manganese and 1% magnesium, while the lid is made from one or two alloys from the 5xxx-series with higher magnesium content [16]. During use and collection, the cans may pick up impurities such as steel, glass and dirt. These impurities and compounds from the lacquer may contaminate the aluminum metal upon remelting (X_{01}). Some of the material is lost due to incomplete

collection of UBCs, or because of remelting losses (X_{30}). The recycled material is used in the production of new bodies (X_{32}) [17] after a delay equal to the average time spent from production of the can material until it arrives at the remelting facility as used scrap. Primary aluminum and alloying elements are added for lid production (X_{01}) and for adjusting the composition and mass of the body (X_{02}). It is assumed that the impurity may also be an alloying element in the lid, and that it is not closely controlled in the production of the body material, i.e. it is allowed to accumulate.

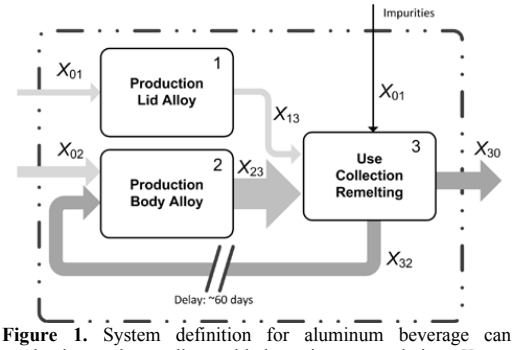

Figure 1. System definition for aluminum beverage can production and recycling, with impurity accumulation. X_{ij} are material flows. The can consists of two parts, the body and the lid, where only the body material is produced from end-of-life scrap.

Mathematical model description and parameter estimation

The goal of the model is to investigate how the collection rate and contamination rate affect the accumulation of an impurity in the body material when the overall mass flows are constant, i.e. to find the concentration in X_{23} after n recycling loops and in steady state. For simplicity, the impurity inflow, X_{01}, is defined as impurities ending up in the recycled material X_{23}; i.e. contaminations that appear in UBCs which are removed before or during remelting are not considered. Model parameters are summarized and defined in Table 1. The concentration of the impurity in flow X_{ij} is expressed as c_{ij}.

The lid's average share of the total can weight is reported from 18 to 22% [18-20]; 20% was used as a representative value. The end-of-life (EOL) recycling rate, as defined here, depends on the collection rate, the yield during scrap pre-processing (shredding), and the yield during remelting. These are respectively estimated as 54.2% (USA 2011) [5], 99% [19] and 95% [19], giving an overall EOL recycling rate (*RR*) of 51%. Note that the collection rate is here defined as the amount of cans entering recycling divided by the amount of cans sold (i.e. it takes into account import unfilled of cans), as suggested by the Container Recycling Institute.

It was recently estimated that typical titanium content from lacquer in UBCs is 0.4% of the can weight [6]. As a conservative estimate it was assumed that one quarter of this ends up as an impurity in the remelted aluminum.

Table 1. Model parameters and definitions.

Symbol	*Description*	*Definition*	*Value*
w_{lid}	Mass share of the lid	$w_{lid} = \frac{X_{13}}{X_{13} + X_{23}}$	0.20 [18-20]
RR	End-of-life recycling rate	$RR = \frac{X_{32} - X_{01}}{X_{23} + X_{13}}$	51% (USA 2011) [5, 19]
h	Rate of impurity contamination	$h = \frac{X_{01}}{X_{32} - X_{01}}$	assumed = 0.1% [6]
c_{lid}	Conc. in lid material	$c_{lid} = c_{13}$	assumed = 0
$c0_{body}$	Initial conc. in body material	$c0_{body} = c_{23}^{n=0}$	assumed = 0

Assuming that the inflow of impurities is small compared to the aluminum flows ($X_{01} << X_{32}$), the concentration in the body material after n loops can be expressed as a function of the concentration after $n-1$ loops:

$$c_{23}^{n} = \theta + RR \cdot c_{23}^{n-1} \tag{1}$$

where

$$\theta = \frac{RR}{1 - w_{lid}} \cdot (w_{lid} c_{lid} + h) \tag{2}$$

This gives:

$$c_{23}^{n=1} = \theta + RR \cdot c0_{body} \tag{3.a}$$

$$c_{23}^{n=2} = \theta \cdot (1 + RR) + RR^2 \cdot c0_{body} \tag{3.b}$$

etc. After n loops, the concentration can be expressed as:

$$\begin{aligned} c_{23}^{n} &= RR^n \cdot c0_{body} + \theta \sum_{i=1}^{n} RR^{i-1} \\ &= RR^n \cdot c0_{body} + \theta \frac{1 - RR^n}{1 - RR} \end{aligned} \tag{4}$$

The steady state concentration is found by letting $n \to \infty$:

$$c_{23}^{ss} = \theta \frac{1}{1 - RR} \tag{5}$$

Note that the results are only valid as long as the amount of recycled material is less than or equal to amount required for body production, i.e. in this case $RR \leq 0.80$. For higher recycling rates, the material will either have to be used in lid production or in other applications.

A sensitivity analysis was performed on the concentration over time by quantifying the system for different recycling rates and assuming a constant value for the contamination rate, h = 0.1%. The steady state concentration was calculated as a function of recycling rate, and a sensitivity analysis with respect to contamination rate was carried out.

Results

Steady state concentration of impurities

The steady state concentration in the body material as a function of end-of-life recycling rate is shown in Figure 2 for different values of the contamination rate. As the recycling rate grows toward 100%, the concentrations are approaching infinity, as can be seen in (5), where the denominator goes to zero. However, as long as only the body material absorbs scrap, it is not possible to go beyond 80%. For a given recycling rate, the steady state concentration is directly proportional to the contamination rate, h. The curve shape is thus independent of this parameter.

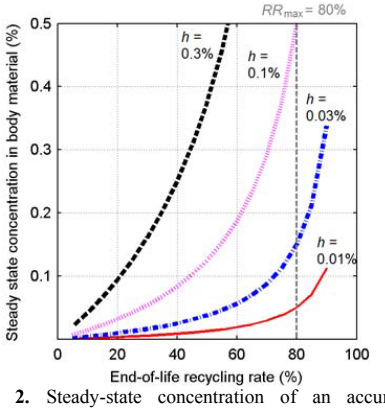

Figure 2. Steady-state concentration of an accumulating impurity in the can body, as a function of end-of-life recycling rate, shown for different values of the contamination rate, h.

Dynamics of impurity accumulation

The concentration in the body material as it develops over time is shown in Figure 3 for different values of the recycling rate. For recycling rates less than ~55%, the concentration will stabilize relatively fast: After 5 loops through use and recycling, the material has already reached its steady state composition, as can be seen by the plateau. At higher recycling rates the accumulation takes longer, and the steady state level increases disproportionally. It takes about 15 loops before steady state is reached with a 75% recycling rate.

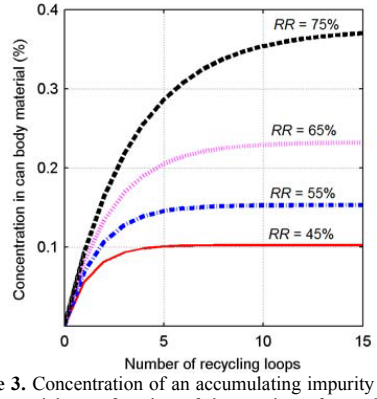

Figure 3. Concentration of an accumulating impurity in the can body material as a function of the number of recycling loops, shown for different values of the end-of-life recycling rate, RR. Accumulation lasts longer for high recycling rates, and reaches progressively higher steady-state levels.

Discussion and conclusions

Model limitations

The model presented here is a highly simplified representation of real recycling systems, and was used to demonstrate some fundamental properties of impurity accumulation. It is therefore useful to ask whether the same conclusions would hold in reality.

Production scrap was not included in the model. The effect of this simplification depends on whether the impurity enters the system in the production chain or in the use/end-of-life management stage. For example, an impurity contained in the lacquer may already be present in some of the manufacturing scrap, although most of the production scrap is generated before this stage. Similarly, iron contamination may originate from equipment used for remelting and scrap handling. In such cases, the accumulation will be intensified by the generation and recycling of new scrap. If on the other hand the impurity only enters the system in the use phase or during collection, the recycling of new scrap does not significantly influence the steady state concentration, as long as the collection and recycling of it is close to 100% and done in a closed-loop fashion (recycling into the same alloy).

It was assumed here that collected cans are recycled into new cans in the same region. In reality, UBC scrap is also used in other products, and may be exported to other regions, thereby redirecting the impurities associated with it as well. Industry associations and other institutions that publish recycling rates do not distinguish between different uses of the scrap, and this information is generally not available in statistics. It is therefore possible that the recycling rate of UBCs, as it is normally defined, increases without any effect on impurity levels in cans. Hence, the conclusions from this work apply to closed-loop systems. While this may be a good approximation for beverage can recycling in the U.S. today, most aluminum alloys are recycled in an open-loop fashion, with cast alloys for automotive applications being the main scrap absorbers [21, 22]. However,

increased scrap supply from products with long lifetimes may necessitate a higher degree of closed-loop recycling in the future [23].

In the quantification of the system all parameters were set as constant over time. The validity of this assumption may be assessed by looking at Figure 3. It can be seen that accumulation, at current U.S. recycling rates, happens over a relatively short period of time. The Aluminum Association claims that each recycling loop may take as little as 60 days [24]. Even assuming an average of twice this time, the steady state concentration is reached within less than two years, while the consumption of aluminum beverage cans in the U.S. has been stable over a period of 10 years [25]. In regions with rapidly growing consumption, additional primary material is needed to account for the growth that occurs between one recycling loop and the next, leading to a somewhat lower impurity concentration until consumption stabilizes. This is also the reason why the results here cannot be directly extrapolated to other markets such as building or transport, where lifetimes are much longer and consumption growth higher.

The example calculations included only a rough estimate of the contamination rate, h, for one element (titanium). The inflow of impurities, X_{01}, is not directly observed in reality, but may be estimated by mass balance. This would require knowledge of the average composition of can lid and body materials that are used in the given region, and measurements of the composition of remelted material. Individual producers routinely check the composition of their material, but such information is not publicly available. At the moment it is therefore difficult to draw conclusions about specific impurity elements and their current and future levels. Because scrap compositions are determined by the practices of all producers in the system, a higher level of knowledge requires a coordinated effort by the whole industry.

Conclusions

Despite the aforementioned limitations, the model can provide some fundamental insights into the accumulation of impurities in a closed-loop recycling system. Most importantly, the steady state concentration will increase more rapidly than the recycling rate. As an example, consider the goal of the Aluminum Association of reaching 75% recycling for UBCs [26]. This corresponds to a 71% end-of-life recycling rate, RR, as it is defined here. From today's level of 51%, the resulting change in steady state impurity concentration can be calculated with Equation 5, or observed in Figure 2. Such increase in recycling rate will lead to a steady state impurity concentration which is 2.35 times today's level. A single producer may be able to produce with this level of recycled content today, but if the whole industry did so, the quality of scrap would be affected by accumulation. This implies that better control of impurities in scrap handling, preprocessing and remelting must be developed in parallel with increased collection, unless significantly higher concentrations can be tolerated.

The results also indicated a time frame for reaching steady state concentrations in impurity accumulating recycling systems. At current U.S. recycling rates, this occurs within approximately 5 recycling loops. Considering the relatively slow rate of change of parameters in the system, it is likely that impurity levels are presently in steady state, i.e. not accumulating over time. Rapid changes in collection rate, contamination, or the introduction of new alloying elements in the lid may be followed by a transition period to a new steady state concentration. The time needed depends on the collection rate, but will in general be less than 15 recycling loops, or assuming that each loop takes 120 days, less than 6 years.

Acknowledgment

We thank Andres Tominaga for help with data gathering and literature survey.

References

1. International Energy Agency, *Energy technology transitions for industry*. 2009, Paris: IEA Publications.
2. J.M. Allwood, J.M. Cullen, R.L. Milford, *Options for Achieving a 50% Cut in Industrial Carbon Emissions by 2050.* Environ Sci Technol, 2010. **44**(6): p. 1888-1894.
3. International Aluminium Institute, *Global aluminium recycling: a cornerstone of sustainable development*, 2009.
4. Container Recycling Institute. *Aluminum Used Beverage Can recycling Rate: Europe, US, and Canada 2010*. [10.12.2013]; Available from: http://www.container-recycling.org/index.php/factsstatistics/aluminum/125-aluminum-data.
5. *Calculating the Aluminum Can Recycling Rate*. [10.11.2013]; Available from: http://www.container-recycling.org/index.php/calculating-aluminum-can-recycling-rate.
6. N. Li, K. Qiu, *Study on Delacquer Used Beverage Cans by Vacuum Pyrolysis for Recycle.* Environ Sci Technol, 2013.
7. W.B. Steverson, *MRFs and UBCs: a concern yet an opportunity*, in *Light Metals 1995*, J. Evans, Editor 1995, TMS-AIME.
8. R. Kirchain, A. Cosquer, *Strategies for maintaining light metal reuse: Insights from modeling of firm-wide raw materials availability and demand.* Resources, Conservation and Recycling, 2007. **51**(2): p. 367-396.
9. G. Gaustad, E. Olivetti, R. Kirchain, *Toward sustainable material usage: evaluating the importance of market motivated agency in modeling material flows.* Environ Sci Technol, 2011. **45**(9): p. 4110-7.
10. H. Hatayama, et al., *Evolution of aluminum recycling initiated by the introduction of next-generation vehicles and scrap sorting technology.* Resources, Conservation and Recycling, 2012. **66**: p. 8-14.
11. H. Hatayama, et al., *Dynamic Substance Flow Analysis of Aluminum and Its Alloying Elements.* Materials Transactions, 2007. **48**(9): p. 2518-2524.
12. A. van Schaik, et al., *Dynamic modelling and optimization of the resource cycle of passenger vehicles.* Minerals Engineering, 2002. **15**(11): p. 1001-1016.
13. A. van Schaik, M.A. Reuter, K. Heiskanen, *The influence of particle size reduction and liberation on the recycling rate of end-of-life vehicles.* Minerals Engineering, 2004. **17**(2): p. 331-347.

14. J. Green, M. Skillingberg, *Recyclable aluminum rolled products.* Light Metal Age, 2006(August).
15. The Aluminum Association, *Aluminum: The Element of Sustainability - A North American Aluminum Industry Sustainability Report.* 2011.
16. Hydro Aluminium Rolled Products Packaging and Building. *Coil for aluminium beverage cans*. [10.21.2013]; Available from: http://www.hydro.com/pagefiles/55888589/BeverageCans.pdf.
17. D.A. Doutre, *LiMCA and its Contribution to the Development of the Aluminum Beverage Container and UBC Recycling*, in *2011 Guthrie Symposium Proceedings* 2011.
18. S. Yoshida, H. Baba, *A New Used Aluminum Beverage Can Recycling System.* Proceedings of the 12th International Conference on Aluminium Alloys, 2010.
19. PE Americas, *Life Cycle Impact Assessment of Aluminum Beverage Cans.* 2010, Washington, DC, USA: Aluminum Association, Inc.
20. A. Detzel, J. Mönckert, *Environmental evaluation of aluminium cans for beverages in the German context.* The International Journal of Life Cycle Assessment, 2009. **14**(S1): p. 70-79.
21. A. Gesing, R. Wolanski, *Recycling light metals from end-of-life vehicle.* JOM, 2001. **53**(11): p. 21-23.
22. S.K. Das, J.A.S. Green, J.G. Kaufman, *The development of recycle-friendly automotive aluminum alloys.* JOM, 2007. **59**(11): p. 47-51.
23. R. Modaresi, D.B. Müller, *The role of automobiles for the future of aluminum recycling.* Environ Sci Technol, 2012. **46**(16): p. 8587-94.
24. The Aluminum Association. *U.S. Aluminum Can Recycling Reached 54.2 percent in 2008*. 2009 [10.12.2013]; Available from: http://www.aluminum.org/AM/.
25. Container Recycling Institute. *Aluminum can sales and recycling in the US*. 2006 [12.10.2013]; Available from: http://www.container-recycling.org/index.php/factsstatistics/data-archive.
26. The Aluminum Association. *Aluminum Can Extends Lead as Most Recycled Beverage Container*. 2012 [10.12.2013]; Available from: http://www.aluminum.org/AM/.

Paper II

Component- and alloy-specific modeling for evaluating aluminum recycling strategies for vehicles

Modaresi, R.; Løvik, A. N.; Müller, D. B., JOM, 2014, 66 (11): 2262-2271

Supporting information available from:

http://link.springer.com/article/10.1007/s11837-014-0900-8

JOM, Vol. 66, No. 11, 2014
DOI: 10.1007/s11837-014-0900-8

Component- and Alloy-Specific Modeling for Evaluating Aluminum Recycling Strategies for Vehicles

ROJA MODARESI,[1,2] AMUND N. LØVIK,[1,3] and DANIEL B. MÜLLER[1,4]

1.—Industrial Ecology Programme (IndEcol), Department of Energy and Process Engineering (EPT), Norwegian University of Science and Technology (NTNU), 7491 Trondheim, Norway. 2.—e-mail: roja.modaresi@ntnu.no. 3.—e-mail: amund.lovik@ntnu.no. 4.—e-mail: daniel.mueller@ntnu.no

Previous studies indicated that the availability of mixed shredded aluminum scrap from end-of-life vehicles (ELV) is likely to surpass the capacity of secondary castings to absorb this type of scrap, which could lead to a scrap surplus unless suitable interventions can be identified and implemented. However, there is a lack of studies analyzing potential solutions to this problem, among others, because of a lack of component- and alloy-specific information in the models. In this study, we developed a dynamic model of aluminum in the global vehicle stock (distinguishing 5 car segments, 14 components, and 7 alloy groups). The forecasts made up to the year 2050 for the demand for vehicle components and alloy groups, for the scrap supply from discarded vehicles, and for the effects of different ELV management options. Furthermore, we used a source-sink diagram to identify alloys that could potentially serve as alternative sinks for the growing scrap supply. Dismantling the relevant components could remove up to two-thirds of the aluminum from the ELV stream. However, the use of these components for alloy-specific recycling is currently limited because of the complex composition of components (mixed material design and applied joining techniques), as well as provisions that practically prevent the production of safety-relevant cast parts from scrap. In addition, dismantling is more difficult for components that are currently penetrating rapidly. Therefore, advanced alloy sorting seems to be a crucial step that needs to be developed over the coming years to avoid a future scrap surplus and prevent negative energy use and emission consequences.

INTRODUCTION

Aluminum is used in the form of many different alloys with variable concentrations of alloying elements, such as copper, manganese, magnesium, silicon, iron, and zinc. The high and increasing complexity of alloys presents recycling challenges, particularly because these alloying elements, with the exception of magnesium,[1] cannot be removed cost effectively through refining due to thermodynamic constraints.[2–4] Thus, the aluminum scrap that is recovered as mixed fractions (e.g., shredded products that contain various alloys and other materials) typically cannot be used to produce alloys contained in these products. Thus far, the aluminum industry has been able to recycle a wide variety of alloys primarily by increasing the alloying element levels of the material to create foundry cast alloys, which have a higher tolerance for impurities but often require either additional alloying elements or the dilution of scrap with clean primary material to attain the necessary material qualities.[1,4,5] However, there are clear indications that blending and dilution are becoming less effective as the amount of the old scrap supply is increasing faster than demand for secondary casting applications that can absorb mixed scrap, resulting in a potential surplus of low-quality scrap.[6–10]

To make use of all the aluminum scrap in the future and thus benefit from the potential energy and emission savings, it is therefore of utmost importance to identify alternative recycling strategies that are better suited to address the growing complexity of aluminum products. Of particular

 (Published online March 26, 2014)

relevance is the recycling of automotive applications because (I) they account for a broad range of different alloys, (II) they represent already today the largest market for secondary aluminum castings, and (III) they are responsible for a very strong increase in wrought aluminum demand. According to our previous study,[8] a scrap surplus can be avoided only by separating the wrought and cast aluminum fractions and using wrought scrap as raw material for rolling and extrusion alloys. The model used in that study allows for robust identification of the problem; however, its high aggregation level limits the evaluation of practical solutions because of the multitude of aluminum-containing components in automobiles and their highly complex alloys. Another group has developed a dynamic optimization model for end-of-life vehicles (ELV) recycling and demonstrated that product design by particle size reduction and liberation of material during shredding plays an important role in the composition and quality of recycling streams,[11,12] whereas others have investigated designs for recycling and optimization of refining and recycling processes,[1,2,13,14] Because automotive aluminum usage is expected to grow more rapidly in components consisting of wrought aluminum,[9,13,15–18] it is important to identify components with wrought alloys or develop new "recycling friendly" alloys for these applications that could serve as intermediate reservoirs (sink alloys); such small-scale recycling practices have already begun. For example, Nissan collects and recycles aluminum wheels to construct suspension part and has developed pilot technology for bumper-to-bumper recycling.[19]

Although all the aforementioned models provide important insights into the effectiveness of strategies both technically and economically, they cannot forecast simultaneously scrap supply and aluminum demand both on a component and alloy basis, which is necessary to test whether the separated scrap fractions could be used in new vehicles. Consequently, the models cannot identify alternative strategies by which to avoid or delay filling the bottom reservoir of secondary cast alloys, such as closing-alloy cycles or recycling toward intermediate reservoirs that may have the capacity to use different types of wrought alloy scrap. The source-sink diagram (Fig. 1) illustrates the potential for the typical automobile alloys to act as scrap sinks from several source alloys using the maximum recycled content as an indicator. As indicated by the white diagonal in the figure, all alloy scrap can be recycled to their original alloy ("closed-alloy cycle") with minimal need for the dilution or addition of alloying elements, but potential sink alloys are limited.

In this study, we developed a component-alloy model of the global vehicle stock. The component-alloy model is used to forecast the demand for sink alloys and the supply of source alloys within a vehicle system, and the source-sink alloy diagram (Fig. 1) is used to identify potential sink alloys that could serve as intermediate reservoirs. Furthermore, the model is used to assess the influence of different ELV strategies (dismantling versus alloy sorting) on scrap composition. This study is an initiation and development based on a European project for estimating aluminum alloys and components in ELVs for European Aluminium Association (EAA) and International Aluminium Institute (IAI).

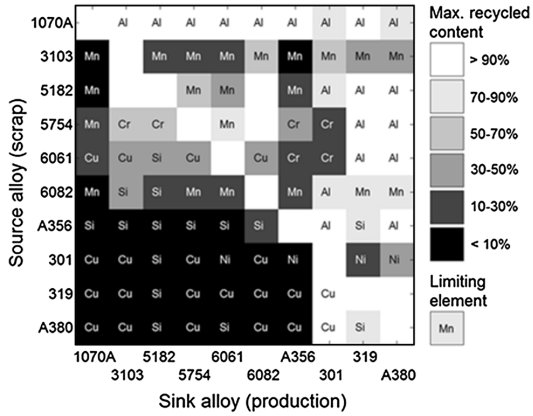

Fig. 1. Options and constraints for recycling paths of typical automotive aluminum alloys due to alloying elements. The different colors indicate the percentage of a source alloy (scrap) that could be used in the production of a sink alloy. There is a clear potential in recycling wrought alloys (4-digit names) into cast alloys, such as alloys 319 and A380, shown by the lighter shades to the right. Another potential sink alloy is alloy 6082, which could absorb a mixture of typical wrought alloys. The limiting element is shown inside each square. Magnesium is not considered because it can be removed by chlorination. Calculations are based on compositional limits from industry standards.[20,21]

We address the following questions: How is the changing use of aluminum in cars components expected to influence alloy demand and scrap composition in the next decades on a global scale? What are the most promising intermediate reservoirs (sink alloys), and which alloys are most suitable as raw material sources? In which components can these source alloys be found, and what are the prospects of obtaining these source alloys through dismantling? What changes can be made from the system perspective with respect to ELV management practices to increase recycling in the future?

METHODOLOGY

System Definition

Figure 2 illustrates the global aluminum cycle related to passenger cars. The system includes passenger car production, use, and ELV management. Passenger cars are broken down into 5 car segments (S1–S5), 14 car components (C1–C14), and 7 alloy groups (A1–A7). Cars enter the use phase and provide services to society during their lifetime. After the use phase, the cars collected for

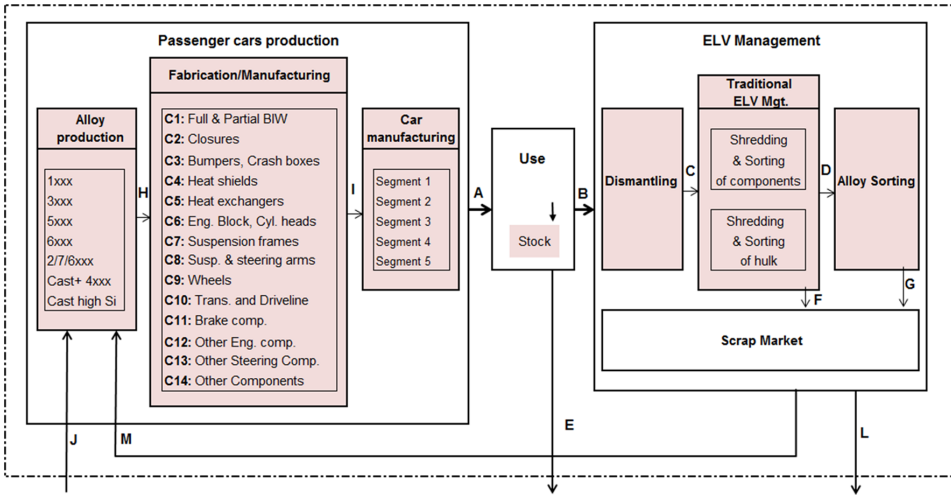

Fig. 2. System definition for the global automotive aluminum cycle.

recycling enter the ELV management process, in which some components are dismantled and kept separate from the shredding process, while the remaining components are usually shredded and sorted by air knife, magnetic sorting, sink float, or eddy current, which results in one mixed aluminum scrap fraction. Further alloy sorting may be introduced, for example, based on laser-induced breakdown spectroscopy (LIBS) or hand sorting. The overall loss of aluminum from shredding and sorting processes is shown as a flow leaving the system (L). Flow M is the ELV scrap that is recycled to produce alloys in combination with a flow J consisting of dross, turnings, new and old scrap from other applications, and primary aluminum and alloying elements.

Model Formulation

Determining the Vehicle Stock and Flow

At the core of the model is a global dynamic material flow analysis (MFA) model for the vehicle stock in use, which determines the number of cars that flow to the use phase (A) annually based on population, car ownership, and assumed vehicle lifetimes (normal distribution function). The principle of the model is described in a previous study,[6] and the Supplementary Information (SI) explains the specific aspects to this application.

Differentiating Vehicle Segments, Components, and Alloys

For a specific year t, the flow of aluminum in specific car segments and components in new vehicles ($N_{\mathrm{Al}}^{(\mathrm{S,C})}(t)$) is determined by the number of vehicles inflow in each segment ($\mathrm{N}^{(\mathrm{S})}(t)$), and the average aluminum mass of the component in that specific segment ($m_{\mathrm{Al}}^{(\mathrm{S,C})}(t)$). The aluminum flows that enter use in vehicle segment S and component C are determined by the following equation:

$$N_{\mathrm{Al}}^{(\mathrm{S,C})}(t) = N^{(\mathrm{S})}(t) * m_{\mathrm{Al}}^{(\mathrm{S,C})}(t) \quad (1)$$

For each of these 14 component groups, the content of various alloy classes (1xxx, 3xxx, 5xxx, 6xxx, 2xxx/7xxx/6xxx with Cu content $>1\%$, 4xxx + low-impurity cast alloys, and cast high-Si alloys (high-impurity cast alloys) are defined, and based on the experts' opinion, it is assumed that the alloy content is constant for the entire period of time. The outflow from the use phase, with the same resolution of alloys, groups, and segments, is calculated based on a normal lifetime distribution function.

ELV Management

For each component group (C1–14) reaching the ELV management, three ELV indexes are defined. According to the experts' view on technical and economical viability of part dismantling, these three distinctions are as follows: (I) One fraction that is dismantled under the current practice, (II) another that has potential for dismantling, (III) and the remaining share that will be shredded under all circumstances. For the dismantling strategy, we assumed that the first two fractions of each component are dismantled.

Parameter Estimation

Detailed documentation on parameter estimation, such as population (Pop), vehicle ownership (Vp), and lifetime (L), is available in the Supplementary Information section. A summary of all the parameter estimation is shown in Fig. 3.

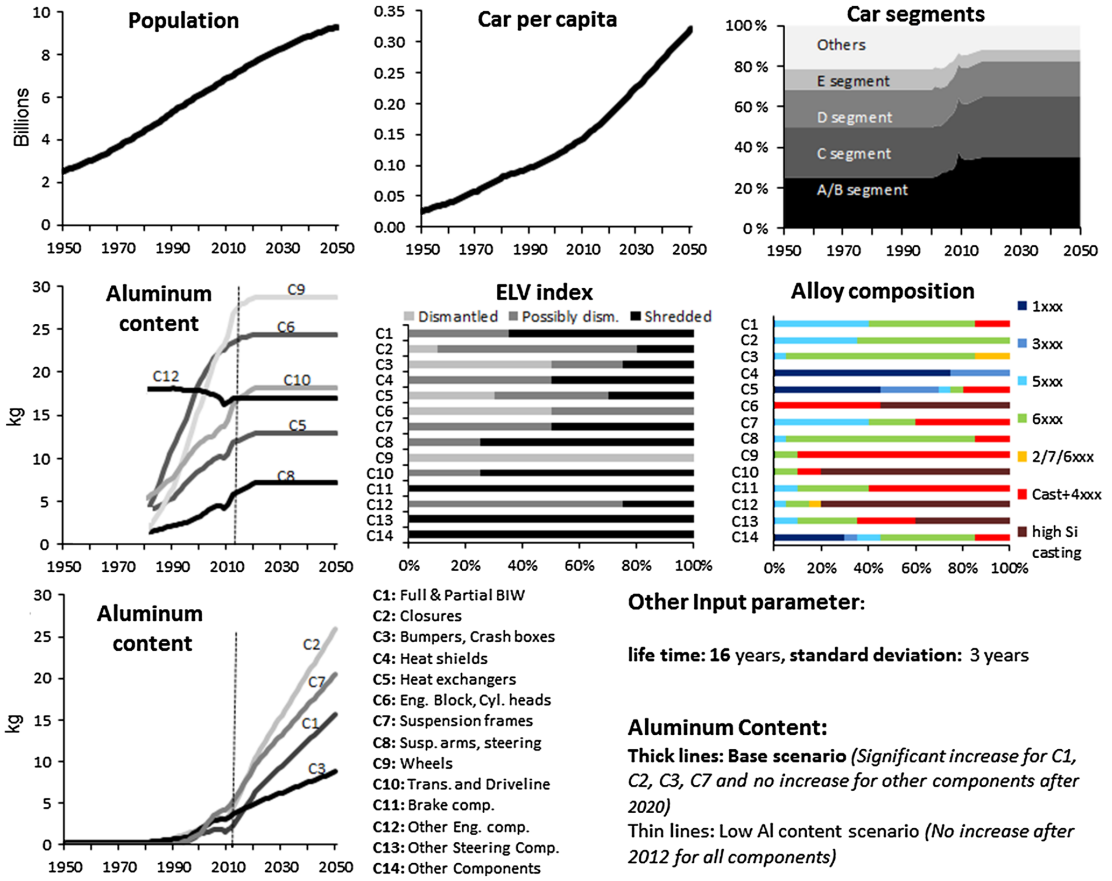

Fig. 3. Input parameters for the dynamic model.

Segments Splits ($N^{(S)}$ (t))

We learned from our previous study[6] that drive technology does not have a major effect because of a late penetration in the market. Therefore, the passenger car fleet is divided into five segments. S1 is A/B segment mini/small cars, S2 is C segment medium cars (small family cars), S3 is D segment large cars (large family cars), S4 is E segment executive cars (executive cars), and S5 includes the rest of the vehicle types (F segment luxury cars + S segment sport coupes). Market share data for different segments are available from 2000 to 2012, and a projection for 2017 on the global scale.[22] For the years prior to 2000, the segment share of the year 2000 is assumed, and the future segmentation share is assumed unchanged after 2017.

Aluminum Content for Vehicle Components ($m^{(C)}_{(Al)}(t)$)

The 14 components in this study are shown in Table I.

Data for the European aluminum content in 14 component groups and 5 segments between 1980 and 2020 are provided by the EAA and the Ducker studies.[23,24] The European aluminum amounts are used as the global assumption because European passenger car production corresponds to one-third of the global production.[15] Moreover, European cars use less aluminum than North American cars but more than Japanese and Asian cars.[16] Figure 3 shows the weighted average aluminum content in 14 components over time for the base scenario and a low-aluminum content scenario. Expert predictions and different studies have confirmed that aluminum growth will most likely be in BIW, closures, bumpers and crash boxes, and suspension frames.[16,17,23,24] The base scenario is based on experts' assumptions until 2020. After 2020, the aluminum content is assumed to remain constant except for component groups C1, C2, C3, and C7, which are assumed to increase. BIW (C1) and closures (C2) have the highest potential to grow, and it is suggested by experts to assume that the average aluminum content will be

Table I. Relevant component groups for aluminum used in passenger cars

Component	Manufactured Vehicle Part(s)
C1	Full body in white (BIW) and partial BIW
C2	Closures
C3	Bumpers and crash boxes
C4	Heat shields
C5	Heat exchangers
C6	Engine block and cylinder heads
C7	Suspension frames
C8	Suspension and steering arms
C9	Wheels
C10	Transmission and driveline
C11	Brake components
C12	All other engine components (pistons, housing for starter/dynamo, housing for water/oil, pump, oil pan, fuel injection system, cylinder head cover, support plates, *etc*.)
C13	All other steering components
C14	All other interior and exterior components

2.5 times greater in 2050 than in 2020. Subsequently, growth potential for bumpers and crash boxes (C3), and suspension frames (C7) are assumed two times greater in 2050 compared to 2020. In contrast to the base scenario, which is optimistic in aluminum use and governed by the ongoing light weighting trend, the low-aluminum scenario assumes that there will be no change in aluminum content after 2012.

Alloy Composition for Vehicle Groups

For the production of each of the 14 component groups, different alloy categories can be used (Fig. 3). It was suggested by experts to assume that the type of alloys used for a given component does not change over time because of lack of such detailed data. The following are the alloy categories: 1xxx, 3xxx, 5xxx, 6xxx, 2xxx/7xxx/6xxx with Cu $>1\%$, 4xxx + cast alloys (AlSi, AlMg) with low alloying/impurity content ($<0.5\%$ each), and cast alloys with high silicon content and higher alloying/impurity contents. Cast alloys with a low impurity content are primarily used in wheels, brake and steering components, structural body castings, and some of the engine parts and suspension frames, which in current practice are generally made from primary aluminum or wrought alloy fabrication scrap because of mandated properties and high cost for new alloy specifications and product design. Cast alloys with a high tolerance for impurities are primarily used in engine blocks and cylinder heads, transmissions and drivelines, and several steering subcomponents, and they have a high potential to accept scrap in their production.

Alloys Selection

The alloys selected from the typical alloys in automobiles for the source-sink diagram and are explained briefly in this section. More information is available in the Supplementary Information.

1070A This alloy has intermediate impurity levels between 1050 and 1100. The capacity to absorb scrap is close to zero for 1xxx series; however, they could be used as source material for any of the other alloys shown.

3103 The 3xxx-series alloys might be important from a recycling perspective because manganese, the main alloying element, is undesirable in many other alloys. Its main applications are fins and tubes in heat exchangers because of their high formability and corrosion resistance and medium strength.[18] Typical alloys are 3003 and 3103.[25]

5182 and 5754 Alloy 5754 is a typical choice when temperatures could exceed 80°C; in other cases, alloy 5182 may be used when increased strength is needed.[26–28]

6061 and 6082 Alloys 6061 and 6082 are typical selections when a higher strength is required, for example, in bumpers, suspension arms or wheels.[27–29] Alloy 6061 is more common in the United States, and alloy 6082 is more common in Europe.[5,28]

A356, 301, 319, and A380 The 3xx-series are the most widely used of all cast alloys. Silicon levels may reach up to 20%, and there is often a high concentration of other alloying elements.[20] Alloy A356 was chosen as an example of a primary cast alloy; it is widely used in wheels and other structural components, such as suspension frames or BIW.[5,28,30] Alloy A301 is used in pistons, contains approximately 1% Ni, and is included in the figure primarily to illustrate how the use of less common alloying elements can influence recycling. Alloys A319 and A380 are primarily used in cylinder heads and engine blocks[5,28] are the most important secondary alloys in terms of production volume,[31] and currently the main sinks for scrap.

ELV Index

ELV indexes are based on expert assumptions that consider economical feasibilities with currently available technology (Fig. 3).

ELV Collection Rate

In the United States, more than 95% of retired cars enter a comprehensive recycling system.[32] No definite global statistics are available regarding the number of ELVs that ends up in recycling plants, and therefore, the U.S. collection rate is used in the model.

ELV Management Efficiency

In ELV management, several losses may occur. There is aluminum loss during the shredding process to other systems, where several undesirable metals that cause contamination in the recycling system, such as Fe, Cu, Mg, and Zn, can enter the stream. In the system definition, there is a flow leaving ELV management, which represents the overall scrap loss during the ELV processes (L). In this study, the shredder yield is assumed to be 90%.[33] Scrap remelting losses are also considered in the ELV management process and are assumed to be 8%.[33] The resulting overall yield from ELV management is 83%. Flow M leaves the ELV management system to be recycled into new alloys for use in passenger cars.

RESULTS AND DISCUSSION

Figure 4 illustrates the aggregate simulation results for the alloy groups entering use in the form of vehicles (flow A) and the alloy groups recovered from ELV management in the form of scrap (flow M). Three alloy classes dominate automotive aluminum use, which is reflected in both new vehicles and scrap: cast alloys with high impurity tolerance ("cast high Si"), cast alloys with low impurity content ("4xxx + cast alloys"), and 6xxx alloys. For the base scenario, the demand for 6xxx alloys is expected to grow by a factor of three between 2010 and 2030, from 2.3 to 6.5 million metric tons (MMT), and the total demand for cast alloys is estimated to increase in the same period by a factor of two, from 5.4 to 11.5 MMT. Figure 4 also confirms many other previous studies that the total scrap supply is expected to surpass the demand for high-impurity cast alloys in the next few years. Because the cast high-Si alloys currently are the only relevant sink alloy class, this graph highlights the importance and urgency of identifying alternative sink alloys for automotive aluminum scrap that can act as intermediate reservoirs. In addition, the figure shows the need for effective strategies by which to separate alloys sufficiently to reach the required qualities of these sink alloys. Figure 5 illustrates flows of components (area of circles) and their alloy composition (colors) in new vehicles entering use (flow A) and in scrap recovered from ELV management (flow M) in 2030. Flow M is determined for component dismantling before shredding and alloy sorting to assess the effectiveness of dismantling and alloy sorting in the changing context. The overall scrap supply is expected to grow to 9.3 MMT in 2030. In addition, the share of wrought alloys in ELV scrap increases from 35% in 2010 to 43% in 2030. This mixed scrap from shredders can be used only for cast high-Si content alloy demand, which is expected to grow to 5.1 MMT in 2030, and it is significantly less than the expected ELV scrap in 2030. Therefore, without sorting or dismantling and under the assumption that no dilution is required for the production of cast, high-Si content alloys, there

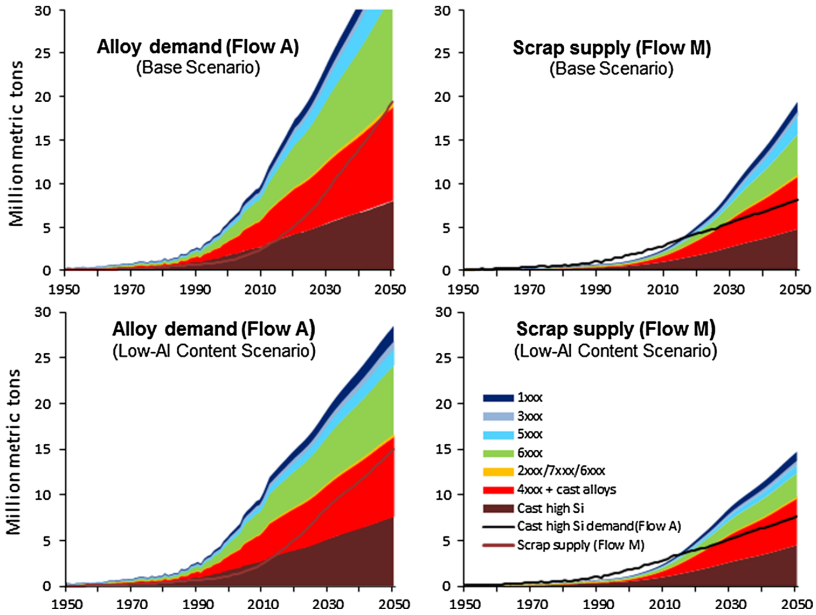

Fig. 4. Global passenger cars alloy demand and scrap supply for the base scenario and the low-Al content scenario. The graphs on the left show the alloys demand (flow A) and the total scrap supply (brown lines). The graphs on the right show the scrap supply (flow M) of different alloys and cast high-Si alloy demand (black lines).

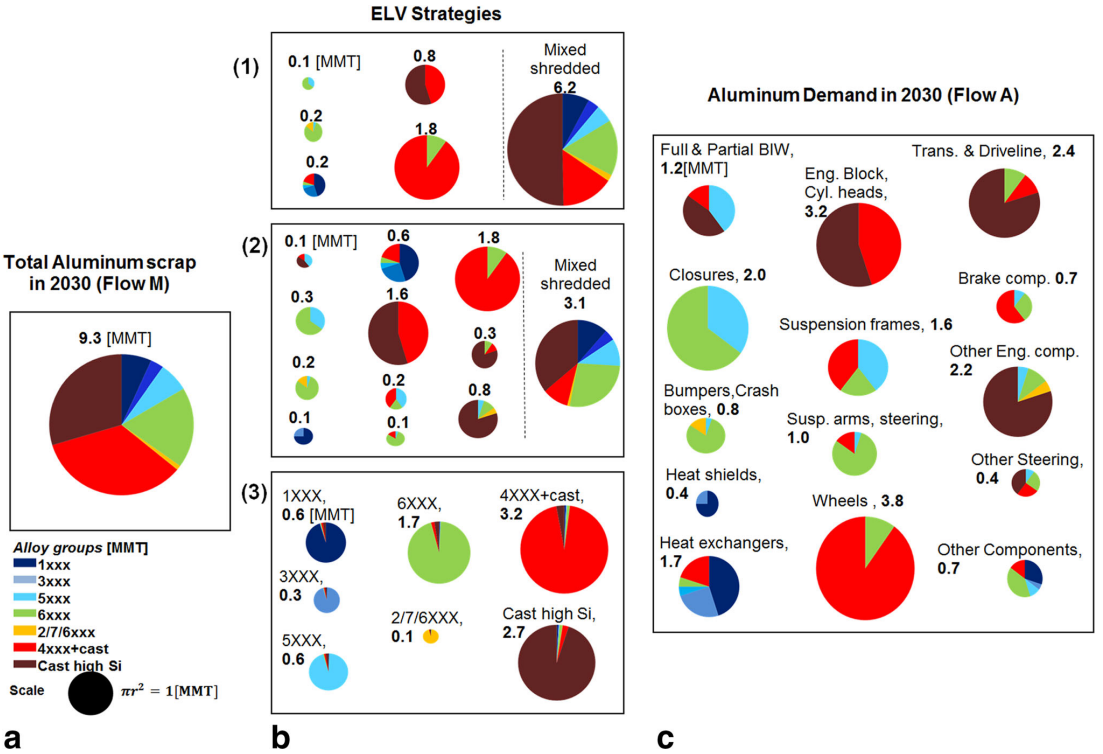

Fig. 5. The figure shows a snapshot for the year 2030: (a) total aluminum scraps (flow M); (b) ELV strategies considering (1) current dismantling strategy, (2) intensive dismantling strategy, and (3) alloy sorting; and (c) aluminum demand for car components (flow A).

will be a scrap surplus of approximately 4.2 MMT in 2030.

An ambitious dismantling strategy prior to shredding would reduce the shredded scrap bulk by approximately 67% in 2030 (from 9.3 to 3.1 MMT). Even with the high dismantling option, in the absence of component-to-component recycling, available scrap that can only be used to produce cast high-Si alloys would increase the demand and create a surplus in 2030 (including the cast high Si alloys in dismantled components). By introducing alloy sorting after shredding, there would be a greater possibility to use scrap in intermediate reservoirs, although the scrap streams would still be mixtures of different alloys within each series. The proposed alloy sorting requires high-tech facilities such as LIBS to minimize the impurities. A cost-benefit analysis is needed because the facilities are expensive.

To recover and recycle all the aluminum from ELVs within the automotive sector, an analysis of the alloy flows on a component-by-component level is required (Fig. 6). Cast alloys with a high impurity tolerance, the most attractive sink alloys, are primarily used in engine blocks and cylinder heads, other engine parts, transmissions, and drivelines. All of these components are suitable candidates for component-to-component recycling, but their future as an important sink alloy is in danger due to the downsizing of internal combustion engines and the introduction of alternative powertrains. In contrast, aluminum wheels have the largest, yet unused potential for component-to-component recycling. They are the largest component group, they are easy to dismantle, and they use homogenous alloys. Nonetheless, obsolete wheels are currently used mainly as a source of scrap for cast high-Si components. Wheel-to-wheel recycling is impeded by the fact that automobile producers' practice requires safety-relevant components to be made from primary material only. Changing the specifications for wheels to allow for component-to-component recycling would be expensive for the automobile manufacturers because it would require the development of improved casting processes, investments in new equipment, and costly technical tests, where the urgency for such a change would likely come from the aluminum recycling industry. Using wheels scrap to produce suspension arms is technically possible,[19] even though the demand for suspension arms is not high enough to absorb a large amount of wheels scrap. Bumpers and crash boxes have changed their

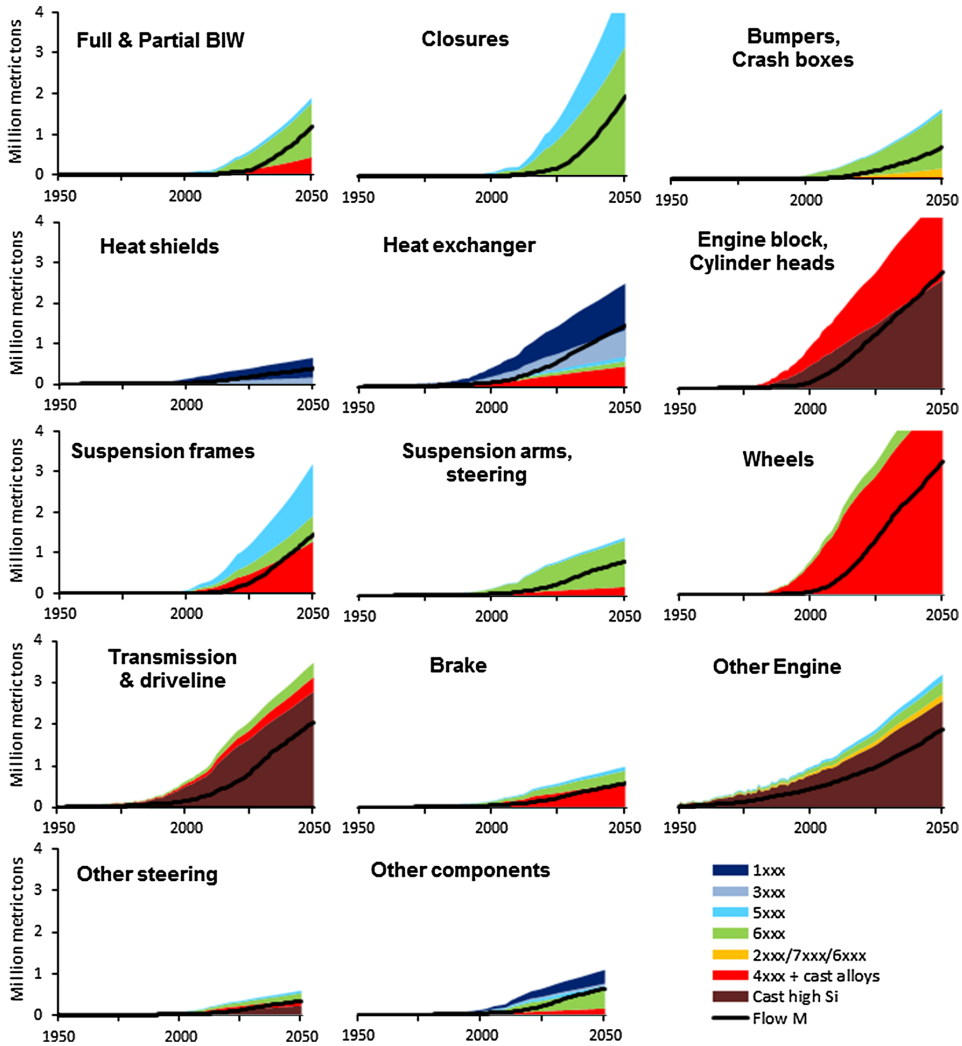

Fig. 6. Global alloy demand for 14 major car components versus the overall scrap (flow M) for the base scenario from components.

composition. Although they used to be made of zinc-containing 7xxx alloys, they consist today mainly of 6xxx alloys. Although bumper-to-bumper recycling is technically possible with some of the existing practices in recycling plants,[19] it is practically limited to bumpers made of 6xxx alloys because bumpers made from 7xxx are no longer produced and 6xxx alloys are very ineffective in absorbing 7xxx alloys because of their high zinc content. Such shifts in alloy use toward higher purity within a component group can pose severe limits to recycling. The model used here cannot treat such changes in component composition and may thus produce too optimistic results; however, these changes resulting from the component composition are deemed less important than the changes from increased penetration of aluminum components in general and should not affect the main conclusions.

CONCLUSION

Drastic changes in ELV management practices are necessary to make use of the growing potential for recycling and to avoid an unusable surplus of aluminum scrap. The main solution options recognized in this study are as follows:

1. Further dismantling and efficient component-to-component recycling may require new standards for the production of safety-related components made from scrap. Enhanced dismantling as long

as the dismantled parts are keeping separate from the mixed shredded scrap could be a very effective strategy. Wheels, closures, suspension frames, heat exchangers, bumpers, and crash boxes are recognized as the best candidates for component-to-component recycling. Wheels are a key scrap flow that needs to be redirected and can make a very large contribution to mitigating scrap surplus if recycled into an intermediate reservoir.
2. Alloy sorting of mixed shredded scrap for components that are too expensive to dismantle. Additional alloy sorting requires further advanced technology development (such as LIBS) and high penetration of such technologies in the market to avoid impurities in the scrap stream.
3. New recycling-friendly alloys are being developed for both wrought and cast applications, which are functioning as "intermediate reservoirs." Although intermediate reservoirs may not be the final solution to the alloy problem, they could be important in a transition phase by delaying the problem while more advanced separation techniques are developed.

It is important to look for alternative sink alloys. The most versatile sinks are cast alloys, such as 301, 319 and A380; however, these alloys have high alloying element content, making them the least flexible source alloys because they can only be recycled into similar alloys. Other than these cast alloys, there are few other alloys that can absorb mixed scrap. One option could be to use alloy 6082 as a sink for a mixture of wrought alloys.

ACKNOWLEDGEMENTS

This work is funded by Norsk Hydro and was developed based on the Mines on Wheels project co-funded by EAA and IAI. The authors thank all the experts from EAA and IAI, particularly Christian Leroy and Patrik Ragnarsson, who helped in database framing, Peter Furrer for the aluminum in automobile data input, and Georg Rombach from Norsk Hydro for his support from the aluminum industry perspective.

ELECTRONIC SUPPLEMENTARY MATERIAL

The online version of this article (doi:10.1007/s11837-014-0900-8) contains supplementary material, which is available to authorized users.

REFERENCES

1. A. Gesing and R. Wolanski, *JOM* 53 (11), 21 (2001).
2. G. Gaustad, E. Olivetti, and R. Kirchain, *J. Ind. Ecol.* 14, 286 (2010).
3. E.V. Verhoef, G.P.J. Dijkema, and M.A. Reuter, *J. Ind. Ecol.* 8, 23 (2004).
4. G. Rombach, *Sustainable Metals Management*, ed. A. von Gleich, R.U. Ayres, and S. Gößling-Reisemann (Amsterdam, The Netherlands: Springer, 2006), pp. 295–312.
5. European Aluminium Association, *The Aluminium Automotive Manual*, http://www.alueurope.eu/aam/.
6. R. Modaresi and D.B. Müller, *Environ. Sci. Technol.* 46, 8587 (2012).
7. G. Rombach, R. Modaresi, and D.B. Müller, *World Metall. ERZMETALL* 65, 157 (2012).
8. H. Hatayama, I. Daigo, Y. Matsuno, and Y. Adachi, *Resour. Conserv. Recycl.* 66, 8 (2012).
9. A. Gesing, *JOM* 56 (8), 18 (2004).
10. P. Zapp, G. Rombach, and W. Kuckshinrichs, European Metallurgical Conference (2003), p. 339.
11. A. van Schaik, M.A. Reuter, and K. Heiskanen, *Miner. Eng.* 17, 331 (2004).
12. A. van Schaik, M.A. Reuter, U.M.J. Boin, and W.L. Dalmijn, *Miner. Eng.* 15, 1001 (2002).
13. G. Gaustad, E. Olivetti, and R. Kirchain, *Resour. Conserv. Recycl.* 58, 79 (2012).
14. M.A. Reuter, *Waste Biomass Valoriz.* 2, 183 (2011).
15. Q.-N. Huynh, *The Automobile Industry Pocket Guide 2013* (Brussels, Belgium: ACEA, European Automobile Manufacturers Association, 2013), http://www.acea.be/uploads/publications/POCKET_GUIDE_13.pdf.
16. Ducker Worldwide, *Update on North American Light Vehicle Aluminum Content Compared to the Other Countries and Regions of the World*, http://www.drivealuminum.org/research-resources/PDF/Research/2009/2009-Ducker-Report.pdf (2008).
17. Ducker Worldwide, *Aluminum in 2012 North American Light Vehicles*, http://www.drivealuminum.org/research-resources/PDF/Research/2011/NorthAmericanReport-2011-Ducker.pdf (2011).
18. J.G. Kaufman, *Materials Selection*, ed. M. Kutz (New York: Wiley, 2007).
19. NissanMotor Application of Recycled Material, http://www.nissan-global.com/EN/ENVIRONMENT/CAR/RECYCLE/USED/RECYCLING_MATERIAL/ (2014).
20. ASTM B179-11, *Standard Specification for Aluminum Alloys in Ingot and Molten Forms for Castings from All Casting Processes* (2011).
21. The Aluminum Association, *International Alloy Designations and Chemical Composition Limits for Wrought Aluminum and Wrought Aluminum Alloys* (Washington, DC: The Aluminum Association Inc., 2009).
22. M. Robinet, IHS Automotive Consulting, USA, Global Production Segment, Private Communication (2012).
23. Ducker Worldwide, *EAA Aluminium Penetration in Cars 2012*, http://www.alueurope.eu/wp-content/uploads/2012/04/EAA-Aluminium-Penetration-in-cars_Final-Report-Public-version.pdf (2012).
24. The Aluminum Association's Aluminum Transportation Group (ATG), *Auto Aluminum Usage Hits All-Time High, Expected to Aggressively Accelerate*, http://www.digitaljournal.com/pr/412575#ixzz1YTT2NhBv (2012).
25. H. Rossel, *Light Metals*, ed. B. Welch (TMS, 1998), pp. 1217–1223.
26. I.N. Fridlyander, V.G. Sister, O.E. Grushko, V.V. Berstenev, L.M. Sheveleva, and L.A. Ivanova, *Met. Sci. Heat Treat.* 44, 365 (2002).
27. R. Koganti and J. Weishaar, *SAE Int. J. Manuf. Mater.* 1, 491–502 (2008).
28. J.C. Benedyk, *Materials, Design and Manufacturing for Lightweight Vehicles*, ed. P.K. Mallick (Cambridge, U.K.: Woodhead Publishing Ltd., 2010).
29. G. Yotsuya and R. Yamauchi, *SAE Int. J. Manuf. Mater.* 6, 124–130 (2012). doi:10.4271/2012-32-0094.
30. M.A. Tirelli, M.A. Colosio, and J.C. Santos, *SAE Technical Paper Series* 36 (2011).
31. E.L. Bray, *USGS Aluminum Minerals Yearbook 2011* (Washington, DC: U.S. Geological Survey, 2012).
32. B.J. Jody, E.J. Daniels, C.M. Duranceau, J.A. Pomykala, Jr., and J.S. Spangenberger, Argonne National Laboratory, U.S.

Department of Energy, Center for Transportation Research, http://www.es.anl.gov/Energy_systems/CRADA_Team/publications/End%20of%20life%20vehicle%20recycling%20Technology%20review.pdf (2010).

33. J. Julius and S. Mutz, *Automotive Recycling-Aluminium Recovery from End of Life Vehicles* (Brussels, Belgium: Report Prepared for European Aluminium Association (EAA), 2008).

Paper III

Long-term strategies for increased recycling of automotive aluminum and its alloying elements

Løvik, A. N.; Modaresi, R.; Müller, D. B., Environ. Sci. Technol., 2014, 48 (8): 4258-4265.

Supporting information available from:

http://pubs.acs.org/doi/suppl/10.1021/es405604g

Environmental Science & Technology

Policy Analysis

pubs.acs.org/est

Long-Term Strategies for Increased Recycling of Automotive Aluminum and Its Alloying Elements

Amund N. Løvik,* Roja Modaresi, and Daniel B. Müller*

Industrial Ecology Programme and Department of Energy and Process Engineering, Norwegian University of Science and Technology, NO-7491, Trondheim, Norway

Supporting Information

ABSTRACT: Aluminum recycling currently occurs in a cascading fashion, where some alloys, used in a limited number of applications, absorb most of the end-of-life scrap. An expected increase in scrap supply in coming decades necessitates restructuring of the aluminum cycle to open up new recycling paths for alloys and avoid a potential scrap surplus. This paper explores various interventions in end-of-life management and recycling of automotive aluminum, using a dynamic substance flow analysis model of aluminum and its alloying elements with resolution on component and alloy level (*vehicle-component-alloy-element* model). It was found that increased component dismantling before vehicle shredding can be an effective, so far underestimated, intervention in the medium term, especially if combined with development of safety-relevant components such as wheels from secondary material. In the long term, automatic alloy sorting technologies are most likely required, but could at the same time reduce the need for magnesium removal in refining. Cooperation between the primary and secondary aluminum industries, the automotive industry, and end-of-life vehicle dismantlers is therefore essential to ensure continued recycling of automotive aluminum and its alloying elements.

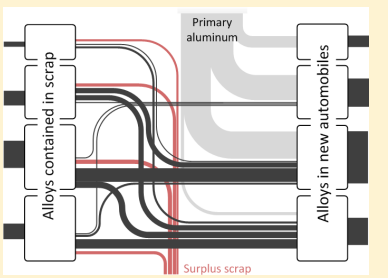

1. INTRODUCTION

Aluminum production is energy intensive and causes significant greenhouse gas emissions, recently estimated to 1.1% of world total (CO_2 eq.).[1] Material flow models have shown that scrap availability will increase, enabling industry to meet demand with a higher share of postconsumer scrap than today's ~20%.[1−3] An increased share of secondary production can significantly reduce energy use and emissions, but poses a challenge for the industry with regard to material quality because of the large diversity of aluminum alloys and the limited number of applications that can currently absorb end-of-life scrap.[4,5]

Dynamic material flow models are ideal for investigating such problems because they can be used to forecast future availability and demand of different types of scrap as well as qualitative changes within each type. Early models with a focus on scrap quality, developed for the European market, indicated that scrap supply would increase faster than the demand for traditional secondary alloys, thus pointing at a potential problem with scrap utilization.[6,7]

Hatayama and colleagues[8] applied a regional model of aluminum use and recycling to China, Europe, Japan, and the United States, making assumptions about the alloys used in the relevant sectors (*sector-alloy-element* model) to find the chemical composition of scrap flows. They connected this to an optimization procedure for blending of different raw materials that determines the maximum scrap utilization, and concluded that a regional scrap surplus in the United States and Europe may be absorbed in Japan and China through trade of scrap today, whereas in 2050 the four regions together will be a net exporter of scrap. In a follow-up study,[9] a similar model was used to show that introduction of electric and hybrid-electric vehicles can intensify the regional scrap surplus by lowering the demand for secondary cast alloys.

Gaustad and colleagues developed a dynamic material flow model with chemical element resolution and an optimization procedure,[10] and use this to demonstrate the importance of scrap segregation for a case of aluminum recycling from three sectors (beverage cans, buildings and automotive) in the United States. However, this study uses a simplified representation of aluminum use by including only selected components. For example, automobiles are represented as three parts (castings, bumpers and body sheet), with no attempt to quantify the relative share of these, and assuming a single alloy used for each of them. Although indicating a problem, the conclusions from these models[6−10] regarding scrap surplus are limited by the regional system boundaries: rapidly developing regions such as India, South-East Asia, or Latin America, could absorb the surplus scrap and thereby delay the problem. To make statements about the timing, it is necessary to use a global system boundary.

Modaresi and Müller[11] developed a dynamic model of aluminum in automobiles worldwide, distinguishing between wrought, primary cast, and secondary cast aluminum. Maximum

Received: December 16, 2013
Revised: March 20, 2014
Accepted: March 21, 2014
Published: March 21, 2014

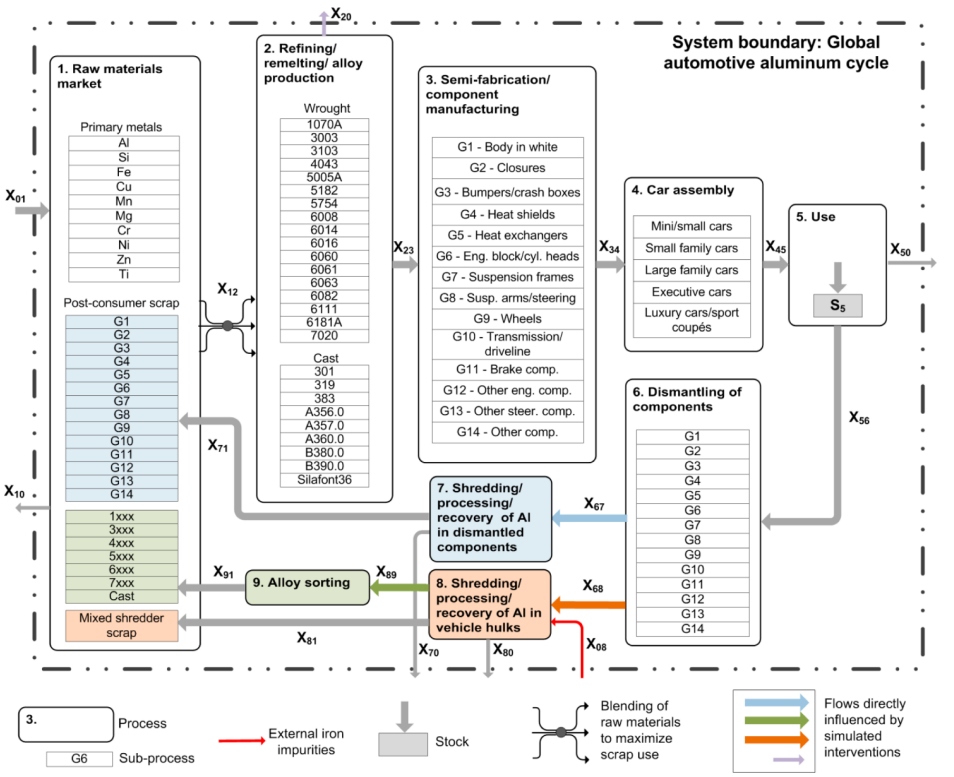

Figure 1. System definition of the global use, production and recycling of aluminum and its alloying elements in automobiles. A layered model tracks aluminum and the most common alloying elements through the use and recycling of alloys and components in vehicles. Detailed flows, for example, which alloys are used in specific components, are not shown, but included in the model.

scrap use was estimated by assuming that up to 56% of the mass of cast alloys is scrap (70% of cast alloys are secondary, and they contain up to 80% old scrap). They found that without any intervention, aluminum scrap supply from automobiles is likely to exceed demand in the same sector between 2014 and 2023, where the variation in timing is due to different assumptions for the model drivers and key parameters such as population, vehicle ownership or scrap dilution rate. This indicates a strong need to restructure recycling paths, since automotive castings function as the bottom reservoir in a recycling cascade that includes all aluminum products. However, the model lacks the component level resolution which is needed to simulate alternative strategies, as well as the chemical element resolution necessary to quantify the capacity for scrap use in other applications than the traditional secondary castings.

These previous material flow studies were mostly concerned with problem identification, which is reflected in the architecture of the models. Automotive aluminum was represented in a simplified way: as a collection of alloys,[6,8,9] as example components made of single alloys,[10] or as cast/wrought material.[7,11] In reality, aluminum is used in a very wide range of components.[12] The choice of alloy for a given application depends on material property requirements, which in the case of automotive components leads to an extreme diversity in chemical composition. Under the assumption that all automotive aluminum enters the same scrap stream through shredding of the vehicle hulk, the component level becomes irrelevant since it has no influence on the average composition of the scrap. However, dismantling of selected components before shredding enables segregation of scrap streams with different compositions, determined by the alloys used in these components. To be able to assess interventions in end-of-life vehicle management, it is therefore necessary to include a component level in the model. Moreover, some component groups have a much larger growth potential than others: By relating the alloy use to components, it is possible to create a more realistic forecast of future alloy demand and scrap quality.

These issues were recently addressed with a model for forecasting global scrap availability from vehicles in 14 different component groups and 7 alloy types (*vehicle-component-alloy* model), as well as the demand for these in new vehicles.[13] Although giving a detailed understanding of future alloy demand and scrap supply from automobiles, the model still lacks chemical element resolution and a procedure to quantify possible scrap surplus, and cannot fully assess the effect of interventions, or identify alternative recycling paths.

The chemical element resolution is needed because the possibility of utilizing scrap ultimately depends on its chemical composition, and due to thermodynamic limitations there is a lack of viable refining options for all alloying elements except magnesium.[14,15] Magnesium is often removed from molten

Table 1. Conditions Explored in Model Simulations

condition	description	implemented
low dismantling	representing current level of component dismantling (e.g., 100% of wheels, 10% of closures, 50% of bumpers and crash boxes, 0% of heat shields, 50% of engine blocks and cylinder heads, 0% of other engine components).	yes
high dismantling	representing a maximum level of dismantling with current technology (e.g., 100% of wheels, 80% of closures, 75% of bumpers and crash boxes, 50% of heat shields 100% of engine blocks and cylinder heads, 75% of other engine components).	no
alloy sorting	sorting of mixed shredded aluminum into 8 categories of alloys with 90% success rate.	no
recycled material used in safety-relevant cast parts	end-of-life scrap used in the production of safety-relevant cast parts (*body-in-white, suspension frame, suspension arms and steering, wheels, brake components, other steering components, other components*)	no
demagging used	magnesium removal during refining is used.	yes

aluminum to achieve the low levels required in the most common secondary cast alloys, typically by injecting a mixture of an inert gas and chlorine gas into the melt.[16] Because of the high value of magnesium, costs associated with the process, and chlorine emissions[17] it is desirable to reduce the extent of this practice.

In the present work we attempt to overcome the aforementioned limitations with a newly developed model that integrates: (1) a global dynamic material flow model of aluminum in automobiles; (2) component-level resolution; (3) alloy resolution; (4) chemical element resolution of alloys and scrap, combined with optimization procedure to quantify the scrap surplus and recycling paths under maximum scrap utilization. We focus on the automotive subsystem, because it has been identified as the most critical sector,[4,8,11] being both the main scrap sink in the system and largest source of it. The architecture of the model (*vehicle-component-alloy-element*) allows for a more realistic representation of interventions based on component characteristics, whereas the optimization procedure determines the quantitative impact of them and can point out new recycling paths for the industry by indicating alloys and components that could function as intermediate reservoirs in the cascade. By analyzing model simulations for different conditions and interventions in end-of-life treatment and recycling, we address the following questions: (1) What recycling paths of alloys and components are likely under current practice in ELV management and auto manufacturing? (2) Which interventions or combinations of interventions can most effectively open up new recycling paths and thus mitigate scrap surplus in the long term?

2. MATERIALS AND METHODS

We used a layered material flow analysis framework to evaluate the future recycling potential and pathways of aluminum scrap within the automotive subsystem. An implicit assumption is that other sectors of use, such as buildings or consumer durables, can absorb their own scrap in the future, but have a limited capacity to utilize scrap from automobiles. This is likely due to the large variety of alloys in the automotive sector and the presence of cast alloys with high concentrations of alloying elements, whereas for example the vast majority of extruded building products are made from a few quite similar alloys of the 6xxx series and can easily be separated from other types.[18] The first place to look for improvements is therefore within the automotive subsystem itself.

We track aluminum as components, alloys, and chemical elements through the global system of vehicle use, production and end-of-life management, as illustrated in Figure 1. The core of the stock-driven model, developed in previous works,[11,13] gives a forecast of the aluminum components entering and leaving use through historic data and future projections of world population and car ownership. By constructing a recipe for the alloys used in various components we arrive at a range of material compositions that needs to be produced by proper blending of primary aluminum and alloying elements with the scrap materials available at end-of-life. For each year, the model determines: (1) stock of vehicles in use, S_5, from population and vehicle ownership; (2) vehicles leaving use, X_{56} and X_{50}, by lifetime distribution and production in previous years; (3) demand for new vehicles in five segments, X_{45}, from a balance equation of stock change and outflow; (4) aluminum metal in new components, X_{34}, and alloys needed for these, X_{23}; (5) availability of scrap of different compositions, X_{71}, X_{81} and X_{91}, by past alloy use and ELV management criteria; (6) optimal blending of scrap and primary metals to produce the alloys needed and the exact composition of alloys in X_{12}, by a linear program. The linear program minimizes the use of primary aluminum and alloying elements, and does not consider the difference in price between scrap types or the balancing of supply and demand through price changes. The quality of scrap and the amounts available in a given year are decided by the historic aluminum use in different components, the simulated utilization (blending) of scrap in the past, and the current practice in ELV management. Along the chain there are losses due to: incomplete collection, X_{50}; shredder dust and incomplete sorting from other materials, X_{80} and X_{70}; oxidation during remelting and magnesium removal, X_{20}. In addition, there may be a loss from the system due to surplus scrap, X_{20}.

Forming and manufacturing scrap were excluded from the model, because closed loop recycling of new scrap into the same alloy or very similar alloy is something that is either done already, or could relatively easily be achieved in the future by scrap segregation at source or automatic sorting technologies.[19,20] We do not consider this one of the main limitations for the system in the future. If we assume closed loop recycling of all new scrap, this flow will have no influence on the system's capacity to absorb end-of-life scrap, and including it in the model will only introduce unnecessary calculations in the optimization procedure. A complete description of the system definition, mathematical model formulation, parameter estimation and data sources is in the Supporting Information (SI).

The timing and magnitude of a potential scrap surplus depend on many factors, including but not limited to future population growth, vehicle ownership, and the market penetration of electrical vehicles. Previous work has indicated that a scrap surplus is likely to occur within a wide range of scenarios for these parameters.[11] Therefore, we focus on interventions in the industry (end-of-life vehicle management, secondary aluminum industry, component manufacturers), which may enable increased scrap utilization in the future.

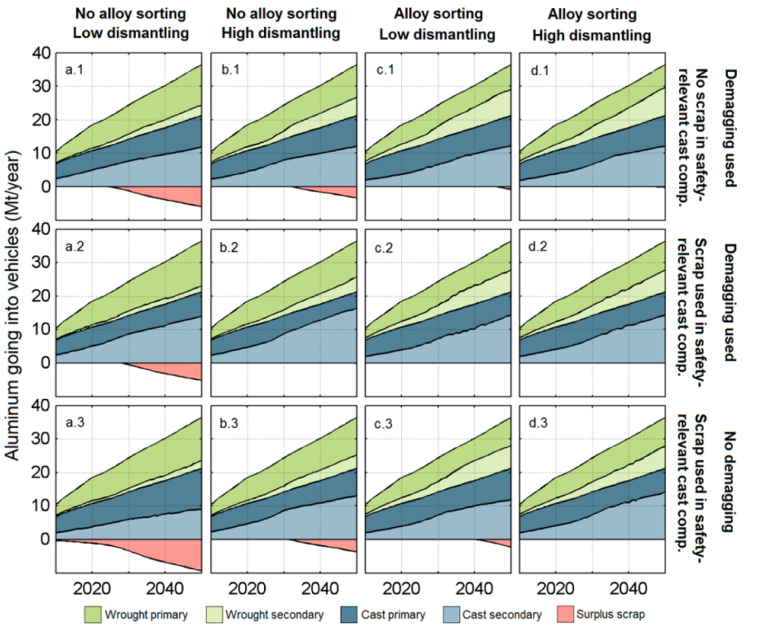

Figure 2. Simulated future production of wrought and cast aluminum for vehicles, and the relative share covered by primary and secondary sources under combinations of interventions in ELV management and scrap sorting (columns) and restrictions in aluminum/auto manufacturing industry (rows). A combination of better scrap segregation and recycling into safety-relevant cast components is necessary to avoid surplus scrap until 2050 (b.2, c.2, d.2−3). Increased dismantling combined with alloy sorting eliminated the need for magnesium removal during refining (d.2).

The model was run for different scenarios of ELV management and alloy production, assuming that the whole industry will adapt a given strategy. This can shed light on the ultimate potential of interventions, though in reality they would only be implemented gradually. The interventions include: (1) different levels of component dismantling before shredding; (2) advanced alloy sorting of mixed shredded aluminum by laser-induced breakdown spectroscopy (LIBS); (3) with and without recycled material in safety-relevant cast components; (4) with and without magnesium removal during refining. An overview of interventions can be found in Table 1, and details are in the SI.

Dismantling is already being done for some component groups, mainly for the purpose of reuse or remanufacturing of parts,[21] but can also be an effective way of segregating scrap of different qualities by taking advantage of the component-specific use of alloys. We assume that components, once dismantled, are kept apart from each other to obtain separate scrap streams. It is also assumed that dismantled aluminum parts are completely separated from particles of other metals. Assumptions regarding current and possible future levels of dismantling are based on a comprehensive evaluation by industry experts for a project with the European Aluminium Association and the International Aluminium Institute.[13,22]

LIBS sorting is a promising technology that enables high-speed automatic sorting of aluminum particles based on their chemical composition, but so far only being used on a small scale with production scrap.[19,20] We assume that alloys can be identified by the series they belong to (1xxx, 3xxx, 4xxx, 5xxx, 6xxx, 7xxx, cast low Cu, cast high Cu) with a 90% success rate, and that the failed 10% are distributed evenly between the other categories.

Safety-relevant cast components, such as wheels or space frame nodes, must have a combination of high strength and ductility to be able to withstand impacts. This requires a very low level of impurities, especially iron, which can only be achieved using primary metal.[23,24] We consider a widespread use of old scrap in such components as a separate intervention because it will require extensive testing, possibly adjustment of company-specific alloy specifications, and substantial coordination between refiners, foundries and auto manufacturers.

Finally, the possibility of reducing the practice of magnesium removal (demagging) in parallel with recycling into safety-relevant components was investigated as a separate strategy by running the model without the option of magnesium removal in the refining/remelting process.

3. RESULTS

The flows of primary- and recycled aluminum into the stocks of cast and wrought automotive components in use are shown for all simulations from 2010 to 2050 in Figure 2 together with the available scrap which could not be utilized due to material composition constraints. Simulation a.1, representing current practice, resulted in a scrap surplus from 2025 that grows to 28% of available scrap in 2050. An increased level of dismantling (b.1) delayed the surplus until 2033, and reduced the magnitude to 16% of available scrap in 2050. Alloy sorting of the mixed shredded fraction gave similar results for both levels of dismantling (c-d.1): the surplus was further delayed until 2047 (low dism.) and 2048 (high dism.). In these simulations (a-d.1), recycling into safety-relevant cast components was excluded. By lifting this constraint (a-d.2), an increased amount of scrap could be utilized and surplus was avoided for the whole time period in the simulations with

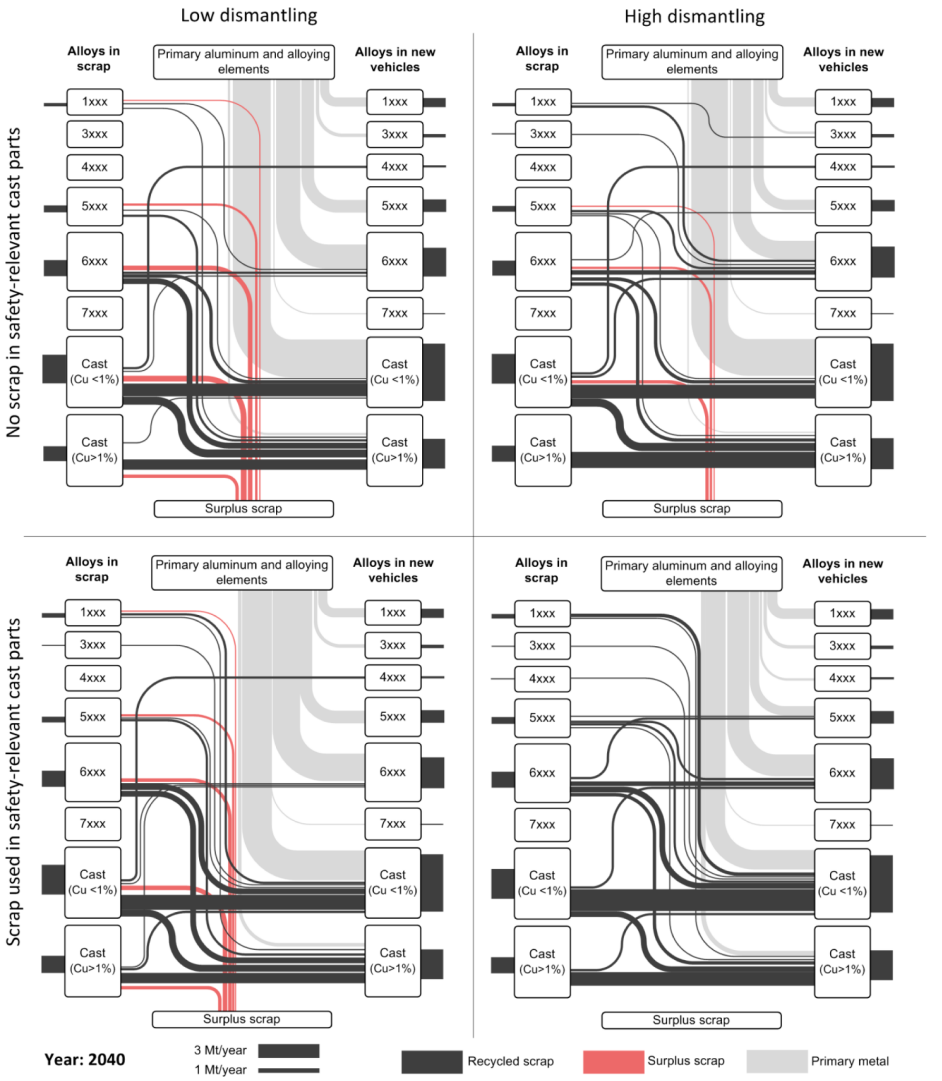

Figure 3. The automotive aluminum recycling cascade illustrates the pathways of alloys contained in scrap as they are recycled into new alloys in 2040. A "closed loop" is not achieved in most cases because of incomplete separation at end-of-life. By utilizing intermediate scrap reservoirs (low-Cu cast and 6xxx) and taking full advantage of dismantling as a scrap segregation measure, surplus may be avoided (bottom right). Flows smaller than 0.5% of the total are not shown.

increased dismantling and/or alloy sorting. The third row shows the results when magnesium removal during refining was excluded. Here, scrap surplus was avoided only by combining alloying sorting and increased dismantling (d.3).

Alloys and their compositions were tracked throughout the system. Scrap streams, such as dismantled engine blocks, wheels or the mixed shredded fraction, contain a variety of alloys. Because of this mixing, it is often not possible to recycle a scrap alloy into the same. For example, all 1xxx alloys that are contained in the mixed shredded scrap will necessarily be transformed to a lower purity alloy upon recycling. This leads to a "cascade" of recycling where some alloys absorb most of the scrap, and others act as sources of scrap only. Figure 3 visualizes this cascade in 2040 for four of the simulations by showing the pathways taken by the main alloy groups through recycling. The high-Cu cast alloys act as the bottom reservoir in the system. They absorb large amounts of scrap from all other alloys, but cannot in turn be used as a source for other alloys. As seen from the lower half of the figure, the system's performance is improved by allowing recycling into safety-relevant cast components. Scrap with the right composition is available in large amounts due to the high dismantling rate for wheels and the low variation in alloys used for that purpose. Redirecting this scrap to an intermediate reservoir frees up capacity in alloys with a high tolerance for impurities to absorb more of the mixed scrap. When combined with a high level of

dismantling (lower right of Figure 3), the 6xxx alloys and low-Cu cast alloys both act as intermediate reservoirs, thereby slowing down the cascading behavior of the system. In all simulations, the surplus occurred mainly for the mixed shredded scrap, such that the relative magnitudes of the red flows in Figure 3 always reflect the constituents of this scrap. Many of the wrought alloys (1xxx, 5xxx, 6xxx) are pulled out of the system as "passengers" in mixed shredded scrap because of limited dismantling, instead of being used to produce these alloys again. There is low utilization of scrap in wrought alloys, the only significant absorber being the 6xxx alloys.

The chemical composition of mixed shredded scrap is expected to change significantly within the coming decades as shown in Figure 4. Three major trends were observed: (1) decreasing silicon concentration, (2) decreasing copper concentration, and (3) increasing magnesium concentration. This reflects the recent and expected future penetration of wrought aluminum, which on average contain less silicon and copper, but more magnesium. Increased dismantling will amplify the trend, since it has a larger potential for cast than wrought components. The concentration of copper shows the largest change, down from almost 1% in 2010 with low dismantling to 0.2% in 2040 with high dismantling.

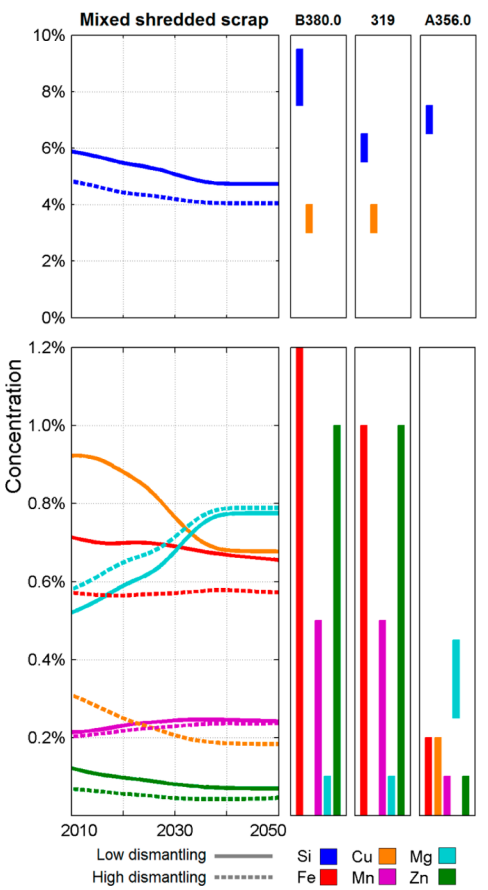

Figure 4. Simulated future chemical composition of mixed shredded automotive aluminum scrap under different degrees of component dismantling (left), and composition limits for some important cast alloys (right). The concentration of magnesium increases, while silicon and copper decreases, due to increased penetration of wrought components. The composition of mixed scrap is diverging from the specifications of traditional secondary alloys (B380.0, 319) but is still very far from typical primary cast alloys (A356.0). This trend is amplified by increased dismantling, because it mostly targets the secondary cast components.

4. DISCUSSION

Scrap surplus is a consequence of the dynamics of in-use stocks and complexity in the recycling system. Mixing of different materials prevents closed-loop recycling and leads to a recycling cascade where alloys play different roles as sources or sinks of scrap. Such systems depend on growing in-use stocks of the sinks to ensure sufficient scrap demand. Parameters in the model may be divided into two groups based on whether they influence (1) the growth rate of the in-use stocks, or (2) the complexity of the system. In group (1) are the drivers such as population, vehicle ownership and the lifetime of cars which determine the in-use stock over time and the number of vehicles entering and leaving use. Because scrap surplus is closely related to stock saturation, these factors have a large influence on the timing of the problem. However, it was found in a previous study the effect is small within a wide range of future scenarios due to the amount of aluminum already existing in use and the relatively slow rate of change for the drivers.[11] Increased growth rate of population or vehicle ownership, or longer lifetime, may delay the problem but not permanently solve it due to the eventual saturation of in-use stocks. Similarly, large-scale penetration of electrical cars may reduce the demand for secondary cast components, and thus intensify the problem and the need for better scrap segregation.[9,11] Other sectors of use were not included in the model, while in reality some scrap from these sectors is being absorbed by the secondary cast alloys for automobiles. Due to large in-use stocks, it is expected that scrap supply from these sectors, particularly buildings, also increases in the future.[25] It is therefore unlikely that the system can be reversed so that these sectors absorb scrap from automobiles. In group (2) are the number of alloys, the chemical composition limits of these, their relative use in various components, all the parameters that influence scrap segregation at end-of-life (e.g., accuracy of alloy sorting technologies), and the contamination rate for external impurities such as free iron or copper. Changes in these parameters may influence the time and magnitude of scrap surplus as well as the effectiveness of dismantling and alloy sorting. For example, a large diversity in alloys for closures will make dismantling of these a less effective option. Because complexity in the recycling system is a cause of surplus, most model simplifications can inherently lead to more optimistic results. One important limitation of the model is that although 26 different alloys were used, the specifications found in industry standards are relatively wide and there is a significant degree of overlap between them. Typically, a lower and upper limit is defined for 1−3 of the alloying elements, while for the rest, only the upper limit is given and the lower limit is zero. Nevertheless, these minor alloying elements are often added. Examples include iron for improved high-pressure die casting process, titanium or boron for grain refining, zirconium to influence recrystallization and antimony or strontium for modification of the microstructure.[26,27] Moreover, each company has its own internal alloy specifications with stricter

impurity limits. Hence, the real diversity of automotive aluminum alloys is larger than what is captured by the model. Another important simplification is that the relative use of different alloys for a given component was assumed to be constant over time. For most components this reflects reality well given the resolution of the model (e.g., cast 3xx.x wheels have always been the dominant technology for this component), but there are exceptions: bumper technology has moved from 7xxx sheet to 6xxx extrusions.[28] Such changes may inhibit recycling if the alloys become obsolete before they are recycled.

Only one external impurity, iron, was included in the model, and it was assumed that it only enters the system through shredding of the vehicle hulk. Other contaminations in the mixed shredded scrap, such as copper, zinc or nonmetallic inclusions may further inhibit recycling, but were not included due to a lack of quantitative estimates. Moreover, dismantled parts will contain impurities to varying degrees. One important future limitation to closed-loop recycling of wrought alloys may be the use of steel rivets, which are difficult to separate from aluminum sheet during recycling.[29] An increased concentration of iron leads to lower formability of the sheet material,[30] which is currently a limiting factor for aluminum use in more complex closures such as doors and liftgates. [31]

The model does not consider the relationships between scrap supply, demand and prices; in other words the simulations reflect a situation where both scrap supply and demand are price inelastic. A surplus of scrap will lead to significantly lower prices and have repercussions throughout the system of ELV management, scrap processing, recycling and component manufacturing, potentially increasing the competitiveness of secondary aluminum versus other materials. However, the short-run price elasticities of scrap supply and demand have been shown to be very low, which confirms the validity of the model.[32]

Most of the model limitations lead to an underestimate of alloying element and impurity concentrations in scrap, or idealize scrap blending possibilities; hence the conclusions drawn here regarding interventions must be regarded as best-case results. Nevertheless, it is possible to point out some directions in which the system must develop to facilitate aluminum recycling in the future.

In simulation a.1, representing current European ELV management, scrap surplus occurred from 2025, which is 7 years later than in the base scenario of our previous model.[11] Maximum recycled content was previously fixed as 56% and 0% for cast and wrought alloys respectively. In the current model, where maximum recycled content is determined by the chemical composition of scrap and alloys, maximum recycled content was found to be 51% and 13% for cast and wrought respectively in 2025 (Figure 2, a.1), increasing to 55% and 19% in 2040. The increased recycled content in wrought alloys and an updated population scenario are the main reasons for delayed scrap surplus compared to the previous model. This result shows that current dismantling practice can already alleviate some of the pressure on the traditional scrap absorbers by liberating components which can be recycled into wrought alloys. In the long term however, additional measures are needed to ensure full utilization of scrap.

An increased level of dismantling delayed the scrap surplus until 2033 (Figure 2, b.1). As can be seen in the upper part of Figure 3, a higher level of dismantling enables significant recycling into the 6xxx alloys (41% recycled content). However, because of the restriction of not using scrap in safety-relevant cast components such as wheels, this measure has little effect on the recycled content in cast alloys, which is already close to 100% for the high-Cu alloys. Alloy sorting delayed the surplus until 2047 and 2048 with low and high level of dismantling respectively, by enabling a recycled content of about 50% in 5xxx and 64% in 6xxx alloys. The results indicate that advanced alloy sorting of mixed shredded scrap is more effective than intensified dismantling. However, such sorting technologies − although promising − have yet to be proven effective for sorting of dirty end-of-life scrap.[20]

The use of recycled material in safety-relevant cast parts had a large impact on the results, and is a key development that needs to take place to avoid scrap surplus in the long term. However, it is only effective when combined with better scrap segregation to reach sufficient quality. Again, impurities not included in the model, for example, attached to dismantled parts, may cause problems in practice. For example, iron levels below 0.2% are usually required to achieve sufficient ductility in cast wheels or nodes used in space frames.[24] Current recycling of used wheels into steering system parts by Nissan is a first step toward development of intermediate scrap reservoirs.[33]

The results showed that the removal of magnesium during refining is a necessary element of the current recycling system (Figure 2, a.3), without which there would already be a surplus of scrap today. Due to the increased penetration of wrought alloys, the concentration of magnesium in mixed scrap is expected to increase to about one and a half times its current level (Figure 4). Hence, it is likely that efforts to reduce chlorine emissions from demagging must be intensified in the future. Because of such emissions and the value of magnesium as an alloying element, it is desirable to keep this element in the cycle. With the most ambitious strategy for scrap segregation, scrap with magnesium can be redirected to applications where it has a value, and removal is no longer needed for full scrap utilization (Figure 2, d.3).

The results confirm that the automotive aluminum sector may go from being a net scrap consumer to a net scrap producer in the coming decade. Based on model simulations, we suggest a tentative list of priorities to enable increased recycling within the sector in the coming decades: (1) increased dismantling of components before shredding, in conjunction with a strategy to develop high-volume applications of 6xxx alloys with a high recycled content; (2) closed-loop recycling of safety-relevant cast parts (mainly wheels); (3) development of technologies for automated sorting of shredded scrap. While the need for such interventions comes from the aluminum industry, the realization of them depends on agents elsewhere in the system.

In the current situation, with a low price difference between primary and secondary material, there is limited economic motivation for investments in scrap segregation technologies or for a wider use of postconsumer scrap. A higher availability of scrap will lead to lower prices and incentivize such new developments. However, in the case of dismantlers, it is unlikely that prices of scrap will have a large influence on how they operate; a study from France showed that about 95% of their revenue comes from selling dismantled components for reuse or remanufacture, and only about 4% comes from selling the vehicle hulk which contains the majority of the aluminum.[34] Sorting technologies such as LIBS are not yet efficient for end-of-life scrap.[20] A larger price difference between scrap types will motivate companies to develop the technology, but only after

the surplus has occurred. Increased scrap use in safety-relevant components may require relaxing the composition limits of alloys. Recent research has shown that the same material properties can be achieved with a higher level of trace elements by modifying the production route.[35] Currently, agreements between refiners and their customers are based on compositional specifications rather than material properties. New developments can only happen through cooperation to define new alloy standards, which will demand extensive material testing. Early recognition of these challenges and collaboration between the different players to explore new technical solutions are essential to ensure that aluminum and its alloying elements are effectively recycled in the future, with associated energy use and emissions reductions.

■ ASSOCIATED CONTENT

Supporting Information

Detailed description of system definition, mathematical model formulation, parameter estimation and data sources. This material is available free of charge via the Internet at http://pubs.acs.org.

■ AUTHOR INFORMATION

Corresponding Authors

*(A.N.L.) Phone: +47-416-97086; e-mail: amund.lovik@ntnu.no.

*(D.B.M) Phone: +47-735-94754; e-mail: daniel.mueller@ntnu.no.

Author Contributions

The manuscript was written through contributions of all authors. All authors have given approval to the final version of the manuscript.

Notes

The authors declare no competing financial interest.

■ ACKNOWLEDGMENTS

We thank Peter Furrer for valuable discussions about aluminum use in automobiles, and Georg Rombach for useful comments on the manuscript.

■ ABBREVIATIONS

ELV end-of-life vehicle

■ REFERENCES

(1) Liu, G.; Bangs, C. E.; Müller, D. B. Stock dynamics and emission pathways of the global aluminium cycle. *Nat. Clim. Change* **2013**, *3*, 338−342.

(2) International Aluminium Institute. *Global Aluminium Recycling Committee, Global Aluminium Recycling Model (GARC)*. 2011.

(3) Martchek, K. Modelling more sustainable aluminium. *Int. J. Life Cycle Assess.* **2005**, *11* (1), 34−37.

(4) Gesing, A.; Wolanski, R. Recycling light metals from end-of-life vehicles. *JOM* **2001**, *53* (11), 21−23.

(5) Das, S. K.; Green, J. A. S.; Kaufman, J. G. The development of recycle-friendly automotive aluminum alloys. *JOM* **2007**, *59* (11), 47−51.

(6) Rombach, G., Future availability of aluminium scrap. In *Light Metals, Proceedings of the 131st TMS Annual Meeting*; Schneider, W. A., Ed. Seattle, WA, 2002; pp 1011−1018.

(7) Zapp, P.; Rombach, G.; Kuchshinrichs, W., Long term supply of aluminium to the European automotive indsutry. In *Proceedings of European Metallurgical Conference EMC 2003*; Waschki, U., Ed.; Hannover, Germany, 2003.

(8) Hatayama, H.; Daigo, I.; Matsuno, Y.; Adachi, Y. Assessment of the recycling potential of aluminum in Japan, the United States, Europe and China. *Mater. Trans.* **2009**, *50* (3), 650−656.

(9) Hatayama, H.; Daigo, I.; Matsuno, Y.; Adachi, Y. Evolution of aluminum recycling initiated by the introduction of next-generation vehicles and scrap sorting technology. *Resour., Conserv. Recycl.* **2012**, *66*, 8−14.

(10) Gaustad, G.; Olivetti, E.; Kirchain, R. Toward sustainable material usage: Evaluating the importance of market motivated agency in modeling material flows. *Environ. Sci. Technol.* **2011**, *45* (9), 4110−7.

(11) Modaresi, R.; Müller, D. B. The role of automobiles for the future of aluminum recycling. *Environ. Sci. Technol.* **2012**, *46* (16), 8587−94.

(12) Miller, W. S.; Zhuang, L.; Bottema, J.; Witterbrood, A. J.; De Smeet, P.; Hazler, A.; Vieregge, A. Recent development in aluminium alloys for the automotive industry. *Mater. Sci. Eng.* **2000**, *A280*, 37−49.

(13) Modaresi, R.; Løvik, A. N.; Müller, D. B. Component- and alloy-specific modeling for evaluating aluminum recycling strategies for vehicles. *JOM* **2014**, DOI: 10.1007/s11837-014-0900-8.

(14) Gaustad, G.; Olivetti, E.; Kirchain, R. Improving aluminum recycling: A survey of sorting and impurity removal technologies. *Resour., Conserv. Recycl.* **2012**, *58*, 79−87.

(15) Nakajima, K.; Takeda, O.; Miki, T.; Matsubae, K.; Nakamura, S.; Nagasaka, T. Thermodynamic analysis of contamination by alloying elements in aluminum recycling. *Environ. Sci. Technol.* **2010**, *44* (14), 5594−5600.

(16) Velasco, E.; Nino, J. Recycling of aluminium scrap for secondary Al-Si alloys. *Waste Manage. Res.* **2011**, *29* (7), 686−93.

(17) Leroy, C. Provision of LCI data in the European aluminium industry Methods and examples. *Int. J. Life Cycle Assess.* **2009**, *14* (S1), 10−44.

(18) Das, S.; Green, J., The recycling of aluminum from building and construction applications. In *Light Metals, Proceedings of the 137th TMS Annual Meeting & Exhibition*, DeYoung, D. H., Ed.; New Orleans, LA, 2008; pp 1113−1118.

(19) Gesing, A.; Harbeck, H., Particle sorting of light-metal alloys and expanded use of manufacturing scrap in automotive, marine and aerospace markets. In *Proceedings of REWAS 2008, Global Symposium on Recycling, Waste Treatment and Clean Technology*, Mishra, B.; Ludwig, C.; Das, S., Eds.; Cancun, Mexico, 2008.

(20) Werheit, P.; Fricke-Begemann, C.; Gesing, M.; Noll, R. Fast single piece identification with a 3D scanning LIBS for aluminium cast and wrought alloys recycling. *J. Anal. At. Spectrom.* **2011**, *26* (11), 2166−2174.

(21) Jody, B. J.; Daniels, E. J.; Duranceau, C. M.; Pomykala Jr., J. A.; Spangenberger, J. S., *End-of-life Vehicle Recycling: State of the Art of Resource Recovery from Shredder Residue*; U.S. Department of Energy, Center for Transportation Research, Energy Systems Division, Argonne National Laboratory, **2010**.

(22) European Aluminium Association; International Aluminium Institute. *Mines on Wheels Project*, 2012.

(23) Furrer, P.; Jones, R.; Ruckstuhl, B. Aluminium Structural Modules. *SAE Technical paper series* **2003**, *2003−01−2771*, 319−324.

(24) Altenpohl, D., *Aluminum: Technology, Applications, and Environment: a Profile of a Modern Metal*, 6th ed.; Aluminum Association: Washington, DC, 1998.

(25) Liu, G.; Muller, D. B. Centennial evolution of aluminum in-use stocks on our aluminized planet. *Environ. Sci. Technol.* **2013**, *47* (9), 4882−8.

(26) Aleris International Inc. Aluminium Casting Alloys. http://www.aleris.com/what-we-offer/literature-exhibitions/product-information (accessed December 16, 2013)

(27) Carlberg, T.; Jaradeh, M.; Kamgou Kamga, H. Solidification studies of automotive heat exchanger materials. *JOM* **2006**, *58* (11), 56−61.

(28) European Aluminium Association. The aluminium automotive manual. http://www.alueurope.eu/aam/ (accessed December 16, 2013).

(29) Briskham, P.; Blundell, N.; Han, L.; Hewitt, R.; Young, K.; Boomer, D., Comparison of self-pierce riveting, resistance spot welding and spot friction joining for aluminium automotive sheet. *SAE Tech. Pap. Ser.* **2006**, *2006−01−0774*.
(30) Das, S. K.; Yin, W.; Wen, X.; Liu, Y.; Ningileri, S. Formability evaluation of recycle-friendly automotive aluminum alloys. *SAE Int. J. Mater. Manuf.* **2008**, *1* (1), 503−510.
(31) Verbrugge, M. W.; Krajewski, P. E.; Sachdev, A. K., Challenges and opportunities relative to increased usage of aluminum within the automotive industry. In *Light Metals, Proceedings of the technical sessions presented by the TMS Aluminium Committee at the TMS 2010 Annual Meeting & Exhibition*, Johnson, J. A., Ed.; TMS (The Minerals, Metals & Materials Society: Seattle, WA, 2010.
(32) Blomberg, J.; Hellmer, S. Short-run demand and supply elasticities in the West European market for secondary aluminium. *Resour. Policy* **2000**, *26* (1), 39−50.
(33) Nissan Motor Company Recycling of Aluminum Wheels; http://www.nissan-global.com/EN/ENVIRONMENT/CAR/RECYCLE/USED/RECYCLING_MATERIAL/ (accessed November 12, 2013)
(34) Agence de l'Environnement et de la Maîtrise de l'Energie, *Economic study on the management of end-of-life vehicles*. 2003. http://www2.ademe.fr/servlet/KBaseShow?sort=-1&cid=96&m=3&catid=17618&p1=00&p2=00 (accessed March 18, 2014)
(35) Fragner, W.; Baumgartner, K.; Suppan, H.; Hummel, M.; Bösch, D.; Höppel, H.-W.; Uggowitzer, P. J., Using scrap in recycling alloys for structural applications in the automotive industry. In *Light Metals 2014*; Grandfield, J., Ed.; TMS (The Minerals, Metals & Materials Society: San Diego, CA, 2014.

Paper IV

The global anthropogenic gallium system: determinants of demand, supply and efficiency improvements

Løvik, A. N.; Restrepo, E.; Müller, D. B., Environ. Sci. Technol., 2015, 49(9):5704-5712.

Supporting information available from:

http://pubs.acs.org/doi/suppl/10.1021/acs.est.5b00320

Environmental Science & Technology

Article

pubs.acs.org/est

The Global Anthropogenic Gallium System: Determinants of Demand, Supply and Efficiency Improvements

Amund N. Løvik,*[,†] Eliette Restrepo,[†,‡] and Daniel B. Müller[†]

[†]Industrial Ecology Programme and Department of Energy and Process Engineering, Norwegian University of Science and Technology (NTNU), NO-7491, Trondheim, Norway

[‡]Empa, Swiss Federal Laboratories for Materials Science and Technology, CH-9014, St. Gallen, Switzerland

Supporting Information

ABSTRACT: Gallium has been labeled as a critical metal due to rapidly growing consumption, importance for low-carbon technologies such as solid state lighting and photovoltaics, and being produced only as a byproduct of other metals (mainly aluminum). The global system of primary production, manufacturing, use and recycling has not yet been described or quantified in the literature. This prevents predictions of future demand, supply and possibilities for efficiency improvements on a system level. We present a description of the global anthropogenic gallium system and quantify the system using a combination of statistical data and technical parameters. We estimated that gallium was produced from 8 to 21% of alumina plants in 2011. The most important applications of gallium are NdFeB permanent magnets, integrated circuits and GaAs/GaP-based light-emitting diodes, demanding 22−37%, 16−27%, and 11−21% of primary metal production, respectively. GaN-based light-emitting diodes and photovoltaics are less important, both with 2−6%. We estimated that 120−170 tons, corresponding to 40−60% of primary production, ended up in production wastes that were either disposed of or stored. While demand for gallium is expected to rise in the future, our results indicated that it is possible to increase primary production substantially with conventional technology, as well as improve the system-wide material efficiency.

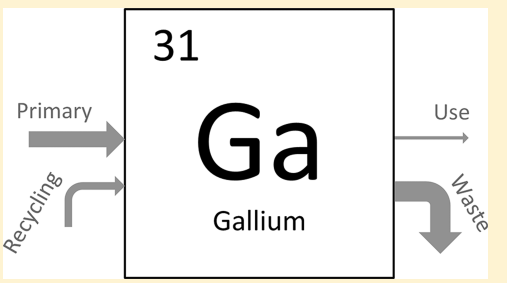

1. INTRODUCTION

Technological development relies heavily on novel use of materials, and is often enabled by geochemically scarce elements. This is especially so for low-carbon technologies such as wind power and photovoltaics (PV). Moreover, the same elements are used in other fast growing applications such as consumer electronics. The production of scarce elements is usually geographically concentrated and linked to other scarce elements or base metals through coproduction.[1] This combination of rapidly growing use and potential restrictions in the production chain has led to concerns about whether the future supply of scarce elements will be sufficient to meet demand from emerging technologies. Recent reports commissioned by the United States department of Energy and the European Union have attempted to evaluate the criticality of metals or mineral resources by looking at economic importance and potential supply risk.[1,2] However, due to the wide scope of the reports and limited data there are many open questions remaining about individual metals. A more in-depth understanding is provided by the description and quantification of stocks and flows throughout the global system of production, manufacturing, use and recycling, known as an element's "cycle". While the global cycles of key industrial metals such as iron, copper, and aluminum are well described, only a few such studies have been performed for scarce elements.[3] Recent additions to this body of literature includes works on the indium, platinum, tellurium, and rare earth element cycles.[4−8]

Gallium has been labeled as critical because of rapidly growing use, importance for low carbon technologies and being produced only as a coproduct of other metals, mainly aluminum.[1] Primary production of gallium is now around four times higher than it was before 2010.[9,10] This rapid growth has been attributed to higher content of gallium arsenide (GaAs) in mobile phones, especially smartphones, increasing use of light-emitting diodes and penetration of thin-film PV based on copper indium gallium diselenide (CIGS).[11,12] However, the relative importance of these different applications for primary gallium demand is not known. Furthermore, there is a lack of knowledge about waste flows along the production chain and the products from which the metal could be recovered at end of life. Previous studies on the criticality of gallium have mostly not used a systems approach,[2,12−14] and included only selected applications.[2,13,14] All of these include forecasts for future supply and demand, but are severely limited by lack of knowledge about the current system. The two studies

Received: January 19, 2015
Revised: April 17, 2015
Accepted: April 17, 2015
Published: April 17, 2015

DOI: 10.1021/acs.est.5b00320
Environ. Sci. Technol. 2015, 49, 5704−5712

that used a systems approach to investigate the present situation suffer from a lack of quantitative information and details on applications and processes.[15,16]

Here, we present the first substance flow analysis of gallium on a global level. We first characterize the system by describing each process, then quantify the flows through production, refining, manufacturing, use, and recycling, and determine the relative importance of major applications for primary gallium demand. The quantification relies on a combination of statistical data and technical parameters such as materials yield in the manufacturing processes. With this approach, we accomplish two goals: quantification of a system with few statistical data available, and identification of the technical parameters that govern raw material demand and supply and the magnitude of waste flows. The results contribute to a better understanding of how emerging technologies might influence demand for gallium, indicate the potential for increasing primary production, and reveal options for improvement of system-wide material efficiency.

2. MATERIALS AND METHODS

2.1. System Description. *Geological Resources.* Gallium occurs mainly as a trace element in earth's crust, with an estimated average mass fraction of about 17 ppm.[17] The world average gallium mass fraction in bauxite, the main resource for gallium extraction, has been estimated to 57 ppm, with regional averages mostly between 28 ppm (Western Guanxi, China) and 75 ppm (Caribbean).[18]

Primary Production. Gallium metal is produced as a byproduct, mainly from the Bayer process for alumina production and to a lesser degree from the hydrometallurgical route for zinc production.[19] In the Bayer process, gallium accumulates in the alkaline solution used to dissolve bauxite.[20] Part of the gallium may be extracted, while the rest ends up in the waste (red mud) or as an impurity in aluminum.

Secondary Production. Recycling of gallium from industrial scrap is commonly done, while no end-of-life recycling is known to occur.[21] The most important type of industrial scrap is GaAs in various forms: bulk crystal pieces, test wafers, broken wafers, and slurries from grinding and cutting.[22,23] Bulk GaAs and clean wafers may be recycled internally at the crystal growth facilities by direct remelting. Such recycling is defined as part of the wafer production process here (reflected in a higher process yield). Recycled gallium metal may be further refined to obtain the same grades as from primary metal.

Refining. Refining of the metal to a purity of 99.9999% (6N) or higher for electronic applications is achieved by a combination of methods.[24] Purification from 4N to 7N by fractional crystallization could have a material yield in the range 70−80%.[25] However, the discarded material is reintroduced at an earlier stage in the process chain for an overall yield close to 100%.[26] This recovery is here defined as part of the refining process.

Production of Intermediate Compounds and Substrates. The most common gallium-containing compounds are GaAs, gallium nitride (GaN), gallium phosphide (GaP), copper indium gallium diselenide (CIGS), and related alloys with indium or aluminum. These are either grown as single crystals and cut into wafers or produced directly from precursor gases or other sources during the device fabrication process. The wafer production process generates a large amount of waste due to cutting and polishing, part of which is recycled.[22,27]

Fabrication. Semiconductor devices such as integrated circuits (ICs) and light emitting diodes (LEDs) consist of a few microns thick deposition layer on top of the much thicker substrate. Integrated circuits and GaAs/GaP-based LEDs are mainly produced on GaAs substrates.[28] GaN-based LEDs are produced on substrates of sapphire (Al_2O_3) or silicon carbide (SiC),[29] and therefore require very little gallium per device. Material yields in deposition for LEDs and ICs are normally less than 20% and can be as low as 1%,[30] while the yield in thin film PV production is higher, typically 30−60% assuming sputtering deposition.[31]

The substrates for ICs and LEDs are much thicker than what is required for the operation of the device, 450−675 μm,[32] and is therefore thinned to a thickness of 50−100 μm in a "backgrinding" process.[33] Cutting, wafer breakage, and non-working devices further contribute to a total material loss that may reach above 90% including substrate material.[33−35]

In the production of NdFeB magnets, Ga is often added at approximately 0.5 wt % to improve magnetic properties, corrosion resistance, and the production process.[11,36,37] Material losses in fabrication are typically 20−40% of the starting material.[38,39] Although it is common to recycle neodymium from the production scrap, gallium is not recovered in this process.[39]

End-Use. GaN-based LEDs (violet, blue, green, white) are mainly used in general lighting, automotive and as backlighting for liquid crystal displays.[40] GaAs/GaP-based LEDs (red, orange, yellow) are used in automotive dashboards and exterior lights, traffic lights, full-color displays and many other signage and display applications.[41] GaAs ICs are mainly used in mobile phones and other wireless communication devices and infrastructure. More than 50% of the demand in 2011 has been attributed to mobile phones.[42] The most important applications of NdFeB magnets are computers, electric motors and audio systems, each responsible for about 30% of demand.[43]

Waste Management. Currently, there is no recovery of gallium from end-of-life products. The main end-of-life waste streams are, due to the end uses, end-of-life vehicles and waste electrical and electronic equipment. Current recycling processes favor the recovery of bulk metals (steel, aluminum and copper) and precious metals, while gallium ends up as an impurity in recycled metals or in waste slags.[44−46]

2.2. System Quantification. Published statistics on gallium production and use are scarce. The United States Geological Survey (USGS) estimates global primary production, refinery production from primary metal, as well as capacities for these and secondary production.[19] However, they publish end-use statistics only for the United States, which is markedly different from the global average because of a concentration of LED and magnet producers in Asia. Most flows in the system were therefore quantified using global production data, market data and transfer coefficients. A detailed explanation of the calculations is given in the Supporting Information, and is summarized in the following: (i) Primary production data was taken from the USGS,[19] and typical yield was used to estimate the input of Bayer liquor into the extraction process. A model of gallium accumulation in Bayer liquor, similar to that used by Hudson,[20] was used to estimate the distribution ratio between Bayer liquor and alumina. Typical gallium concentration in aluminum was used to verify the ratio ending up in red mud. Along with concentrations in bauxites and bauxite production, this enabled

DOI: 10.1021/acs.est.5b00320
Environ. Sci. Technol. 2015, 49, 5704−5712

Table 1. Parameters, Estimated Values, Uncertainties and Probability Distributions Used for Monte Carlo Simulation[a]

description	mean	stand. dev.	prob. dist.	ref.
bauxite mining	259 ·10^6 tons	10%	normal	49
Ga conc. in bauxite	49 ppm	15%	normal	18
Ga conc. in bauxite used for Ga recovery	33 ppm	15%	normal	18
Share of bauxite used in Bayer proc.	0.85	0.05	beta	50
alumina production	92 × 10^6 tons	10%	normal	49
fraction of Ga in bauxite going to red mud	0.63	0.1	beta	20
fraction of dissolved Ga going to alumina	0.6	0.15	beta	20
yield in gallium recovery from Bayer liquor	0.95	0.03	beta	51,52
primary gallium production	292 tons	15%	normal	19
primary gallium production from zinc route	4 tons	25%	normal	19
refined gallium production	160 tons	10%	normal	53
concentration of gallium in alumina	80 ppm	25%	normal	54
yield in secondary production	0.9	0.05	beta	26
trimethylgallium production	22 tons	15%	normal	48
GaAs semi-insulating (SI) substrate prod.	2.12 × 10^8 cm^2	15%	normal	42
GaAs semicond. sub. prod. relative to GaAs SI sub. prod.	0.84	15%	normal	47
GaP substrate prod. relative to GaAs SI substrate prod.	0.096	15%	normal	47
GaN substrate prod. relative to GaAs SI substrate prod.	0.014	25%	normal	47
sapphire and SiC substr. prod. relative to GaAs SI substr.	1.84	15%	normal	47
thickness of GaAs substrates for IC fabrication	650 μm	5%	normal	22,32
thickness of other substrates	560 μm	10%	normal	32
yield in trimethylgallium production	0.92	0.05	beta	55
yield in crystal growth and substrate production	0.35	0.03	beta	22
collection rate, crystal growth and substrate prod. scrap	0.63	0.1	beta	22
yield in MOCVD deposition	0.11	0.05	beta	30
yield in MBE deposition	0.07	0.03	beta	30
yield in sputtering deposition	0.45	0.1	beta	31
wafer breakage and nonworking devices loss, fabrication	0.08	0.03	beta	34,35,56,57
backgrinding loss in IC fabrication	0.86	0.02	beta	33,57
backgrinding/epitaxial lift-off loss in LED fab.	0.83	0.08	beta	58−60
dicing and edge loss in device fabrication	0.16	0.03	beta	35,61
collection rate broken wafers and nonworking devices scrap	0.7	0.1	beta	[b]
collection rate backgrinding and dicing scrap from IC fabs.	0.1	0.2	beta	[c]
collection rate backgrinding/epitaxial lift-off scrap, LED	0.3	0.2	beta	[d]
LED deposition layer thickness	4 μm	15%	normal	62−66
integrated circuit deposition layer thickness	2 μm	25%	normal	67,68
CIGS deposition layer thickness	1.5 μm	15%	normal	31
concentration of gallium in CIGS	0.34 g/cm^3	5%	normal	31
efficiency of CIGS cells	0.118	0.005	beta	31
standard test conditions PV	1000 W/m^2	-		69
CIGS PV production capacity	1.6 GW	15%	normal	70
PV total production capacity	46 GW	15%	normal	70
new installed PV electricity generation capacity	30 GW	15%	normal	70
power electronics deposition layer thickness	5 μm	15%	normal	71
power electronics GaN market	7 mill. $	25%	normal	72
power electronics substrate area per unit value	0.17 cm^2/$	25%	normal	72
gallium use in NdFeB magnet production	85 tons	20%	normal	39[e]
material yield in NdFeB magnet production	0.7	0.1	beta	38,39

[a]Uncertainties are given as absolute (equivalent to percentage points) for transfer coefficients, and as relative to the mean for other parameters. [b]Assumed that broken wafers are collected, devices are not. [c]Assumed most slurries are not recycled. [d]Assumed 30% of backgrinding/epitaxial lift-off scrap recycled, mainly from epitaxial lift-off. [e]Estimate is for 2014.

estimating the Ga amount in bauxite consumed in the Bayer process with Ga extraction versus Ga in bauxite consumed in the Bayer process without Ga extraction. (ii) Primary refined production was taken from the USGS.[19] (iii) An estimate of the global market for compound semiconductor substrates in terms of area, as well as the use of trimethylgallium, were derived from various market analyst reports.[42,47,48] The demand for trimethylgallium was verified by back-calculation from substrate areas, deposition layer thickness and deposition yields. Substrate thickness and yields in wafer production and trimethylgallium synthesis were used to estimate the demand for refined gallium. The excess refined gallium, possibly ending up in stockpiles, was calculated by mass balance. The amount of gallium ending up in final products was estimated from fabrication yields, taking into account wafer breakage, nonworking devices and dicing as well as the large material losses

DOI: 10.1021/acs.est.5b00320
Environ. Sci. Technol. 2015, 49, 5704−5712

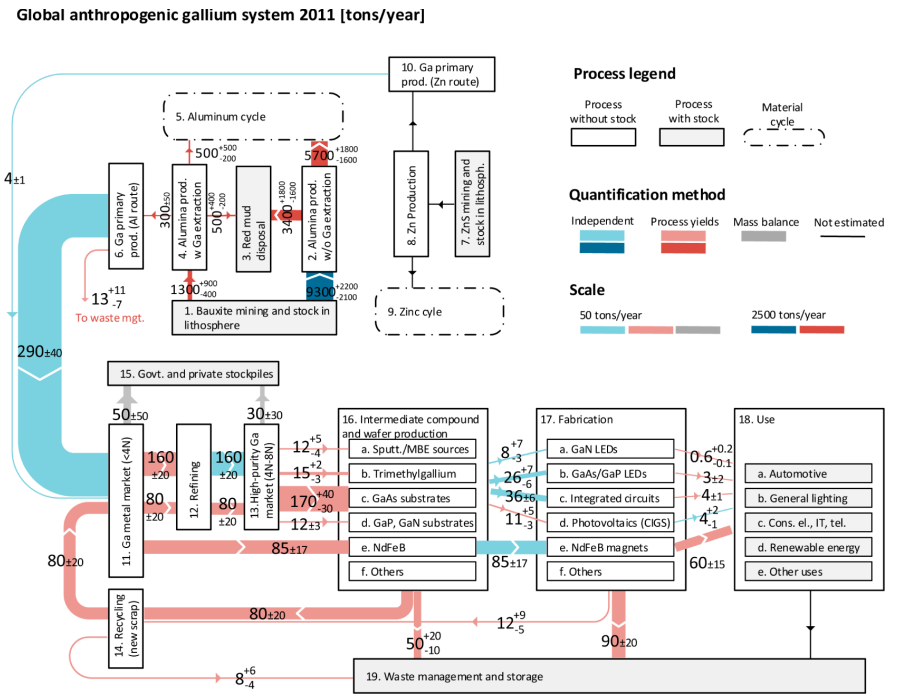

Figure 1. Global system of gallium production, refining, fabrication, use and recycling. Quantified flows are given as median ±84th and 16th percentile (equivalent to mean ± one standard deviation if variable has a normal distribution) of Monte Carlo simulation. Process inputs and outputs may not add up to the same number due to rounding. Colors indicate quantification method. Note that the flows in the upper part (dark colors) are shown in a different scale.

associated with backgrinding of the substrates and epitaxial lift-off. (iv) A separate approach was used for CIGS, where the demand for refined gallium was back-calculated from installed solar power, efficiencies, penetration of CIGS in the PV market, thickness of thin films, gallium concentration, and deposition yield. (v) An estimate of world demand for gallium for use in NdFeB magnets in 2014 was obtained directly from Molycorp Inc., a major producer of both refined gallium and NdFeB magnets. The estimate is based on measured concentration of gallium in magnets and world production of magnets. (vi) Gallium use in power electronics was estimated based on market value, device size and deposition layer thickness. (vii) The aforementioned steps also led to estimates of scrap flows. Collected scrap was estimated based on known practice to recycle or not recycle different types of scrap. Recycling process yield was used to estimate the supplied secondary production from new scrap. It was assumed that all recycled material is refined to high purity. An upper limit for stockpiling of unrefined gallium metal was also estimated by mass balance.

Decomposition of gallium flows into use and in intermediate compounds according to application was calculated as part of the quantification process explained above. For primary gallium demand and total gallium metal demand, it was calculated from the flows of gallium going into each application, production yields and the estimated recycling rates for production scrap from each application. Primary production needed for a given application was defined as the flow into use of the application plus all nonrecycled losses associated with its production chain, calculated by process yields and recycling rates; it thus represents the total needed primary production if only this application was produced. All parameters with values and estimated uncertainties are given in Table 1.

2.3. Uncertainty Analysis. A Monte Carlo simulation (10^5 iterations) was conducted to obtain final estimates of flows and their uncertainties. For each parameter, the uncertainty (standard deviation) was estimated based on the type and reliability of the reference, as well as knowledge of the individual processes. For example, the uncertainty of the yield in crystal growth and substrate production is estimated as below 5 percentage points (pp), since there is essentially one way to do it, and the majority of material losses from cutting and similar operations are impossible to avoid with current technology. On the other hand, uncertainties for scrap collection rates were judged as 10−20 pp, since the estimates are only based on rough knowledge of which types of scrap are usually recycled. A beta distribution was used for all transfer coefficients such as process yields. The beta distribution is useful for this purpose because it is limited between 0 and 1, it allows for asymmetric distributions (e.g., when a process yield is close to 100%), and because it is not necessary to make additional assumptions about the shape: for a given mean and standard deviation, there is only one solution for the parameters α and β of the beta distribution.[73] For all other parameters, a normal distribution was used. Uncertainties and distributions are summarized in Table 1.

DOI: 10.1021/acs.est.5b00320
Environ. Sci. Technol. 2015, 49, 5704−5712

3. RESULTS

3.1. System Quantification. Figure 1 shows the quantified gallium cycle for the year 2011. Values are given as the median, the 16th percentile and the 84th percentile of the Monte Carlo simulation results, equivalent to mean ± one standard deviation if the variable is normally distributed. The total flow of gallium in mined bauxite flows is around 11 000 tons, or about 40 times the current primary production of gallium. The majority of this gallium ends up in red mud or enters the aluminum cycle as an impurity, because (i) only a small share of bauxite is used for Ga recovery and (ii) even with Ga recovery, the amount extracted is smaller than the amount lost. Uncertainties in this part of the system are large, and in general larger above than below the median, meaning that losses and hence the share of bauxite already used for Ga extraction could potentially be much higher.

Flows of primary and secondary gallium are in the same order of magnitude, with larger uncertainties on the secondary side due to uncertainties in collection rates. Estimated demand of primary metal amounts to 210 ±30 tons in 2011, corresponding to 73% of the primary production. The gap is analyzed further in the discussion, section 4.1. Large material losses occur both in the production of wafers and in fabrication. While most of the scrap from wafer production is recycled, the majority from fabrication is landfilled or otherwise stored. The total loss, excluding that from the Bayer process and primary extraction, is 140^{+30}_{-20} tons/year, with an estimated 50^{+20}_{-10} tons from wafer and intermediate compound production (process 16), 90 ± 20 tons from device fabrication (process 17) and 8^{+6}_{-4} tons from recycling (process 14). The largest material losses after primary production occur in production of GaAs substrates (40^{+20}_{-10} tons), fabrication of ICs (30^{+5}_{-8} tons), fabrication of NdFeB magnets (24^{+11}_{-8} tons) and fabrication of GaAs/GaP-based LEDs (17 ± 6 tons) (details not shown in Figure 1). Although substantial amounts of gallium are used to produce semiconductors, the actual semiconductor applications embody only relatively small amounts; most of the gallium is lost during the manufacturing process. Only 13 ±3 tons of gallium enter the use phase in semiconductor applications, while 60^{+15}_{-14} tons enter use as an alloying element in NdFeB magnets. Gallium content in end-of-life products was not estimated, but is expected to be much lower due to the rapid growth in all major applications and the extended lifetime of products. Gallium use in power electronics was found to be insignificant (less than 10 kg in 2011) and will not be discussed further.

3.2. Demand Drivers. Figure 2 shows the decomposition of four flows in the system according to which of the five major applications they are driven by, with the median, 16th percentile and 84th percentile. Figure 2b) represents the market for refined and unrefined gallium. Refined gallium, needed for all major applications except magnets, is dominated by GaAs/GaP-based (red, orange, yellow) LEDs and ICs, because of the need for GaAs substrates. It is estimated that a significant share of scrap from substrate production is recycled, leading to a lower need for primary metal for these applications in Figure 2a). The amount of primary metal needed for semiconductor applications adds up to 130 ±30 tons/year. Figure 2c) shows the gallium contained in substrates and intermediate compounds, illustrating how a large share of the material is lost in the production of substrates for GaAs/GaP-based LEDs and ICs. At the stage of final products entering use there is very little gallium left in LEDs, ICs and PV. Blue, violet and white LEDs are at this stage insignificant in terms of gallium content, while red, orange and yellow LEDs, ICs and PV are all around 5 tons/year. Contrary to the use in semiconductors, most of the gallium used in magnets enter the final application. The flow into use, and most likely also the end-of-life flows, are therefore completely dominated by gallium in magnets.

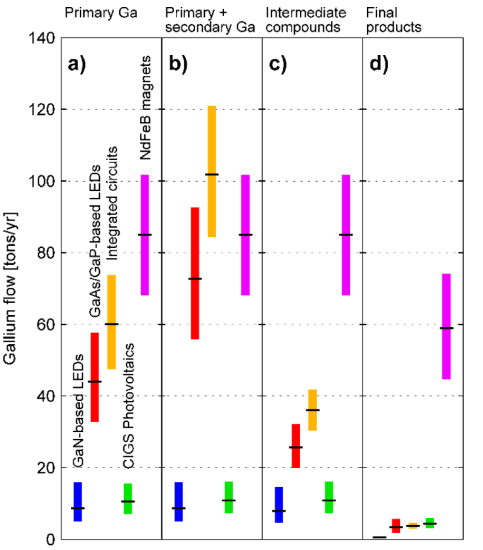

Figure 2. Decomposition of flows: (a) primary production, (b) primary and secondary production, (c) intermediate compounds production, d) products entering use; according to application in 2011. The black horizontal lines indicate the median; the colored bars show the 16−84% confidence interval. Primary production needed for a given application equals the flow into use of the application plus all losses associated with its production chain; it thus represents the total needed primary production if only this application was produced.

4. DISCUSSION

4.1. Gallium Demand. Semiconductor applications such as ICs and LEDs are frequently listed as the most important applications of gallium, and the recent growth in gallium production has been attributed to rapid demand increase from these.[2,12,19] According to our results, however, these applications only demand about 130 tons primary gallium, or 44% of the world production. An estimated 85 tons, corresponding to 29% of primary production, were used in the production of NdFeB permanent magnets, while the remaining 27% were not accounted for. Possible explanations for this disparity include (i) overestimation of production or underestimation of demand, (ii) stockpiling of gallium by national governments, (iii) stockpiling of gallium by industry and private investors, (iv) demand from other applications. The difference between estimated primary production and demand was 80 ±50 tons, indicating that errors in the estimates most likely cannot explain the entire gap. Some national governments are known to build up and hold strategic stockpiles of gallium and other critical metals. Japan and South Korea hold or plan relatively small stockpiles of gallium (60 days of domestic consumption), the United States does not stockpile

DOI: 10.1021/acs.est.5b00320
Environ. Sci. Technol. 2015, 49, 5704−5712

gallium, while China has a stockpile of unknown magnitude.[74] There have been reports of the Chinese State Reserve Bureau buying as much as 50 tons in a single event.[75,76] Some companies offer ownership of physical metal stocks to private investors,[74] but the magnitude of such stocks is not known. There are a number of applications of gallium which were not included in this study, for example low melting point alloys, catalysts, lithium thionyl chloride batteries, medical applications, piezoelectric materials, phosphors and transparent conductive oxides.[11] It has been estimated that these other applications were responsible for 14% of demand in 2010.[11] We conclude that the gap between estimated demand and supply is most likely due to other applications and stockpiling.

Further growth is likely in most applications. While LEDs are expected to be gradually replaced by organic LEDs in backlighting applications, a rapid penetration in general lighting and automotive has been projected.[29,40] Proliferation of smartphones and wireless technology in general may drive the demand for GaAs-based integrated circuits further. However, competing silicon-based technology is expected to take a larger market share in the future.[42] The future demand from photovoltaics and magnets will be highly dependent on the penetration of gallium-containing technology in these markets, as well as the overall demand for these applications. While future market penetration is very difficult to predict, we have seen that the potential growth is very large: the penetration rate of CIGS in the photovoltaics market is currently around 3%.[70] It has been estimated that the average gallium content in NdFeB magnets is 0.2 wt %,[39] which could translate to a 40% penetration rate assuming that Ga is normally added at 0.5 wt % when it is used. Furthermore, demand for solar panels and permanent magnets is expected to increase fast with expansion of renewable energy and electrified transport.[43,77] In combination, these changes could drive gallium demand to several times the current production. Such demand increases may result in a necessity to increase gallium recovery not only from primary production, but also from manufacturing and end-of-life management over the coming decades.

4.2. Gallium Supply. We estimated that globally, 8−21% of the extraction potential for gallium from the Bayer process was used in 2011, indicating that there is still room for increasing primary production using conventional resources and technologies. A large share of the gallium in bauxite ends up in red mud and as an impurity in alumina. Loss to red mud is difficult to avoid, as the amount of dissolved gallium is closely related to the amount of dissolved aluminum hydroxides. Loss to alumina may be possible to reduce substantially by extracting gallium more frequently from the Bayer liquor, that is, at lower concentrations. This would reduce the amount precipitated to alumina, as it is proportional to the concentration in the liquor. However, a lower concentration may also lead to lower efficiency in the extraction phase (process 6 in Figure 1). In addition to the existing extraction routes, gallium may also be produced from aluminous clay,[78] fly ash from coal combustion[79,80] or gasification,[81] and phosphorus flue dust.[82]

The majority of primary gallium is produced in China, which had about 75% of world production capacity in 2012.[19] Assuming that the same share applies to actual production, we can estimate that about 40% of the Chinese gallium extraction potential was utilized in 2011. This number is however subject to large uncertainties, mainly due to limited information about gallium concentration in Chinese bauxites. The number used here, 28 ppm, is low compared to other regions and based on data from only one deposit in the Western Guanxi province.[18]

4.3. System-Wide Efficiency Improvements. The largest losses in the system occur in (i) production of GaAs substrates, (ii) fabrication of ICs, (iii) fabrication of NdFeB magnets, and (iv) fabrication of GaAs/GaP-based LEDs. These losses may be reduced by increased recycling of production scrap, or improved material yield in the production processes. Recycling of production scrap is technically feasible today, but may be limited by economics. Most of the nonrecycled production scrap is in the form of slurries or filter media with a relatively low concentration of gallium,[83] implying higher transportation costs, lower recovery rates and a more demanding process. In current wafer production it is difficult to reduce the waste generation substantially, since the method depends on cutting the ingot into wafers. Increased recycling is therefore the most important measure in this part of the production chain. In device fabrication, however, there are opportunities to reduce wastes substantially. Wastes are mainly generated from the backgrinding process when the substrate thickness is reduced from around 600−100 μm or less. Reducing the wafer thickness would lead to less wastes from backgrinding, but would simultaneously increase wafer breakage.

A technology known as epitaxial lift-off has the potential to eliminate most waste from semiconductor device fabrication.[58,84] After devices have been produced on the wafer, a new carrier substrate of a different material is attached on top of the devices and the original GaAs substrate is removed by selective etching of an AlGaAs layer. This process is already being used in the fabrication of GaAs/GaP-based LEDs to replace the light-absorbing GaAs substrate with a metallic light-reflecting layer and a less expensive carrier substrate of silicon or aluminum nitride.[60] The original substrate can then be reused to produce new devices, which removes the need for the backgrinding process altogether and at the same time reduces GaAs consumption in device fabrication by more than 90%, assuming multiple reuses. Reuse of substrates has also been demonstrated for thin-film GaAs solar cells, which could enable large-scale terrestrial employment of the most efficient single junction solar cells.[85] It is not known whether epitaxial lift-off is feasible for GaAs-based ICs.

Material efficiency in the production of GaN-based LEDs and CIGS PV may become more important in the future if these technologies see continued growth. Due to the small amounts of gallium entering use in semiconductor devices it is unlikely that end-of-life recycling of these will play a major role. A more important question, due to the substantial use of gallium in magnets, is whether effective recycling of gallium as an alloying element in end-of-life NdFeB magnets will be achieved. With increased penetration of CIGS photovoltaics, end-of-life recycling of these could also become a substantial source of gallium.

■ ASSOCIATED CONTENT

Supporting Information

Detailed description of system, procedure for calculating the flows, Monte Carlo simulation, and a table with detailed results for flows to and from subprocesses. The Supporting Information is available free of charge on the ACS Publications website at DOI: 10.1021/acs.est.5b00320.

DOI: 10.1021/acs.est.5b00320
Environ. Sci. Technol. 2015, 49, 5704−5712

AUTHOR INFORMATION

Corresponding Author

*Phone: +47 41 69 70 86, +41 079 667 98 74; fax: +47 73 59 35 80; e-mail: amund.lovik@ntnu.no, amund.loevik@gmail.com.

Author Contributions

The manuscript was written through contributions of all authors. All authors have given approval to the final version of the manuscript.

Notes

The authors declare no competing financial interest.

ACKNOWLEDGMENTS

We thank Brian Jaskula, Eric Higham, Todd Hall, James Herchenroeder, Shiban Tiku and Stefan Eichler for data clarifications and valuable information on industry processes.

ABBREVIATIONS

6N	99.9999%
CIGS	copper indium gallium diselenide
IC	integrated circuit
LED	light emitting diode
MBE	molecular beam epitaxy
MOCVD	metalorganic chemical vapor deposition
PV	photovoltaics
SI	semi-insulating
TMG	trimethylgallium
USGS	United States Geological Survey

REFERENCES

(1) *Report on Critical Raw Materials for the EU: Report of the Ad hoc Working Group on defining critical raw materials*; European Commission: Brussels, 2014; http://ec.europa.eu/enterprise/policies/raw-materials/files/docs/crm-report-on-critical-raw-materials_en.pdf (accessed January 9, 2015).

(2) *Critical Materials Strategy*; U.S. Department of Energy: Washington DC, 2011; http://energy.gov/sites/prod/files/DOE_CMS2011_FINAL_Full.pdf (accessed January 9, 2015).

(3) Chen, W.-Q.; Graedel, T. E. Anthropogenic cycles of the elements: A critical review. *Environ. Sci. Technol.* **2012**, *46* (16), 8574−8586.

(4) Yoshimura, A.; Daigo, I.; Matsuno, Y. Global substance flow analysis of indium. *Mater. Trans.* **2013**, *54* (1), 102−109.

(5) Du, X.; Graedel, T. E. Uncovering the end uses of the rare earth elements. *Sci. Total Environ.* **2013**, *461*−*462*, 781−784.

(6) Du, X.; Graedel, T. E. Global in-use stocks of the rare earth elements: A first estimate. *Environ. Sci. Technol.* **2011**, *45* (9), 4096−4101.

(7) Kavlak, G.; Graedel, T. E. Global anthropogenic tellurium cycles for 1940−2010. *Resour. Conserv. Recycl.* **2013**, *76*, 21−26.

(8) Nansai, K.; Nakajima, K.; Kagawa, S.; Kondo, Y.; Suh, S.; Shigetomi, Y.; Oshita, Y. Global flows of critical metals necessary for low-carbon technologies: The case of neodymium, cobalt, and platinum. *Environ. Sci. Technol.* **2014**, *48* (3), 1391−1400.

(9) United States Geological Survey. *Mineral Commodity Summaries 2010: Gallium*; Jaskula, B. W., Ed, 2010; http://minerals.usgs.gov/minerals/pubs/commodity/gallium/mcs-2010-galli.pdf (accessed March 25, 2015).

(10) United States Geological Survey. *Mineral Commodity Summaries 2015: Gallium*; Jaskula, B. W., Ed., 2015; http://minerals.usgs.gov/minerals/pubs/commodity/gallium/mcs-2015-galli.pdf (accessed March 25, 2015).

(11) Butcher, T.; Brown, T. Gallium. In *Critical Metals Handbook*; Gunn, G., Ed.; John Wiley & Sons, 2014; pp 150−176.

(12) *Report on Critical Raw Materials for the EU: Critical raw materials profiles*; European Commission: Brussels, 2014; http://ec.europa.eu/enterprise/policies/raw-materials/files/docs/crm-report-on-critical-raw-materials_en.pdf (accessed January 9, 2015).

(13) Katrak, F. E.; Agarwal, J. C. Gallium: Long-run supply. *JOM* **1981**, *33* (9), 33−36.

(14) Angerer, G.; Erdmann, L.; Marscheider-Weidemann, F.; Scharp, M.; Lüllmann, A.; Handke, V.; Marwede, M. *Rohstoffe für Zukunftstechnologien: Einfluss des branchenspezifischen Rohstoffbedarfs in rohstoffintensiven Zukunftstechnologien auf die zukünftige Rohstoffnachfrage*; Fraunhofer Institut für System- und Innovationsforschung ISI, Institut für Zukunftsstudien und Technologiebewertung IZT GmbH: Stuttgart, 2009; http://www.isi.fraunhofer.de/isi-wAssets/docs/n/de/publikationen/Schlussbericht_lang_20090515_final.pdf (accessed January 9, 2015).

(15) Wittmer, D.; Scharp, M.; Bringezu, S.; Ritthoff, M.; Erren, M.; Lauwigi, C.; Giegrich, J. *Umweltrelevante Metallische Rohstoffe: Meilensteinbericht des Arbeitsschrittes 2.1 des Projekts "Materialeffizienz und Ressourcenshconung" (MaRess)*; Wuppertal Institut fur Klima, Umwelt, Energie GmbH: Wuppertal, Germany, 2011; http://ressourcen.wupperinst.org/downloads/MaRess_AP2_1.pdf (accessed January 9, 2015).

(16) Yarahmadi Dehnavi, P. Global cycle of gallium production, use and potential recycling. Master's thesis, Royal Institute of Technology (KTH): Stockholm, Sweden, 2013; http://www2.lwr.kth.se/Publikationer/PDF_Files/LWR_EX_13_23.pdf (accessed September 24, 2014).

(17) Burton, J. D.; Culkin, F.; Riley, J. P. The abundances of gallium and germanium in terrestrial materials. *Geochim. Cosmochim. Acta* **1959**, *16* (1−3), 151−180.

(18) Schulte, R. F.; Foley, N. K. *Compilation of Gallium Resource Data for Bauxite Deposits:* U.S. Geological Survey Open-File Report 2013-1272; 2014; http://pubs.usgs.gov/of/2013/1272/ (accessed November 21, 2014).

(19) United States Geological Survey. Gallium. In *2012 minerals Yearbook*; Jaskula, B. W., Ed., Washington DC, 2014; http://minerals.usgs.gov/minerals/pubs/commodity/gallium/myb1-2012-galli.pdf (accessed January 9, 2015).

(20) Hudson, L. K. Gallium as a by-product of alumina manufacture. *J. Met.* **1965**, *17* (9), 948−951.

(21) Graedel, T. E.; Allwood, J.; Birat, J. P.; Reck, B. K.; Sibley, S. F.; Sonnemann, G.; Buchert, M.; Hagelüken, C. *Recycling Rates of Metals—A Status Report, A Report of the Working Group on the Global Metal Flows to the International Resource Panel*; United Nations Environment Programme, 2011. http://www.unep.org/resourcepanel/Portals/24102/PDFs/Metals_Recycling_Rates_110412-1.pdf (accessed January 9, 2015).

(22) Eichler, S. Green gallium arsenide (GaAs) substrate manufacturing. In *2012 International Conference on Compound Semiconductor Manufacturing Technology*; CS ManTech: Boston, Massachusettes, 2012.

(23) Kramer, D. A. *Gallium and Gallium Arsenide: Supply, Technology, And Uses*; U.S. Department of the Interior, Bureau of Mines: Pittsburgh, PA, 1988; http://archive.org/details/galliumgalliumar00kram (accessed September 24, 2014).

(24) Greber, J. F. Gallium and Gallium Compounds. In *Ullmann's Encyclopedia of Industrial Chemistry*; Wiley-VCH Verlag GmbH & Co. KGaA: Weinheim, Germany, 2000.

(25) Yamamura, T.; Kato, H.; Ohgami, T.; Tayama, K.; Okuda, K.; Dowa Mining Co., Ltd. Refining Process for High Purity Gallium for Producing Compound Semiconductor and Apparatus for the Same. Patent EP1099770 (*A1*), 2007.

(26) Hall, T. *Personal communication with Todd Hall, Manager, Raw Material Procurement & Sales*; Molycorp Rare Metals Inc., Utah, November 2014, 2014.

(27) Jurisch, M.; Börner, F.; Bünger, T.; Eichler, S.; Flade, T.; Kretzer, U.; Köhler, A.; Stenzenberger, J.; Weinert, B. LEC- and VGF-growth of SI GaAs single crystals—recent developments and current issues. *J. Cryst. Growth* **2005**, *275* (1−2), 283−291.

DOI: 10.1021/acs.est.5b00320
Environ. Sci. Technol. 2015, 49, 5704−5712

(28) Weimar, A. High brightness LEDs: Manufacturing and applications. In *2011 International Conference on Compound Semiconductor Manufacturing Technology*, CS ManTech: Indian Wells, California, 2011.
(29) Grady, T.; Thompson, K.; Crow, A. M.; Ridsdale, D. *LED Spotlight*; Edison Investment Research: London, UK, 2013; http://www.edisoninvestmentresearch.com/sectorreports/LEDreportJune2013.pdf (accessed January 9, 2015).
(30) Izumi, S.; Shirahama, H.; Kouji, Y. Environmental safety issues for molecular beam epitaxy platform growth technology. *J. Cryst. Growth* **2001**, *227*−*228*, 150−154.
(31) Marwede, M.; Reller, A. Estimation of life cycle material costs of cadmium telluride- and copper indium gallium diselenide-photovoltaic absorber materials based on life cycle material flows. *J. Ind. Ecol.* **2014**, *18* (2), 254−267.
(32) Freiberger Compound Materials. GaAs wafers specifications http://www.freiberger.com/en/products/gaas-wafers/specifications.html (accessed July 24, 2014).
(33) Wei, R.-C.; Wang, H.-W.; Chin, C.-C.; Chiang, S.; Her, J.; Chen, P.-W.; Huang, K.; Hua, C.-H. Yield improvement for thin 50 μm GaAs product line. In *2012 International Conference on Compound Semiconductor Manufacturing Technology*; CS ManTech: Boston, MA, 2012.
(34) Darley, B.; Singh, M.; Santos, P.; Ambrocio, E.; Tiku, S. GaAs Wafer Breakage Reduction. In *2014 International Conference on Compound Semiconductor Manufacturing Technology*; CS ManTech: ; Denver, Colorado, 2014.
(35) Ho, W.-J.; Liu, J.; Chou, H. C.; Wu, C. S.; Tsai, T. C.; Chang, W. D.; Chou, F.; Wang, Y. C. Manufacturing of GaAs ICs for wireless communications applications. *Journal of Semiconductor Technology and Science* **2006**, *6* (3), 136−145.
(36) Bai, G.; Gao, R. W.; Sun, Y.; Han, G. B.; Wang, B. Study of high-coercivity sintered NdFeB magnets. *J. Magn. Magn. Mater.* **2007**, *308* (1), 20−23.
(37) Mizoguchi, T.; Sakai, I.; Niu, H.; Inomata, K.; Tsutai, A. Permanent Magnet. US Patent 4,935,075, June 19, 1990. http://worldwide.espacenet.com/publicationDetails/biblio?CC=US&NR=4935075A&KC=A&FT=D (accessed March 25, 2015).
(38) Binnemans, K.; Jones, P. T.; Blanpain, B.; Van Gerven, T.; Yang, Y.; Walton, A.; Buchert, M. Recycling of rare earths: a critical review. *J. Clean. Prod.* **2013**, *51*, 1−22.
(39) Herchenroeder, J. Personal communication with James Herchenroeder; Vice President Technology; Molycorp Magnequench, March 2015.
(40) Baumgartner, T.; Wunderlich, F.; Wee, D.; Jaunlich, A.; Sato, T.; Erxleben, U.; Bundy, G.; Bundsgaard, R. *Lighting the Way: Perspectives on the Lighting Market*; McKinsey & Company, Inc., 2011; http://www.mckinsey.com/~/media/mckinsey/dotcom/client_service/Automotive%20and%20Assembly/Lighting_the_way_Perspectives_on_global_lighting_market_2012.ashx (accessed January 9, 2015).
(41) Broell, M.; Sundgren, P.; Rudolph, A.; Schmid, W.; Vogl, A.; Behringer, M. New developments on high-efficiency infrared and InGaAlP light-emitting diodes at OSRAM Opto Semiconductors. In *Proc. SPIE 9003, Light-Emitting Diodes: Materials, Devices, and Applications for Solid State Lighting XVIII, 90030L*, San Francisco, CA, 2014; Vol. *9003*, pp 1−6.
(42) Higham, E. GaAs industry overview and forecast: 2011− 2016. In *28th International Conference on Compound Semiconductor Manufacturing Technology*; CS ManTech: ; New Orleans, LA, 2013; pp 13−16.
(43) Habib, K.; Wenzel, H. Exploring rare earths supply constraints for the emerging clean energy technologies and the role of recycling. *J. Clean. Prod.* **2014**, *84*, 348−359.
(44) Schleup, M.; Hagelüken, C.; Kuehr, R.; Magalini, F.; Maurer, C.; Meskers, C.; Mueler, E.; Wang, F. Recycling—From e-waste to resources; Sustainable Innovation and Technology Transfer Sector Studies; UNEP-StEP, 2009. http://www.unep.org/pdf/Recycling_From_e-waste_to_resources.pdf (accessed December 17, 2014).
(45) Widmer, R.; Du, X.; Haag, O.; Restrepo, E.; Wäger, P. A. Scarce metals in conventional passenger vehicles and end-of-life vehicle shredder output. *Environ. Sci. Technol.* **2015**, *49* (7), 4591−4599.
(46) Reuter, M.; Hudson, C.; van Schaik, A.; Heiskanen, K.; Meskers, C.; Hagelüken, C. *Metal Recycling: Opportunities, Limits, Infrastructure, A Report of the Working Group on the Global Metal Flows to the International Resource Panel.*; United Nations Environment Programme, 2013, http://www.unep.org/resourcepanel/Portals/24102/PDFs/Metal_Recycling-Full_Report_36dpi_130919.pdf (accessed May 22, 2014).
(47) Yole Développement. Press release: A comprehensive survey of usage and markets for: GaAs, GaP, InP, SiC, Sapphire and bulk-GaN http://www.yole.fr/iso_upload/news/2010/cssubstrates_june2010.pdf (accessed October 24, 2014).
(48) Compound Semiconductor. Demand For Key Raw Material To Double As LED Market Booms http://www.compoundsemiconductor.net/csc/news-details/id/19736670/name/Demand-for-key-raw-material-to-double-as-LED-marketboom.html (accessed September 5, 2014).
(49) United States Geological Survey. Bauxite and alumina. In *2012 Minerals Yearbook*; Bray, E. L., Ed.; United States Geological Survey: Washington DC, 2014.
(50) United States Geological Survey. Bauxite and Alumina Statistics and Information http://minerals.usgs.gov/minerals/pubs/commodity/bauxite/ (accessed November 19, 2014).
(51) Kou, X.; Li, S.; Liu, Q.*New Method for Extracting Gallium from Bayer Mother Liquor through Chelating Resin*; Xi An Sunresin Technology Ltd, Patent CN102321802 (B), 2013. http://worldwide.espacenet.com/publicationDetails/biblio?CC=CN&NR=102321802B&KC=B&FT=D (accessed September 9, 2014).
(52) Puvvada, G. V. K. Liquid−liquid extraction of gallium from Bayer process liquor using Kelex 100 in the presence of surfactants. *Hydrometallurgy* **1999**, *52* (1), 9−19.
(53) Jaskula, B. W. Private communication with Brian W. Jaskula, beryllium, gallium and lithium commodity specialist; National Minerals Information Center, U.S. Geological Survey, Reston, Virginia, USA, December 2014.
(54) Senel, E.; Walmsley, J. C.; Diplas, S.; Nisancioglu, K. Liquid metal embrittlement of aluminium by segregation of trace element gallium. *Corros. Sci.* **2014**, *85*, 167−173.
(55) Revin, M. V.; Artemov, A. N.; Sazonova, E. V. A new synthetic route to trimethylgallium. *Russ. J. Appl. Chem.* **2013**, *86* (9), 1359−1363.
(56) Hand, T.; Farmosa, S.; Welborn, J.; Nercessian, D. Successful GaAs backend process improvement. In *27th International Conference on Compound Semiconductor Manufacturing Technology*; CS ManTech: Boston, MA, 2012.
(57) Tiku, S. Private communication with Shiban Tiku, Manager, New Product Introduction; Skyworks Solutions, Inc., Woburn MA, August 2014.
(58) Cheng, C.; Shiu, K.; Li, N.; Han, S.; Shi, L.; Sadana, D. K. Epitaxial lift-off process for gallium arsenide substrate reuse and flexible electronics. *Nat. Commun.* **2013**, *4*, 1577.
(59) Marktech Optoelectronics. LED Chips and Materials, various data sheets http://www.marktechopto.com/products.cfm?p=LED-Chips-and-Materials (accessed November 20, 2014).
(60) Epistar Corporation. LED Products, various data sheets http://www.epistar.com.tw/_english/01_product/07_search.php (accessed November 20, 2014).
(61) Zuhlke, H.-U.; Eberhardt, G.; Ullmann, R. TLS-Dicing—An innovative alternative to known technologies. In *Advanced Semiconductor Manufacturing Conference, 2009. ASMC '09. IEEE/SEMI*; 2009; pp 28−32.
(62) Zhu, D.; Humphreys, C. J. Low-cost high-efficiency GaN LED on large-area Si substrate. In *28th International Conference on Compound Semiconductor Manufacturing Technology*; CS ManTech: New Orleans, Louisiana, 2013; pp 269−272.
(63) Ryu, H.-Y.; Jeon, K.-S.; Kang, M.-G.; Choi, Y.; Lee, J.-S. Dependence of efficiencies in GaN-based vertical blue light-emitting

DOI: 10.1021/acs.est.5b00320
Environ. Sci. Technol. 2015, 49, 5704−5712

diodes on the thickness and doping concentration of the n-GaN layer. *Opt. Express* **2013**, *21* (S1), A190−A200.
(64) Tsai, Y.-J.; Lin, R.-C.; Hu, H.-L.; Hsu, C.-P.; Wen, S.-Y.; Yang, C.-C. Novel electrode design for integrated thin-film GaN LED package with efficiency improvement. *IEEE Photonics Technol. Lett.* **2013**, *25* (6), 609−611.
(65) Schreiner, R.; Boyd, A. R.; Rockenfeller, O.; Kaeppeler, J.; Schineller, B.; Heuken, M. Led structures grown on 200 mm diameter sapphire and silicon substrates. In *2010 International Conference on Compound Semiconductor Manufacturing Technology*; CS ManTech: Portland OR, 2010.
(66) Hao, G.-D.; Wang, X.-L. Enhancement of light-extraction efficiency in AlGaInP light-emitting diodes using evanescent wave coupling effect. *Appl. Phys. Lett.* **2013**, *103*, 231112.
(67) Byoung, G. M.; Hyung, S. Y.; Jong-Min, L.; Seong-Il, K.; Hae, C. K.; Il-Hwan, C.; Kyung, W. J. Dependences of the characteristics of an InGaP/GaAs HBT for applications in power amplifiers on the structural parameters. *J. Korean Phys. Soc.* **2011**, *59* (21), 435.
(68) Tseng, H.-C.; Li, J.-K.; Chen, T.-W. Thermal-Stability Enhancement of InGaP/GaAs Collector-Up HBTs. *IEEE Trans. Device Mater. Reliab.* **2011**, *11* (3), 387−390.
(69) *Test Methods for Electrical Performance of Nonconcentrator Terrestrial Photovoltaic Modules and Arrays Using Reference Cells*; E44 Committee, ASTM International, 2012. http://enterprise.astm.org/SUBSCRIPTION/filtrexx40.cgi?REDLINE_PAGES/E1036.htm (accessed October 14, 2014).
(70) Masson, G.; Latour, M.; Rekinger, M.; Theologitis, I.-T.; Papoutsi, M. *Global market outlook for photovoltaics 2013−2017*; European Photovoltaic Industry Association: Brussels, Belgium, 2013. http://www.epia.org/fileadmin/user_upload/Publications/GMO_2013_-_Final_PDF.pdf (accessed January 15, 2015).
(71) Extance, A.; Yole Développement. GaN-on-silicon wafers: the enabler of GaN power electronics. *Power Dev'*. 2012. http://www.yole.fr/iso_upload/Mag/PowerDev_January2012_IR.pdf (accessed November 4, 2014).
(72) Marketsandmarkets. Gallium Nitride (GaN) Semiconductor Devices (Discretes & ICs) Market, Global Forecast & Analysis (2012−2022) http://www.marketsandmarkets.com/PressReleases/gallium-nitride-semiconductor.asp (accessed August 28, 2014).
(73) Kennedy, D. J.; Montgomery, D. C.; Quay, B. H. Data quality. *Int. J. Life Cycle Assess.* **1996**, *1* (4), 199−207.
(74) Risk & Policy Analysts Ltd. *Stockpiling of Non-Energy Raw Materials: Final Report*; European Commission, Directorate-General for Enterprise and Industry: Brussels, Belgium, 2012. http://ec.europa.eu/enterprise/policies/raw-materials/files/docs/stockpiling-report_en.pdf (accessed September 4, 2014).
(75) Gallium price falls as overcapacity minimises impact of SRB buying 50 tonnes http://www.metalbulletin.com/Article/3290225/Gallium-price-falls-as-overcapacity-minimises-impact-of-SRB-buying-50-tonnes.html#axzz3GycNazcQ (accessed October 23, 2014).
(76) Chinese gallium price rises on SRB purchase http://www.metalbulletin.com/Article/3091212/Chinese-gallium-price-rises-on-SRB-purchase.html#axzz3GycNazcQ (accessed October 24, 2014).
(77) IEA. *Energy Technology Perspectives 2014*; Organisation for Economic Co-operation and Development: Paris, 2014. http://www.iea.org/etp/etp2014.
(78) Orbite Aluminae Inc. Orbite: A strategic gallium producer http://www.orbitealuminae.com/media/upload/filings/Gallium_Version_1_1.pdf (accessed Setember 26, 2014).
(79) Fang, Z.; Gesser, H. D. Recovery of gallium from coal fly ash. *Hydrometallurgy* **1996**, *41* (2−3), 187−200.
(80) Gutiérrez, B.; Pazos, C.; Coca, J. Recovery of gallium from coal fly ash by a dual reactive extraction process. *Waste Manag. Res.* **1997**, *15* (4), 371−382.
(81) Font, O.; Querol, X.; Juan, R.; Casado, R.; Ruiz, C. R.; López-Soler, Á.; Coca, P.; Peña, F. G. Recovery of gallium and vanadium from gasification fly ash. *J. Hazard. Mater.* **2007**, *139* (3), 413−423.
(82) Xu, K.; Deng, T.; Liu, J.; Peng, W. Study on the recovery of gallium from phosphorus flue dust by leaching with spent sulfuric acid solution and precipitation. *Hydrometallurgy* **2007**, *86* (3−4), 172−177.
(83) Torrance, K. W.; Keenan, H. E.; Hursthouse, A. S.; Stirling, D. Measurement of arsenic and gallium content of gallium arsenide semiconductor waste streams by ICP-MS. *J. Environ. Sci. Health Part A* **2010**, *45* (4), 471−475.
(84) Konagai, M.; Sugimoto, M.; Takahashi, K. High efficiency GaAs thin film solar cells by peeled film technology. *J. Cryst. Growth* **1978**, *45*, 277−280.
(85) Bauhuis, G. J.; Mulder, P.; Haverkamp, E. J.; Huijben, J. C. C. M.; Schermer, J. J. 26.1% thin-film GaAs solar cell using epitaxial lift-off. *Sol. Energy Mater. Sol. Cells* **2009**, *93* (9), 1488−1491.

DOI: 10.1021/acs.est.5b00320
Environ. Sci. Technol. 2015, 49, 5704−5712

Supporting information to:

The global anthropogenic gallium system: Determinants of supply, demand and efficiency improvements

Amund N. Løvik[†]*, *Eliette Restrepo*[†‡], *Daniel B. Müller*[†]

[†] Industrial Ecology Programme and Department of Energy and Process Engineering, Norwegian University of Science and Technology (NTNU), NO-7491, Trondheim, Norway

[‡] Empa, Swiss Federal Laboratories for Materials Science and Technology, CH-9014, St. Gallen, Switzerland

Corresponding author:

* E-mail: amund.lovik@ntnu.no, amund.loevik@gmail.com; phone: +47 41 69 70 86, +41 079 667 98 74; fax: +47 73 59 35 80

This supporting information includes 24 pages, 3 figures and 3 tables.

Contents

1. System description S2
2. Quantification of flows and decomposition S6
3. Monte Carlo simulation S18
4. Detailed results S19
5. References S21

1. System description

The system definition is shown in Figure S1.

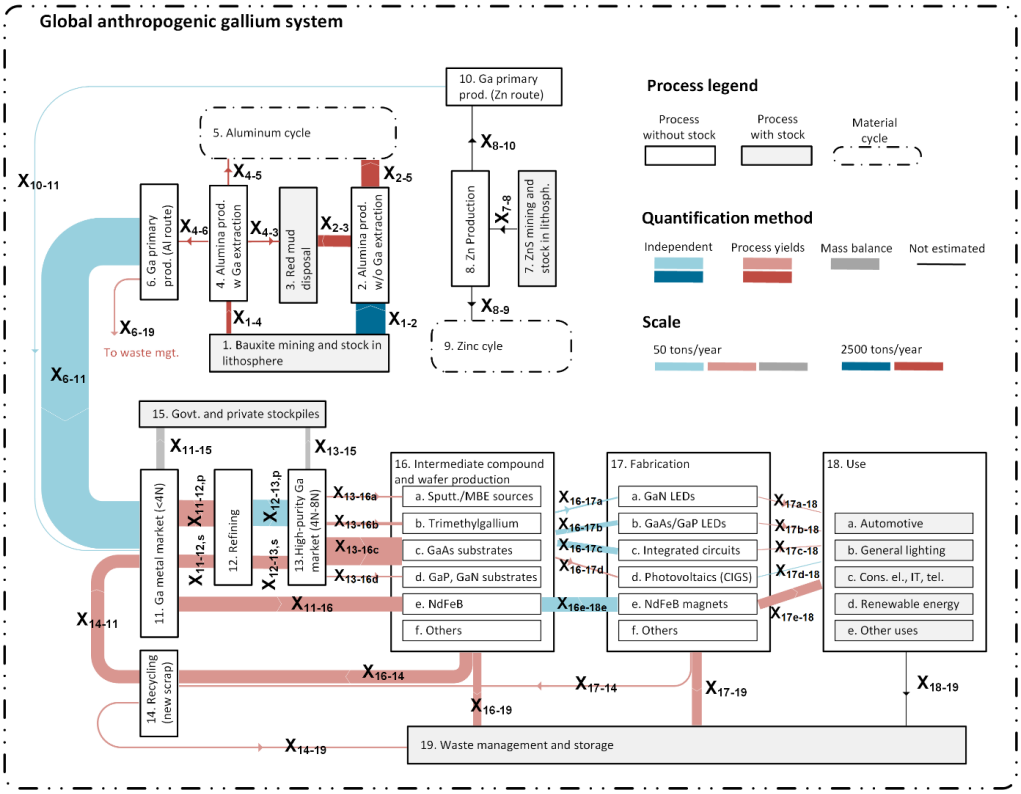

Figure S1 System definition of the global system of gallium production, manufacturing, use and recycling. Flows to and from sub-processes 16a-e and 17a-e were also estimated.

Geological resources. Gallium occurs mainly as a trace element in earth's crust, with an estimated average concentration of about 17 ppm.[1] Minerals in which gallium forms a substantial part have been found only in uneconomic quantities.[2] Elevated concentrations are found in aluminum-containing rocks and minerals such as bauxite (<10-180 ppm), micas (7-170 ppm) and corundum (100 ppm), due to its chemical similarity to aluminum. Enrichments are also present in zinc blende (2-110 ppm) and magnetite (20-90 ppm). The world average gallium concentration in bauxite resources has been estimated to 57 ppm, with regional averages mostly between 28 ppm (Western Guanxi, China) and 75 ppm (Caribbean).[3]

Primary production. Gallium metal is produced as a by-product, mainly from the Bayer process for alumina production and to a lesser degree from the hydrometallurgical route for zinc production.[4] Alternative routes that are currently not used for large-scale production include recovery from aluminous clay,[5] fly ash from coal combustion[6,7] or gasification,[8] and phosphorous flue dust.[9] In the Bayer process, aluminum minerals in bauxite rock are dissolved

in a sodium hydroxide solution, separated from iron oxides and silicates by filtration and then precipitated as aluminum hydroxide. About 30-50% of the gallium in bauxite will remain undissolved and therefore be disposed of in the so-called red mud together with iron oxides, silicates and undissolved aluminum hydroxides.[10,11] The alkaline solution (Bayer liquor) is recycled to process the next batch of bauxite. Gallium will accumulate in the liquor until it reaches a steady-state concentration, i.e. when the amount dissolved from bauxite equals the amount precipitated as an impurity in alumina.[12] When the concentration reaches a certain level, the liquor may be removed from the Bayer process to extract gallium in a series of processing steps. The most common method is the ion exchange process in which an organic compound is used to preferentially adsorb gallium. Further processing separates gallium from the organic resin and metallic impurities, and finally gallium metal is produced by electrolysis.[11]

Secondary production. Recycling of gallium from industrial scrap is commonly done, while no end-of-life recycling is known to occur.[13] The most important type of industrial scrap is GaAs in various forms: bulk crystal pieces, test wafers, broken wafers and slurries from grinding and cutting.[14,15] Bulk GaAs and clean wafers may be recycled internally at the crystal growth facilities by direct remelting.[14] From less pure scrap, gallium is typically recovered by dissolving GaAs in a hot acidic solution such as nitric acid, precipitation of Ga_2O_3, re-dissolution and electrolysis.[15,16] Another method involves heating the GaAs material to evaporate arsenic and obtain Ga_2O_3.[16] Recycled gallium metal may be further refined to obtain the same grades as from primary metal.

Refining. Refining of the metal to a purity of 99.9999% (6N) or higher for electronic applications, is achieved by a combination of methods such as vacuum refining,[17] washing with aqueous acids and alkalis, fractional crystallization,[18] zone melting[19,20] and/or single crystal growth.[21] Purification may also be conducted on gallium compounds such as gallium trichloride, which is sometimes produced directly at the gallium metal plant.[22] The overall yield of the refining process depends on the final purity and the methods used. As an example, purification from 4N to 7N by fractional crystallization could have a material yield in the range 70-80%.[23] However, the discarded material is reintroduced at an earlier stage in the process chain for an overall yield close to 100%.[24] This recovery is here defined as part of the refining process.

Production of intermediate compounds and substrates. The majority of gallium demand arises from its use in compound semiconductors, the most common ones being GaAs, gallium nitride (GaN), indium gallium nitride ($In_xGa_{1-x}N$, hereafter InGaN), gallium phosphide (GaP), aluminum gallium indium phosphide ($(Al_{1-x}Ga_x)_yIn_{1-y}P$, hereafter AlGaInP) and copper indium gallium diselenide ($CuIn_xGa_{1-x}Se_2$, CIGS). These are either grown as single crystals and cut into wafers or produced directly from precursor gases or other sources during the device fabrication process. GaAs and GaP single crystal ingots are produced by two techniques, the liquid-encapsulated Czochralski process and the vertical gradient freeze process. Both involve directional solidification of a single crystal from a melt to produce a cylinder-shaped ingot with a diameter of 50-200 mm and length of up to 300 mm.[25] The sides of the ingot are trimmed to an even diameter, the cone-shaped ends are cut off, and the ingot is sawed into thin wafers (<1mm thick) that are polished and used as substrates for device fabrication. Bulk losses such as the cone-shaped ends are usually recycled internally, while the wastes from sawing, trimming, polishing and etching are sent to an external recycler or disposed of.[14]

The other gallium-containing compounds are mainly produced during device fabrication by metalorganic chemical vapor deposition (MOCVD), molecular beam epitaxy (MBE) or sputtering deposition. These processes are described under "fabrication". The main precursor gas for MOCVD of gallium compounds is trimethylgallium (TMG), $Ga(CH)_3$. TMG is synthesized from gallium trichloride and a metal alkyl such as trimethylaluminum,[26,27] or directly from gallium metal and methyl iodide.[28] Evaporation sources for MBE consist of pure gallium metal, while sputtering targets for CIGS production can be pure gallium metal or gallium in alloys with indium and/or copper.

Fabrication. Semiconductor devices such as integrated circuits (ICs) and light emitting diodes (LEDs) consist of a few microns thick *deposition layer* on top of the much thicker substrate. GaAs is used both for the substrate and the deposition layer in GaAs-based ICs and LEDs, and as substrate for GaAs/GaP-based LEDs.[29] GaN-based LEDs are produced on substrates of sapphire (Al_2O_3) or silicon carbide (SiC),[30] and therefore require very little gallium per device. The deposition layer is produced by MOCVD or MBE.[31] In an MOCVD process, precursor gases such as TMG and ammonia flow across the substrate surface in a reaction chamber to produce an epitaxial film of the desired compound. The MBE process is conducted in a vacuum chamber, where the low pressure causes the pure elemental sources (e.g. gallium metal) to sublimate. The beam of sublimated atoms is directed toward the heated substrate, and a thin film is formed. LEDs are mainly produced with MOCVD,[29] while ICs are produced with both MOCVD and MBE.[31,32] Thin film CIGS solar cells can be produced with a variety of techniques. Vacuum-based methods such as co-evaporation and sputtering are most common; methods with higher material utilization rates are being developed.[33,34] Material yields in deposition for LEDs and ICs are normally less than 20% and can be as low as 1%,[35] while the yield in thin film PV production is higher, typically 30-60% assuming sputtering deposition.[36]

The substrates for ICs and LEDs are much thicker than what is required for the operation of the device, 450-675 μm,[37] and is therefore thinned to a thickness of 50-100 μm in a "backgrinding" process to enable denser packaging and better heat dissipation.[38] Each wafer is normally used to produce up to several thousand identical devices, which are separated by cutting, leading to some additional loss. Finally, wafer breakage and non-working devices contribute to a total material loss that may reach above 90% including substrate material.[38–40] The majority of this loss is due to the backgrinding process.

In the production of NdFeB magnets, Ga is often added at approximately 0.5%wt to improve magnetic properties, corrosion resistance and the production process.[2,41,42] The magnets are produced by melting the constituent elements to form an alloy, milling to a fine powder, pressing, sintering and machining into the final shape. Material losses are typically 20-40% of the starting material.[43,44] Although it is common to recycle neodymium from the production scrap, gallium is not recovered in this process.[44]

End-use.

GaN-based LEDs are used to produce light with color ranging from ultraviolet to green.[45] The most important application is as a component of white LEDs, where a blue or ultraviolet LED is combined with a phosphor. White LEDs are today used in all key lighting markets such as residential, offices, outdoor, architectural and automotive; however, the penetration is still low compared to other lighting technologies. In addition, white LEDs are extensively used for backlighting in liquid crystal displays, especially in handsets and portable computers.[46]

GaAs/GaP-based LEDs can produce light with color ranging from green to red. They are used in automotive dashboards and exterior lights, traffic signal lighting, full-color displays and many other signage and display applications.[47] In the future, increased use may be seen in indoor general lighting where they can be used to improve the color temperature of white LED lamps.[48] Red LEDs can also be used together with green and blue LEDs to produce white light, but this is more expensive and therefore much less used than the phosphor-based white LED.[49]

GaAs ICs are mainly used in mobile phones and other wireless communication devices and infrastructure. More than 50% of the demand in 2011 has been attributed to mobile phones,[32] the majority of which comes from power amplifiers used to strengthen the signal before it is transmitted through the antenna. Due to the wide variety of air interface standards (e.g. GSM, EDGE, CDMA, LTE) and frequency bands, new handsets contain several power amplifiers for international compatibility including older standards.[32]

The main applications for NdFeB magnets are computers, electric motors and audio systems, each responsible for about 30% of demand.[50]

Waste management.

Currently, there is no recovery of gallium from end-of-life products, mainly due to the low concentrations with respect to other materials in the products, but also due to the lack of technologies for its recovery from end-of-life products.

The main end-of-life waste streams are, due to the end uses, end-of-life vehicles (ELV) and waste electrical and electronic equipment (WEEE). Gallium in automobiles is mainly in lighting systems and electrical motors;[51] in electronics it is found in printed circuit boards.[52] Typical recycling of ELV favors the recovery of bulk metals such as steel and aluminum and it can include depollution, dismantling, shredding and recovery of materials.[53] After shredding, gallium is found mainly in the automobile shredder residue (ASR) and in low concentrations in the bulk aluminum fractions, most likely as a native impurity in the base metal.[54] The ASR is subsequently incinerated or landfilled. Some processes exist to recover precious metals after incineration.[55] However, in such processes gallium is transferred to slags from which it is not recovered.[56]

Recycling of WEEE can include depollution, dismantling, crushing, separation and recovery of materials. As for ELV, it favors the recovery of bulk metals (steel, aluminum and copper), as well as the recovery of precious metals.[57] The final recovery of these metals is carried out in copper smelters or in integrated metals smelters in which gallium is transferred to slags and not recovered.[56]

2. Quantification of flows and decomposition

The system variables (flows) are listed and described in Table S1. $X_{m\text{-}n}$ refers to the flow from process *m* to process *n*. Letters *a-f* designate sub-processes, letters *p* and *s* stand for primary and secondary material respectively, *sc* stands for semiconductor applications (light emitting diodes, integrated circuits and photovoltaics), and *pe* stands for power electronics . All system variables refer to the gallium content in the flows.

Table S1 System variables. All variables refer to the gallium content in the flows.

Variable name	*Description of flow*
$X_{1\text{-}2}$	Bauxite input to non-Ga Bayer process
$X_{1\text{-}4}$	Bauxite input to Ga-extr. Bayer process
$X_{2\text{-}3}$	Red mud from non-Ga Bayer process
$X_{2\text{-}5}$	Alumina from non-Ga Bayer process
$X_{4\text{-}3}$	Red mud from Ga-extr. Bayer process
$X_{4\text{-}5}$	Alumina from Ga-extr. Bayer process
$X_{4\text{-}6}$	Gallium entering extraction process from Bayer route
$X_{6\text{-}11}$	Primary production of gallium metal from Bayer route
$X_{6\text{-}19}$	Loss from extraction process
$X_{6\text{-}11}$	Primary gallium to refining
$X_{10\text{-}11}$	Primary production of gallium metal from zinc route
$X_{11\text{-}15}$	Primary unrefined gallium going into stockpiles
$X_{11\text{-}12,p}$	Refined gallium from primary production
$X_{11\text{-}12,s}$	Refined gallium from recycling
$X_{14\text{-}11}$	Recycled material going to refining
$X_{14\text{-}19}$	Loss from recycling
$X_{13\text{-}15}$	Gallium going into stockpiles
$X_{13\text{-}16a}$	Refined gallium used in production of sputtering targets and MBE sources
$X_{13\text{-}16b}$	Refined gallium used in the production of TMG
$X_{13\text{-}16c}$	Refined gallium used in the production of GaAs substrates
$X_{13\text{-}16d}$	Refined gallium used in the production of GaP and GaN substrates
$X_{13\text{-}16f}$	Refined gallium used for other purposes
$X_{13\text{-}16}$	Consumption of refined gallium
$X_{16b\text{-}19}$	Loss from production of TMG
$X_{16c\text{-}19}$	Loss from production of GaAs substrates
$X_{16d\text{-}19}$	Loss from production of GaP and GaN substrates
$X_{16\text{-}19}$	Loss to landfills from compound production
$X_{16c\text{-}14}$	Recycling from production of GaAs substrates
$X_{16d\text{-}14}$	Recycling from production of GaP and GaN substrates
$X_{16\text{-}14}$	Recycling from compound production
$X_{16a\text{-}17}$	Consumption of sputtering targets and MBE sources
$X_{16b\text{-}17}$	Consumption of TMG
$X_{16c\text{-}17}$	Consumption of GaAs substrates
$X_{16d\text{-}17}$	Consumption of GaP and GaN substrates
$X_{16\text{-}17}$	Consumption of intermediate compounds

Table S1 cont.

Variable name	*Description of flow*
$X_{16a\text{-}17c}$	Use of sputtering targets and MBE sources for ICs
$X_{16a\text{-}17d}$	Use of sputtering targets and MBE sources for PV
$X_{16b\text{-}17a}$	Use of TMG for production of GaN LEDs
$X_{16b\text{-}17b}$	Use of TMG for production of GaP/GaAs LEDs
$X_{16b\text{-}17c}$	Use of TMG for production of ICs
$X_{16b\text{-}17f,\ pe}$	Use of TMG for production of power electronics
$X_{16b\text{-}17}$	Total use of TMG (estimated from substrates area)
$X_{16c\text{-}17b}$	Use of GaAs substrates for GaP/GaAs LEDs
$X_{16c\text{-}17c}$	Use of GaAs substrates for ICs
$X_{16d\text{-}17b}$	Use of GaP substrates for GaP LEDs
$X_{16d\text{-}17f}$	Use of GaN substrates for lasers and other applications
$X_{16e\text{-}17e}$	Use of NdFeB to produce magnets
$X_{17a\text{-}19}$	Scrap lost from production of GaN LEDs
$X_{17b\text{-}19}$	Scrap lost from production of GaP/GaAs LEDs
$X_{17c\text{-}19}$	Scrap lost from production of ICs
$X_{17d\text{-}19}$	Scrap lost from production of PV
$X_{17e\text{-}19}$	Scrap lost from production of NdFeB magnets
$X_{17f,\ pe\text{-}19}$	Scrap lost from production of power electronics
$X_{17\text{-}19}$	Total scrap loss to landfills from fabrication of devices
$X_{17b\text{-}14}$	Collected scrap from production of GaP, GaAs LEDs
$X_{17c\text{-}14}$	Collected scrap from production of ICs
$X_{17d\text{-}14}$	Collected scrap from production of PV
$X_{17\text{-}14}$	Total collected scrap from fabrication
$X_{17a\text{-}18}$	Total use of GaN LEDs
$X_{17b\text{-}18}$	Total use of GaP/GaAs LEDs
$X_{17c\text{-}18}$	Total use of ICs
$X_{17d\text{-}19}$	Total use of PV
$X_{17e\text{-}18}$	NdFeB magnets entering use
$X_{17f,\ pe\text{-}18}$	Total use of power electronics
$X_{17\text{-}18}$	Total gallium entering use

The system was quantified using a combination of statistical data, market data and technical process parameters. The parameters used in the quantification are listed in Table S2.

Table S2. Parameters used in the quantification of the system.

Symbol	*Description*
B	Bauxite mining
c_0	Ga concentration in bauxite
c_1	Ga concentration in bauxite used for Ga recovery
a	Share of bauxite used in Bayer process
A	Alumina production
b	Fraction of Ga in bauxite going to red mud
p	Fraction of dissolved Ga going to alumina
y_1	Yield in gallium recovery from Bayer liquor
Y	Primary gallium production
Z	Primary gallium production from zinc route
R	Refined gallium production
c_2	Concentration of gallium in alumina
T	Trimethylgallium production
G_1	GaAs semi-insulating (SI) substrate prod.
g_2	GaAs semiconducting substrate production relative to GaAs SI substrate production
g_3	GaP substrate production relative to GaAs SI substrate production
g_4	GaN substrate production relative to GaAs SI substrate production
g_5	Sapphire and SiC substrate production relative to GaAs SI substrate
d_1	Density of GaAs
d_2	Density of GaP
d_3	Density of GaN
m_1	Molar mass of Ga
m_2	Molar mass of As
m_3	Molar mass of P
m_4	Molar mass of N
t_{1a}	Thickness of GaAs substrates for IC fabrication
t_{1b}	Thickness of other substrates
y_4	Yield in trimethylgallium production
y_5	Yield in crystal growth and substrate production
r_2	Collection rate, crystal growth and substrate production scrap
y_7	Yield in MOCVD deposition
y_9	Yield in MBE deposition
y_{10}	Yield in sputtering deposition
q_1	Wafer breakage and non-working devices loss, fabrication
q_2	Backgrinding loss in IC fabrication
q_4	Backgrinding/epitaxial lift-off loss in LED fabrication
q_3	Dicing and edge loss in device fabrication
M	Mass of gallium used in production of magnets
y_{11}	Yield in fabrication of NdFeB magnets
r_4	Collection rate broken wafers and non-working devices scrap
r_5	Collection rate backgrinding and dicing scrap from IC fabricators
r_6	Collection rate backgrinding/epitaxial lift-off scrap, LED
t_2	LED deposition layer thickness
t_4	Integrated circuit deposition layer thickness
t_5	CIGS deposition layer thickness
c_4	Concentration of gallium in CIGS
W_1	CIGS PV production capacity
W_2	PV total production capacity
W_3	New installed PV electricity generation capacity
t_6	Power electronics deposition layer thickness
W_4	Power electronics GaN market
w	Power electronics GaN substrate area per unit value

Calculation of flows

The equations used to quantify the flows are explained in the following.

Primary production from zinc route:

$$X_{10\text{–}11} = Z$$

Primary production from aluminum route estimated as total primary production minus production from zinc route:

$$X_{6\text{–}11} = Y - Z$$

Loss during extraction from Bayer liquor estimated from process output and yield y_1 in the extraction process:

$$X_{6\text{–}19} = \frac{(\mathrm{Y} - \mathrm{Z})(1 - \mathrm{y}_1)}{y_1}$$

Input to Bayer liquor extraction process also estimated from process yield:

$$X_{4\text{–}6} = \frac{(Y - Z)}{y_1}$$

Ga ending up in alumina estimated from transfer coefficient p:

$$X_{4\text{–}5} = \frac{X_{4\text{–}6} p}{1 - p}$$

Likewise, Ga ending up in red mud was calculated from transfer coefficient b:

$$X_{4\text{–}3} = \frac{X_{4\text{–}6} b}{(1 - b)(1 - p)}$$

The amount of Ga entering the Bayer process *with* Ga extraction was back-calculated from output and the transfer coefficients b and p which designate the fractions ending up in red mud and alumina (as fraction of the gallium dissolved, i.e. not going to red mud) respectively.

$$X_{1\text{–}4} = \frac{X_{4\text{–}6}}{(1 - p)(1 - b)}$$

The amount of Ga entering the Bayer process *without* Ga extraction was estimated from the total bauxite production times the share of bauxite used for alumina production times the average concentration of Ga in bauxites minus the amount entering the Bayer process *with* Ga extraction:

$$X_{1\text{–}2} = Bac_0 - X_{1\text{–}4}$$

Ga to red mud from Bayer process *without* Ga extraction was estimated from transfer coefficient b:

$$X_{2\text{–}3} = X_{1\text{–}2} b$$

Ga to alumina from Bayer process *without* Ga extraction was estimated by mass balance (input minus the fraction ending up in red mud):

$$X_{2-5} = X_{1-2} - X_{2-3}$$

Refined Ga production was taken directly from statistics:

$$X_{12-13,p} = R$$

Since the yield was assumed to be 100%, the input to the refining process is the same as the output:

$$X_{11-12,p} = R$$

Sources of gallium used in molecular beam epitaxy (MBE) for integrated circuits (IC) was estimated from area of GaAs wafers used for IC production (semi-insulating wafers), G_1, times the thickness of the deposition layer, the density of GaAs, the share of ICs produced with MBE, the molar masses of gallium and arsenic, as well as the epitaxy yield factor, y_9:

$$X_{16a-17c} = \frac{G_1 t_4 d_1 (1-h_1) 10^{-6} m_1}{(m_1 + m_2) y_9}$$

Ga in trimethylgallium (TMG) consumed was estimated from the consumption of TMG times the concentration of gallium in TMG:

$$X_{16b-17} = Tc_3$$

Ga in GaAs semiconducting (SC) substrates for LEDs was estimated from the area of GaAs semi-insulating (SI) substrates, the area of SC substrates relative to SI substrates, the thickness of SC wafers, the density of GaAs and molar masses of Ga and As:

$$X_{16c-17b} = g_2 G_1 t_{1b} d_1 \frac{m_1}{m_1 + m_2} 10^{-6}$$

Ga in GaAs substrates for ICs was estimated from the area of GaAs SI substrates, the thickness of SI wafers, the density of GaAs and the molar masses of Ga and As:

$$X_{16c-17c} = G_1 t_{1a} d_1 \frac{m_1}{m_1 + m_2} 10^{-6}$$

Total Ga in GaAs substrates was calculated from the sum of Ga in SC and SI substrates:

$$X_{16c-17} = X_{16c-17b} + X_{16c-17c}$$

Ga in GaP substrates was estimated from the area of GaAs SI wafers, the area of GaP wafers relative to GaAs SI wafers, g_3, the thickness of GaP substrates (assumed same as GaAs SC substrates), the density of GaP, and the molar masses of Ga and P. It was assumed that all GaP substrates are used to manufacture light-emitting diodes (LEDs).

$$X_{16d-17b} = g_3 G_1 t_{1b} d_2 \frac{m_1}{m_1 + m_3} 10^{-6}$$

Ga in GaN substrates was estimated from the area of GaAs SI wafers, the area of GaN wafers relative to GaAs SI wafers, g_4, the thickness of GaN wafers (assumed same as GaAs SI substrates), the density of GaN, and the molar masses of Ga and N. It was assumed that all GaN substrates are used to produce solid state lasers (other applications).

$$X_{16d-17f} = g_4 G_1 t_{1a} d_3 \frac{m_1}{m_1 + m_4} 10^{-6}$$

Total Ga in GaP and GaN substrates was calculated from the sum of the two:

$$X_{16d-17} = X_{16d-17b} + X_{16d-17f}$$

Ga in NdFeB semi-finished products was calculated directly from the estimated amount used:

$$X_{16e-17e} = M$$

Ga going into use was calculated by the material yield in fabrication of magnets:

$$X_{17e-18} = y_{11} M$$

The rest of the flows related to magnets were calculated by simple mass balances.

Ga in CIGS photovoltaics (PV) going into use was estimated from the generation capacity of newly installed CIGS PV, the standard test condition irradiance, the efficiency of the cells, the thickness of the deposition layer and the concentration of Ga in the material. The newly installed capacity of CIGS cells is not reported. Therefore, this was estimated from the total newly installed PV capacity W_3 (all technologies), and the share of CIGS in the *production* capacity in the PV industry (W_1/W_2). Since the generation capacity of PV is based on testing under standard conditions (k=1000W/m^2), this value was used to find the area of the cells from the electricity generation capacity.

$$X_{17d-18d} = \frac{W_1 W_3 t_5 c_4 10^5}{W_2 e_1 k}$$

Consumption of sputtering targets (assuming all CIGS cells are produced with sputtering) was back-calculated from the amount of Ga in installed CIGS cells, assumed breakage rate in the manufacturing process, and the yield in sputtering deposition. Note that the uncertainties of these process yield parameters are quite high.

$$X_{16a-17d} = \frac{X_{17d-18d}}{y_{10}(1-q_1)}$$

Scrap collected from CIGS production was estimated from the input to the production process, the deposition yield and the breakage rate in manufacturing, assuming that all broken cells are recycled.

$$X_{17d-14} = X_{16a-17d} y_{10} q_1$$

Uncollected scrap (*i.e.* undeposited Ga) was calculated by mass balance:

$$X_{17d-19} = X_{16a-17d} - X_{17d-14} - X_{17d-18d}$$

Total CIGS into use is equal to the CIGS going into sub-process *18d*:

$$X_{17d-18} = X_{17d-18d}$$

Total use of MBE sources and sputtering targets was calculated from the sum of the two:

$$X_{16a-17} = X_{16a-17c} + X_{16a-17d}$$

The amount of Ga in TMG used for power electronics was estimated from the GaN power electronics market size in monetary value, W_5, the area of GaN wafers per unit value, w, the thickness of the

deposition layer, the density of GaN, and the yield in the deposition process assuming metal-organic chemical vapor deposition (MOCVD).

$$X_{16b-18f,pe} = \frac{m_1}{m_1 + m_4} \frac{W_5 w t_6 d_3 10^{-6}}{y_7}$$

The amount of Ga in power electronics going into use was estimated from the input to the manufacturing process times the deposition yield, breakage loss rate, and dicing loss rate:

$$X_{17f-18,pe} = X_{16b-18f,pe} y_7 (1-q_1)(1-q_3)$$

Uncollected scrap was estimated by mass balance, assuming that no scrap is collected from this process:

$$X_{17f-19,pe} = X_{16b-18f,pe} - X_{17f-18,pe}$$

Total use of intermediate compounds (sputtering/MBE targets and sources, GaAs wafers, GaP wafers, GaN wafers and TMG) was calculated by summing up the individual flows:

$$X_{16-17} = X_{16a-17} + X_{16b-17} + X_{16c-17} + X_{16d-17} + X_{16e-17}$$

Use of refined Ga for producing sputtering targets and MBE sources was set as equal to the consumption of these, assuming no loss in this process or 100% recycling (likely because it is high purity Ga metal and simple manufacturing process).

$$X_{13-16a} = X_{16a-17}$$

Use of refined Ga for TMG production was calculated from TMG consumption, concentration of Ga in TMG and the yield in the production process:

$$X_{13-16b} = T \frac{c_3}{y_4}$$

Use of refined Ga for production of GaAs substrates was calculated from the consumption of GaAs substrates (see individual calculations above), and the yield in substrate production, y_5:

$$X_{13-16c} = \frac{(G_1 t_{1a} + g_2 G_1 t_{1b}) d_1}{y_5} \frac{m_1}{m_1 + m_2} 10^{-6}$$

Likewise, refined Ga for GaP and GaN substrates was back-calculated from the Ga in produced substrates (see equations above) and the substrate production yield, y_5. It was assumed that the substrate production yield is the same as for GaAs substrates.

$$X_{13-16d} = ((g_3 G_1 t_{1b} d_2 \frac{m_1}{m_1 + m_3}) + (g_4 G_1 t_{1b} d_3 \frac{m_1}{m_1 + m_4})) \frac{10^{-6}}{y_5}$$

Total consumption of refined Ga was then calculated by summing up individual flows:

$$X_{13-16} = X_{13-16a} + X_{13-16b} + X_{13-16c} + X_{13-16d}$$

Loss from TMG production process was calculated from input to process times the loss rate (1 minus production yield). It was assumed that none of this is recycled.

$$X_{16b-19} = X_{13-16b}(1-y_4)$$

Uncollected scrap from GaAs substrate production was calculated from process input, production yield and collection rate, r_2:

$$X_{16c-19} = X_{13-16c}(1-y_5)(1-r_2)$$

Likewise, the uncollected scrap from GaP and GaN substrate production were calculated:

$$X_{16d-19} = X_{13-16d}(1-y_5)(1-r_2)$$

Total uncollected scrap from production of intermediate compounds was found by summing up individual flows:

$$X_{16-19} = X_{16b-19} + X_{16c-19} + X_{16d-19}$$

Collected scrap from GaAs substrate production was calculated from process input, yield and collection rate:

$$X_{16c-14} = X_{13-16c}(1-y_5)r_2$$

Collected scrap from GaP and GaN substrate production was estimated by the same procedure:

$$X_{16d-14} = X_{13-16d}(1-y_5)r_2$$

Total amount of collected scrap from production of intermediate compounds was found by summing up the collected scrap from GaAs substrate production and GaP/GaN substrate production:

$$X_{16-14} = X_{16c-14} + X_{16d-14}$$

Use of Ga in TMG for GaN LED (white, blue, violet, green LED) production was estimated from the area of sapphire and silicon carbide substrates relative to GaAs SI substrates, the area of GaAs SI substrates, the thickness of the deposition layer, the density of GaN, the molar masses of Ga and N, and the deposition yield:

$$X_{16b-17a} = g_5 G_1 t_2 d_3 \frac{m_1}{m_1 + m_4} \frac{10^{-6}}{y_7}$$

Use of Ga in TMG for InGaP-based LEDs (red, orange, yellow LEDs) was estimated from the area of GaAs SC substrates and GaP substrates relative to the area of GaAs SI substrates, the area of GaAs SI substrates, the thickness of the deposition layer, the density of GaP, the molar masses of Ga and P, and the deposition yield. The factor 0.15 was introduced to correct for the stoichiometry of the InGaP deposition layer compared to GaP.

$$X_{16b-17b} = (g_2 G_1 + g_3 G_1)0.15 t_2 d_2 \frac{m_1}{m_1 + m_3} \frac{10^{-6}}{y_7}$$

Ga in TMG used for production of integrated circuits was estimated from area of SI substrates, thickness of the deposition layer, the density of GaAs, the molar masses of Ga and As, the share of GaAs ICs produced with MOCVD, and the deposition yield:

$$X_{16b-17c} = G_1 t_4 d_1 10^{-6} \frac{m_1}{m_1 + m_2} \frac{h_1}{y_7}$$

The amount of scrap collected from production of InGaP LEDs was estimated from inputs into the process, the loss rates in the different fabrication stages and the assumed collection rate:

$$X_{17b-14} = X_{16b-17b} y_7 (q_1 r_4 + (1-q_1) q_3 r_6) + (X_{16d-17b} + X_{16c-17b})(q_1 r_4 + (1-q_1) q_4 r_6 + (1-q_1)(1-q_4) q_3 r_6)$$

Scrap collected from production of ICs was estimated from process inputs, losses in the different fabrication stages, and the assumed collection rate:

$$X_{17c-14} = (X_{16a-17c}\, y_9 + X_{16b-17c} y_7)(q_1 r_4 + (1-q_1) q_3 r_5) + X_{16c-17c}(q_1 r_4 + (1-q_1) q_2 r_5 + (1-q_1)(1-q_2) q_3 r_5)$$

The total collected scrap in fabrication was found by summing up individual flows:

$$X_{17-14} = X_{17b-14} + X_{17c-14} + X_{17d-14}$$

The amount of Ga in GaN LEDs going into use was calculated from inputs to the fabrication process, the deposition yield and the loss rates due to breakage/non-functioning devices and dicing:

$$X_{17a-18} = X_{16b-17a} y_7 (1-q_1)(1-q_3)$$

The amount of Ga in InGaP LEDs going into use was calculated from inputs to the fabrication process, deposition yield and loss rates due to breakage/non-functioning devices, dicing and backgrinding/epitaxial lift-off. Note that backgrinding/epitaxial lift-off loss, q_4, is only included for the substrate term, not the deposition layer:

$$X_{17b-18} = X_{16b-17b} y_7 (1-q_1)(1-q_3) + (X_{16c-17b} + X_{16d-17b})(1-q_1)(1-q_4)(1-q_3)$$

The Ga in integrated circuits going into use was calculated from fabrication process inputs, MOCVD and MBE yields and loss rates due to breakage/non-functioning devices, dicing and backgrinding. Note that backgrinding loss only applies to the substrate term:

$$X_{17c-18} = (X_{16a-17c} y_9 + X_{16b-17c} y_7)(1-q_1)(1-q_3) + X_{16c-17c}(1-q_1)(1-q_2)(1-q_3)$$

Total amount of Ga going into use in the form of semiconductor devices (LEDs, ICs, power electronics and CIGS photovoltaics) was calculated by summing up individual flows:

$$X_{17-18} = X_{17a-18} + X_{17b-18} + X_{17c-18} + X_{17d-18} + X_{17f-18,pe}$$

Uncollected scrap from production of GaN LEDs was calculated by mass balance:

$$X_{17a-19} = X_{16b-17a} - X_{17a-18}$$

Uncollected scrap from fabrication of InGaP LEDs was calculated by mass balance:

$$X_{17b-19} = X_{16b-17b} + X_{16c-17b} + X_{16d-17b} - X_{17b-18} - X_{17b-14}$$

Uncollected scrap from fabrication of GaAs ICs was calculated by mass balance:

$$X_{17c-19} = X_{16a-17c} + X_{16b-17c} + X_{16c-17c} - X_{17c-18} - X_{17c-14}$$

Total uncollected scrap from fabrication was found by summing up individual flows:

$$X_{17-19} = X_{17a-19} + X_{17b-19} + X_{17c-19} + X_{17d-19} + X_{17f-19,pe}$$

Recycled material going to refining was calculated from inputs to recycling and the recycling yield, y_3, assuming that all recycled Ga is refined. This is likely, because it is the same companies doing recycling and refining, who mostly serve the semiconductor device industry.

$$X_{11-12,s} = y_3(X_{16-14} + X_{17-14})$$

Refined production from secondary material (production scrap), is assumed to be the same as input to refining, since the refining process has a net yield close to 100%:

$$X_{12-13,s} = X_{11-12,s}$$

Loss from the recycling process was calculated from input to recycling and recycling yield:

$$X_{14-19} = (X_{16-14} + X_{17-14})(1 - y_3)$$

Stockpiling of refined gallium was estimated by mass balance:

$$X_{13-15} = X_{12-13,s} + X_{12-13,p} - X_{13-16}$$

Decomposition of flows (Figure 2 in main paper)

The decomposition of primary Ga demand, demand for refined Ga and demand for Ga in intermediate compounds was done using the following equations:

Primary demand from GaN-based LEDs:

$$Primary_{LED1} = \frac{X_{16b-17a}}{y_4 y_2}$$

Primary demand from InGaP-based LEDs. This takes into account the that some of demand is covered by secondary material (the last two terms).

$$Primary_{LED2} = \frac{X_{16b-17b}}{y_4 y_2} + \frac{X_{16c-17b}}{y_5 y_2} - X_{16c-17b}\frac{(1-y_5)r_2 y_3 y_2}{y_5} - X_{17b-14} y_3 y_2$$

Primary demand from integrated circuits, also taking into account recycling (last two terms):

$$Primary_{IC} = \frac{X_{16a-17c}}{y_2} + \frac{X_{16c-17c}}{y_5 y_2} - X_{16c-17c}\frac{(1-y_5)r_2 y_3 y_2}{y_5} - X_{17c-14} y_3 y_2$$

Primary demand from photovoltaics, also taking into account recycling (second term):

$$Primary_{PV} = \frac{X_{16a-17d}}{y_2} - X_{17d-14} y_3 y_2$$

The total refined metal (primary and secondary) for GaN-based LEDs:

$$Metal_{LED1} = \frac{X_{16b-17a}}{y_4 y_2}$$

The total refined metal (primary and secondary) for InGaP-based LEDs:

$$Metal_{LED2} = \frac{X_{16b-17b}}{y_4 y_2} + \frac{X_{16c-17b}}{y_5 y_2}$$

The total refined metal (primary and secondary) for integrated circuits:

$$Metal_{IC} = \frac{X_{16a-17c}}{y_2} + \frac{X_{16c-17c}}{y_5 y_2}$$

The total refined metal (primary and secondary) for photovoltaics:

$$Metal_{PV} = \frac{X_{16a-17d}}{y_2}$$

Ga in intermediate compounds for GaN-based LEDs:

$$Semi_{LED1} = X_{16b-17a}$$

Ga in intermediate compounds for InGaP-based LEDs:

$$Semi_{LED2} = X_{16b-17b} + X_{16c-17b}$$

Ga in intermediate compounds for integrated circuits:

$$Semi_{IC} = X_{16a-17c} + X_{16c-17c}$$

Ga in intermediate compounds for photovoltaics:

$$Semi_{PV} = X_{16a-17d}$$

Model for accumulation of Ga in Bayer liquor

The fraction of Ga lost to alumina depends on how long the gallium is allowed to accumulate in the Bayer liquor before it is extracted. In the case that no Ga extraction occurs (assuming that the liquor is not discarded after a certain number of loops), the system will reach steady state, and the amount of Ga dissolved in the liquor for each batch will be the same as that precipitated to aluminum hydroxides, *i.e.* the loss to alumina is 100%. This fact, combined with the typical concentration of Ga in aluminum (100-200 ppm),[58] was used to back-calculate how much of the Ga ends up in the red mud, and it was found to be 30-50%. It was assumed that most alumina is produced without a Ga extraction loop, which later was confirmed by quantification of the other flows. To estimate how much gallium is lost to alumina when Ga is extracted from the liquor, it is necessary to make an assumption about how long the gallium is allowed to accumulate, *i.e.*, until what concentration does Ga accumulate before the liquor is removed for Ga extraction. There is not much information available about this, and it is also likely that this varies a lot between different producers. A higher concentration of Ga is better for the extraction process, but leads to a higher loss to alumina. However, since there is currently an oversupply of gallium, it was assumed that a more efficient extraction process is favored over larger amounts produced. We made a model similar to that used by Hudson to estimate the relationship between the number of accumulation cycles and Ga concentration in Bayer liquor. Figure S2 shows how Ga builds up in the Bayer liquor. The model was calibrated against the results presented by Hudson,[12] which gave a distribution coefficient of 0.3 between the concentration of Ga in precipitated hydrates and the concentration in the liquor. We assumed that Ga accumulates in the liquor until it reaches 90% of the steady state concentration, i.e. 0.14 g/l, meaning that 40% of the Ga dissolved from bauxite enters the Ga extraction process.

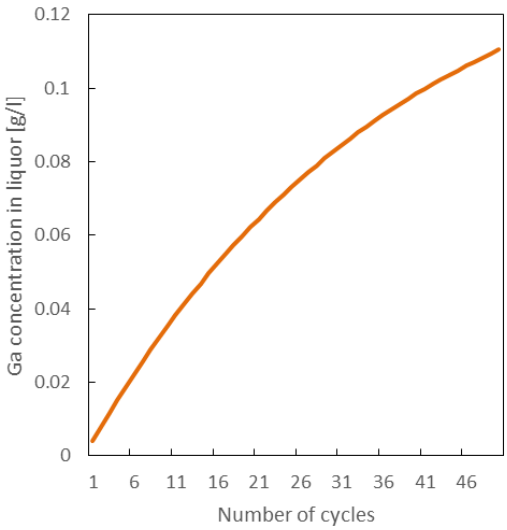

Figure S2. Gallium concentration in Bayer liquor as function of the number of cycles of dissolving bauxite and precipitation of aluminum hydroxide.

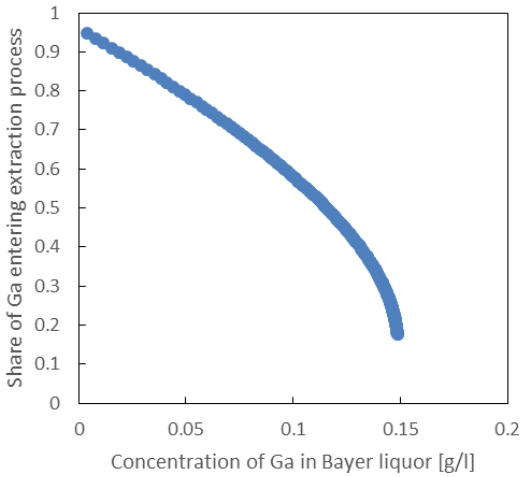

Figure S3. Share of Ga entering extraction process as a function of the concentration to which Ga is allowed to accumulate in the Bayer liquor, assuming 33 ppm Ga in bauxite. Higher concentrations lead to lower amount of Ga entering the extraction process. Steady state can be observed around 0.15 g/l. We assumed that the concentration builds up to 0.14 g/l, which means that 40% of the Ga would enter the extraction process.

3. Monte Carlo simulation

The Monte Carlo simulation was performed with MATLAB.[59] All parameters with uncertainty above zero were treated as random variables. Transfer coefficients (parameters limited between 0 and 1) were given a beta distribution and all other parameters were given a normal distribution. Uncertainties (standard deviations) were estimated based on the quality of data and knowledge about processes. The beta distribution is defined by the parameters α and β, which are related to the standard deviation and mean by the following relations:

$$\alpha = \mu^2 \left(\frac{1-\mu}{\sigma^2} - \frac{1}{\mu} \right)$$

$$\beta = \alpha \left(\frac{1}{\mu} - 1 \right)$$

Using the defined probability distributions, 100 000 sets of the parameters were drawn, and for each of the sets, a complete system quantification was done using the equations in chapter 2 of this supplementary information. Confidence intervals, mean and median were calculated for each system variable.

4. Detailed results

The detailed results of the quantification and Monte Carlo simulation are shown in Table S3. Note that the consumption of TMG, $X_{16b\text{-}17}$ was calculated using two approaches and is therefore listed twice.

Table S3. Results from the Monte Carlo simulation. All values are in metric tons/year.

Variable	***Description***	***Mean***	***Stand. dev.***	***16th percentile***	***Median***	***84th percentile***
$X_{1\text{-}2}$	Bauxite input to non-Ga Bayer process	9290	2284	7124	9254	11504
$X_{1\text{-}4}$	Bauxite input to Ga-extr. Bayer process	1521	993	830	1265	2125
$X_{2\text{-}3}$	Red mud from non-Ga Bayer process	3508	1225	2319	3396	4702
$X_{2\text{-}5}$	Alumina from non-Ga Bayer process	5782	1772	4055	5694	7514
$X_{4\text{-}3}$	Red mud from Ga-extr. Bayer process	605	492	261	476	909
$X_{4\text{-}5}$	Alumina from Ga-extr. Bayer process	613	558	234	462	945
$X_{4\text{-}6}$	Gallium entering extraction process from Bayer route	304	47	257	303	350
$X_{6\text{-}11}$	Primary production of gallium metal from Bayer route	288	44	244	288	332
$X_{6\text{-}19}$	Loss from extraction process	15	10	6	13	25
$X_{6\text{-}11}$	Primary gallium to refining	160	16	144	160	176
$X_{10\text{-}11}$	Primary production of gallium metal from zinc route	4	1	3	4	5
$X_{11\text{-}15}$	Primary unrefined gallium going into stockpiles	47	50	-2	47	96
$X_{11\text{-}12,p}$	Refined gallium from primary production	160	16	144	160	176
$X_{11\text{-}12,s}$	Refined gallium from recycling	82	22	60	80	103
$X_{14\text{-}11}$	Recycled material going to refining	82	22	60	80	103
$X_{14\text{-}19}$	Loss from recycling	9	5	4	8	14
$X_{13\text{-}15}$	Gallium going into stockpiles	27	29	-2	28	56
$X_{13\text{-}16a}$	Refined gallium used in production of sputtering targets and MBE sources	13	5	8	12	17
$X_{13\text{-}16b}$	Refined gallium used in the production of TMG	15	2	12	15	17
$X_{13\text{-}16c}$	Refined gallium used in the production of GaAs substrates	176	34	143	174	209
$X_{13\text{-}16d}$	Refined gallium used in the production of GaP and GaN substrates	12	3	9	12	15
$X_{13\text{-}16}$	Consumption of refined gallium	215	37	179	213	251
$X_{16b\text{-}19}$	Loss from production of TMG	1	1	0	1	2
$X_{16c\text{-}19}$	Loss from production of GaAs substrates	42	15	28	41	57
$X_{16d\text{-}19}$	Loss from production of GaP and GaN substrates	3	1	2	3	4
$X_{16\text{-}19}$	Loss to landfills from compound production	47	16	31	45	62
$X_{16c\text{-}14}$	Recycling from production of GaAs substrates	72	20	53	70	91
$X_{16d\text{-}14}$	Recycling from production of GaP and GaN substrates	5	2	3	5	6
$X_{16\text{-}14}$	Recycling from compound production	77	21	57	75	97
$X_{16a\text{-}17}$	Consumption of sputtering targets and MBE sources	13	5	8	12	17

Table S3 cont.

Variable	*Description*	*Mean*	*Stand. dev.*	*16th percentile*	*Median*	*84th percentile*
$X_{16b\text{-}17}$	Consumption of TMG	13	2	11	13	15
$X_{16c\text{-}17}$	Consumption of GaAs substrates	61	10	51	61	71
$X_{16d\text{-}17}$	Consumption of GaP and GaN substrates	4	1	3	4	5
$X_{16e\text{-}17e}$	Ga in NdFeB to produce permanent magnets	85	17	68	85	102
$X_{16\text{-}17}$	Consumption of intermediate compounds	176	21	155	176	197
$X_{16a\text{-}17c}$	Use of sputtering targets and MBE sources for ICs	1	1	0	1	1
$X_{16a\text{-}17d}$	Use of sputtering targets and MBE sources for PV	12	5	7	11	16
$X_{16b\text{-}17a}$	Use of TMG for production of GaN LEDs	10	8	5	8	15
$X_{16b\text{-}17b}$	Use of TMG for production of InGaP LEDs	0	0	0	0	1
$X_{16b\text{-}17c}$	Use of TMG for production of ICs	1	1	0	1	1
$X_{16b\text{-}17f,\ pe}$	Use of TMG for production of power electronics	0	0	0	0	0
$X_{16b\text{-}17}$	Total use of TMG (estimated from substrates area)	11	8	5	9	16
$X_{16c\text{-}17b}$	Use of GaAs substrates for InGaP LEDs	26	6	20	25	32
$X_{16c\text{-}17c}$	Use of GaAs substrates for ICs	35	6	30	35	41
$X_{16d\text{-}17b}$	Use of GaP substrates for InGaP LEDs	3	1	3	3	4
$X_{16d\text{-}17f}$	Use of GaN substrates for lasers and other applications	1	0	1	1	1
$X_{17a\text{-}19}$	Scrap lost from production of GaN LEDs	9	7	4	7	14
$X_{17b\text{-}19}$	Scrap lost from production of InGaP LEDs	17	6	11	17	23
$X_{17c\text{-}19}$	Scrap lost from production of ICs	28	7	22	29	35
$X_{17d\text{-}19}$	Scrap lost from production of PV	7	4	3	6	10
$X_{17e\text{-}19}$	Scrap lost from production of NdFeB magnets	26	10	16	24	35
$X_{17f,\ pe\text{-}19}$	Scrap lost from production of power electronics	0	0	0	0	0
$X_{17\text{-}19}$	Total scrap loss to landfills from fabrication	87	18	70	86	104
$X_{17b\text{-}14}$	Collected scrap from production of InGaP LEDs	8	5	4	7	14
$X_{17c\text{-}14}$	Collected scrap from production of ICs	5	6	1	3	8
$X_{17d\text{-}14}$	Collected scrap from production of PV	0	0	0	0	1
$X_{17\text{-}14}$	Total collected scrap from fabrication	14	8	7	12	21
$X_{17a\text{-}18}$	GaN LEDs going into use	0.6	0.2	0.5	0.6	0.8
$X_{17b\text{-}18}$	InGaP LEDs going into use	3.7	2.0	1.8	3.4	5.7
$X_{17c\text{-}18}$	ICs going into use	3.9	0.8	3.0	3.8	4.7
$X_{17d\text{-}18}$	PV going into use	4.6	1.5	3.2	4.4	6.0
$X_{17e\text{-}18}$	NdFeB magnets going into use	59	15	45	59	74
$X_{17f,\ pe\text{-}18}$	Power electronics going into use	0.0	0.0	0.0	0.0	0.0
$X_{17\text{-}18}$	Total gallium entering use	72	15	57	72	87

5. References

(1) Burton, J. D.; Culkin, F.; Riley, J. P. The abundances of gallium and germanium in terrestrial materials. *Geochim. Cosmochim. Acta* **1959**, *16* (1–3), 151–180.

(2) Butcher, T.; Brown, T. Gallium. In *Critical Metals Handbook*; Gunn, G., Ed.; John Wiley & Sons, 2014; pp 150–176.

(3) Schulte, R. F.; Foley, N. K. *Compilation of gallium resource data for bauxite deposits: U.S. Geological Survey Open-File Report 2013-1272*; 2014. http://pubs.usgs.gov/of/2013/1272/ (accessed 21 November 2014).

(4) United States Geological Survey. Gallium. In *2012 Minerals Yearbook*; Jaskula, B. W., Ed.; Washington DC, 2014. http://minerals.usgs.gov/minerals/pubs/commodity/gallium/myb1-2012-galli.pdf (accessed 9 January 2015).

(5) Orbite Aluminae Inc. Orbite: A strategic gallium producer http://www.orbitealuminae.com/media/upload/filings/Gallium_Version_1_1.pdf (accessed Sep 26, 2014).

(6) Fang, Z.; Gesser, H. D. Recovery of gallium from coal fly ash. *Hydrometallurgy* **1996**, *41* (2-3), 187–200.

(7) Gutiérrez, B.; Pazos, C.; Coca, J. Recovery of gallium from coal fly ash by a dual reactive extraction process. *Waste Manag. Res.* **1997**, *15* (4), 371–382.

(8) Font, O.; Querol, X.; Juan, R.; Casado, R.; Ruiz, C. R.; López-Soler, Á.; Coca, P.; Peña, F. G. Recovery of gallium and vanadium from gasification fly ash. *J. Hazard. Mater.* **2007**, *139* (3), 413–423.

(9) Xu, K.; Deng, T.; Liu, J.; Peng, W. Study on the recovery of gallium from phosphorus flue dust by leaching with spent sulfuric acid solution and precipitation. *Hydrometallurgy* **2007**, *86* (3–4), 172–177.

(10) Kou, X.; Li, S.; Liu, Q.; Xi An Sunresin Technology Ltd. New method for extracting gallium from Bayer mother liquor through chelating resin. Patent CN102321802 (B), 2013. http://worldwide.espacenet.com/publicationDetails/biblio?CC=CN&NR=102321802B&KC=B&FT=D (accessed 9 September 2014).

(11) Zhao, Z.; Yang, Y.; Xiao, Y.; Fan, Y. Recovery of gallium from Bayer liquor: A review. *Hydrometallurgy* **2012**, *125*, 115–124.

(12) Hudson, L. K. Gallium as a by-Product of Alumina Manufacture. *J. Met.* **1965**, *17* (9), 948–951.

(13) Graedel, T. E.; Allwood, J.; Birat, J. P.; Reck, B. K.; Sibley, S. F.; Sonnemann, G.; Buchert, M.; Hagelüken, C. *Recycling rates of metals - A status report, A report of the working group on the global metal flows to the international resource panel*; United Nations Environment Programme, 2011. http://www.unep.org/resourcepanel/Portals/24102/PDFs/Metals_Recycling_Rates_110412-1.pdf (accessed 9 January 2015).

(14) Eichler, S. Green Gallium Arsenide (GaAs) Substrate Manufacturing. In *2012 International Conference on Compound Semiconductor Manufacturing Technology, CS ManTech 2012*; Boston, Massachusettes, USA, 2012.

(15) Kramer, D. A. *Gallium and gallium arsenide : supply, technology, and uses*; U.S. Dept. of the Interior, Bureau of Mines: Pittsburgh, PA, 1988. http://archive.org/details/galliumgalliumar00kram (accessed 24 September 2014).

(16) Chen, W.-T.; Tsai, L.-C.; Tsai, F.-C.; Shu, C.-M. Recovery of Gallium and Arsenic from Gallium Arsenide Waste in the Electronics Industry. *CLEAN – Soil Air Water* **2012**, *40* (5), 531–537.
(17) Lee, M. S.; Ahn, J. G.; Oh, Y. J. Production of high-purity indium and gallium metals by vacuum refining. *Mater. Trans.* **2002**, *43* (12), 3195–3198.
(18) Fan, J.; Jin, L.; Liu, S.; Liu, W.; Nanjing Jinmei Gallium Co., Ltd. Large-scale production method for preparing high purity gallium. Patent CN102618734 (B), 2013. http://worldwide.espacenet.com/publicationDetails/biblio?CC=CN&NR=102618734B&KC=B&FT=D (accessed 24 September 2014).
(19) Ghosh, K.; Mani, V. N.; Dhar, S. Numerical study and experimental investigation of zone refining in ultra-high purification of gallium and its use in the growth of GaAs epitaxial layers. *J. Cryst. Growth* **2009**, *311* (6), 1521–1528.
(20) Bollong, A. B. I.; Bult, R. P.; Proux, G. T. Method for the zone refining of gallium. Patent US4888051 (A), 1989. http://worldwide.espacenet.com/publicationDetails/biblio?FT=D&date=19891219&DB=&locale=&CC=US&NR=4888051A&KC=A&ND=1 (accessed 23 September 2014).
(21) Greber, J. F. Gallium and Gallium Compounds. In *Ullmann's Encyclopedia of Industrial Chemistry*; Wiley-VCH Verlag GmbH & Co. KGaA: Weinheim, Germany, 2000.
(22) Kern, W. Zone refining of gallium trichloride: Radiochemical method for determining the distribution of components in a column and its application in analyzing the zone refining effectiveness in purifying gallium trichloride. *J. Electrochem. Soc.* **1963**, *110* (1), 60–65.
(23) Yamamura, T.; Kato, H.; Ohgami, T.; Tayama, K.; Okuda, K.; Dowa Mining Co., Ltd. Refining Process for High Purity Gallium for Producing Compound Semiconductor and Apparatus for the Same. Patent EP1099770 (A1), 2007. http://worldwide.espacenet.com/publicationDetails/biblio?CC=EP&NR=1099770B1&KC=B1&FT=D (accessed 10 October 2014).
(24) Hall, T. *Personal communication with Todd Hall, Manager, Raw Material Procurement & Sales, Molycorp Rare Metals Inc., Utah, USA, November 2014*; 2014.
(25) Jurisch, M.; Börner, F.; Bünger, T.; Eichler, S.; Flade, T.; Kretzer, U.; Köhler, A.; Stenzenberger, J.; Weinert, B. LEC- and VGF-growth of SI GaAs single crystals—recent developments and current issues. *J. Cryst. Growth* **2005**, *275* (1–2), 283–291.
(26) Starowieyski, K. B.; Chwojnowski, A.; Jankowski, K.; Lewiński, J.; Zachara, J. Synthesis and purification of trimethylgallium for MOCVD: molecular structure of (KF)4·4(Me3Ga). *Appl. Organomet. Chem.* **2000**, *14* (10), 616–622.
(27) Karch, R.; Rivas-Nass, A.; Frey, A.; Burkert, T.; Woerner, E.; Doppiu, A.; Umicore AG & CO. KG. Process for Preparing Trialkylgallium Compounds. U.S. Patent application 20140256974 A1, 2013. http://patentscope.wipo.int/search/en/WO2013083450 (accessed 9 September 2014).
(28) Revin, M. V.; Artemov, A. N.; Sazonova, E. V. A new synthetic route to trimethylgallium. *Russ. J. Appl. Chem.* **2013**, *86* (9), 1359–1363.
(29) Weimar, A. High Brightness LEDs: Manufacturing and Applications. In *2011 International Conference on Compound Semiconductor Manufacturing Technology, CS ManTech 2011*; Indian Wells, California, USA, 2011.
(30) Grady, T.; Thompson, K.; Crow, A. M.; Ridsdale, D. *LED Spotlight*; Edison Investment Research: London, UK, 2013. http://www.edisoninvestmentresearch.com/sectorreports/LEDreportJune2013.pdf (accessed 9 January 2015).

(31) Pelzel, R. A comparison of MOVPE and MBE growth technologies for III-V epitaxial structures. In *28th International Conference on Compound Semiconductor Manufacturing Technology, CS ManTech 2013*; New Orleans, LA, 2013; pp 105–108.
(32) Higham, E. GaAs Industry Overview and Forecast: 2011 - 2016. In *28th International Conference on Compound Semiconductor Manufacturing Technology, CS ManTech 2013*; New Orleans, LA, 2013; pp 13–16.
(33) Kaelin, M.; Rudmann, D.; Tiwari, A. N. Low cost processing of CIGS thin film solar cells. *Sol. Energy* **2004**, *77* (6), 749–756.
(34) Hibberd, C. J.; Chassaing, E.; Liu, W.; Mitzi, D. B.; Lincot, D.; Tiwari, A. N. Non-vacuum methods for formation of Cu(In, Ga)(Se, S)2 thin film photovoltaic absorbers. *Prog. Photovolt. Res. Appl.* **2010**, *18* (6), 434–452.
(35) Izumi, S.; Shirahama, H.; Kouji, Y. Environmental safety issues for molecular beam epitaxy platform growth technology. *J. Cryst. Growth* **2001**, *227–228*, 150–154.
(36) Marwede, M.; Reller, A. Estimation of Life Cycle Material Costs of Cadmium Telluride- and Copper Indium Gallium Diselenide-Photovoltaic Absorber Materials based on Life Cycle Material Flows. *J. Ind. Ecol.* **2014**, *18* (2), 254–267.
(37) Freiberger Compound Materials. GaAs wafers specifications http://www.freiberger.com/en/products/gaas-wafers/specifications.html (accessed Jul 24, 2014).
(38) Wei, R.-C.; Wang, H.-W.; Chin, C.-C.; Chiang, S.; Her, J.; Chen, P.-W.; Huang, K.; Hua, C.-H. Yield improvement for thin 50 µm GaAs product line. In *2012 International Conference on Compound Semiconductor Manufacturing Technology, CS ManTech 2012*; Boston, MA, 2012.
(39) Darley, B.; Singh, M.; Santos, P.; Ambrocio, E.; Tiku, S. GaAs Wafer Breakage Reduction. In *2014 International Conference on Compound Semiconductor Manufacturing Technology, CS ManTech 2014*; Denver, Colorado, USA, 2014.
(40) Ho, W.-J.; Liu, J.; Chou, H. C.; Wu, C. S.; Tsai, T. C.; Chang, W. D.; Chou, F.; Wang, Y. C. Manufacturing of GaAs ICs for Wireless Communications Applications. *J. Semicond. Technol. Sci.* **2006**, *6* (3), 136–145.
(41) Bai, G.; Gao, R. W.; Sun, Y.; Han, G. B.; Wang, B. Study of high-coercivity sintered NdFeB magnets. *J. Magn. Magn. Mater.* **2007**, *308* (1), 20–23.
(42) Mizoguchi, T.; Sakai, I.; Niu, H.; Inomata, K.; Tsutai, A. Permanent Magnet. US Patent 4,935,075, June 19, 1990. http://worldwide.espacenet.com/publicationDetails/biblio?CC=US&NR=4935075A&KC=A&FT=D
(43) Binnemans, K.; Jones, P. T.; Blanpain, B.; Van Gerven, T.; Yang, Y.; Walton, A.; Buchert, M. Recycling of rare earths: a critical review. *J. Clean. Prod.* **2013**, *51*, 1–22.
(44) Herchenroeder, J. *Personal communication with James Herchenroeder, Vice President Technology; Molycorp Magnequench*; 2015.
(45) Peter, M.; Engl, K.; Baumann, F.; Wirth, R.; Laubsch, A.; Baur, J.; Hahn, B. Recent progress in high efficiency InGaN LEDs. In *2010 Conference on Lasers and Electro-Optics (CLEO) and Quantum Electronics and Laser Science Conference (QELS)*; San Jose, CA, 2010; pp 1–2.
(46) Baumgartner, T.; Wunderlich, F.; Wee, D.; Jaunlich, A.; Sato, T.; Erxleben, U.; Bundy, G.; Bundsgaard, R. *Lighting the way: Perspectives on the lighting market*; McKinsey & Company, Inc., 2011.
(47) Broell, M.; Sundgren, P.; Rudolph, A.; Schmid, W.; Vogl, A.; Behringer, M. New developments on high-efficiency infrared and InGaAlP light-emitting diodes at OSRAM Opto Semiconductors. In *Proc. SPIE 9003, Light-Emitting Diodes: Materials,*

Devices, and Applications for Solid State Lighting XVIII, 90030L; San Francisco, CA, 2014; Vol. 9003, pp 1–6.
(48) He, G.; Zheng, L. Color temperature tunable white-light light-emitting diode clusters with high color rendering index. *Appl. Opt.* **2010**, *49* (24), 4670–4676.
(49) DenBaars, S. P.; Feezell, D.; Kelchner, K.; Pimputkar, S.; Pan, C.-C.; Yen, C.-C.; Tanaka, S.; Zhao, Y.; Pfaff, N.; Farrell, R.; et al. Development of gallium-nitride-based light-emitting diodes (LEDs) and laser diodes for energy-efficient lighting and displays. *Acta Mater.* **2013**, *61* (3), 945–951.
(50) Habib, K.; Wenzel, H. Exploring rare earths supply constraints for the emerging clean energy technologies and the role of recycling. *J. Clean. Prod.* **2014**, *84*, 348–359.
(51) Du, X.; Restrepo, E.; Widmer, R.; Wäger, P. Quantifying the distribution of critical metals in conventional passenger vehicles using input-driven and output-driven approaches: a comparative study. *J. Mater. Cycles Waste Manag.* **2015**.
(52) Blaser, F.; Castelanelli, S.; Wäger, P. A.; Widmer, R. *Seltene Metalle in Elektro- und Elektronikaltgeräten - Vorkommen und Rückwinnungstechnologien*; Bundesamt für Umwelt: Bern, Switzerland, 2011. http://www.bafu.admin.ch/abfall/01472/01478/index.html?lang=de&download=NHzLpZeg7t,lnp6I0NTU042l2Z6ln1acy4Zn4Z2qZpnO2Yuq2Z6gpJCHdYB,gmym162epYbg2c_JjKbNoKSn6A-- (accessed 9 January 2015).
(53) Sakai, S.; Yoshida, H.; Hiratsuka, J.; Vandecasteele, C.; Kohlmeyer, R.; Rotter, V. S.; Passarini, F.; Santini, A.; Peeler, M.; Li, J.; et al. An international comparative study of end-of-life vehicle (ELV) recycling systems. *J. Mater. Cycles Waste Manag.* **2014**, *16* (1), 1–20.
(54) Widmer, R.; Du, X.; Haag, O.; Restrepo, E.; Wäger, P. A. Scarce Metals in Conventional Passenger Vehicles and End-of-Life Vehicle Shredder Output. *Environ. Sci. Technol.* **2015**.
(55) *ZAR Annual Report 2013*; Waste and Resource Management; Stiftung Zentrum für Nachhaltige Abfall- und Ressourcennutzung: Switzerland, 2013. http://www.zar-ch.ch/fileadmin/user_upload/Contentdokumente/Oeffentliche_Dokumente/ZAR_GB_2013_EN_web.pdf (accessed 7 August 2014).
(56) Reuter, M.; Hudson, C.; van Schaik, A.; Heiskanen, K.; Meskers, C.; Hagelüken, C. *Metal Recycling: Opportunities, Limits, Infrastructure, A Report of the Working Group on the Global Metal Flows to the International Resource Panel.*; United Nations Environment Programme, 2013. http://www.unep.org/resourcepanel/Portals/24102/PDFs/Metal_Recycling-Full_Report_36dpi_130919.pdf (accessed 22 May 2014).
(57) Schleup, M.; Hagelüken, C.; Kuehr, R.; Magalini, F.; Maurer, C.; Meskers, C.; Mueler, E.; Wang, F. *Recycling - From e-waste to resources*; Sustainable Innovation and Technology Transfer Sector Studies; UNEP-StEP, 2009. http://www.unep.org/pdf/Recycling_From_e-waste_to_resources.pdf (accessed 17 December 2014).
(58) Senel, E.; Walmsley, J. C.; Diplas, S.; Nisancioglu, K. Liquid metal embrittlement of aluminium by segregation of trace element gallium. *Corros. Sci.* **2014**, *85*, 167–173.
(59) *MATLAB Version 8.1.0.430 (R2013a)*; The MathWorks Inc., 2013.

Paper V

Strategies for securing rising gallium supply under boundary conditions of aluminum stock dynamics

Løvik, A. N.; Restrepo, E.; Müller, D. B., 2015, Submitted to Environmental Science & Technology.

Strategies for securing rising gallium supply under boundary conditions of aluminum stock dynamics

Amund N. Løvik [*] [†] [‡], *Eliette Restrepo* [†] [‡], *Daniel B. Müller* [†] [‡]

[†] Industrial Ecology Programme and Department of Energy and Process Engineering, Norwegian University of Science and Technology (NTNU), NO-7491, Trondheim, Norway

[‡] Empa, Swiss Federal Laboratories for Materials Science and Technology, CH-9014, St. Gallen, Switzerland

ABSTRACT

Future availability of byproduct metals, essential for existing and emerging technologies, is governed by the demand for the more commonly used carrier metals. This linkage, while recognized in past studies, has not been adequately taken into account in resource availability estimates. Here, we assess the future global availability of gallium by comparing scenarios for gallium demand from the five most important applications with the gallium supply potential, which is determined through scenarios for the global cycle of aluminum, the main carrier metal of gallium. We found that longer-term gallium demand is highly uncertain; the gallium supply potential is heavily influenced by the development of the in-use stocks and recycling rates of aluminum; with current applications, a shortage of gallium is unlikely by 2050; however, the gallium industry may need to introduce ambitious recycling- and material efficiency strategies to meet its demand; if in-use stocks of aluminum saturate or even decline, a shift to other gallium sources such as zinc or coal fly ash may be required. Traditional mineral resource classification systems and life cycle impact assessment methods do not account for the linkages between byproduct and carrier metals and therefore require appropriate extensions to provide meaningful information about resource depletion.

INTRODUCTION

The limited availability of metals is often suggested as a possible constraint for widespread use of emerging technologies, such as photovoltaics (PV) and electric vehicles.[1–5] These concerns are justified: Mineral resources are finite stocks in the lithosphere, which possess the capacity to become exhausted. The concept of fixed geological stocks has therefore been used to assess the future availability of a range of metals and other mineral resources,[5–8] and is also used in life cycle impact assessment, such as the abiotic depletion potential in the CML method.[9] However, most metals are not mined primarily for their own sake, but are produced as minor byproducts of more common metals.[10,11] The value of the byproduct metal is, (by definition), too small to justify mining of the mineral, so mining activity is driven exclusively by the demand for the "carrier" metal. As a consequence, future availability of byproduct metals is limited by the anthropogenic flows of the carrier metal, rather than geological stocks of the byproduct metals. This should be taken into account in resource availability estimates by conceptualizing these resources as flows, as illustrated in Fig. 1.

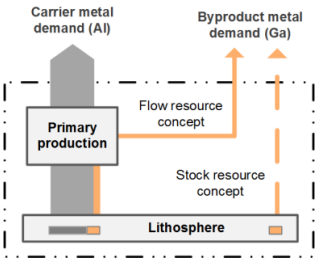

Figure 1 Illustration of the difference between a stock- and flow resource concept for a byproduct metal. The stock resource concept regards the byproduct independently from its carrier metal, *e.g.* by comparing production to reserves in the lithosphere. The flow resource concept links the availability of the byproduct metal directly to the production of the carrier metal. Because availability of the byproduct metal is determined by demand for the carrier metal, the stock resource concept is inadequate for evaluating byproduct metal availability.

The "byproduct constraint" to metal supply was brought to attention by Verhoef et al., and has subsequently been picked up by the research community. In criticality assessments, it is sometimes included, although in a highly simplified manner.[12] For example, in the methodology of Graedel et al., the percentage of the metal produced as a byproduct is weighted and added up with a normalized depletion time (a stock-based concept) and other indicators to arrive at an overall supply risk indicator.[13] Such calculations can be useful to create a list of critical metals that should be monitored, but they do not provide any quantitative estimate of future availability or demand. Only a handful of studies have conceptualized byproduct metals as flow-based resources:[10,14–20] Long and Smith used a simple model to look at large scale employment of GaAs PV and a possible limitation of gallium supply,[18] Verhoef et al. and Nakamura et al. investigated silver and bismuth availability for lead-free solder,[10,14] while Fthenakis, Houari et al., Fizaine, Stamp et al., and Bustamante and Gaustad analyzed availability of tellurium, indium and/or gallium for thin film PV.[15–17,19,20] These studies all take the perspective of a single technological shift and its potential restriction due to resource availability. Demand from other applications is usually modelled as a constant or ignored completely. Only Stamp et al. modelled the use in other applications explicitly, using exponential growth functions; however, they did not model the carrier metal cycle.[19] By focusing only on one application, the hypothesis of a resource constraint may be confirmed, but it may not be rejected: there could always be additional demand from other applications. While it is impossible to include all possible future uses, it would be beneficial to include at least the most important current applications. More importantly, past studies have a limited consideration of the future production of the carrier metals, using either Hubbert curves,[16,17] exponential growth,[15,18,20] static production,[10,14] or no explicit modelling of future supply.[19] None of these approaches link the production of the carrier metal to its in-use stocks or the

service levels provided. Hence, they neither take into account the socio-economic drivers nor stock dynamics, which are decisive factors for the long-term demand for major metals.[21] To address these shortcomings, we explore potential future supply restrictions and mitigation strategies by modeling the linkages between the cycles of gallium and its carrier metal aluminum.

Gallium is produced as a byproduct of aluminum, and is today mainly used in integrated circuits (ICs), light emitting diodes (LEDs), PV, and as an alloying element in neodymium ferrite boron (NdFeB) permanent magnets.[22] Primary production of gallium has grown rapidly in the last years, from below 100 tons/year before 2010 to 440 tons/year in 2014.[23,24] This growth is usually attributed to increasing use of GaAs in mobile phones. Considering the main end uses and applications of gallium, i.e. information technology (IT), telecommunications, energy efficient lighting, renewable energy, and electrified transport, a continued growth in gallium demand is expected. However, gallium supply may be restricted by the development of the aluminum cycle. For example, a slow-down of the growth of aluminum in-use stocks could lead to a drop in demand for primary aluminum and reduce the supply potential of gallium accordingly, a trend which may be exacerbated by efforts to increase scrap collection and recycling efficiency.[25] We therefore address the following research questions: (i) What are likely future trajectories for gallium supply potential, given the influence of stock dynamics in the aluminum cycle? (ii) Under what conditions, relating to expansion of emerging technologies, may primary gallium demand grow beyond supply potential? (iii) Which measures can be taken to ensure sufficient gallium supply for existing and emerging technologies, and how effective are these measures?

METHODS

A dynamic material flow model of the global gallium cycle was developed and used to quantify the demand for primary gallium from the five most important applications, as well as the future supply potential from the bauxite/alumina route. A mathematical description and details on scenario development and data sources are in the SI, and the most important features are explained here. The demand model includes the following key processes: refining to high-purity gallium, crystal growth and substrate production (GaAs, GaP), production of trimethylgallium, fabrication of GaN-LEDs, fabrication of GaAs/GaP-LEDs, fabrication of GaAs ICs, fabrication of CIGS PV, manufacturing of NdFeB permanent magnets, recycling, and use (general lighting, automotive, mobile phones, other IT/telecom. equipment, renewable energy, others). It takes the following inputs: (i) parameters describing the yields, recycling rates and other relevant characteristics of the production chains, from semi-finished product manufacturing to device fabrication and recycling, as well as the lifetimes of products, (ii) time series of demand for the five most important applications: GaN-based LEDs, GaAs/GaP-based LEDs, GaAs ICs, copper indium gallium diselenide (CIGS) PV, and NdFeB magnets, in physical units (device area or mass). The demand model calculates stocks and flows of the gallium system, in particular the global demand for primary gallium.

Input data for group (i) were obtained from a previous quantification of the gallium cycle. [22] The following expected lifetimes were assumed for products in use: 15 years for automobiles,[26] 10 years for general lighting,[27] 3.25 years for mobile phones (estimated in this work), 6 years for other IT and telecom equipment (based on computers),[28] 25 years for PV,[29,30] 20 years for wind turbines,[31] and 8 years for all other applications. The standard deviation of the lifetime probability normal distribution was set to one fifth of the expected lifetime.

The time series data of group (ii) define the differences between the demand scenarios. These were constructed individually for each of the five applications, relying on previously published projections [27,32,33] and smaller models developed in this work which are briefly explained in the following and in detail in the SI. The set of demand projections was generated by combining different development paths for CIGS PV and NdFeB magnets with the baseline projection from LEDs and ICs. For LEDs and ICs, only one scenario was defined (baseline), due to the limited capacity of these applications to cause a significant gallium demand. The scenarios are labeled according to the difference in assumptions for the demand for magnets and PV as well as the penetration of gallium-based technology in these applications: *M* and *m* refer to high and low demand for NdFeB magnets respectively, while the following + or – refers to high (100%) or low (20%) penetration rate of gallium as an alloying element in NdFeB magnets, assumed to be used at 0.5% wt; *P* and *p* refer to high and low demand for PV respectively, while the following + or – refers to high (40%) and low (5%) future penetration rate of CIGS in the PV market. The low magnet and PV demand (*m*, *p*) correspond to the assumed developments in the International Energy Agency (IEA) 6DS (6 degree Celsius) scenario while the high magnet and PV demand (*M, P*) correspond to the 2DS-HR (2 degree Celsius, high renewable energy) scenario.[33]

The projections for gallium in magnets are based on demand scenarios for NdFeB magnets by Habib and Wenzel,[32] (which are again based on the IEA climate change mitigations scenarios) and a logistic function for the penetration rate of gallium alloying in magnet production. Note that even the *m* scenarios involve a large growth due to traditional applications such as computers. The penetration rate of gallium alloying was assumed to saturate at 20% (today's level), or 100% in the – and + scenarios respectively. Mass fraction of gallium in magnets was assumed to remain constant at 0.5% when used.

146 The projections for CIGS PV are based on the IEA scenarios for climate change mitigation
147 (6DS, 4DS, 2DS, 2DS-HR),[33] which give the delivered electricity from PV in TWh, and a
148 logistic function for increased market penetration of CIGS. A stock-driven lifetime based
149 model was used to calculate the required production of PV cells to meet the solar PV electricity
150 supply of the IEA scenarios, assuming a lifetime of 25 years. The 6DS scenario, here equivalent
151 to *p*, assumes 900 TWh of electricity supplied in 2050, while the 2DS-HR scenario, equivalent
152 to *P*, assumes 6200 TWh.[33] The penetration rate of CIGS was assumed to saturate at 5%, or
153 40% in the –/+ scenario respectively.

154 The projection for ICs was developed in this work, using a stock-driven model for mobile
155 phones, penetration rate of smartphones in the market, and number and size of GaAs chips in
156 smart phones and standard mobile phones. Historic data on sales of standard phones and
157 smartphones were used to calibrate a logistic function for the future penetration rate of
158 smartphones, assuming saturation at 90% (from 54% in 2013). The number of mobile phones
159 per capita was also calibrated as a logistic function, assuming saturation at 1.05 (0.9 in 2013).
160 Historic data on the number and size of GaAs power amplifiers was gathered from suppliers
161 and technical papers.

162 The LED area entering use was broken down into general lighting, liquid crystal display
163 backlighting, automotive, and signage and others. Projections are based on lighting market
164 scenarios by McKinsey & Company,[27] which indicate that LED lighting will have a market
165 share above 70% in most general lighting sectors by 2020. It was assumed that LED market
166 share saturates at 90% in the 2030's for general lighting, automotive and signage and others.
167 For backlighting, it was assumed to approach zero, as LEDs are expected to be replaced by
168 organic LED. The scenarios result in an increase from 10 bn. mm^2 GaN-LED device area
169 entering use in 2012, to 80 bn. mm^2 in 2050. GaAs/GaP-LED grows from 10 bn. mm^2 in 2012

to 35 bn. mm^2 in 2050. Note that the amount of gallium required per area LED is much higher for GaAs/GaP than for GaN, due to the use of sapphire or silicon carbide substrates in the latter.

Projections of the supply potential were calculated from previously published scenarios for the global aluminum cycle that determine the level of alumina production,[25] average gallium mass fraction in bauxite produced today (49 ppm),[34,35] loss rate to red mud (38%), loss rate to alumina (60% of what remains after red mud loss), and extraction yield (95%).[22] The alumina projections are determined by saturation level of aluminum in-use stocks (L = 200 kg/cap, M = 400 kg/cap, H = 600 kg/cap), saturation time (2050, 2075, 2100), and whether near-perfect collection of scrap is implemented (*NPC*) or not (*BAU*), using a stock-driven material flow model.[25] Gallium production from other raw material sources, such as zinc leach residue (< 3% of production) and coal fly ash (currently not used), were not included in the model.

RESULTS

Fig. 2 shows historic primary production, refining to high purity, modelled demand and supply potential under different scenarios, and the contributions from each application to demand in 2050. The supply potential in 2050 ranges from 1700 tons/year (NPC L2100) to 11000 tons/year (BAU H2075). The effect of the different conditions in the aluminum cycle can be observed by comparing other scenarios to the lowest projection, NPC L2100. Aluminum scrap collection greatly influences the gallium supply potential: Without implementation of near-perfect collection, the supply potential projection instead reaches 2900 tons/year in 2050 (BAU L2100), 70% higher than with near-perfect collection. Saturation time has a relatively small impact (NPC L2050), giving a supply potential of 1900 tons/year in 2050, but may lead to a lower supply potential in the second half of the century. With a medium saturation level (NPC M2100), the supply potential reaches 4300 tons/year in 2050, which is higher than all demand

194 projections except the maximum (M+P+). The highest supply potential scenarios (BAU
195 H2075, NPC H2075) remain far above any of the demand scenarios.

196

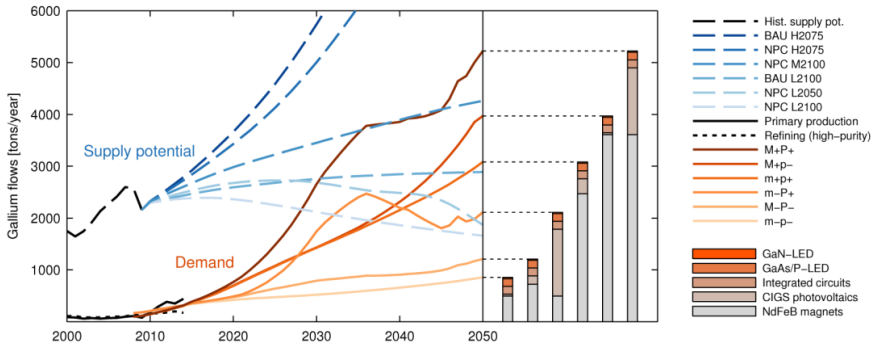

197

198 **Figure 2** Modelled world primary Ga demand and supply potential, and historic primary
199 production and refining (left). Supply potential projections vary due to different saturation
200 levels (*L* = 200 kg/cap, *M* = 400 kg/cap, *H* = 600 kg/cap) and time (2050, 2075, 2100) of
201 aluminum in-use stocks, and whether near-perfect collection (*NPC*) of aluminum scrap is
202 implemented or not (*BAU* = business as usual). Demand projections vary due to different
203 development paths for Ga in NdFeB magnets and CIGS photovoltaics. *M* = high magnet
204 demand, *m* = low magnet demand, *P* = high PV demand, *p* = low PV demand, +/- indicate high
205 or low penetration of gallium-containing technology in the magnet- or PV markets. Breakdown
206 of primary Ga demand into the five applications in 2050 for the different scenarios (right).

207

208 The lowest demand projection (*m-p-*) is mainly a continuation of current trends. Demand for
209 NdFeB magnets continues to grow fast, while the share of magnets produced with gallium as
210 an alloying element remains at today's level (~20%), resulting in a gallium demand from

magnets that increases from about 85 tons/year today to 500 tons/year in 2050. Demand for PV grows slightly and the share of CIGS in the PV market remains similar as today (5%), causing a growth from around 10 tons/year to 40 tons/year in 2050 for PV applications. The demand growth for ICs slows down significantly after 2020, due to saturation of smart phones in the handset market and the number of mobile phones per capita globally. In 2050, the demand for primary gallium due to ICs has grown to 150 tons/year, from today's 60 tons/year. Rapid penetration of LEDs in the general lighting and automotive markets drives a growing demand for both types of LEDs. However, this is somewhat dampened by the expected replacement of LED-backlit liquid crystal displays with organic LED technology. The primary gallium requirements of LEDs reach 150 tons/year and 30 tons/year from GaAs/GaP-LEDs and GaN-LEDs respectively. In total, primary gallium demand amounts to 900 tons/year in 2050, which is still far below the lowest supply potential at 1700 tons/year.

The second lowest demand scenario (M-P-) involves high demand for magnets and PV, corresponding to the IEA *2DS-HR*, while the penetration rates of gallium-containing technologies in the magnet- and PV markets remain the same as today. This scenario leads to a demand of 1200 tons/year in 2050. High PV and magnet demand alone does not drive gallium demand beyond the supply potential; it only occurs when the penetration rate of CIGS or gallium alloying in magnets increases from today's level. The next scenario, *m-P+*, illustrates the highest modelled demand from CIGS. A rapid growth in PV deployment together with an increased market penetration of CIGS from 3% to 40% causes demand to exceed the lowest supply potential curve around 2030. Gallium demand peaks at 2500 tons/year in 2036 due to slower growth of the PV in-use stock, and declines to 2100 tons/year in 2050. The *m+p+* scenario shows the effect of increased penetration rate of CIGS and gallium alloying in magnets without the rapid demand increase for PV and magnets driven by climate change mitigation. In this case, primary demand grows steadily to pass the minimum supply potential in 2038, and

reaches 3100 tons/year in 2050. It should be noted that even in the *6DS* scenario, demand for magnets is expected to increase significantly from today's level.[32] Increased market share of gallium-containing magnets would not on its own cause such a dramatic change. The *M*+*p*- scenario shows the maximum contribution of magnets, causing demand to reach 4000 tons/year in 2050. The combined effect of high PV demand, high magnet demand, and increased penetration rates of CIGS and gallium alloying in magnets can be seen in the *M*+*P*+ scenario. Here, demand exceeds the lowest supply potential curve already in 2029, and reaches 5200 tons/year in 2050.

The model results start from 2008, which allows for comparison with the reported primary production in recent years. In 2008 and 2009, most scenarios give results that are reasonably close to the reported primary production. From 2010, the reported primary production diverges from the reported high purity refining and the model results. Among the most common applications, all but NdFeB magnets require high purity gallium. It therefore seems very likely that the large growth seen in recent years is in part due to this application. The scenarios with a high penetration rate of gallium in magnets show a similar rate of growth as the reported production, but with about two years delay.

There are many options to reduce the demand for primary gallium. However, the effectiveness of these options may change significantly over the next decades (Figure 3). Due to the possible shift of importance from ICs and LEDs toward magnets and PV, the impact of individual measures can be very different in 2015 and 2050. In 2015, the most effective measure is to improve collection of scrap from crystal growth and substrate production. An improvement from 63% collection rate to 98% could reduce primary gallium demand with 16%. A reduced substrate thickness from 650 µm to 450 µm could lower primary demand with 13%. However, this supposes that process yields remain constant, which is unlikely due to the

nature of the production process: thinner wafers break more often, and imply more scrap from cutting per kg output. Other options include recycling of gallium from magnet production scrap (from 0% to 98% collection rate: -10% demand), improved yield in crystal growth and substrate production (from 35% to 50%: -10% demand), and improved collection of IC fabrication scrap (from 10% to 98%, -9% demand). In 2050 in the M+P+ scenario, the most effective measures would be recycling of gallium from magnet fabrication scrap (-16% demand), reduced thickness of CIGS cells (-12%), improved collection of scrap from PV fabrication (-11%) or improved yield in sputtering deposition (-11%). End-of-life (EOL) recycling has almost no effect in 2015, but could contribute significantly in 2050. Some of the measures are redundant. For example, improved yield in the substrate production process has a very small effect after the introduction of near perfect collection. Increased yield in secondary production on the other hand, would have a higher impact if introduced together with increased scrap collection for recycling. The effects of individual interventions discussed here are dependent on the context of the overall system, and are therefore not cumulative.

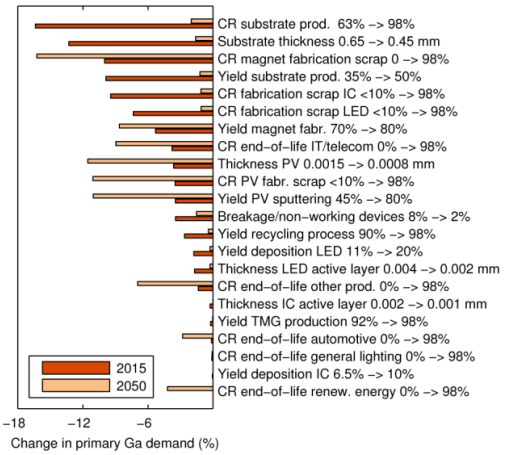

Figure 3 Effect of system improvements on world primary gallium demand in 2015, and 2050 under the maximum demand scenario (M+P+). *CR* = collection rate, the share given scrap collected for Ga recovery. Note that some scrap flows, e.g. magnet production scrap, are recycled today, but not for Ga recovery. The large effect of reducing substrate thickness originates from reduced losses in device manufacturing; lower yield in substrate manufacturing is not taken into account.

Industry can use a portfolio of measures to secure gallium supply in the case of maximum demand and minimum supply potential (see cumulative effects for scenario M+P+ in Figure 4). On the supply side, there is a high potential for reducing the loss of gallium to alumina by extracting gallium more frequently from the Bayer liquor, possibly increasing the supply potential by as much as 50%. An additional 3% increase may be obtained by improving the efficiency of the extraction process itself. Combined, these changes would lead to a 55% increase in supply and a 51% reduction of demand, which is just enough to avoid a shortage.

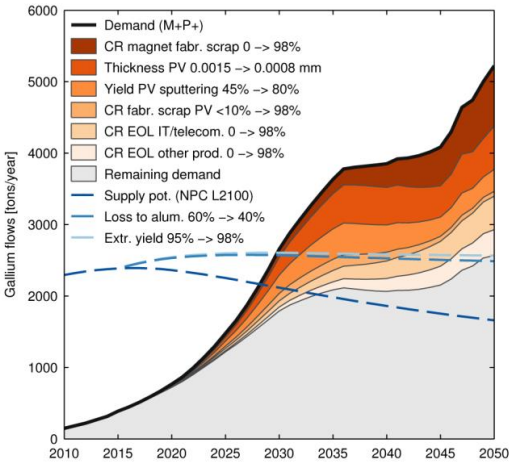

Figure 4 Example of how to ensure sufficient availability of Ga under the maximum demand projection (M+P+) and minimum supply projection (NPC L2100), through gradual system improvements. Parameters were changed linearly to reach the best value in 2050. Areas (white to red) show cumulative effect of individual improvements on demand when they are applied in the order from top to bottom. Dashed lines show the supply potential: minimum scenario (dark blue) with reduced loss to alumina (middle blue), with both supply side measures (light blue). *CR* = collection rate, *EOL* = end-of-life.

DISCUSSION

This analysis did not include an estimation of the potential demand from other applications, such as low melting point alloys, catalysts and piezoelectric materials.[36] To contribute significantly to future gallium demand, these applications would have to grow by several orders of magnitude. Although it seems unlikely, this possibility cannot be ruled out completely. It was further assumed that the average gallium mass fraction in bauxite remains at the current level of 49 ppm, varying between 28 ppm (Western Guanxi, China) and 75 ppm (Caribbean)

gallium by mass. While in the next few decades, average gallium content in mined bauxite is likely to remain similar to today's, this may change in the longer term. The largest known bauxite reserves are found in Australia and Guinea. While Australian bauxites have a relatively high gallium content (59 ppm), data for those of Guinea were not available. Measurements for African bauxites (43 ppm) [34] are on average slightly lower than the current global average, however, the variation within Africa is large.

We found that demand for gallium from current applications may exceed the future supply potential if the following two conditions are met: (i) the market share of gallium-containing technologies, CIGS or gallium alloying of NdFeB magnets, increases significantly from today's level, (ii) the aluminum in-use stock grows slowly to approach a saturation level of 200 kg/cap. Rapidly increasing demand from NdFeB magnets seems likely given past development, while CIGS producers face tough competition from other technologies, and have not been able to increase their market share lately.[24,37] Integrated circuits and LEDs appear not to have the potential to cause large increases in demand for primary gallium although significant growth is expected. An aluminum in-use stock of 200 kg/cap is similar to current levels in the United Kingdom, France or Spain, but lower than current levels of Japan (~350 kg/cap), Germany and Austria (~400 kg/cap), or The United States and The Netherlands (>500 kg/cap).[25] Reaching this level globally by the end of the century still implies significant growth from today's level of 100 kg/cap, and can be regarded as a likely development.

If demand grows beyond the supply potential, there are many opportunities for reducing primary gallium demand or increasing the supply potential. Recycling of manufacturing scrap can have a large impact on the overall material efficiency in the system, but may be severely limited by economics. Gallium recovery from recycling of NdFeB manufacturing scrap is currently not economic [38] because gallium prices are low [24,39] and the value of neodymium in

magnets is more than 10 times that of gallium. Similarly, both the price and weight fraction in CIGS of gallium are smaller than that of indium.[40–42] End-of-life recycling could play an important role in the future, but is economically even less attractive than recycling of production scrap. Most of the gallium entering use is as an alloying element at less than 1% of the mass in NdFeB magnets, which again constitute a small part of the product in which they are used. Today, not even neodymium is recovered from this end-of-life material.[43] Improved yield and thickness reductions in manufacturing of CIGS can have a large effect on primary demand, and are likely developments to reduce costs,[17,29] but may render recycling less economic. Similar yield improvements cannot be expected for magnets. However, gallium in NdFeB magnets is not essential, but is used for minor improvements of the properties.[44,45] Hence, gallium in magnets may in the future act as a buffer: its use can be reduced if gallium demand for other applications is rising, short term or long term. Stockpiling of the byproduct metal on expectations of high demand in the future may be regarded as a viable strategy, particularly if production of the carrier metal is expected to decline. However, the large uncertainties related to future demand and the high investment risks may discourage such measures. Environmental impacts and energy requirements of extraction, possibly with no associated benefit for many years, provide another argument against this strategy.

We conclude that a constraint to future use of gallium-containing technologies due to gallium supply is unlikely over the coming decades. Nevertheless, a move from primary to secondary production and substantial material efficiency improvements may be needed to meet demand, possibly already before 2030. Beyond 2050, stock saturation in the aluminum cycle could further reduce gallium supply potential and necessitate a shift towards alternative primary sources such as zinc leach residue or coal fly ash. Coal fly ash could provide a source of gallium

355 in the same order of magnitude as from bauxite per year,[46] with extraction efficiency above
356 60%.[47] Large stocks of gallium also exist in red mud holding ponds as a result of past alumina
357 production. Depending on the cost of extraction from alternative sources compared to the cost
358 of increased recycling and yield improvements, shift to alternative sources may happen earlier.

359 This study demonstrated that the future supply potential from bauxite is highly dependent on
360 the development of the aluminum cycle. For other byproduct metals, the future resource
361 availability may be even more complex. For example, the use of zinc is closely related to that
362 of steel, leading some authors to discuss whether a saturation of the steel stock would also
363 imply saturation of the zinc stock, with further implications for indium extraction as a
364 byproduct of zinc.[19] Tellurium is another example for which resource availability assessments
365 would benefit from a more refined development of scenarios for future in-use stocks and
366 primary production of the carrier metal, copper.

367 In the case presented here, there is virtually no technological correlation between the use of
368 the two metals, aluminum and gallium, which justifies an independent development of supply
369 potential and demand scenarios. In other cases however, the opposite might be true, for
370 example the linkage between copper production and tellurium supply. While a technology such
371 as CdTe thin-film PV may be limited by tellurium availability, its deployment will require large
372 amounts of copper,[4] and therefore simultaneously increase the supply potential of tellurium.
373 Such indirect correlations between the demand for a byproduct metal and its supply potential
374 may be modelled, as has been done in case studies on the introduction of lead free solder.[10,14]
375 Realizing the importance of such linkages, a natural methodological development would be the
376 integration of several metal production and use systems in one model. While this could allow
377 for a better representation of linkages, such integration would lead to highly complex models
378 that may have limited usefulness for systems understanding. Order of magnitude changes of

demand for minor metals are, as illustrated here, driven by technological shifts rather than socio-economic variables such as population and affluence. The detailed knowledge of individual technologies and their production systems thus required to create reasonable scenarios may be difficult to reconcile with a complete integration of many material cycles in one model. A possible way forward could be development of integrated scenarios only for carrier metals (Al, Sn, Ni, Cu, Pb, Zn, Cr),[10] which can consistently take into account the correlation between their use, socioeconomic drivers and stock dynamics. Resource availability of byproduct metals could then be evaluated over these background scenarios through case studies incorporating detailed knowledge of relevant applications and production systems.

Using gallium as an example, this study showed that an assessment of the practical future resource availability of byproduct metals requires an understanding of their linkages with their carrier metals as well as a shift in the conceptualization of these resources as flows rather than stocks. As a consequence of the flow nature of byproduct mining, resource depletion of the byproduct metals is caused by the mining of the carrier metal. Extraction of a byproduct metal only reduces its concentration in carrier metal or mining waste. Current assessments of resource availability are based on resource classification systems that exclusively focus on stocks of mineral resource deposits and neglect the flow nature of byproduct mining. They are therefore insufficient to provide meaningful insights into practical future resource availability for byproduct metals. Since most of the metals considered to be critical are mined as byproducts of carrier metals, it is of highest importance to complement and harmonize efforts for the standardization of mineral information systems with efforts to characterize metal cycles and their linkages.

The absence of causality between byproduct extraction and geological depletion also has important consequences for how these resources should be considered in life cycle assessments.

For example, in the CML method for life cycle impact assessment, an abiotic depletion potential is calculated for a metal from annual production and reserves.[9] We argue that such depletion potential should not be assigned to byproduct metals, at least when production is far below the supply potential. To the extent that depletion of geological resources is taking place, it is driven by extraction of the carrier metal. This point has not been taken up in recent discussions on abiotic resource depletion in LCA,[48,49] even though the majority of metals are produced as byproducts.

ASSOCIATED CONTENT

Supporting Information Available.

System definition, mathematical model description, data sources and scenario development can be found in the Supporting Information. This material is available free of charge via the Internet at http://pubs.acs.org.

AUTHOR INFORMATION

Corresponding Author

* (A.N.L.); e-mail: amund.lovik@ntnu.no, amund.loevik@gmail.com; phone: +47 41 69 70 86, +41 79 667 98 74; fax: +47 73 59 35 80

Author Contributions

The manuscript was written through contributions of all authors. All authors have given approval to the final version of the manuscript.

Notes

The authors declare no competing financial interest.

ACKNOWLEDGMENTS

We thank Gang Liu for aluminum productions scenarios, Komal Habib for NdFeB magnet production scenarios, and Brian Jaskula, Eric Higham, Todd Hall, James Herchenroeder, Shiban Tiku and Stefan Eichler for data clarifications and information on industry processes.

ABBREVIATIONS

BAU – business as usual, CIGS – copper indium gallium diselenide, CR – collection rate, EOL – end-of-life, IC – integrated circuit, IEA – international energy agency, LCA – life cycle assessment, LED – light emitting diode, NPC – near-perfect collection, PV – photovoltaics

REFERENCES

(1) Graedel, T. E.; Harper, E. M.; Nassar, N. T.; Reck, B. K. On the materials basis of modern society. *Proc. Natl. Acad. Sci.* **2015**, *112* (20), 6295–6300.

(2) Feltrin, A.; Freundlich, A. Material considerations for terawatt level deployment of photovoltaics. *Renew. Energy* **2008**, *33* (2), 180–185.

(3) Kushnir, D.; Sandén, B. A. The time dimension and lithium resource constraints for electric vehicles. *Resour. Policy* **2012**, *37* (1), 93–103.

(4) Hertwich, E. G.; Gibon, T.; Bouman, E. A.; Arvesen, A.; Suh, S.; Heath, G. A.; Bergesen, J. D.; Ramirez, A.; Vega, M. I.; Shi, L. Integrated life-cycle assessment of electricity-supply scenarios confirms global environmental benefit of low-carbon technologies. *Proc. Natl. Acad. Sci.* **2015**, *112* (20), 6277–6282.

(5) Alonso, E.; Field, F. R.; Kirchain, R. E. Platinum Availability for Future Automotive Technologies. *Environ. Sci. Technol.* **2012**, *46* (23), 12986–12993.

(6) Gordon, R. B.; Bertram, M.; Graedel, T. E. Metal stocks and sustainability. *Proc. Natl. Acad. Sci.* **2006**, *103* (5), 1209–1214.

(7) Zuser, A.; Rechberger, H. Considerations of resource availability in technology development strategies: The case study of photovoltaics. *Resour. Conserv. Recycl.* **2011**, *56* (1), 56–65.

(8) Elshkaki, A.; Graedel, T. E. Dynamic analysis of the global metals flows and stocks in electricity generation technologies. *J. Clean. Prod.* **2013**, *59*, 260–273.

(9) Guinée, J. B.; Gorrée, M.; Heijungs, R.; Huppes, G.; Kleijn, R.; Koning, A. de; Oers, L. van; Wegener Sleeswijk, A.; Suh, S.; Udo de Haes, H. A.; et al. *Handbook on life cycle assessment. Operational guide to the ISO standards.*; Kluwer Academic Publishers: Dordrecht, 2002.

(10) Verhoef, E. V.; Dijkema, G. P. J.; Reuter, M. A. Process Knowledge, System Dynamics, and Metal Ecology. *J. Ind. Ecol.* **2004**, *8* (1-2), 23–43.

(11) Graedel, T. E.; Harper, E. M.; Nassar, N. T.; Nuss, P.; Reck, B. K. Criticality of metals and metalloids. *Proc. Natl. Acad. Sci.* **2015**, *112* (14), 4257–4262.

(12) Achzet, B.; Helbig, C. How to evaluate raw material supply risks—an overview. *Resour. Policy* **2013**, *38* (4), 435–447.

(13) Graedel, T. E.; Barr, R.; Chandler, C.; Chase, T.; Choi, J.; Christoffersen, L.; Friedlander, E.; Henly, C.; Jun, C.; Nassar, N. T.; et al. Methodology of Metal Criticality Determination. *Environ. Sci. Technol.* **2012**, *46* (2), 1063–1070.

(14) Nakamura, S.; Murakami, S.; Nakajima, K.; Nagasaka, T. Hybrid Input−Output Approach to Metal Production and Its Application to the Introduction of Lead-Free Solders. *Environ. Sci. Technol.* **2008**, *42* (10), 3843–3848.

(15) Fizaine, F. Byproduct production of minor metals: Threat or opportunity for the development of clean technologies? The PV sector as an illustration. *Resour. Policy* **2013**, *38* (3), 373–383.

(16) Houari, Y.; Speirs, J.; Candelise, C.; Gross, R. A system dynamics model of tellurium availability for CdTe PV. *Prog. Photovolt. Res. Appl.* **2014**, *22* (1), 129–146.

(17) Fthenakis, V. Sustainability of photovoltaics: The case for thin-film solar cells. *Renew. Sustain. Energy Rev.* **2009**, *13* (9), 2746–2750.

(18) Long, L. W.; Smith, S. Possible material supply constraints for photovoltaic solar cells. *Min. Congr. J.* **1980**, *66* (7), 43–44.

(19) Stamp, A.; Wäger, P. A.; Hellweg, S. Linking energy scenarios with metal demand modeling–The case of indium in CIGS solar cells. *Resour. Conserv. Recycl.* **2014**, *93*, 156–167.

(20) Bustamante, M. L.; Gaustad, G. Challenges in assessment of clean energy supply-chains based on byproduct minerals: A case study of tellurium use in thin film photovoltaics. *Appl. Energy* **2014**, *123*, 397–414.

(21) Müller, D. B.; Wang, T.; Duval, B. Patterns of Iron Use in Societal Evolution. *Environ. Sci. Technol.* **2011**, *45* (1), 182–188.

(22) Løvik, A. N.; Restrepo, E.; Müller, D. B. The Global Anthropogenic Gallium System: Determinants of Demand, Supply and Efficiency Improvements. *Environ. Sci. Technol.* **2015**, *49* (9), 5704–5712.

(23) United States Geological Survey. Minerals Yearbook: Gallium, various years 1988-2012; Jaskula, B. W., Kramer, D. A., Eds.; 2014.

(24) United States Geological Survey. Mineral Commodity Summaries 2015: Gallium; Jaskula, B. W., Ed.; 2015.

(25) Liu, G.; Bangs, C. E.; Müller, D. B. Stock dynamics and emission pathways of the global aluminium cycle. *Nat. Clim. Change* **2012**, *3*, 338–342.

(26) Oguchi, M.; Fuse, M. Regional and Longitudinal Estimation of Product Lifespan Distribution: A Case Study for Automobiles and a Simplified Estimation Method. *Environ. Sci. Technol.* **2015**, *49* (3), 1738–1743.

(27) Baumgartner, T.; Wunderlich, F.; Wee, D.; Jaunlich, A.; Sato, T.; Erxleben, U.; Bundy, G.; Bundsgaard, R. *Lighting the way: Perspectives on the lighting market*; McKinsey & Company, Inc., 2011. http://www.mckinsey.com/~/media/mckinsey/dotcom/client_service/Automotive%20and%20Assembly/Lighting_the_way_Perspectives_on_global_lighting_market_2012.ashx (accessed January 9, 2015)

(28) Babbitt, C. W.; Kahhat, R.; Williams, E.; Babbitt, G. A. Evolution of Product Lifespan and Implications for Environmental Assessment and Management: A Case Study of Personal Computers in Higher Education. *Environ. Sci. Technol.* **2009**, *43* (13), 5106–5112.

(29) IEA. *Solar Photovoltaic Energy*; Organisation for Economic Co-operation and Development: Paris, 2010.

(30) Turkenburg, W. C.; Arent, D. J.; Bertani, R.; Faaij, A.; Hand, M.; Krewitt, W.; Larson, E. D.; Lund, J.; Mehos, M.; Merrigan, T.; et al. Chapter 11 - Renewable Energy. In *Global Energy Assessment - Toward a Sustainable Future*; Cambridge University Press and International Institute for Applied Systems Analysis: Cambridge, UK; New York, NY, USA and Laxenburg, Austria, 2012; pp 761–900.

(31) Rademaker, J. H.; Kleijn, R.; Yang, Y. Recycling as a Strategy against Rare Earth Element Criticality: A Systemic Evaluation of the Potential Yield of NdFeB Magnet Recycling. *Environ. Sci. Technol.* **2013**, *47* (18), 10129–10136.

(32) Habib, K.; Wenzel, H. Exploring rare earths supply constraints for the emerging clean energy technologies and the role of recycling. *J. Clean. Prod.* **2014**, *84*, 348–359.

(33) IEA. *Energy Technology Perspectives 2014*; Organisation for Economic Co-operation and Development: Paris, 2014.

(34) Schulte, R. F.; Foley, N. K. *Compilation of gallium resource data for bauxite deposits: U.S. Geological Survey Open-File Report 2013-1272*; 2014. http://pubs.usgs.gov/of/2013/1272/ (accessed November 21, 2014)

(35) United States Geological Survey. Bauxite and alumina. In *2012 Minerals yearbook*; Bray, E. L., Ed.; United States Geological Survey: Washington DC, 2014.

(36) Butcher, T.; Brown, T. Gallium. In *Critical Metals Handbook*; Gunn, G., Ed.; John Wiley & Sons, 2014; pp 150–176.

(37) Masson, G.; Latour, M.; Rekinger, M.; Theologitis, I.-T.; Papoutsi, M. *Global market outlook for photovoltaics 2013-2017*; European Photovoltaic Industry Association: Brussels, Belgium, 2013. http://www.epia.org/fileadmin/user_upload/Publications/GMO_2013_-_Final_PDF.pdf (accessed January 15, 2015)

(38) Herchenroeder, J. *Personal communication with James Herchenroeder, Vice President Technology; Molycorp Magnequench*; 2015.

(39) United States Geological Survey. Mineral Commodity Summaries 2015: Rare earths; Gambogi, J., Ed.; 2015.

(40) Marwede, M.; Reller, A. Estimation of Life Cycle Material Costs of Cadmium Telluride- and Copper Indium Gallium Diselenide-Photovoltaic Absorber Materials based on Life Cycle Material Flows. *J. Ind. Ecol.* **2014**, *18* (2), 254–267.

(41) Tolcin, A. C. Indium. In *Mineral Commodity Summaries*; United States Geological Survey, 2015.

(42) United States Geological Survey. Gallium. In *2012 Minerals Yearbook*; Jaskula, B. W., Ed.; Washington DC, 2014.

(43) Graedel, T. E.; Allwood, J.; Birat, J. P.; Reck, B. K.; Sibley, S. F.; Sonnemann, G.; Buchert, M.; Hagelüken, C. *Recycling rates of metals - A status report, A report of the working group on the global metal flows to the international resource panel*; United Nations Environment Programme, 2011. http://www.unep.org/resourcepanel/Portals/24102/PDFs/Metals_Recycling_Rates_110412-1.pdf (accessed June 18, 2014)

(44) Bai, G.; Gao, R. W.; Sun, Y.; Han, G. B.; Wang, B. Study of high-coercivity sintered NdFeB magnets. *J. Magn. Magn. Mater.* **2007**, *308* (1), 20–23.

(45) Mizoguchi, T.; Sakai, I.; Niu, H.; Inomata, K.; Tsutai, A. Permanent Magnet. US Patent 4,935,075, June 19, 1990.

(46) Licht, C.; Peiró, L. T.; Villalba, G. Global Substance Flow Analysis of Gallium, Germanium, and Indium: Quantification of Extraction, Uses, and Dissipative Losses within their Anthropogenic Cycles. *J. Ind. Ecol.* **2015**.

(47) Font, O.; Querol, X.; Juan, R.; Casado, R.; Ruiz, C. R.; Lopez-Soler, A.; Coca, P.; Garcia Pena, F. Recovery of gallium and vanadium from gasification fly ash. *J. Hazard. Mater.* **2007**, *139* (3), 413–423.

(48) Klinglmair, M.; Sala, S.; Brandão, M. Assessing resource depletion in LCA: a review of methods and methodological issues. *Int. J. Life Cycle Assess.* **2013**, *19* (3), 580–592.

(49) Rørbech, J. T.; Vadenbo, C.; Hellweg, S.; Astrup, T. F. Impact Assessment of Abiotic Resources in LCA: Quantitative Comparison of Selected Characterization Models. *Environ. Sci. Technol.* **2014**, *48* (19), 11072–11081.

Supporting information to:

Strategies for securing rising gallium supply under boundary conditions of aluminum stock dynamics

Amund N. Løvik [*] [†] [‡], *Eliette Restrepo* [†] [‡], *Daniel B. Müller* [†] [‡]

[†] Industrial Ecology Programme and Department of Energy and Process Engineering, Norwegian University of Science and Technology (NTNU), NO-7491, Trondheim, Norway

[‡] Empa, Swiss Federal Laboratories for Materials Science and Technology, CH-9014, St. Gallen, Switzerland

[*] Corresponding author: Amund N. Løvik, Department of Energy and Process Engineering, Norwegian University of Science and Technology (NTNU), NO-7491, Trondheim, Norway; tel: +47 41697086/+41 796679874; e-mail: amund.lovik@ntnu.no/amund.loevik@gmail.com

This document stands as supporting information for the article: "Strategies for securing rising gallium supply under boundary conditions of aluminum stock dynamics".

Pages: 36

Number of figures: 10

Number of tables: 6

Contents

1. System definition S3
2. Model formulation S5
3. Parameter estimation S14
4. Scenario development S14
    4.1 Stock dynamics model S14
    4.2 Gallium supply S16
    4.3 LEDs S17
    4.4 Integrated circuits S20
    4.5 Photovoltaics S25
    4.6 NdFeB magnets S27
5. Sensitivity analysis and system improvements S29
    5.1 Sensitivity analysis S29
    5.2 Modeled system improvements S30
6. References S32

1. System definition

We used a somewhat simplified system definition compared to our previous work where we quantified the 2011 anthropogenic gallium system. This is because some flows, e.g. into stockpiles, were not included in the scenario analysis. The system variable names are the same as in the previous work.[1]

The system definition is shown in Figure S1.

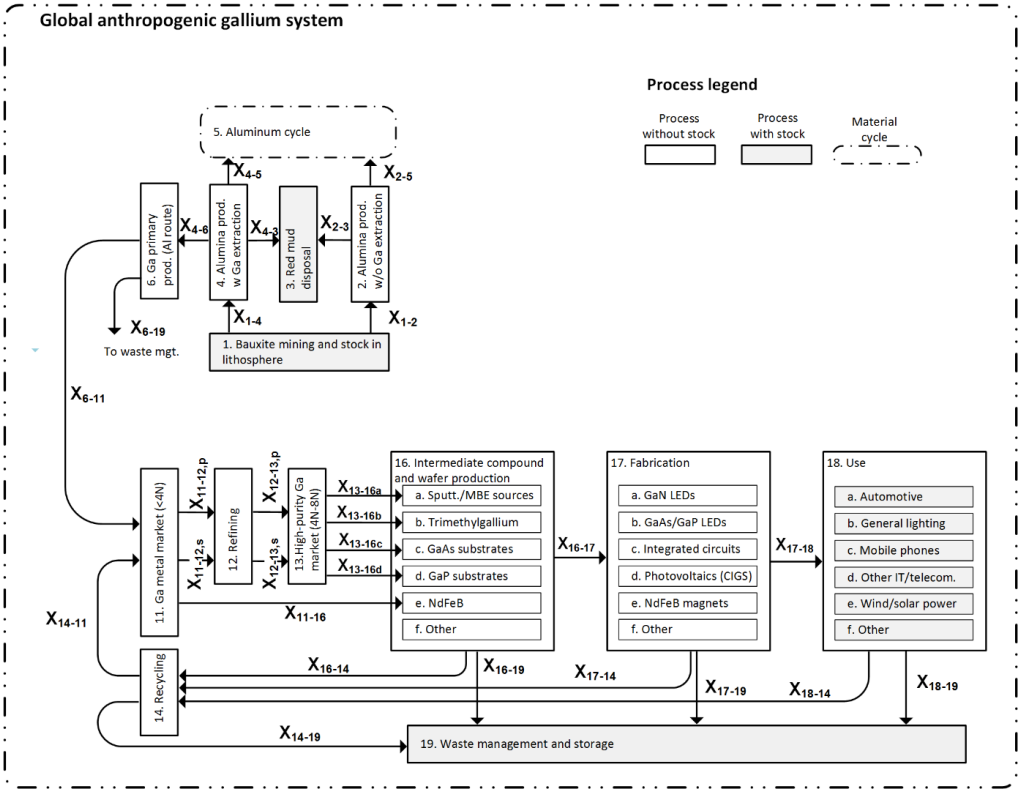

Figure S1 System definition of the global system of gallium production, manufacturing, use and recycling. Sub-flows to and from sub-processes 16a-e and 17a-e were also estimated.

The system variables are listed in Table S1. All variables refer to the gallium content. In addition, flows between sub-processes, e.g. $X_{17a\text{-}18b}$ (GaN-LEDs used in general lighting), were calculated.

Table S1 Description of system variables.

Variable name	*Description of variable*	*Units*
$X_{1\text{-}2}$	Bauxite input to non-Ga Bayer process	tons
$X_{1\text{-}4}$	Bauxite input to Ga-extr. Bayer process	tons
$X_{2\text{-}3}$	Red mud from non-Ga Bayer process	tons
$X_{2\text{-}5}$	Alumina from non-Ga Bayer process	tons
$X_{4\text{-}3}$	Red mud from Ga-extr. Bayer process	tons
$X_{4\text{-}5}$	Alumina from Ga-extr. Bayer process	tons
$X_{4\text{-}6}$	Gallium entering extraction process from Bayer route	tons
$X_{6\text{-}11}$	Primary production of gallium metal from Bayer route	tons
$X_{6\text{-}19}$	Loss from extraction process	tons
$X_{6\text{-}11}$	Primary gallium to refining	tons
$X_{11\text{-}12,p}$	Refined gallium from primary production	tons
$X_{11\text{-}12,s}$	Refined gallium from recycling	tons
$X_{14\text{-}11}$	Recycled material going to refining	tons
$X_{14\text{-}19}$	Loss from recycling	tons
$X_{13\text{-}16}$	Consumption of refined gallium	tons
$X_{16\text{-}19}$	Loss to landfills from compound production	tons
$X_{16\text{-}17}$	Total use of intermediate compounds in fabrication	tons
$X_{16\text{-}14}$	Recycling from compound production	tons
$X_{17\text{-}19}$	Total scrap loss to landfills from fabrication of devices	tons
$X_{17\text{-}14}$	Total collected scrap from fabrication	tons
Y	Maximum production of gallium from Bayer route with conventional methods	tons

2. Model formulation

A mathematical model was used to estimate the demand for refined and primary gallium as well as the maximum production by conventional methods (i.e. from the Bayer route). Scenarios were developed for the demand for the most important gallium-containing products and the maximum supply from the Bayer process. In the mathematical model, the driver for maximum supply is the mass of bauxite entering the Bayer process. The drivers of demand are: the area of GaN-LED chips entering use, the area of GaAs/GaP-LED chips entering use, the area of GaAs integrated circuit (IC) chips entering use, the area of CIGS photovoltaic cells entering use, the mass of gallium contained in NdFeB magnets entering use. Table S2 lists the drivers. The development of the scenarios for the individual application areas and bauxite entering the Bayer process is explained in section 3.

Table S2. Drivers of demand and maximum supply in scenarios for future development of the anthropogenic gallium system.

Description	*Symbol*	*Units*	*No. scenarios*	*Scenario reference*
Bauxite entering Bayer process	B	mill. tons/year	18	Liu et al. [2]
GaN-LED entering use	A_{LED1}	m^2/year	1	McKinsey and Company [3]
GaAs/GaP-LED entering use	A_{LED2}	m^2/year	1	McKinsey and Company [3]
GaAs Integrated circuits entering use	A_{IC}	m^2/year	1	This work
CIGS photovoltaics entering use	A_{PV}	m^2/year	12	IEA,[4] EPIA [5], this work
Gallium in NdFeB magnets entering use	M_{mag}	tons/year	9	Habib and Wenzel [6]

In addition to the drivers, a number of parameters were used to estimate other flows in the system. The selection of these parameters and the determination of mathematical relationships between the different flows were largely based on previous work,[1] and is explained in the following.

The model parameters are listed in Table S3.

Table S3 Description of model input parameters. All process parameters, down to prod. of GaP substrates, from [1].

Group	*Description*	*Symbol*	*Value*	*Units*
Primary prod.	Mass fraction of Ga in bauxite	x_1	$4.91 \cdot 10^{-5}$	kg/kg
	Fraction of Ga lost to red mud	k_1	0.38	1
	Fraction of Ga lost to alumina	k_2	0.60	1
	Extraction yield from Bayer liquor	y_1	0.95	1
Secondary prod.	Yield in recycling of wafer production scrap	y_2	0.92	1
	Yield in recycling of fabrication scrap (devices)	y_3	0.80	1
	Yield in recycling of end-of-life scrap	y_4	0.80	1
Fabr. of LEDs	Loss rate due to dicing of LEDs	k_3	0.31	1
	Loss rate due to non-working devices LED	k_4	0.08	1
	Thickness of LED chips	t_1	$1.4 \cdot 10^{-4}$	m
	Thickness of deposition layer of LEDs	t_2	$4 \cdot 10^{-6}$	m
	Deposition yield MOCVD	y_5	0.11	1
	Share of GaP/GaAs LEDs fabricated on GaAs substrates	h_1	0.88	1
	Collection rate of backgrinding/epitaxial lift-off scrap LEDs	r_1	0.30	1
	Collection rate other LED fab. scrap	r_2	0	1
Fabr. of IC	Loss rate due to dicing of integrated circuits	k_5	0.15	1
	Loss rate due to non-working devices IC	k_6	0.08	1
	Thickness of integrated circuit chips	t_3	$1.0 \cdot 10^{-4}$	m
	Thickness of deposition layer	t_4	$2.0 \cdot 10^{-6}$	m
	Deposition yield MBE	y_6	0.07	1
	Share of integrated circuits produced with MOCVD	h_2	0.67	1
	Collection rate backgrinding scrap IC	r_3	0.10	1
	Collection rate other scrap IC fab.	r_4	0	1
Fabr. PV	Loss rate due to non-working photovoltaics	k_7	0.08	1
	Deposition yield photovoltaics	y_7	0.45	1
	Deposition layer thickness CIGS	t_7	$1.5 \cdot 10^{-6}$	m
	Collection rate non-working photovoltaics scrap	r_5	0.70	1
	Collection rate other photovoltaics scrap	r_6	0	1
Prod. NdFeB magnets	Yield in production of NdFeB magnets	y_8	0.70	1
	Collection rate of magnet scrap for gallium recycling	r_{14}	0	1
Prod. sputtering targets/MBE sources	Yield in production of sputtering targets/MBE sources	y_9	1	1
Prod. of TMG	Yield in production of TMG	y_{10}	0.92	1
Prod. GaAs substrates	Thickness of GaAs substrates	t_5	$6.53 \cdot 10^{-4}$	m
	Yield in production of GaAs substrates	y_{11}	0.35	1
	Collection rate GaAs substrate production scrap	r_7	0.63	1
Prod. GaP substrates	Thickness of GaP substrates	t_6	$5.62 \cdot 10^{-4}$	m
	Yield in production of GaP substrates	y_{12}	0.35	1
	Collection rate GaP substrate production scrap	r_8	0.63	1
Use	Share of GaN-LEDs used in automotive	w_a	0.02	1
	Share of GaN-LEDs used in general lighting	w_b	0.22	1
	Share of GaN-LEDs used in mobile phones	w_c	0.08	1
	Share of GaN-LEDs used in other consumer electronics and IT/telecom eq.	w_d	0.54	1
	Share of GaN-LEDs used in wind/solar power	w_e	0	1
	Share of GaN-LED used in other applications	w_f	0.15	1
	Share of GaAs/GaP-LEDs used in automotive	q_a	0.12	1
	Share of GaAs/GaP-LEDs used in general lighting	q_b	0.17	1
	Share of GaAs/GaP-LEDs used in mobile phones	q_c	0.03	1
	Share of GaAs/GaP-LEDs used in other consumer electronics and IT/telecom eq.	q_d	0.20	1
	Share of GaAs/GaP-LEDs used in wind/solar power	q_e	0	1
	Share of GaAs/GaP-LEDs used in other applications	q_f	0.49	1
	Share of ICs used in automotive	u_a	0	1
	Share of ICs used in general lighting	u_b	0	1
	Share of ICs used in mobile phones	u_c	0.55	1
	Share of ICs used in other IT/telecom eq.	u_d	0.37	1
	Share of ICs used in wind/solar power	u_e	0	1
	Share of ICs used in other applications	u_f	0.08	1
	Share of PV used in automotive	z_a	0	1
	Share of PV used in general lighting	z_b	0	1

Table S3 cont.

Group	*Description*	*Symbol*	*Value*	*Units*
	Share of PV used in mobile phones	z_c	0	1
	Share of PV used in IT/telecom. eq.	z_d	0	1
	Share of PV used in wind/solar energy	z_e	1	1
	Share of PV used in other applications	z_f	0	1
	Share of magnets used in automotive	v_a	0.03	1
	Share of magnets used in general lighting	v_b	0 [a]	1
	Share of magnets used in mobile phones	v_c	0 [a]	1
	Share of magnets used in other IT/telecom. eq.	v_d	0.60 [a]	1
	Share of magnets used in wind/solar power	v_e	0.01 [a]	1
	Share of magnets used in other applications	v_f	0.36 [a]	1
End-of-life	Collection rate for automotive EOL gallium scrap	r_9	0	1
	Collection rate for general lighting EOL gallium scrap	r_{10}	0	1
	Collection rate for consumer electronics, IT, telecom eq. EOL gallium scrap	r_{11}	0	1
	Collection rate for renewable energy EOL scrap	r_{12}	0	1
	Collection rate for other EOL scrap	r_{13}	0	1
	Expected lifetime of automobiles	μ_a	15	years
	Expected lifetime of general lighting	μ_b	10	years
	Expected lifetime of mobile phones	μ_c	3.25	years
	Expected lifetime of other consumer electronics, IT and telecom eq.	μ_d	6	years
	Expected lifetime of photovoltaics	μ_{e1}	25	years
	Expected lifetime of wind turbines	μ_{e2}	20	years
	Expected lifetime of other applications	μ_f	8	years
Materials	Concentration of Ga in GaN	c_1	5.12	g/cm^3
	Concentration of Ga in GaAs	c_2	2.56	g/cm^3
	Concentration of Ga in GaP	c_3	2.87	g/cm^3
	Concentration of Ga in AlInGaP	c_4	0.96	g/cm^3
	Concentration of Ga in CIGS	c_5	0.34	g/cm^3

[a] Value changes over time depending on scenario, shown for 2010.

The following procedure was used to quantify flows based on drivers and parameters. Any parameter and flow is a function of time in these calculations, although not indicated. However, many parameters were assumed constant over time.

The amount of gallium going into use in GaN-LEDs is determined by the demand for GaN-LED area, the thickness of the deposition layer and the concentration of gallium in GaN:

$$X_{17a-18} = A_{LED1} t_2 c_1 \tag{2.1}$$

Gallium in TMG required to produce GaN-LEDs is determined by deposition yield, losses due to dicing of LEDs and losses due to non-working devices:

$$X_{16b-17a} = \frac{X_{17a-18}}{y_5(1-k_3)(1-k_4)} \tag{2.2}$$

The amount of scrap lost from fabrication of GaN-LEDs is determined by mass balance and the collection rate:

$$X_{17a-19} = \left(X_{16b-17a} - X_{17a-18}\right)(1-r_2) \tag{2.3}$$

The amount of scrap collected from the production of GaN-LEDs is calculated by mass balance:

$$X_{17a-14} = X_{16b-17a} - X_{17a-18} - X_{17a-19} \tag{2.4}$$

GaAs/GaP-LEDs going into use, calculated from device area, thickness of device and deposition layer, as well as the concentration of Ga in GaAs and GaP:

$$X_{17b-18} = A_{LED2} h_1 \left((t_1 - t_2) c_2 + t_2 c_4 \right) + A_{LED2} (1 - h_1) t_1 c_3 \tag{2.5}$$

TMG needed for GaAs/GaP LEDs, calculated from device area, thickness, concentrations and the losses and yields in different fabrication steps:

$$X_{16b-17b} = A_{LED2} \frac{h_1 t_2 c_4 + (1 - h_1) t_2 c_3}{(1 - k_3)(1 - k_4) y_5} \tag{2.6}$$

GaAs substrates needed for LEDs, calculated from device area, substrate thickness, concentration of Ga and fabrication losses from non-working devices and dicing:

$$X_{16c-17b} = A_{LED2} \frac{h_1 t_5 c_2}{(1 - k_3)(1 - k_4)} \tag{2.7}$$

GaP substrates needed for LEDs, calculated by the same method as for GaAs substrates:

$$X_{16d-17b} = A_{LED2} \frac{(1 - h_1) t_6 c_3}{(1 - k_3)(1 - k_4)} \tag{2.8}$$

Collected fabrication scrap from GaAs/GaP LEDs, from process yields and collection rates:

$$\begin{aligned} X_{17b-14} = {} & \frac{A_{LED2}}{(1 - k_3)(1 - k_4)} \left(h_1 \, \mathrm{c}_2 (t_5 - t_1 - t_2) \, \mathrm{r}_1 + h_1 \, \mathrm{c}_2 (\mathrm{t}_1 - t_2) k_3 k_4 r_2 \right) \\ & + \frac{A_{LED2}}{(1 - k_3)(1 - k_4)} \left((1 - h_1)(t_6 - t_1 + t_2) c_3 r_1 + (1 - h_1)(t_1 - t_2) c_3 k_3 k_4 r_2 \right) + X_{16b-17b} (1 - y_5) r_2 \end{aligned} \tag{2.9}$$

Lost scrap from fabrication of GaAs/GaP LEDs, by mass balance:

$$X_{17b-19} = X_{16b-17b} + X_{16c-17b} + X_{16d-17b} - X_{17b-14} - X_{17b-18} \tag{2.10}$$

Integrated circuits into use, calculated by device area demand, thickness and concentration of Ga:

$$X_{17c-18} = A_{IC} t_3 c_2 \tag{2.11}$$

MBE targets for integrated circuits, from device area, deposition layer thickness, concentration, share of devices produced by MBE, fabrication losses and yields:

$$X_{16a-17c} = \frac{A_{IC} t_4 c_2 (1-h_2)}{(1-k_5)(1-k_6) y_6} \tag{2.12}$$

TMG for integrated circuits, calculated by the same method as MBE targets:

$$X_{16b-17c} = \frac{A_{IC} t_4 c_2 h_2}{(1-k_5)(1-k_6) y_5} \tag{2.13}$$

GaAs substrates for integrated circuits, calculated from device area, substrate thickness, concentration and fabrication loss rates:

$$X_{16c-17c} = \frac{A_{IC} t_5 c_2}{(1-k_5)(1-k_6)} \tag{2.14}$$

Collected scrap from fabrication of integrated circuits, calculated from loss rates and process yields in different steps of the fabrication process as well as collection rates:

$$X_{17c-14} = A_{IC} c_2 (t_5 + t_4 - t_3) r_3 + \frac{A_{IC} c_2 t_3 k_5 k_6 r_4}{(1-k_5)(1-k_6)} + X_{16a-17c}(1-y_6)\,r_4 + X_{16b-17a}(1-y_5) r_4 \tag{2.15}$$

Uncollected scrap from fabrication of integrated circuits, calculated by mass balance:

$$X_{17c-19} = X_{16a-17c} + X_{16b-17c} + X_{16c-17c} - X_{17c-18} - X_{17c-14} \tag{2.16}$$

Gallium in CIGS photovoltaics entering use, calculated from solar cell area, thickness of deposition layer and concentration of gallium in CIGS:

$$X_{17d-18} = A_{PV} t_7 c_4 \tag{2.17}$$

Sputtering targets used in fabrication of photovoltaics, calculated from solar cell area, thickness of deposition layer, concentration in CIGS, deposition yield and overall fabrication loss rate:

$$X_{16a-17d} = A_{PV} t_7 c_4 \frac{1}{y_7 (1-k_7)} \tag{2.18}$$

Collected scrap from fabrication of CIGS PV, calculated from solar cell area, thickness of deposition layer, concentration, fabrication losses, process yields and collection rates:

$$X_{17d-14} = A_{PV} t_7 c_4 \left(\frac{1}{(1-k_7)} k_7 r_5 + \frac{1}{y_7 (1-k_7)} (1-y_7) r_6 \right) \tag{2.19}$$

Uncollected scrap from fabrication of CIGS PV, calculated by mass balance:

$$X_{17d-19} = X_{16a-17d} - X_{17d-18} - X_{17d-14} \tag{2.20}$$

Gallium entering use as alloying element in NdFeB magnets, given directly from scenario output:

$$X_{17e-18} = M_{mag} \tag{2.21}$$

Uncollected scrap from magnet production is calculated from production yield and collection rate:

$$X_{17e-19} = X_{17e-18} \frac{\left(1-y_8\right)}{y_8}\left(1-r_{14}\right) \tag{2.22}$$

Input into magnet fabrication equal to mass entering use divided by fabrication yield:

$$X_{16e-17e} = X_{17e-18} \frac{1}{y_8} \tag{2.23}$$

Collected scrap from magnet fabrication is calculated from process yield and collection rate:

$$X_{17e-14} = X_{16e-17e}\left(1-y_8\right)r_{14} \tag{2.24}$$

Total Ga going into use is calculated by summing up individual applications:

$$X_{17-18} = X_{17a-18} + X_{17b-18} + X_{17c-18} + X_{17d-18} + X_{17e-18} \tag{2.25}$$

Refined gallium used in the production of sputtering targets and MBE sources, calculated from use of sputtering targets and MBE sources in fabrication, and yield in the production of these:

$$X_{13-16a} = \left(X_{16a-17c} + X_{16a-17d}\right)\frac{1}{y_9} \tag{2.26}$$

Since yield is assumed 100%, the lost scrap from manufacturing of MBE sources and sputtering targets is zero:

$$X_{16a-19} = 0 \tag{2.27}$$

Likewise, collected scrap is zero:

$$X_{16a-14} = 0 \tag{2.28}$$

Refined gallium used in the production of TMG, calculated by use of TMG in fabrication and yield in production of TMG:

$$X_{13-16b} = \left(X_{16b-17a} + X_{16b-17b} + X_{16b-17c} \right) \frac{1}{y_5} \tag{2.29}$$

Gallium lost from TMG production calculated by input of refined gallium and production yield:

$$X_{16b-19} = X_{13-16b} \left(1 - y_5 \right) \tag{2.30}$$

Gallium collected for recycling from TMG production is zero because collection rate is assumed to be zero:

$$X_{16b-14} = 0 \tag{2.31}$$

Refined gallium used in production of GaAs substrates calculated from the use of substrates in fabrication and the yield in production of substrates:

$$X_{13-16c} = \left(X_{16c-17b} + X_{16c-17c} \right) \frac{1}{y_{11}} \tag{2.32}$$

Uncollected scrap from production of GaAs substrates calculated from process input, production yield and collection rate:

$$X_{16c-19} = X_{13-16c} \left(1 - y_{11} \right) \left(1 - r_7 \right) \tag{2.33}$$

Collected scrap calculated from process input, yield and collection rate:

$$X_{16c-14} = X_{13-16c} \left(1 - y_{11} \right) r_7 \tag{2.34}$$

Refined gallium used in the production of GaP substrates, calculated from the demand for GaP substrates and production yield:

$$X_{13-16d} = \frac{X_{16d-17b}}{y_{12}} \tag{2.35}$$

Collected scrap from production of GaP substrates calculated from process input, yield and collection rate:

$$X_{16d-14} = X_{13-16d} \left(1 - y_{12} \right) r_8 \tag{2.36}$$

Uncollected scrap from production of GaP substrates calculated from process input, yield and collection rate:

$$X_{16d-19} = X_{13-16d} \left(1 - y_{12} \right) \left(1 - r_8 \right) \tag{2.37}$$

Input of gallium metal in production of NdFeB is equal to output from the same process (assumed 100% yield of gallium in production):

$$X_{11\text{–}16e} = X_{16e\text{–}17e} \tag{2.38}$$

The loss from NdFeB production is zero:

$$X_{16e\text{–}19} = 0 \tag{2.39}$$

Likewise, the collected gallium is zero:

$$X_{16e\text{–}14} = 0 \tag{2.40}$$

The input into each end-use from each application type was calculated by multiplying the total use of a product (e.g. integrated circuits) with the share going to the given end-use. These equations are all of the same form; one example is given below, for integrated circuits going into "other IT/telecom. equipment:

$$X_{17c\text{–}18d} = w_d X_{17c\text{–}18} \tag{2.41}$$

End-of-life flows, $X_{18a\text{-}19}$, $X_{18b\text{-}19}$, $X_{18c\text{-}19}$, $X_{18d\text{-}19}$, $X_{18e\text{-}19}$, $X_{18a\text{-}14}$, $X_{18b\text{-}14}$, $X_{18c\text{-}14}$, $X_{18d\text{-}14}$ and $X_{18e\text{-}14}$, were calculated based on lifetime distribution functions and expected lifetimes of the products. The procedure is explained generally in chapter 3.1 under "inflow-driven model". The distribution between process 14 and 19 (i.e. collected and uncollected scrap), was calculated by collection rates.

Recovered metal from recycling is equal to the inputs of different scrap types times recycling yields:

$$X_{14\text{–}11} = y_2 X_{16\text{–}14} + y_3 X_{17\text{–}14} + y_4 X_{18\text{–}14} \tag{2.42}$$

Loss from recycling process calculated by mass balance:

$$X_{14\text{–}19} = X_{16\text{–}14} + X_{17\text{–}14} + X_{18\text{–}14} - X_{14\text{–}11} \tag{2.43}$$

Input of secondary material to refining is set equal to recycled gallium, assuming all recycled gallium is refined:

$$X_{11\text{–}12,s} = X_{14\text{–}11} \tag{2.44}$$

Refined secondary material set equal to input of secondary material to refining (assuming 100% yield due to internal recycling loops in refining):

$$X_{12\text{–}13,\mathrm{s}} = X_{11\text{–}12,s} \tag{2.45}$$

Refined primary material calculated by mass balance from demand and refined secondary material:

$$X_{12\text{–}13,p} = X_{13\text{–}16} - X_{12\text{–}13,s} \tag{2.46}$$

Input of primary metal to refining set equal to demand for refined primary material (assuming 100% refining yield):

$$X_{11\text{–}12,p} = X_{12\text{–}13,p} \tag{2.47}$$

Required primary production is equal to the input of primary material to refining plus gallium used in NdFeB:

$$X_{6\text{–}11} = X_{11\text{–}12,p} + X_{11\text{–}16e} \tag{2.48}$$

Input into primary production (extraction from Bayer liquor) is calculated from primary production and extraction yield:

$$X_{4\text{–}6} = \frac{X_{6\text{–}11}}{y_1} \tag{2.49}$$

Losses from primary production calculated by mass balance:

$$X_{6\text{–}19} = X_{4\text{–}6} - X_{6\text{–}11} \tag{2.50}$$

Input to Bayer process with gallium extraction calculated from input to extraction process, loss rate to red mud and loss rate to alumina:

$$X_{1\text{–}4} = \frac{X_{4\text{–}6}}{\left(1-k_1\right)\left(1-k_2\right)} \tag{2.51}$$

Loss to red mud calculated by input to Bayer process with Ga extraction and loss rate:

$$X_{4\text{–}3} = k_1 X_{1\text{–}4} \tag{2.52}$$

Loss to alumina calculated by input to Bayer process with Ga extraction and loss rates:

$$X_{4\text{–}5} = k_2\left(1-k_1\right)X_{1\text{–}4} \tag{2.53}$$

Maximum primary production from bauxite is calculated from mass fraction of Ga in bauxite, total bauxite input to Bayer process, loss rate to red mud, loss rate to alumina and extraction yield:

$$Y = x_1 B\left(1-k_1\right)\left(1-k_2\right)y_1 \tag{2.54}$$

3. Parameter estimation

Most of the parameters used in the model were estimated in a previous work [1]. Some additional parameters were used here, mainly the average lifetimes of end-use products. We used 15 years for automobiles [7], 10 years for general lighting (LEDs) [3], 3.25 years for mobile phones (estimated in this work), 6 years for other IT and telecom equipment (based on computers) [8], 25 years for photovoltaics [9,10], 20 years for wind turbines [11], and 8 years for all other applications. The standard deviation of the lifetime probability distribution function was always set to one fifth of the expected lifetime. The data used for scenario development are explained in the scenario development section.

4. Scenario development

4.1 Stock dynamics model

For some of the application areas, we used dynamic models based on a lifetime distribution function and mass balance in the use phase. A general explanation of this model will be given here; the difference between each application arises from different input data and lifetime assumptions.

Inflow-driven model:

The inflow-driven model takes the sales, I_c, in cohort year c of a product as the starting point. We used a normal distribution to represent the probability of a product to reach end of life after a given time in use. This is then used to estimate the outflow, O_t, from the use phase in all future years t:

$$O_{c,t} = I_c f_{t-c} \tag{4.1}$$

where f_{t-c} is the probability of reaching end-of-life in the year t. The total outflow in year t is then:

$$O_t = \sum_{c=c_0}^{t} I_c f_{t-c} \tag{4.2}$$

Note that this includes the year when the age of the product is 0, i.e. products that leave use the same year as they are produced, which may be a significant share for products with a short lifetime. The factor

f_{t-c} is given by the lifetime distribution function, in this case a normal distribution. For $t=c$, the probability of a product leaving use the same year as it is being sold, is:

$$f_0 = k\left(cdf\left(0.5, \mu, \sigma\right) - cdf\left(0, \mu, \sigma\right)\right) \tag{4.3}$$

where k is a correction factor to account for the portion of the normal distribution that lies below zero, μ is the expected lifetime, σ is the standard deviation of the lifetime distribution function, and *cdf* is the cumulative distribution function, defined as:

$$cdf\left(x, \mu, \sigma\right) = \int_{-\infty}^{x} \frac{1}{\sigma\sqrt{2\pi}} \exp\frac{-(x-\mu)^2}{2\sigma^2} dx' \tag{4.4}$$

The correction factor is calculated as:

$$k = \left(1 - cdf\left(0, \mu, \sigma\right)\right)^{-1} \tag{4.5}$$

The probability of leaving use in all other years is given by:

$$f_{t-c} = k\left(cdf\left(t-c+0.5, \mu, \sigma\right) - cdf\left(t-c-0.5, \mu, \sigma\right)\right) \tag{4.6}$$

If sales (inflow) are given, the in-use stock can be calculated by mass balance from the initial stock plus the stock change (inflow minus outflow) in all subsequent years:

$$S_t = S_0 + \sum_{t'=t_1}^{t} \left(I_{t'} - O_{t'}\right) \tag{4.7}$$

where the outflow has already been calculated using the above equations.

Stock-driven model

A stock-driven model may be used to derive the required inflow (sales) from a predefined in-use stock. We used this approach to create scenarios for future demand, given a pattern of in-use stock development. In this method we use the same relations between inflow, outflow and the stock as defined

above, only that the stock change is calculated first, then the outflow from previous inflows, and finally the required inflow in the given year. This approach has been described in previous works, and will not be elaborated further here.[12]

4.2 Gallium supply

The maximum supply of primary gallium, assuming current technology and practice for extraction, was calculated based on scenarios for primary production of aluminum. Scenarios for the aluminum cycle have been developed and analyzed by Liu et al.[2] They used a stock-driven MFA model to derive production from nine different development paths of the per-capita in-use stock, where the paths are distinguished by stock saturation level (200, 400, 600 kg/cap) and stock saturation time (2050, 2075, 2100). In addition, they combined the stock development patterns with different measures for reducing energy demand and greenhouse gas emissions from the aluminum cycle: near perfect collection of scrap, and material yield improvements. After stock saturation, secondary production may replace a large share of the primary production, such that a characteristic peak in primary production is observed some years before saturation. Primary production of aluminum drives the demand for alumina from the Bayer process, and therefore defines an upper limit for gallium extraction from conventional resources. We used the scenarios from Liu et al. for bauxite input to the Bayer process, assumed that the average mass fraction of Ga in bauxite remains the same as today, and assumed the same coefficients for loss to red mud and alumina. The bauxite flows for the various scenarios are shown in Figure S2.

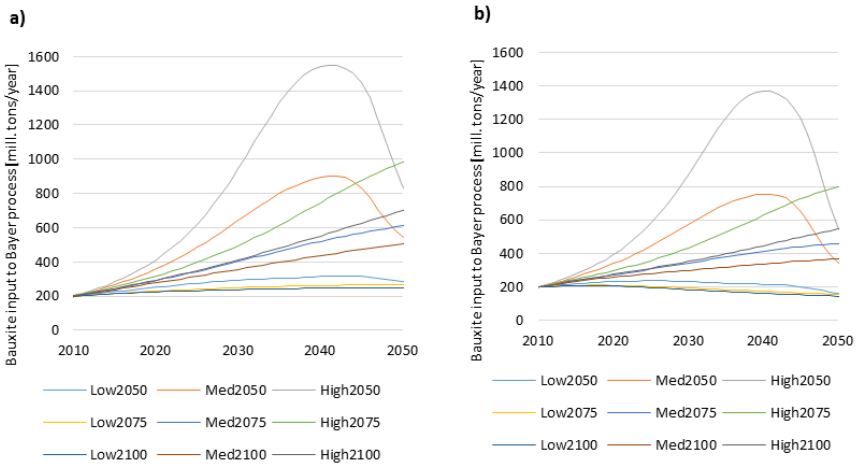

Figure S2. Bauxite input to Bayer process in different scenarios. a) No action; b) near perfect collection.

4.3 LEDs

For our purpose, LEDs can be divided into two main types: i) green, blue, violet, ultraviolet and white LEDs based on the GaN/InGaN system, from now on called GaN-based and ii) infrared, red, orange, yellow and green LEDs based on the GaAs, GaP, InGaP or AlInGaP system, from now on called GaAs/GaP-based. The former are mainly produced on substrates of sapphire (Al_2O_3) or silicon carbide (SiC), while the latter are produced on substrates of GaAs or GaP. We previously estimated the amount of gallium in each of these types from the production of substrates.[1] However, to say something about the future demand, it is also necessary to know which products the LEDs are used in. There are several market reports that estimate the revenue from different applications of LEDs. Table S4 shows the estimated revenue-based market breakdown in 2011 for GaN-based LEDs, high-brightness LEDs and the total LED market from three different sources.

Table 4. The LED market breakdown. Note that the application categories are from the HB-LED market report. The two others have more detailed categories, which have been aggregated in this table.

	Market share		
	Total LED market [13]	*HB-LED* [14]	*GaN LED market* [15]
Market value	$10 bn.	$9 bn.	$8 bn.
Mobile appliances	19%	16%	12%
Large display backlight	35%	30%	47%
Lighting	25%	23%	21%
Automotive	6%	12%	5%
Signs and signals	14%	10%	5%
Other applications	1%	9%	9%

These estimates of the market breakdown are not consistent. For example, the HB-LED market for automotive is estimated to be about twice as large as the total LED market and "Other applications" is estimated to be only 1% of the total market while being 9% in the two other markets. Some of these inconsistencies are probably due to different definitions of the categories, while others simply illustrate the large uncertainties in such estimates. Nevertheless, these reports give some indication about the importance of different markets.

GaN-based LEDs

We took the total demand for sapphire and silicon carbide substrates as a starting point in 2011, and assumed that the price of an LED is proportional to the chip size, such that the breakdown of the substrate use into different application areas is the same as the revenue-based breakdown shown in the last column of Table 1. The total production of sapphire and silicon carbide substrates for LEDs was according to Yole Développement about 1.16 times that of semi-insulating (SI) GaAs in 2008, and expected to grow

to 2.9 times that of SI GaAs in 2013.[16] A simple extrapolation of this relative size combined with an estimate of the SI GaAs substrate market size in 2011 [17] gives a rough estimate of 39,000 m^2 of sapphire and silicon carbide substrate produced in 2011. However, another source indicates that only about half of the production was used due to massive oversupply of substrates in 2011 and 2012.[18] This source estimates that in 2011, about 30,000 m^2 of sapphire substrates were produced while the demand from LEDs was about 15,000 m^2. Silicon carbide substrates for LEDs were estimated to 2,400 m^2 in 2011.[16] It has been estimated that about 115 billion GaN-based LED chips were produced in 2011 while the demand was about 80 billion chips.[15] From these numbers we can estimate the average chip size as 0.1 mm^2, where we assumed a loss of 37% of the area in fabrication. This loss rate was estimated based on a wafer size of 76.2 mm (3 inches) diameter, a 5 mm wide unused edge zone, 0.03 mm cut trench and 8% loss rate due to non-working devices and breakage. An average chip size of 0.1 mm^2 seems plausible, while somewhat low: chips for mobile phone backlighting and keypads are usually smaller, but chips for general lighting can be around 1 mm^2 (data sheets for various LED chips were obtained from the webpages of major producers: Epistar, Cree and Luxtaltek).[19–21]

GaAs/GaP-based LEDs

These LEDs produce infrared, red, orange, yellow or green light. They are mainly used in colored LED displays (e.g. for advertisement), signage, traffic lights, automotive turn lights and stop lights, and in colored indicator lamps. There is very little information available on the relative importance of the different applications for the overall demand of GaAs semiconducting substrates. According to a report from the United States Geological Survey, signage (including outdoor displays) was by far the most important category in 2010, before handheld electronic devices. However, this report seems to overestimates the amount of red LEDs in mobile phones, as mobile phones almost exclusively use blue LEDs with yellow phosphors to create backlight. Only high end TVs and monitors use red, green and blue (RGB) LEDs for backlighting.[22] Assuming that at most 25% of these large LCDs used the RGB-type LEDs, we can conclude that less than 10% of this market is comprised of GaAs/GaP-based LEDs. Some red LEDs are also used in general lighting. Architectural lighting has been the early adopter of LED lighting, where the ability to adjust color is often the motivation for using LEDs.[3] It has been estimated that architectural lighting comprised about 70% of the general lighting LED market in 2011.[3] Assuming that at most 50% of architectural LEDs are RGB and only white GaN-based LEDs in other general lighting, we get an estimated maximum of 10% GaAs/GaP-based LEDs in general lighting. Traffic lights can be assumed to have 2/3 GaAs/GaP -based LEDs to produce red and orange light, the green being produced with GaN-based LEDs. In signage and outdoor LED displays we assume 50% GaAs/GaP -based and 50% GaN-based (full color displays would have 1/3 GaAs/GaP-based LEDs, while single color displays can have up to 100% GaAs/GaP-based LEDs). In the automotive sector, the

highest penetration rates for LEDs are found in the interior instrument panel (~80%), stoplights (~40%), daytime running lights (~15%) and mirror turn lights (~10%).[23] Based on these penetration rates and the relative market size of different lighting components, we estimated that LEDs in automotive applications are currently 20% GaN-based and 80% GaAs/GaP-based. Based on these assumptions for GaAs/GaP share in each application category, and the market values of these (Table 1), we can estimate the following market breakdown of GaAs/GaP -based LEDs in 2011: 19% LCD backlighting, 14% general lighting, 27% automotive, 40% signage, traffic lights and other.

Future demand from key LED applications

As far as possible, we based the scenarios for future LED demand on a lighting market report from McKinsey & Company.[3] They used an economic model to make forecasts of the demand for lighting units in different application areas and with different lighting technologies. The report covers general lighting (including residential, hospitality, outdoor, office, architectural, shop, industrial), backlighting for LCD screens (handsets, TVs, PC monitors and laptop computers) and automotive, from 2010 to 2020. According to this report, the LED general lighting and automotive markets will be about 10 and 3 times larger in 2020 than in 2010. In backlighting, LEDs are expected to reach a maximum around 2020 due to OLED (organic LED) screens taking over the market from LCD screens. Accordingly, it is expected that the demand for GaN-based white LEDs will grow dramatically. For GaAs/GaP-based LEDs we expect a less dramatic change since these have already reached a higher penetration rate (e.g. in traffic lights, signage, automotive).

Current demand for GaN-based and GaAs/GaP-based LEDs in the four main application areas (general lighting, backlighting, automotive, signage and others) was estimated as explained in the above paragraphs. For general lighting and backlighting we used the following approach to create scenarios for the area of LED chips going into use: i) the relative change in demand until 2020 from each application area was estimated from the McKinsey report (except signage and others); ii) after 2020 we assumed that demand growth is driven by population growth and increased penetration of LED lighting (which until 2020 was estimated in the McKinsey report). The penetration rates were assumed to follow a logistic curve that saturates at 90% in the future (for general lighting) or goes down to 0% (for backlighting).

For automotive applications, the McKinsey report only covers the headlamp, which is currently not the main application of LEDs in cars. The penetration rate of LEDs in different automotive components are approximately: 5% in headlamp; 15% in daytime running lights and fog lamp, 10% in side lamps, 30% in rear lamps and 85% in interior (including dashboard).[23] From these rates, we estimate that GaN-based LEDs had an 8% penetration rate in 2014, and GaAs/GaP-based LEDs had a 35% penetration rate in 2014. We created scenarios by assuming that these will grow to 85% in 2030 and 2025 respectively, and

saturating at 90%. The number of cars going into use was taken from a previous work, where this was estimated using a stock-driven model of the vehicle stock, with population scenario from the UN and cars per capita scenario from the International Energy Agency.[24]

For signage and others, we assumed a moderate growth by assuming a current LED penetration rate of 70% that grows to 85% in 2020 and saturates at 90%, again using a logistic function. The relative growth in LED demand was calculated as a product of the relative population growth and the relative growth of the penetration rate.

Figure S3 shows the scenarios for LED demand in terms of chip area going into use.

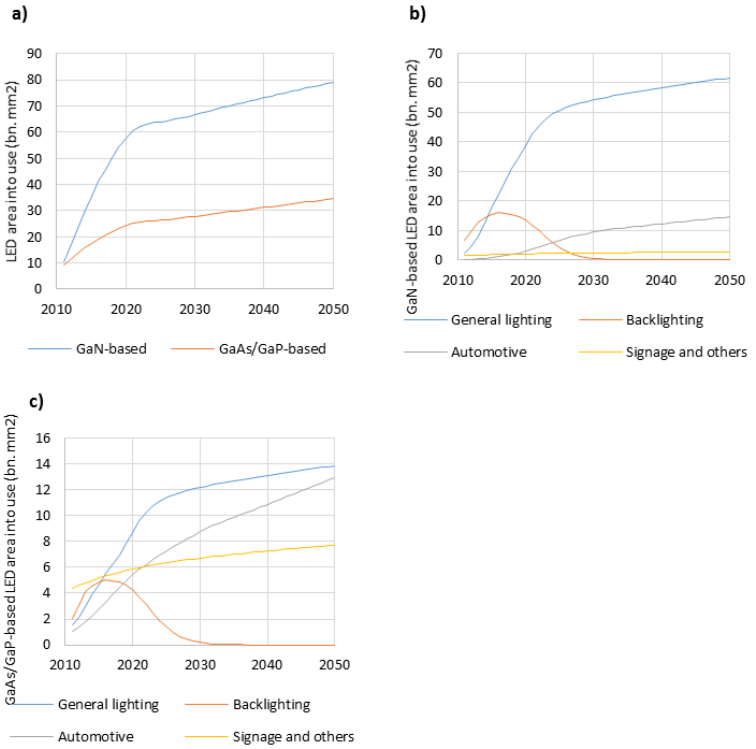

Figure S3 Area of LEDs going into use in the modelled scenario, a) divided by type of LED, b) GaN-based LEDs by application, c) GaAs/GaP-based LED by application.

4.4 Integrated circuits

The market for GaAs integrated circuits was in 2011 dominated by mobile phones (handsets), with 55% of semi-insulating substrate area demand.[17] The second most important use was in other wireless communication (e.g. laptop and tablet computers and wireless infrastructure) with around 20% of substrate area. When developing scenarios for integrated circuits, we used a detailed approach for

handsets. For all other applications, we assumed that the market remains in the same proportion to handsets.

We broke down the mobile phone market into two segments: i) standard mobile phones ii) smartphones. This corresponds roughly to 2G and older technology (i) and 3G/4G technology (ii). The amount of GaAs entering use in mobile phones was calculated as:

$$A_{phones} = I_{phones}\left(x_{standard}a_{standard} + x_{smart}a_{smart}\right) \tag{4.8}$$

Where A_{phones} is the GaAs chip area in mobile phones, I_{phones} is the number of mobile phones sold (calculated from the stock driven model), x is the market share of the indicated technology, and a is the area of GaAs chips per phone for the indicated technology.

Market share of handset technology

The number of standard phones and smartphones sold each year from 2001 to 2013 was compiled from various news reports from Gartner, Inc., a market analysis and advisory company that specializes on IT.[25–34] The market share of smartphones was then modeled as a logistic function with lower value 0 and upper value 0.9, assuming that there will always be a market for cheaper standard phones. Data on handset sales, penetration rate of smartphones and projections are shown in Figure S4.

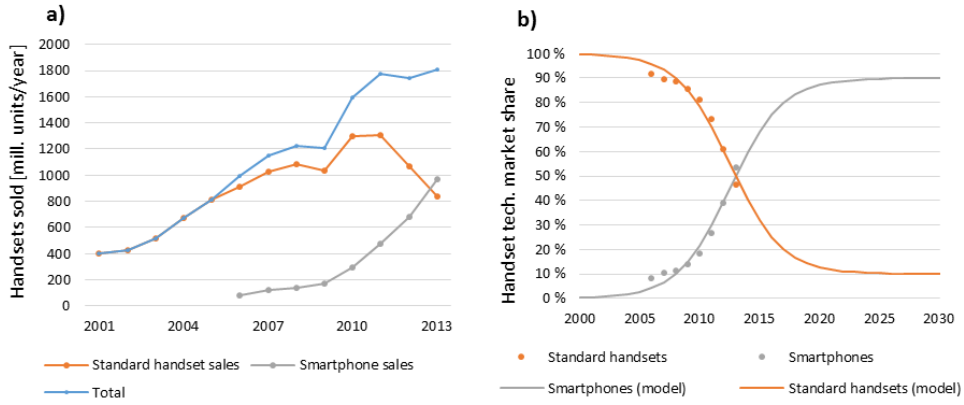

Figure S4. a) World handset sales. b) Market share of smartphones versus standard handsets.

GaAs content in handsets

GaAs is used in the radio frequency (RF) front end of handsets, which is the part between the antenna and the transceiver. Traditionally, GaAs has been used in switches and power amplifiers (PAs), but due to competition from silicon-based technology, it is now mainly used in PAs.[17] It was estimated that 80% of handsets used GaAs technology in 2004,[35] while in 2011 this had grown to about 90%.[36] However, it is expected that the market share GaAs will drop to 75% by 2018 due to competition from silicon-based technology.[36]

A typical architecture of the front end involves one PA module for the 2G frequency bands (up to four bands) and one additional single PA for each band in the 3G/4G modes.[37] The breakdown of the handset market from 2008 to 2014 according to which modes and how many bands the handsets support has been estimated by Bolton.[38] We used this information to estimate the number of 2G PA modules and 3G/4G PAs required in new handsets. The number of 2G PA modules is one per handset (standard and smartphones), while we estimated the average number of 3G/4G PAs per smartphone to be 1.8 in 2008, 2.5 in 2011 and expected to grow to 3.1 in 2014.

A typical size for a 3G/4G PA package is 3x3 mm^2,[39,40] while a 2G PAM is usually around 5x5 mm^2.[41,42] However, only a fraction of the package size is occupied by the GaAs chip. For a 3x3 mm^2 package, the chip occupies about 1.35 mm^2, or 15% of the area. [43] We assumed that the same fraction applies to larger modules, so that the GaAs chip area in a 2G PA module would be approximately 3.75 mm^2. From these data, we estimated that the average GaAs chip area in a standard (2G) handset is 0.90*3.75 mm^2=3.38 mm^2. In a smartphone (3G/4G), we estimate that the average GaAs chip area is 0.90*(3.75 mm^2 + 2.51*1.35 mm^2) = 6.43 mm^2. By adjusting for the growing number of PAs and changing market share of GaAs, we estimated that the corresponding numbers in 2008 and 2014 were 5.26 mm^2 and 6.53 mm^2 respectively in smartphones.

An estimate of the GaAs chip area per handset between 2000 and 2007 was made by Augustine in 2004.[35] It was then reported to grow from 1.5 mm^2 in 2000 to 3.4 mm^2 in 2007, where the latter value was a forecast.

From market data on GaAs substrates,[17] and yields in the fabrication process for integrated circuits,[1] we made a top-down estimate to compare with the previous numbers. The chip area per handset was then found to be 5.4 mm^2 per handset. This is 27% higher than our estimated 4.24 mm^2 from the calculations explained above. Possible explanations for this discrepancy, apart from errors in the estimates, could be: i) use of GaAs in handset switches, ii) time lag between production of substrates. Based on the collected data, we created time series for the average GaAs content in standard handsets and smartphones. For standard handsets, we took 3.75 mm^2 in 2011 as a starting point, assumed this to remain constant in the future, and made a linear extrapolation backwards to the estimates provided by Augustine.[35] For smartphones, we used our own estimates for 2008, 2011 and 2014 based on the number of PAs and a

size of 1.35 mm^2 per 3G/4G PA. For the years in between, we made a linear interpolation, and for the years before and after, we assumed the content to remain constant. Finally, we adjusted all the numbers with a constant factor, to calibrate it towards the top-down estimate based on Higham's estimate of substrate area. The average GaAs chip area in handsets from the different data sources and our model is shown in Figure S5.

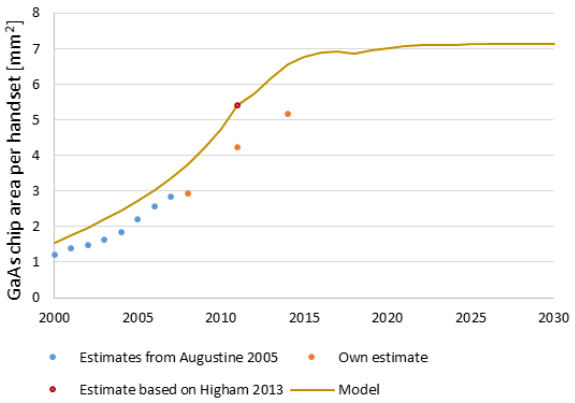

Figure S5. Average GaAs chip area in handsets. The "own estimate" and the estimate based on Augustine only include power amplifiers, while the estimate based on Higham and the model include all use of GaAs in handsets.

To calibrate a stock-driven model, we used global mobile phone subscriptions data from the UN.[44] For many countries, mainly less developed countries, the data seem to overestimate the number of active subscriptions, for example because the data refers to number of registered phone numbers. To correct for this, we assumed that the number of mobile phones in use is equal to 0.9 times the number of subscriptions. The corrected values are shown as blue dots in Figure 4b). We then used these corrected data as inputs in a stock-driven dynamic material flow analysis (MFA) model, and adjusted the lifetime to fit the independent sales estimates from Gartner. We found that an average lifetime of 3.25 years gave the best fit. The sales modelled with the stock-driven model is shown together with the adjusted subscriptions data in Figure S6 a). To make a future projection, we fitted a logistic curve to the calculated number of handsets in use per capita. The best fit was obtained by setting the saturation value to 1.1 mobile phones per capita, which is around current values for countries in Northern Europe. The estimated historic in-use stock (from subscriptions) is shown together with the fitted curve in Figure S6 b).

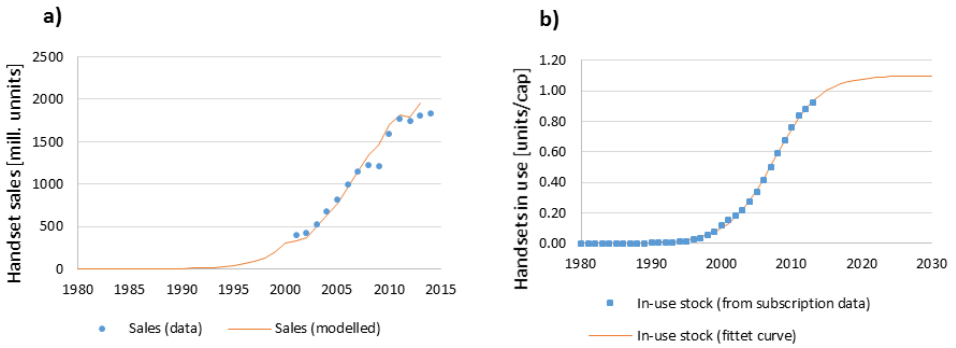

Figure S6. a) Historic sales of mobile phones and the sales estimated with a stock-driven material flow analysis model, using subscriptions as a proxy for in-use stock. b) In-use stock of handsets estimated from subscription data and a logistic curve fitted to this data.

Finally, the calibrated future in-use stock per capita was used in a stock-driven model to produce a scenario for future sales of handsets. Combined with the calibrated market penetration scenarios, this gave the expected future sales of standard handsets and smartphones. These are shown together with the historic data in Figure S7.

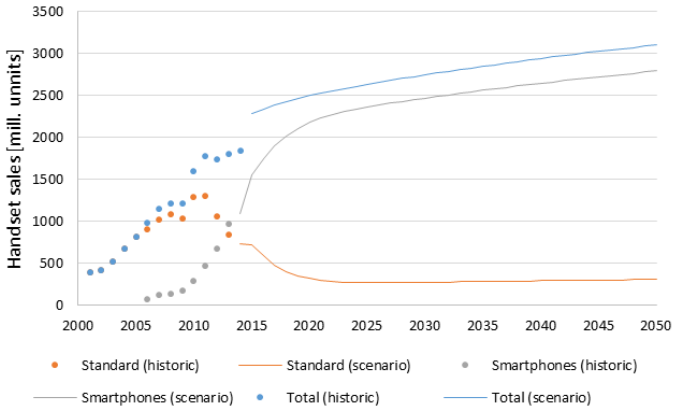

Figure S7. Historic sales of standard phones and smartphones, and scenarios for future sales.

The resulting scenario for integrated circuits, in terms of area of devices going into use, is shown in Figure S8.

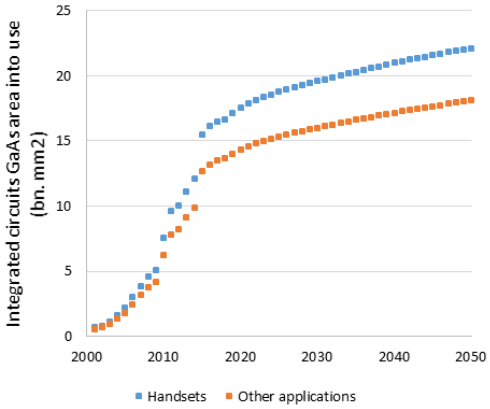

Figure S8. Scenario for GaAs integrated circuit device area going into use.

4.5 Photovoltaics

For future production of copper indium gallium diselenide (CIGS) photovoltaics, we took scenarios from the International Energy Agency (IEA) for photovoltaic power generation as a starting point. Divided by the average capacity factor and the number of hours per year, this gives the installed capacity (in-use stock) of photovoltaics in GW. This was then used as the driver for a stock-driven model, which then estimates the required new installations per year in GW. This was multiplied with the market share of CIGS compared to other PV technologies, and divided by the standard test condition irradiance (1000 W/m^2) and the efficiency of CIGS cells, to find the area of new installed CIGS cells. Table S5 summarizes the parameters used to create the scenarios.

Table S5. Parameters used to create the CIGS scenarios.

Symbol	*Description*	*Units*	*Data source*
E	Delivered electricity from photovoltaics	GWh/year	[4]
w	Capacity factor	1	[9]
K	Total installed PV capacity	GW	-
N_{pv}	New installed PV capacity	GW/year	-
k_{cigs}	Market share of CIGS in PV market	1	[5]
N_{cigs}	New installed CIGS capacity	GW/year	-
S	Standard test conditions irradiance	W/m^2	[45]
e	Efficiency	1	[46], own assumptions
A_{cigs}	Area of new installed CIGS	m^2	-
μ_{pv}	Expected lifetime	years	[9,10]
σ_{pv}	Standard deviation of the lifetime probability distribution	years	own assumption

The calculation procedure is summarized in the following. The in-use stock of PV in GW was calculated from the delivered electricity from PV, the number of hours per year, and the capacity factor:

$$K = \frac{E}{w \cdot 8766h / year} \tag{4.9}$$

The new installed PV capacity per year was then calculated using a stock-driven model and the lifetime parameters, as explained in section 3.1. The area of new installed CIGS cells was calculated from the new installed PV capacity, the market share of CIGS, standard test conditions, and efficiency:

$$A_{cigs} = \frac{N_{pv} k_{cigs}}{S \cdot e} \tag{4.10}$$

We used four scenarios from IEA for the electricity generation from PV, the 6DS, 4DS, 2DS and the 2DS hi-ren.[4] A forecast for the average capacity factor of installed photovoltaic cells was calculated from an IEA scenario for annual power generation and installed capacity, which assumes a slightly increasing capacity factor (15.6% in 2010, 16.2% in 2020, 16.3% in 2030, 16.4% in 2040, and 16.5% in 2050).[9] We assumed an average lifetime of 25 years,[9,10] which is usually taken as a minimum for photovoltaic panels, and 5 years as the standard deviation of the lifetime probability distribution function. The market share of CIGS from 2012 to 2017 was taken from a scenario from the European Photovoltaic Industry Association (EPIA).[5] We then created three scenarios, assuming a lower converging value of 3% and upper converging value of 5%, 20% and 40%, and fitted a logistic function to the data from EPIA and one additional data point, which was set as the converging upper value in 2050. For the efficiency of CIGS cells we assumed that it will increase linearly from the current value of around 11.8%,[46] to reach 15% in 2050. Figure S9 summarizes the key variables and their development over time in the different scenarios.

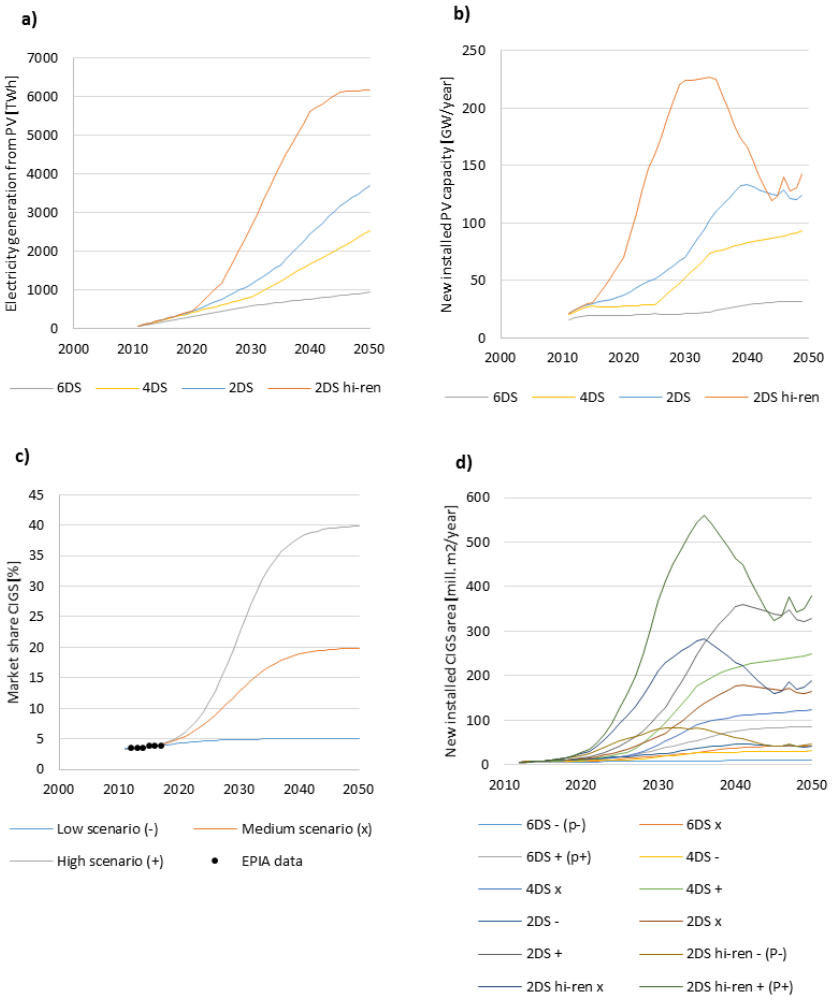

Figure S9. a) Scenarios for electricity generation from photovoltaics, taken from IEA's Energy Technology Perspectives 2014. b) New installed photovoltaics electricity generation capacity, obtained from a stock-driven model of the IEA scenarios. c) Market share of CIGS. Data from EPIA and our own scenarios. d) 12 scenarios for new installed CIGS panels, resulting from combinations of the four scenarios for total PV stock and the 3 scenarios for the market share of CIGS.

4.6 NdFeB magnets

Scenarios for gallium use in NdFeB magnets were developed by decomposing the demand into three factors, the demand for NdFeB magnets, the share of NdFeB magnets using Ga as a dopant, and the concentration of Ga in these magnets:

$$M_{magnets} = M_{NdFeB} k_{Ga-NdFeB} c_{magnets} \tag{4.11}$$

The demand for NdFeB magnets in 2012 was taken from an estimate from Roskill Information Services, presented in a critical raw materials report by the European Commission.[47] For the future demand for NdFeB magnets, we took the scenarios developed by Habib and Wenzel as a starting point.[6] They defined four scenarios, which are supposed to reflect the technological developments analyzed by the IEA in their baseline, BLUE map, and BLUE map high renewables scenarios, as well as an additional scenario that they call "100% renewables". The first three scenarios correspond to the 6DS, 2DS and 2DS hi-ren scenarios respectively, which we used to define the scenarios for CIGS demand. We assumed that the average concentration of neodymium in NdFeB magnets will remain at 26.8%.[47] We note that the scenarios from Habib and Wenzel in general show a very high growth in demand for NdFeB magnets. This may be because they assumed a short lifetime of 10 years for electric vehicles (EVs), and because they assumed that use in computers, audio systems, electric bicycles, and electric motors will grow exponentially with a rate similar to projected economic growth.

The average weight fraction of gallium in NdFeB magnets was around 0.1% in 2014,[1] which is equivalent to 20% of NdFeB magnets containing 0.5% gallium. We assumed that the weight fraction of Ga in NdFeB magnets will be 0.5% when used, which is current practice.[48] Starting from a 20% penetration rate of gallium in magnets, we created three scenarios for how it develops in the future. The first assumes that it remains at 20%; the second assumes that it increases gradually to 60%; the third one assumes that it increases gradually to 100%. In Figure S10, we show how the key parameters and resulting gallium demand for NdFeB magnets develop over time in the different scenarios.

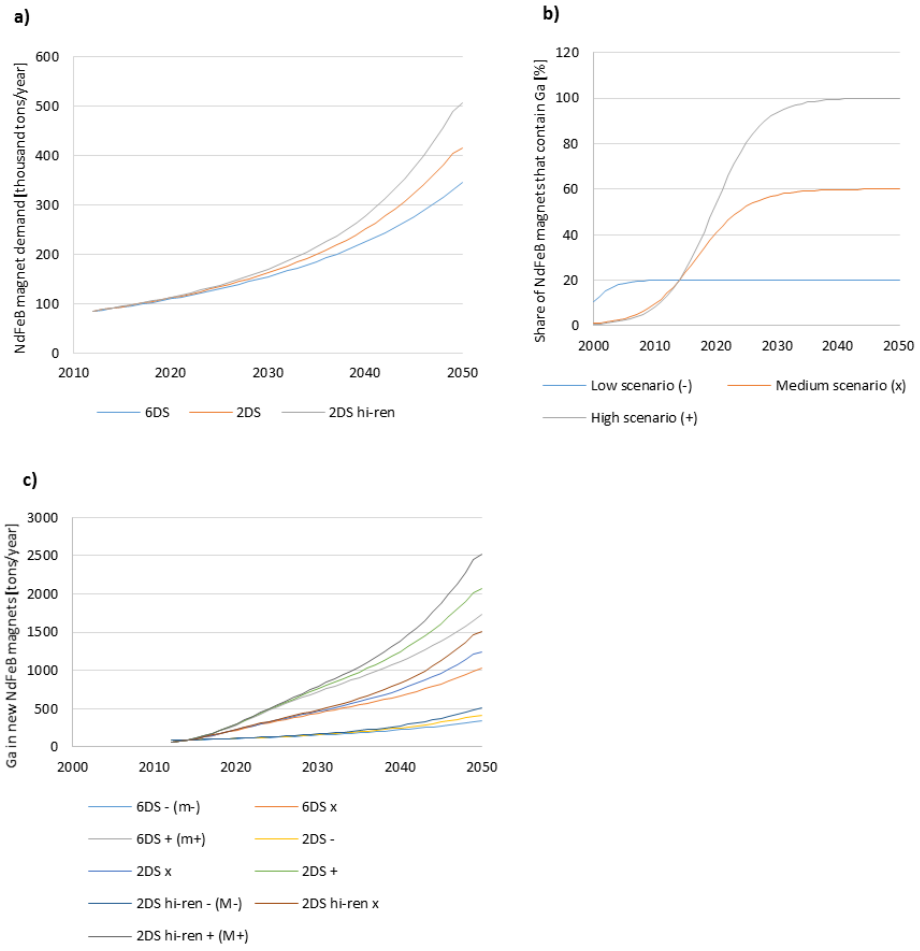

Figure S10. a) Three scenarios for NdFeB magnet demand, based on IEA scenarios and Habib and Wenzel.[6] b) Three scenarios for the share of NdFeB that contain Ga. c) Nine resulting scenarios for Ga in new NdFeB magnets.

5. Sensitivity analysis and system improvements

5.1 Sensitivity analysis

A sensitivity analysis was conducted on the scenarios of minimum supply potential and maximum demand, by changing one parameter at the time. Table S6 shows the list of potential improvements and the corresponding most optimistic parameter changes. Many of the parameters are process yields and scrap collection rates for which it is difficult to set a realistic best value. In these cases we assumed 98% as a "near perfect" improvement.

Table S6 Parameter changes used in sensitivity analysis.

Measure	*Parameters*	*Original value*	*New value*	*Source*
Reduced loss to alumina in Bayer process	k_2	0.60	0.40	*a*
Increased yield in Ga extraction from Bayer liquor	y_1	0.95	0.98	*b*
Increased yield in secondary production	y_2 y_3 y_4	0.92 0.80 0.80	0.98 0.98 0.98	*b*
Reduced substrate thickness of GaAs	t_5	653 µm	450 µm	[49]
Increased yield in TMG production	y_{10}	0.92	0.98	*b*
Increased yield in crystal growth and substrate production	y_{11} y_{12}	0.35 0.35	0.50 0.50	*b*
Increased yield in MOCVD	y_5	0.105	0.20	[50]
Increased yield in MBE	y_6	0.065	0.10	[50]
Increased yield in sputtering deposition	y_7	0.45	0.80	[46]
Reduced breakage and loss from nonworking devices	k_4 k_6 k_7	0.08 0.08 0.08	0.02 0.02 0.02	*b*
Increased collection of fabrication scrap from LEDs	r_1 r_2	0.30 0	0.98 0.98	*b*
Increased collection of fabrication scrap from IC	r_3 r_4	0.10 0	0.98 0.98	*b*
Increased collection of fabrication scrap from PV	r_5 r_6	0.70 0	0.98 0.98	*b*
Increased recycling of Ga from magnet fabrication scrap	r_{14}	0	0.98	*b*
Reduced thickness of LED deposition layer	t_2	4 µm	2 µm	*c*
Reduced thickness of IC deposition layer	t_4	2 µm	1 µm	*c*
Reduced thickness of PV deposition layer	t_7	1.5 µm	0.8 µm	[51]
Increased yield in magnet fabrication	y_8	0.70	0.80	[52]
EOL recycling of gallium from automobiles	r_9	0	0.98	*b*
EOL recycling of gallium from general lighting	r_{10}	0	0.98	*b*
EOL recycling of gallium from IT/telecom. eq.	r_{11}	0	0.98	*b*
EOL recycling of gallium from PV and windmills	r_{12}	0	0.98	*b*
EOL recycling of gallium from other products	r_{13}	0	0.98	*b*

a – Assuming that Bayer liquor is removed for Ga extraction when Ga concentration has reached 100 mg/l instead of 140 mg/l.

b – Assumed near perfect collection or process yields

c – Assumed similar reduction as for PV

5.2 Modeled system improvements

After conducting the sensitivity analysis, the six measures with highest impact on primary Ga demand and the two supply improvements were selected for illustrating a possible solution to a gallium shortage. These were introduced in the model by letting the relevant parameters change linearly from the original value in 2015 to reach the new value (Table S6) in 2050. Measures were applied in the following order:

(i) Recycling of gallium from magnet fabrication scrap, (ii) reduced thickness of CIGS PV cells, (iii) increased yield in sputtering deposition, (iv) increased collection of PV fabrication scrap, (v) EOL recycling of gallium from IT/telecom. equipment, (vi) EOL recycling of gallium from other products, (vii) reduced loss of Ga to alumina, (viii) increased yield in Ga extraction from Bayer liquor.

Supply improvements. The extraction of gallium from Bayer liquor is enabled by the accumulation of gallium that happens upon repeated recycling of the liquor in the process for dissolving and precipitation of aluminum hydroxides.[53] The share of gallium lost to alumina increases with higher concentration in the liquor, and therefore depends on the number of cycles conducted. Hence, it is possible to reduce the loss by extracting gallium more frequently. In the original scenarios, we assumed a loss rate of 60%, equivalent to a concentration of around 140 mg/l. With system improvements, we assume a loss rate of 40%, which would be equivalent to a concentration of around 100 mg/l upon extraction. In addition, we assumed that the extraction efficiency increases from 95% to 98%.

Demand reductions. Recycling of Ga from magnets fabrication scrap was introduced as the first measure, increasing to a collection rate of 98% in 2050. Since Ga is only a very small fraction of the total magnet mass and recycling is currently focused on recovery of neodymium,[52] this must be seen as a very optimistic development. Reduced thickness of CIGS cells and improved deposition yield are expected developments from efforts to cut material costs.[51] The improved values are considered optimistic, but possible. Recycling of CIGS production scrap is mainly focused on recovering indium, but it is also possible to recover gallium.[54] The assumed collection rate in 2050 is considered very optimistic. End-of-life recycling of gallium from IT/telecom. equipment and other products does not take place today. Most of the gallium entering use is contained as an alloying element in NdFeB magnets. As is the case for fabrication scrap, recycling is likely to focus on Nd recovery; gallium recovery from end-of-life products is considered a very optimistic development.

6. References

(1) Løvik, A. N.; Restrepo, E.; Müller, D. B. The Global Anthropogenic Gallium System: Determinants of Demand, Supply and Efficiency Improvements. *Environ. Sci. Technol.* **2015**, *49* (9), 5704–5712.

(2) Liu, G.; Bangs, C. E.; Müller, D. B. Stock dynamics and emission pathways of the global aluminium cycle. *Nat. Clim. Change* **2012**, *3*, 338–342.

(3) Baumgartner, T.; Wunderlich, F.; Wee, D.; Jaunlich, A.; Sato, T.; Erxleben, U.; Bundy, G.; Bundsgaard, R. *Lighting the way: Perspectives on the lighting market*; McKinsey & Company, Inc., 2011. http://www.mckinsey.com/~/media/mckinsey/dotcom/client_service/Automotive%20and%20Assembly/Lighting_the_way_Perspectives_on_global_lighting_market_2012.ashx (accessed January 9, 2015)

(4) IEA. *Energy Technology Perspectives 2014*; Organisation for Economic Co-operation and Development: Paris, 2014.

(5) Masson, G.; Latour, M.; Rekinger, M.; Theologitis, I.-T.; Papoutsi, M. *Global market outlook for photovoltaics 2013-2017*; European Photovoltaic Industry Association: Brussels, Belgium, 2013. http://www.epia.org/fileadmin/user_upload/Publications/GMO_2013_-_Final_PDF.pdf (accessed January 15, 2015)

(6) Habib, K.; Wenzel, H. Exploring rare earths supply constraints for the emerging clean energy technologies and the role of recycling. *J. Clean. Prod.* **2014**, *84*, 348–359.

(7) Oguchi, M.; Fuse, M. Regional and Longitudinal Estimation of Product Lifespan Distribution: A Case Study for Automobiles and a Simplified Estimation Method. *Environ. Sci. Technol.* **2015**, *49* (3), 1738–1743.

(8) Babbitt, C. W.; Kahhat, R.; Williams, E.; Babbitt, G. A. Evolution of Product Lifespan and Implications for Environmental Assessment and Management: A Case Study of Personal Computers in Higher Education. *Environ. Sci. Technol.* **2009**, *43* (13), 5106–5112.

(9) IEA. *Solar Photovoltaic Energy*; Organisation for Economic Co-operation and Development: Paris, 2010.

(10) Turkenburg, W. C.; Arent, D. J.; Bertani, R.; Faaij, A.; Hand, M.; Krewitt, W.; Larson, E. D.; Lund, J.; Mehos, M.; Merrigan, T.; et al. Chapter 11 - Renewable Energy. In *Global Energy Assessment - Toward a Sustainable Future*; Cambridge University Press and International Institute for Applied Systems Analysis: Cambridge, UK; New York, NY, USA and Laxenburg, Austria, 2012; pp 761–900.

(11) Rademaker, J. H.; Kleijn, R.; Yang, Y. Recycling as a Strategy against Rare Earth Element Criticality: A Systemic Evaluation of the Potential Yield of NdFeB Magnet Recycling. *Environ. Sci. Technol.* **2013**, *47* (18), 10129–10136.

(12) Müller, D. B. Stock dynamics for forecasting material flows—Case study for housing in The Netherlands. *Ecol. Econ.* **2006**, *59* (1), 142–156.

(13) Semiconductor-today. Packaged LED market to grow from $11.4bn in 2012 to $17.1bn in 2018. August 9, 2012. http://www.semiconductor-today.com/news_items/2012/AUG/LED_090812.html (accessed Feb 12, 2015)

(14) Semiconductor-today. GaN-based LEDs the main consumer of nitride materials. July 20, 2007. http://www.semiconductor-today.com/news_items/NEWS_2007/JULY_07/YOLE_200707.htm (accessed Mar 6, 2015)

(15) Tao, A. *LED Lighting Market Overview*; IHS IMS Research, 2013. http://www.odmled.com/upfile/file/2013-4/18047541.pdf (accessed Feb 12, 2015)

(16) Yole Développement. Press release: A comprehensive survey of usage and markets for: GaAs, GaP, InP, SiC, Sapphire and bulk-GaN http://www.yole.fr/iso_upload/news/2010/cssubstrates_june2010.pdf (accessed Oct 24, 2014).

(17) Higham, E. GaAs Industry Overview and Forecast: 2011 - 2016. In *28th International Conference on Compound Semiconductor Manufacturing Technology, CS ManTech 2013*; New Orleans, LA, 2013; pp 13–16.

(18) Tuo, D. Trend of Sapphire Substrate Technology and Market Overview; Shanghai, China, 2013. http://www.semiconchina.org/downloadFile/1364362384807.pdf (accessed Feb 11, 2015)

(19) Epistar Corporation. LED Products http://www.epistar.com.tw/_english/01_product/01_overview.php (accessed Feb 12, 2015).

(20) Cree. LED Chips & Materials: Document Library http://www.cree.com/LED-Chips-and-Materials/Document-Library (accessed Feb 12, 2015).

(21) Luxtaltek Corporation. Products http://www.luxtaltek.com/en/products.php (accessed Feb 12, 2015).

(22) Giamello, N. LED Backlighting for LCDs: Options, Design Considerations, and Benefits. SHARP March 2010. http://www.sharpsma.com/sites/default/files/resources/LED%20Backlight%20Whitepaper.pdf (accessed Sep 24, 2014)

(23) Lin, I. Worldwide LED industry - status and outlook; Taipei, Taiwan, 2014. http://prod.ledtaiwan.org/zh/sites/ledtaiwan.org/files/data13/docs/140320__epistar_in_led_executive_summit.pdf (accessed Feb 13, 2015)

(24) Modaresi, R.; Pauliuk, S.; Løvik, A. N.; Müller, D. B. Global Carbon Benefits of Material Substitution in Passenger Cars until 2050 and the Impact on the Steel and Aluminum Industries. *Environ. Sci. Technol.* **2014**, *48* (18), 10776–10784.

(25) Business Wire. Gartner Dataquest Says Fourth Quarter Sales Lead Mobile Phone Market to 6 Percent Growth in 2002 | Business Wire http://www.businesswire.com/news/home/20030310005537/en/Gartner-Dataquest-Fourth-Quarter-Sales-Lead-Mobile#.VImkdSujN8E (accessed Dec 11, 2014).

(26) Gartner Inc. Gartner Says Worldwide Mobile Phone Sales Declined 1.7 Percent in 2012 http://www.gartner.com/newsroom/id/2335616 (accessed Dec 11, 2014).

(27) Gartner Inc. Gartner Says Worldwide Smartphone Sales Soared in Fourth Quarter of 2011 With 47 Percent Growth http://www.gartner.com/newsroom/id/1924314 (accessed Dec 11, 2014).

(28) Gartner Inc. Gartner Says Worldwide Mobile Device Sales to End Users Reached 1.6 Billion Units in 2010; Smartphone Sales Grew 72 Percent in 2010 http://www.gartner.com/newsroom/id/1543014 (accessed Dec 11, 2014).

(29) Gartner Inc. Gartner Says Worldwide Smartphone Sales Reached Its Lowest Growth Rate With 3.7 Per Cent Increase in Fourth Quarter of 2008 http://www.gartner.com/newsroom/id/910112 (accessed Dec 11, 2014).

(30) Gartner Inc. Gartner Says Worldwide Mobile Phone Sales Grew 6 Per Cent in 2008, But Sales Declined 5 Per Cent in the Fourth Quarter http://www.gartner.com/newsroom/id/904729 (accessed Dec 11, 2014).

(31) Gartner Inc. Gartner Says Worldwide Mobile Phone Sales Grew 21 Percent in 2006 http://www.gartner.com/newsroom/id/501734 (accessed Dec 11, 2014).

(32) Gartner Inc. Gartner Says Strong Fourth Quarter Sales Led Worldwide Mobile Phone Sales to 30 Percent Growth in 2004 http://www.gartner.com/newsroom/id/492110 (accessed Dec 11, 2014).

(33) Gartner Inc. Gartner Says Worldwide Combined PDA and Smartphone Shipments Market Grew 57 Percent in the First Half of 2006 http://www.gartner.com/newsroom/id/496997 (accessed Dec 11, 2014).

(34) Gartner Inc. Market Share: Smartphones, Worldwide, 4Q07 and 2007 https://www.gartner.com/doc/619509/market-share-smartphones-worldwide-q (accessed Dec 11, 2014).

(35) Augustine, P. J. Trends and opportunities for gallium arsenide semiconductors in handsets. In *20th International Conference on Compound Semiconductor Manufacturing Technology, CS ManTech 2005*; GaAs Mantech, Incorporated: New Orleans, LA, 2005.

(36) Higham, E. *Private communication with Eric Higham, Director, Advanced Semiconductor Applications at Strategy Analytics; Newton MA; August 2014*.

(37) Cheng, N.; Young, J. P. Challenges and Requirements of Multimode Multiband Power Amplifiers for Mobile Applications. In *2011 IEEE Compound Semiconductor Integrated Circuit Symposium (CSICS)*; 2011; pp 1–4.

(38) Bolton, N. Q. Mobile Device RF Front-End TAM Analysis and Forecast; *International Conference on Compound Semiconductor Manufacturing Technology, CS ManTech 2011*; Indian Wells, California, USA, 2011.

(39) Anadigics Inc. AWT6651 High Efficiency ProEficient UMTS2100 (Band 1) LTE/WCDMA/TD-SCDMA Linear PAM http://www.anadigics.com/sites/default/files/datasheets/AWT6651_Rev_2.3.pdf (accessed Oct 13, 2014).

(40) Skyworks Inc. SKY77185 Power Amplifier Module for WCDMA/HSDPA (1920-1980 MHz) http://www.skyworksinc.com/uploads/documents/200848b.pdf (accessed Oct 13, 2014).

(41) Avago Technologies. ACPM-7868 5x5 mm Power Amplifier Module Linear Quad-Band GSM/EDGE http://www.avagotech.com/pages/en/rf_microwave/amplifiers/linear_power/gsm_pa/ (accessed Oct 13, 2014).

(42) Skyworks Inc. SKY77354 Power Amplifier Module for Quad-Band GSM/GPRS/EDGE http://www.skyworksinc.com/uploads/documents/200890b.pdf (accessed Oct 12, 2014).

(43) Hau, G.; Hussain, A.; Turpel, J.; Donnenwirth, J. A 3x3mm2 LTE/WCDMA dual-mode power amplifier module with integrated high directivity coupler. In *2011 IEEE Bipolar/BiCMOS Circuits and Technology Meeting (BCTM)*; 2011; pp 138–141.

(44) UN Data: Mobile-cellular telephone subscriptions http://data.un.org/Data.aspx?d=ITU&f=ind1Code%3aI271#ITU (accessed Jan 20, 2015).

(45) *Test Methods for Electrical Performance of Nonconcentrator Terrestrial Photovoltaic Modules and Arrays Using Reference Cells*; E44 Committee, ASTM International, 2012. http://enterprise.astm.org/SUBSCRIPTION/filtrexx40.cgi?REDLINE_PAGES/E1036.htm (accessed Oct 14, 2014)

(46) Marwede, M.; Reller, A. Estimation of Life Cycle Material Costs of Cadmium Telluride- and Copper Indium Gallium Diselenide-Photovoltaic Absorber Materials based on Life Cycle Material Flows. *J. Ind. Ecol.* **2014**, *18* (2), 254–267.

(47) European Commission. *Report on Critical Raw Materials for the EU: Critical raw materials profiles*; 2014. http://ec.europa.eu/enterprise/policies/raw-materials/files/docs/crm-report-on-critical-raw-materials_en.pdf (accessed Jan 9, 2015)

(48) Hall, T. *Personal communication with Todd Hall, Manager, Raw Material Procurement & Sales, Molycorp Rare Metals Inc., Utah, USA, November 2014*; 2014.

(49) Freiberger Compound Materials. GaAs wafers specifications http://www.freiberger.com/en/products/gaas-wafers/specifications.html (accessed Jul 24, 2014).

(50) Izumi, S.; Shirahama, H.; Kouji, Y. Environmental safety issues for molecular beam epitaxy platform growth technology. *J. Cryst. Growth* **2001**, *227–228*, 150–154.

(51) Fthenakis, V. Sustainability of photovoltaics: The case for thin-film solar cells. *Renew. Sustain. Energy Rev.* **2009**, *13* (9), 2746–2750.

(52) Herchenroeder, J. *Personal communication with James Herchenroeder, Vice President Technology; Molycorp Magnequench*; 2015.

(53) Hudson, L. K. Gallium as a by-Product of Alumina Manufacture. *J. Met.* **1965**, *17* (9), 948–951.

(54) Zimmermann, Y.-S.; Niewersch, C.; Lenz, M.; Kül, Z. Z.; Corvini, P. F.-X.; Schäffer, A.; Wintgens, T. Recycling of Indium From CIGS Photovoltaic Cells: Potential of Combining Acid-Resistant Nanofiltration with Liquid–Liquid Extraction. *Environ. Sci. Technol.* **2014**, *48* (22), 13412–13418.